Density Model for Sei Whale (*Balaenoptera borealis*) for the U.S. East Coast: Supplementary Report

Duke University Marine Geospatial Ecology Lab*

Model Version 6.5 - 2016-04-21

Citation

When referencing our methodology or results generally, please cite our open-access article:

Roberts JJ, Best BD, Mannocci L, Fujioka E, Halpin PN, Palka DL, Garrison LP, Mullin KD, Cole TVN, Khan CB, McLellan WM, Pabst DA, Lockhart GG (2016) Habitat-based cetacean density models for the U.S. Atlantic and Gulf of Mexico. Scientific Reports 6: 22615. doi: 10.1038/srep22615

To reference this specific model or Supplementary Report, please cite:

Roberts JJ, Best BD, Mannocci L, Fujioka E, Halpin PN, Palka DL, Garrison LP, Mullin KD, Cole TVN, Khan CB, McLellan WM, Pabst DA, Lockhart GG (2016) Density Model for Sei Whale (*Balaenoptera borealis*) for the U.S. East Coast Version 6.5, 2016-04-21, and Supplementary Report. Marine Geospatial Ecology Lab, Duke University, Durham, North Carolina.

Copyright and License

Revision History

Version	Date	Description of changes
1	2013-05-08	Initial version with climatological predictor variables.
2	2014-03-01	Reformulated density model using a Horvitz-Thompson estimator. Eliminated GAM for group size (consequence of above). Added group size as a candidate covariate in detection functions (benefit of above). Added survey ID as a candidate covariate in NOAA NARWSS detection functions. Took more care in selecting right-truncation distances. Fitted models with contemporaneous predictors, for comparison to climatological. Switched SST and SST fronts predictors from NOAA Pathfinder to GHRSST CMC0.2deg L4. Changed SST fronts algorithm to use Canny operator instead of Cayula-Cornillon. Switched winds predictors from SCOW to CCMP (SCOW only gives climatol. estimates.) Added DistToEddy predictors, based on Chelton et al. (2011) eddy database. Added cumulative VGPM predictors, summing productivity for 45, 90, and 180 days. Added North Atlantic Oscillation (NAO) predictor; included 3 and 6 month lags. Transformed predictors more carefully, to better minimize leverage of outliers. Implemented hybrid hierarchical-forward / exhaustive model selection procedure. Model selection procedure better avoids concurvity between predictors. Allowed GAMs to select between multiple formulations of dynamic predictors. Adjusted land mask to eliminate additional estuaries and hard-to-predict cells.
3	2014-05-20	Fixed bug in temporal variability plots. Density models unchanged.

*For questions, or to offer feedback about this model or report, please contact Jason Roberts (jason.roberts@duke.edu)

4	2014-06-02	Added Reclassification of Ambiguous Sightings section, which was accidentally omitted. Density models unchanged.
5	2015-01-17	TODO: Describe changes.
6	2015-01-18	Switched back to a four season model, using seasons from version 4.
6.1	2015-01-19	Restricted Fall season model to the surveyed area of the northeast.
6.2	2015-03-06	Updated the documentation. No changes to the model.
6.3	2015-05-14	Updated calculation of CVs. Switched density rasters to logarithmic breaks. No changes to the model.
6.4	2015-09-28	Updated the documentation. No changes to the model.
6.5	2016-04-21	Switched calculation of monthly 5% and 95% confidence interval rasters to the method used to produce the year-round rasters. (We intended this to happen in version 6.3 but I did not implement it properly.) Updated the monthly CV rasters to have value 0 where we assumed the species was absent, consistent with the year-round CV raster. No changes to the other (non-zero) CV values, the mean abundance rasters, or the model itself.

Survey Data

Survey	Period	Length (1000 km)	Hours	Sightings
NEFSC Aerial Surveys	1995-2008	70	412	14
NEFSC NARWSS Harbor Porpoise Survey	1999-1999	6	36	0
NEFSC North Atlantic Right Whale Sighting Survey	1999-2013	432	2330	797
NEFSC Shipboard Surveys	1995-2004	16	1143	6
NJDEP Aerial Surveys	2008-2009	11	60	0
NJDEP Shipboard Surveys	2008-2009	14	836	0
SEFSC Atlantic Shipboard Surveys	1992-2005	28	1731	3
SEFSC Mid Atlantic Tursiops Aerial Surveys	1995-2005	35	196	0
SEFSC Southeast Cetacean Aerial Surveys	1992-1995	8	42	1
UNCW Cape Hatteras Navy Surveys	2011-2013	19	125	0
UNCW Early Marine Mammal Surveys	2002-2002	18	98	0
UNCW Jacksonville Navy Surveys	2009-2013	66	402	0
UNCW Onslow Navy Surveys	2007-2011	49	282	0
UNCW Right Whale Surveys	2005-2008	114	586	0
Virginia Aquarium Aerial Surveys	2012-2014	9	53	0
Total		895	8332	821

Table 2: Survey effort and sightings used in this model. Effort is tallied as the cumulative length of on-effort transects and hours the survey team was on effort. Sightings are the number of on-effort encounters of the modeled species for which a perpendicular sighting distance (PSD) was available. Off effort sightings and those without PSDs were omitted from the analysis.

Season	Months	Length (1000 km)	Hours	Sightings
Winter	Dec Jan Feb Mar	274	2099	20
Spring	Apr May Jun	298	2001	659
Summer	Jul Aug Sep	225	3575	99
Fall	Oct Nov	99	657	43

Table 3: Survey effort and on-effort sightings having perpendicular sighting distances, summarized by season.

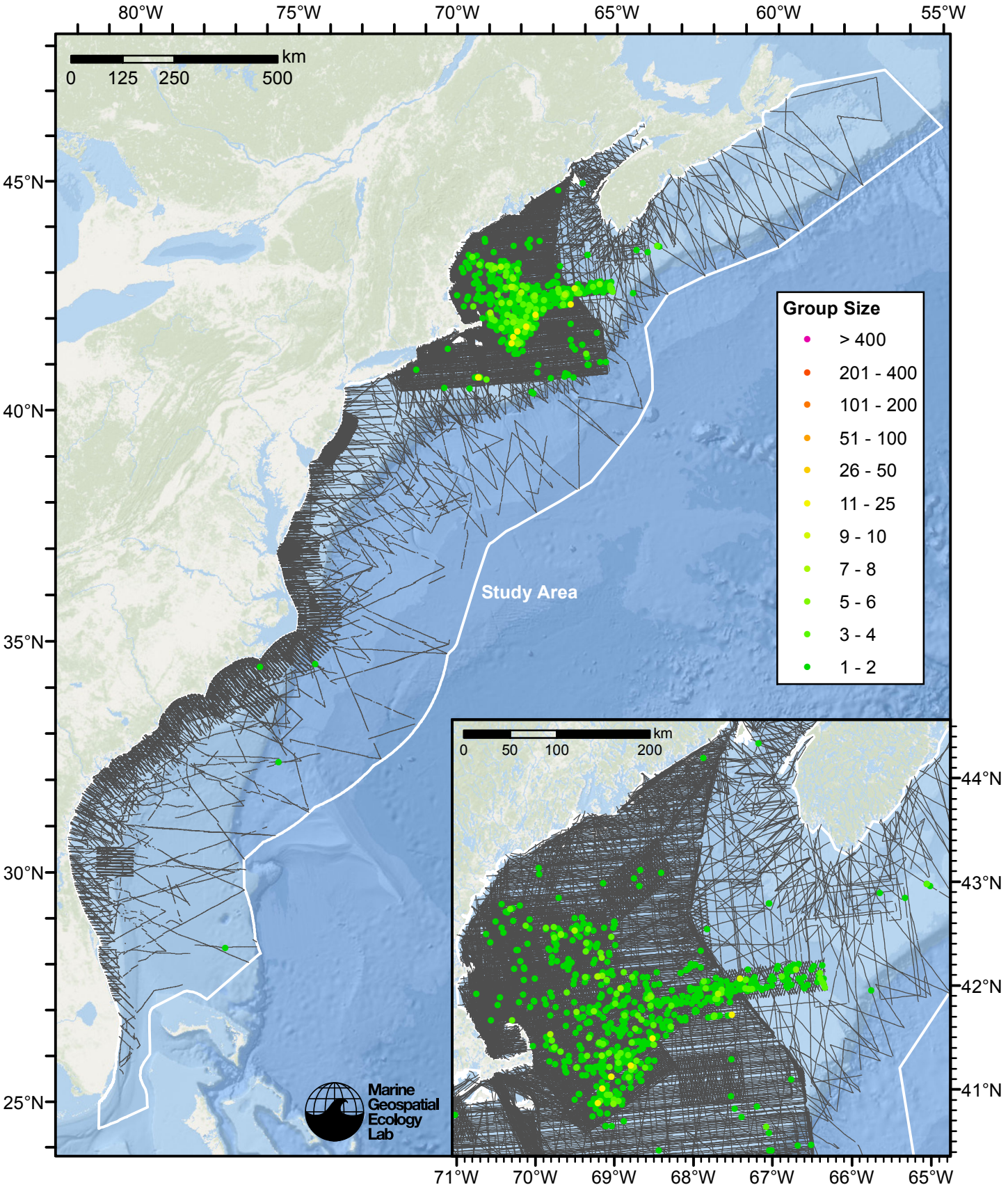

Figure 1: Sei whale sightings and survey tracklines.

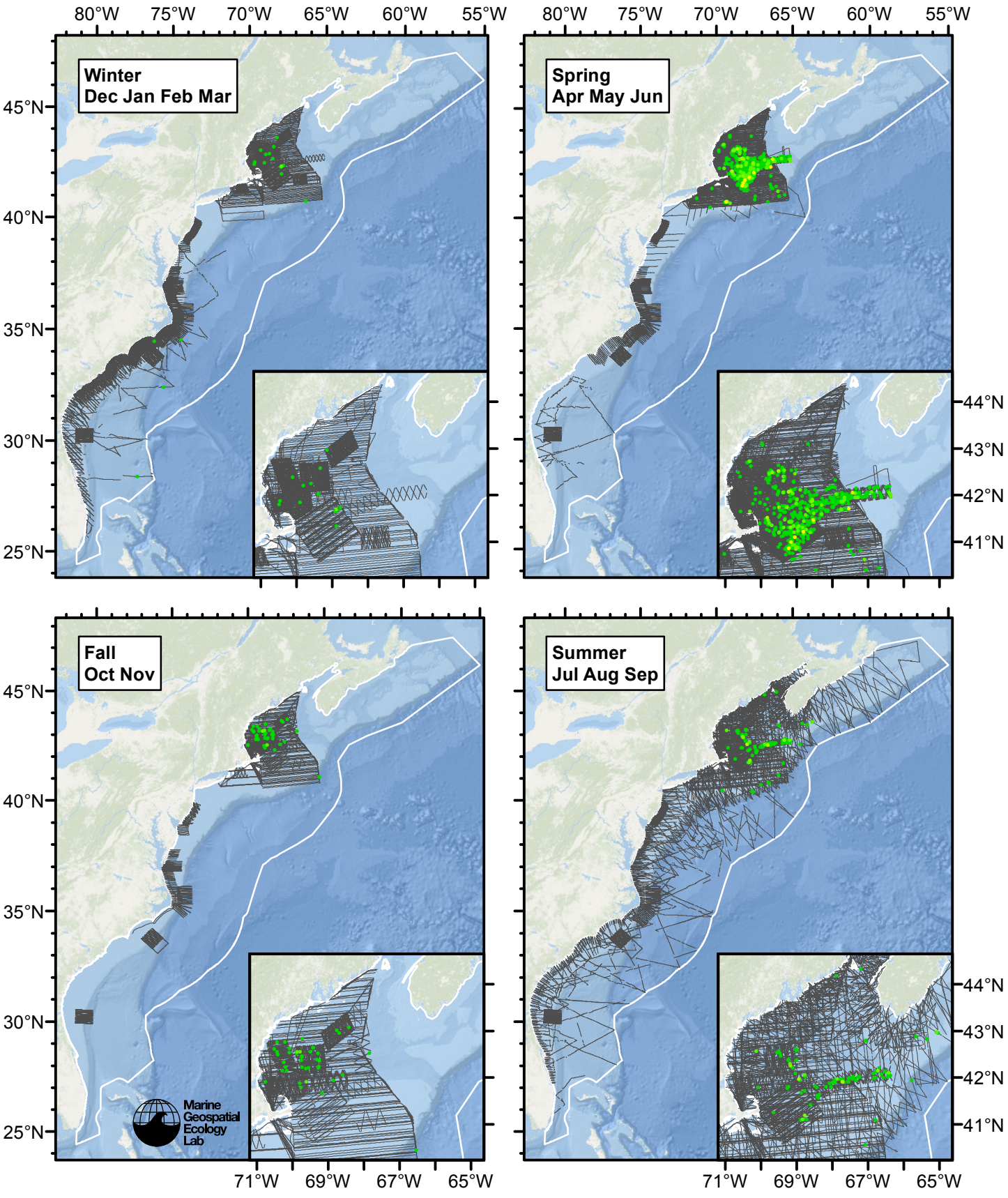

Figure 2: Sei whale sightings and survey tracklines, by season. Sighting colors are the same as the previous figure.

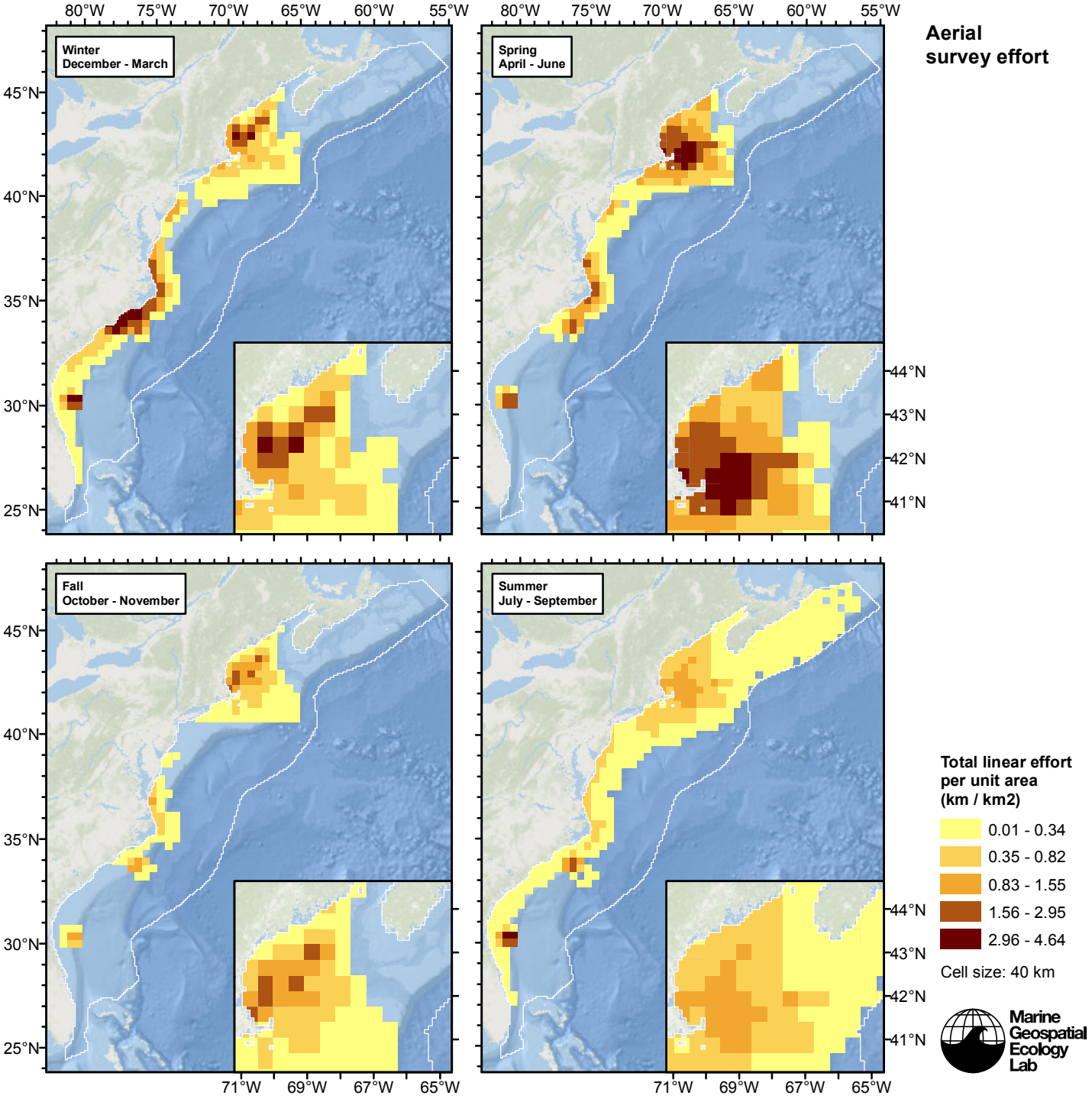

Figure 3: Aerial linear survey effort per unit area.

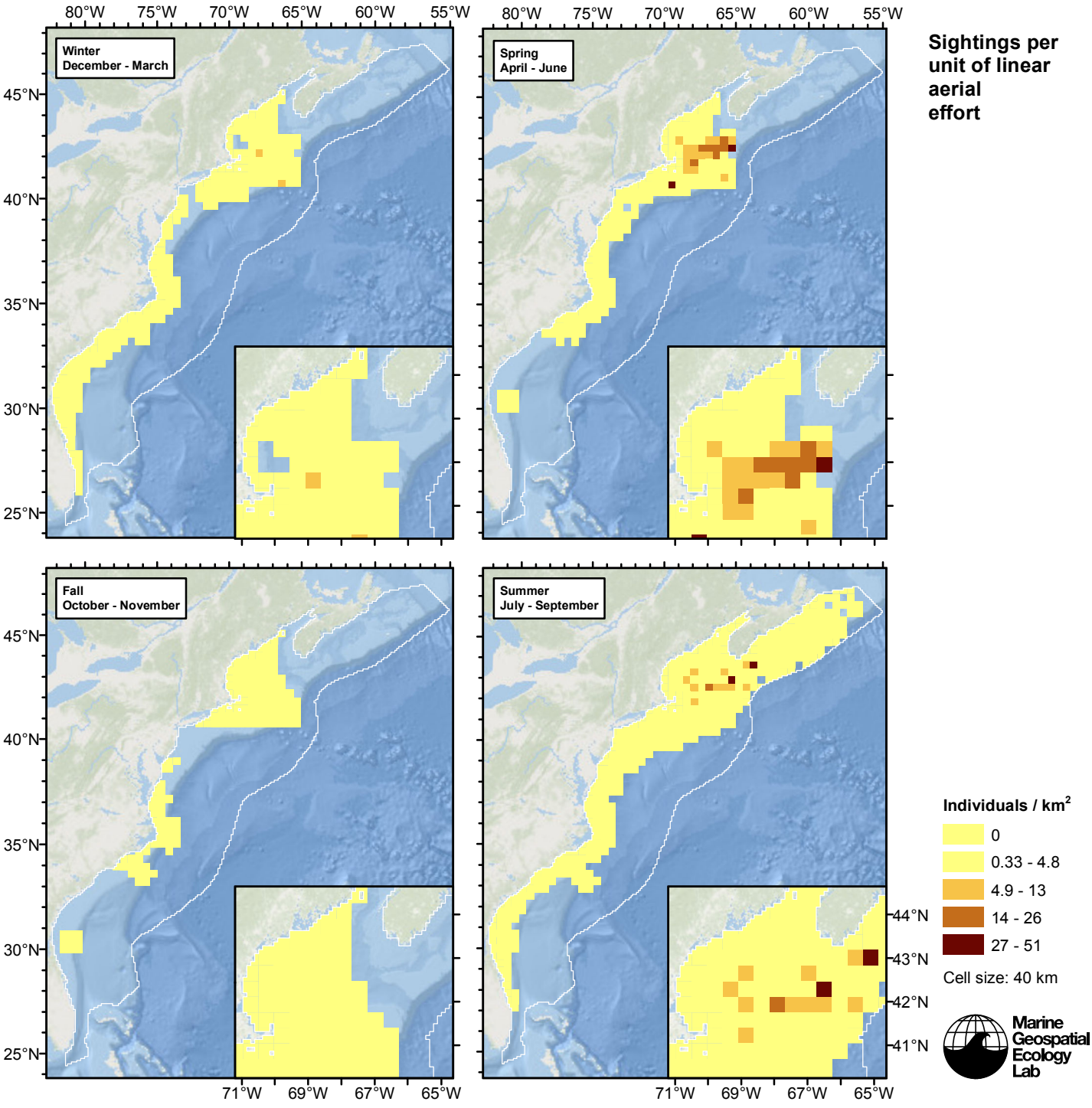

Figure 4: Sei whale sightings per unit aerial linear survey effort.

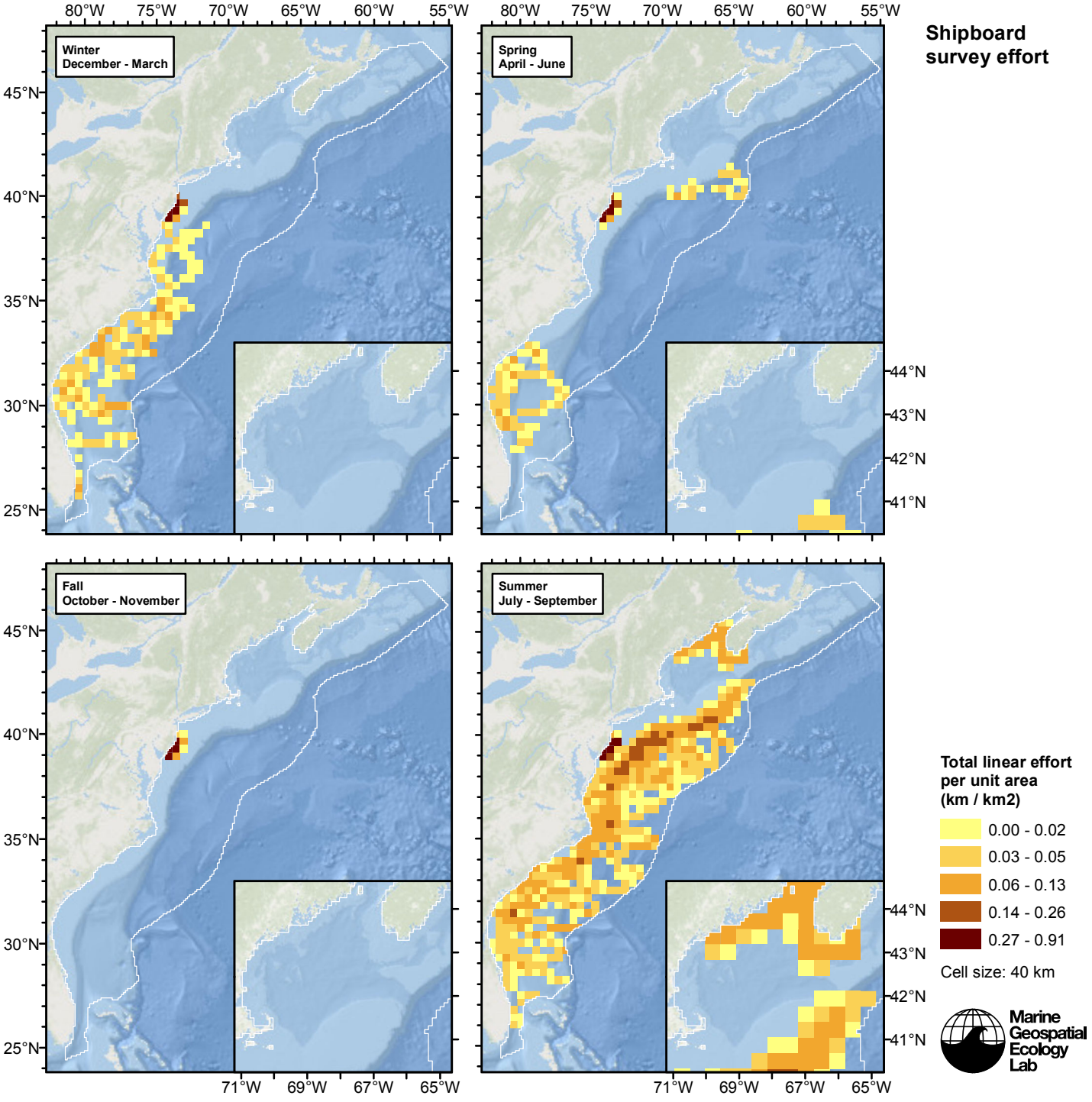

Figure 5: Shipboard linear survey effort per unit area.

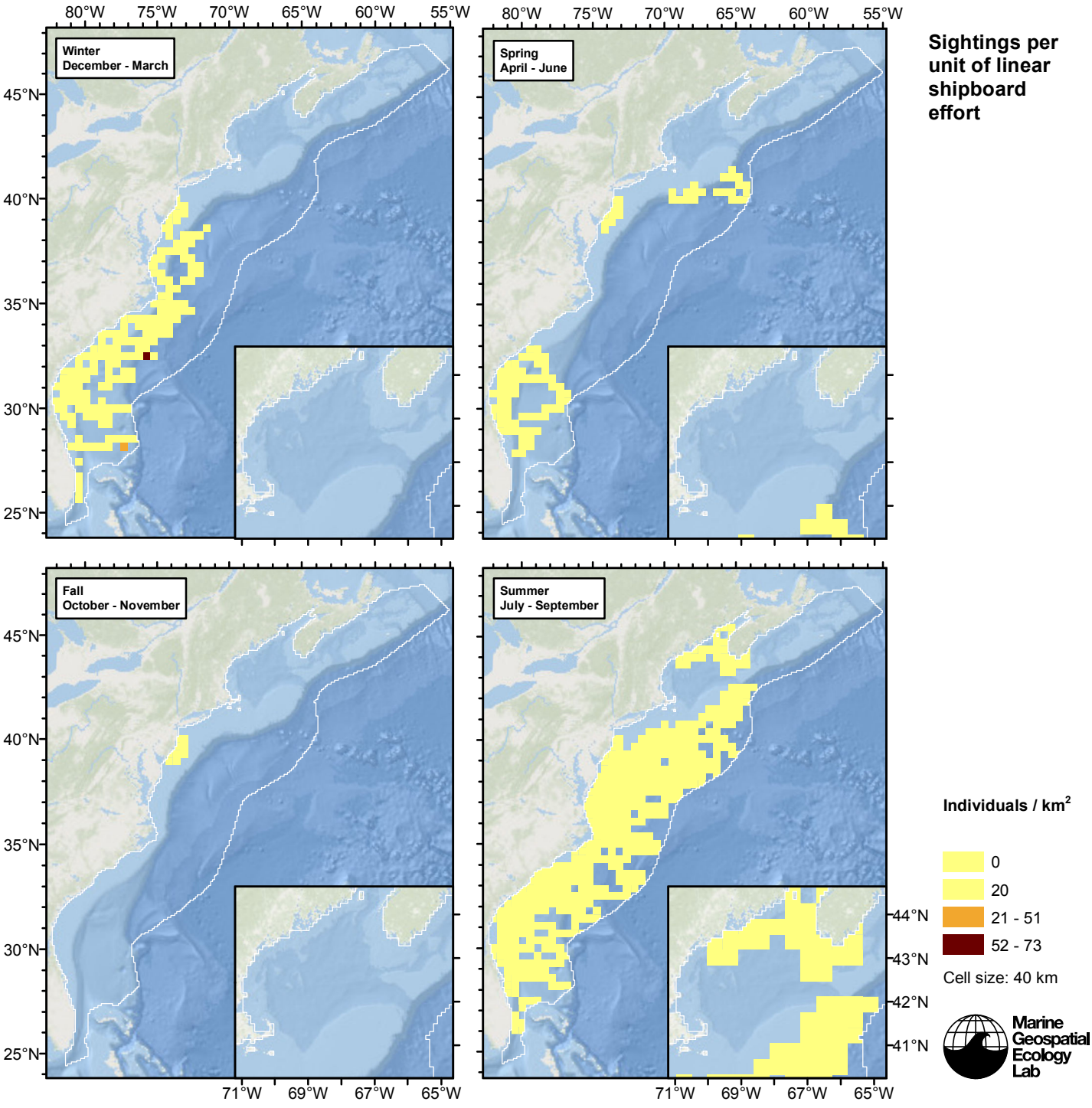

Figure 6: Sei whale sightings per unit shipboard linear survey effort.

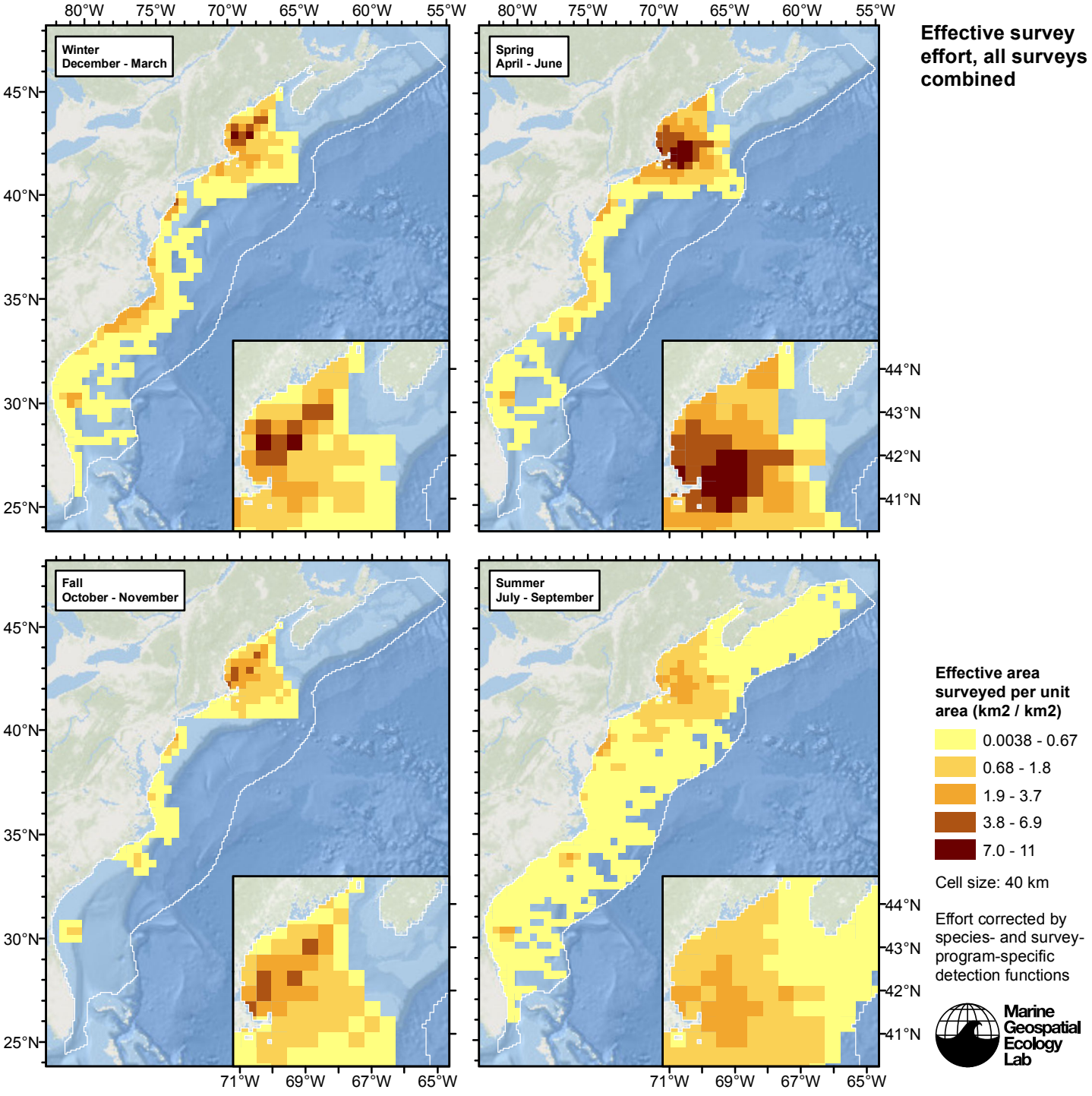

Figure 7: Effective survey effort per unit area, for all surveys combined. Here, effort is corrected by the species- and survey-program-specific detection functions used in fitting the density models.

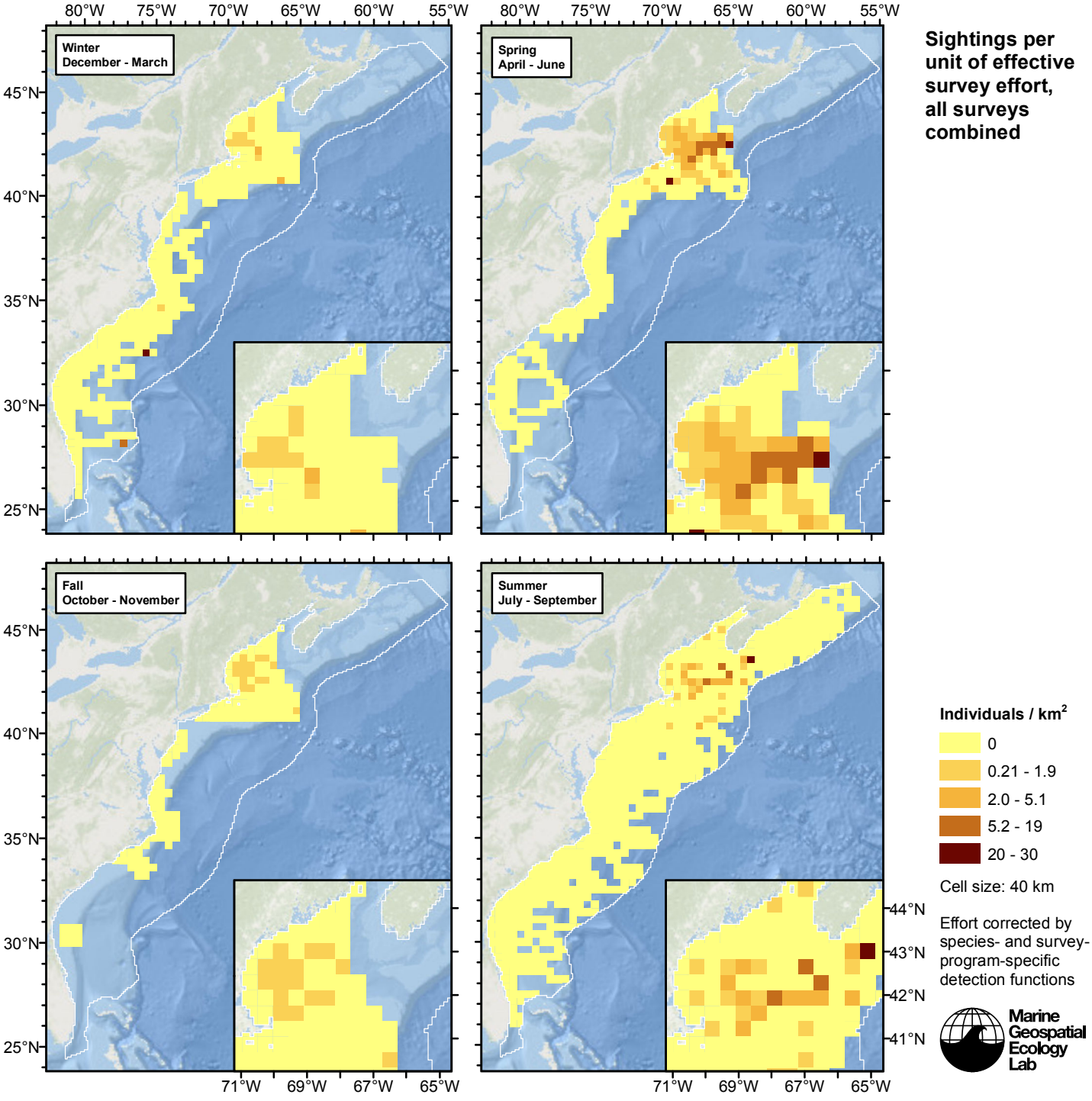

Figure 8: Sei whale sightings per unit of effective survey effort, for all surveys combined. Here, effort is corrected by the species- and survey-program-specific detection functions used in fitting the density models.

Reclassification of Ambiguous Sightings

Observers occasionally experience difficulty identifying species, due to poor sighting conditions or phenotypic similarities between the possible choices. For example, observers may not always be able to distinguish fin whales from sei whales (Tim Cole, pers. comm.). When this happens, observers will report an ambiguous identification, such as "fin or sei whale".

In our density models, we handled ambiguous identifications in three ways:

1. For sightings with very generic identifications such as "large whale", we discarded the sightings. These sightings represented a clear minority when compared to those with definitive species identifications, but they are uncounted animals and our density models may therefore underestimate density to some degree.

2. For sightings of certain taxa in which a large majority of identifications were ambiguous (e.g. "Globicephala spp.") rather than specific (e.g. "Globicephala melas" or "Globicephala macrorhynchus"), it was not tractable to model the individual species so we modeled the generic taxon instead.

3. For sightings that reported an ambiguous identification of two species (e.g. "fin or sei whale") that are known to exhibit different habitat preferences or typically occur in different group sizes, and for which we had sufficient number of definitive sightings of both species, we fitted a predictive model that classified the ambiguous sightings into one species or the other.

This section describes how we utilized the third category of ambiguous sightings in the density models presented in this report.

For the predictive model, we used the cforest classifier (Hothorn et al. 2006), an elaboration of the classic random forest classifier (Breiman, 2001). First, we trained a binary classifier using the sightings that reported definitive species identifications (e.g. "fin whale" and "sei whale"). The training data included all on-effort sightings, not just those in the focal study area. We used the species ID as the response variable and oceanographic variables or group size as predictor variables, depending on the species. We used receiver operating characteristic (ROC) curve analysis to select a threshold for classifying the probabilistic predictions of species identifications made by the model into a binary result of one species or another; for the threshold, we selected the value that maximized the Youden index (see Perkins and Schisterman, 2006).

Then, for all sightings reporting the ambiguous identification, we reclassified the sighting as either one species or the other by processing the predictor values observed for that sighting through the fitted model. We then included the reclassified sightings in the detection functions and spatial models of density. The sightings reported elsewhere in this document incorporate both the definitive sightings and the reclassified sightings.

Reclassification of "Balaenoptera borealis/physalus" in the East Coast Region

Density Histograms

These plots show the per-species distribution of each predictor variable used in the reclassification model. When a variable exhibits a substantially different distribution for each species, it is a good candidate for classifying ambiguous sightings as one species or the other.

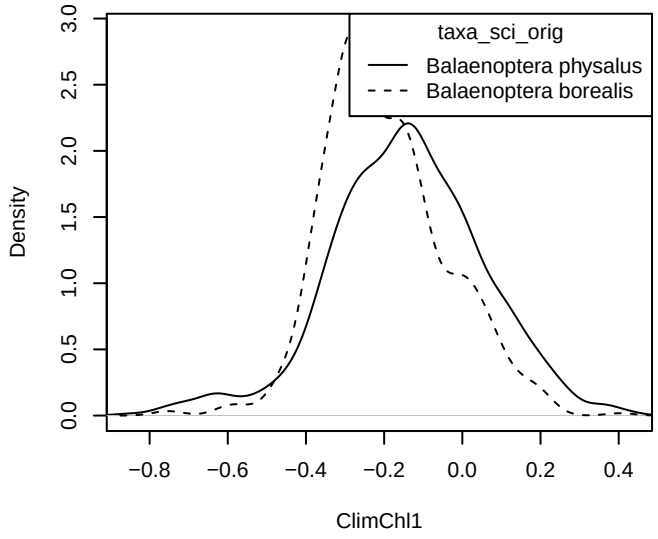

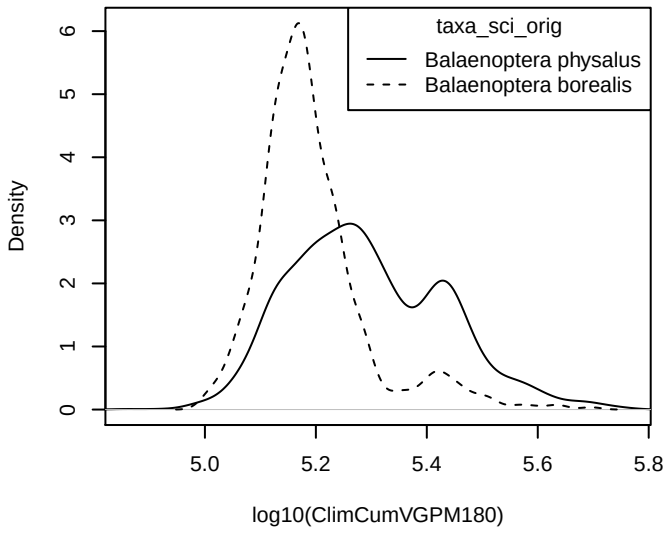

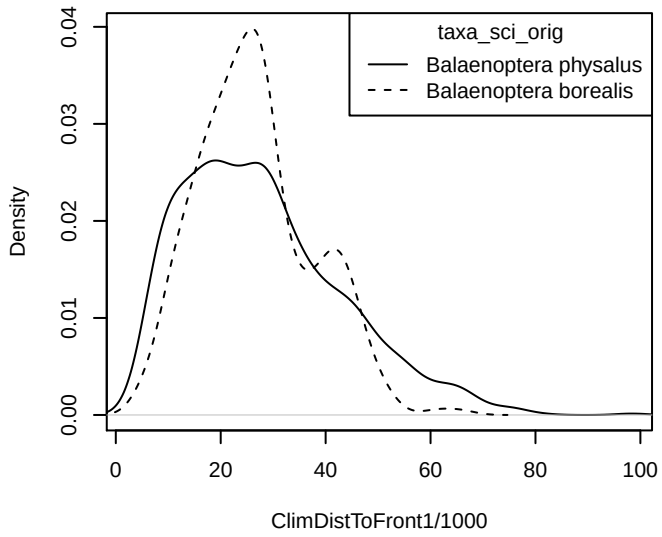
taxa_sci_orig
Balaenoptera physalus
Balaenoptera borealis
Density
0.00
0.01
0.02
0.03
0.04
0
20
40
60
80
100
ClimDistToFront1/1000

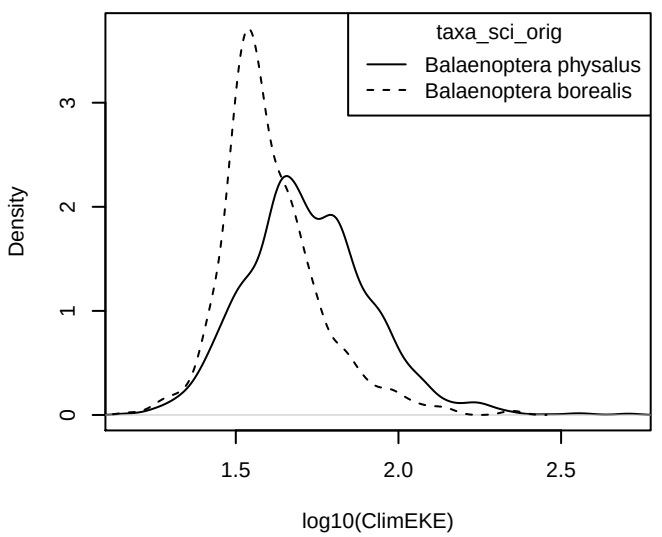
taxa_sci_orig
Balaenoptera physalus
Balaenoptera borealis
Density
0
1
2
3
1.5
2.0
2.5
log10(ClimEKE)

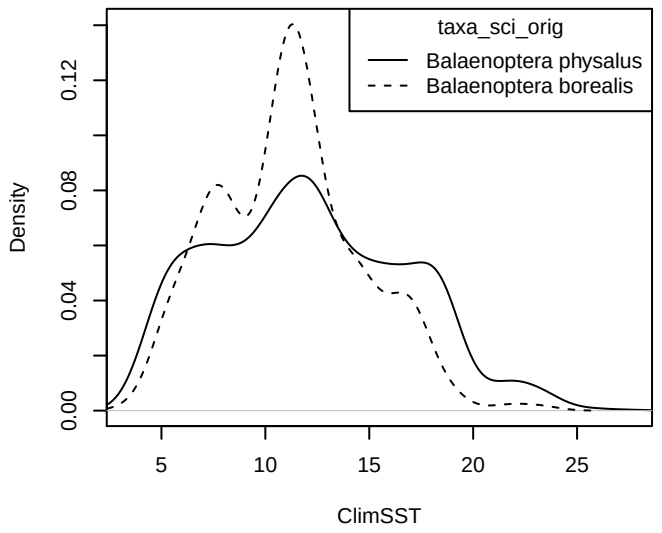
taxa_sci_orig
Balaenoptera physalus
Balaenoptera borealis
Density
0.00
0.04
0.08
0.12
5
10
15
20
25
ClimSST

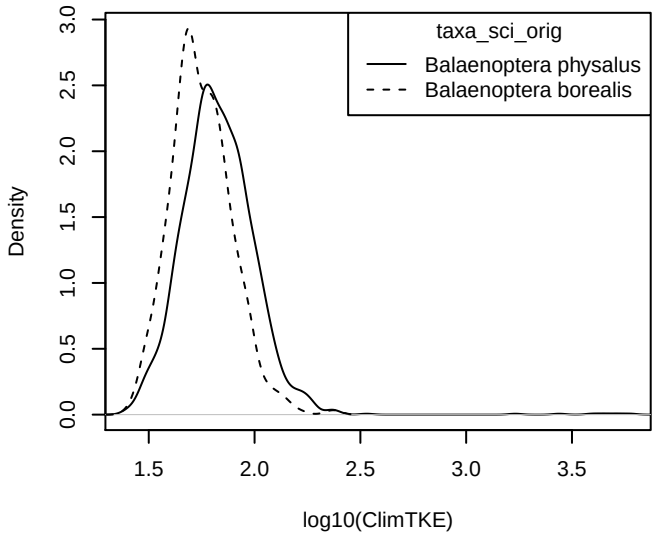
taxa_sci_orig
Balaenoptera physalus
Balaenoptera borealis
Density
0.0
0.5
1.0
1.5
2.0
2.5
3.0
1.5
2.0
2.5
3.0
3.5
log10(ClimTKE)

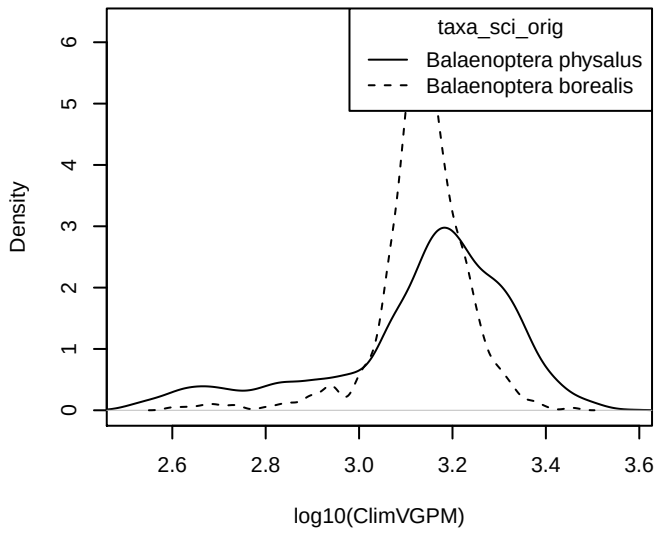
taxa_sci_orig
Balaenoptera physalus
Balaenoptera borealis
Density
0
1
2
3
4
5
6
2.6
2.8
3.0
3.2
3.4
3.6
log10(ClimVGPM)

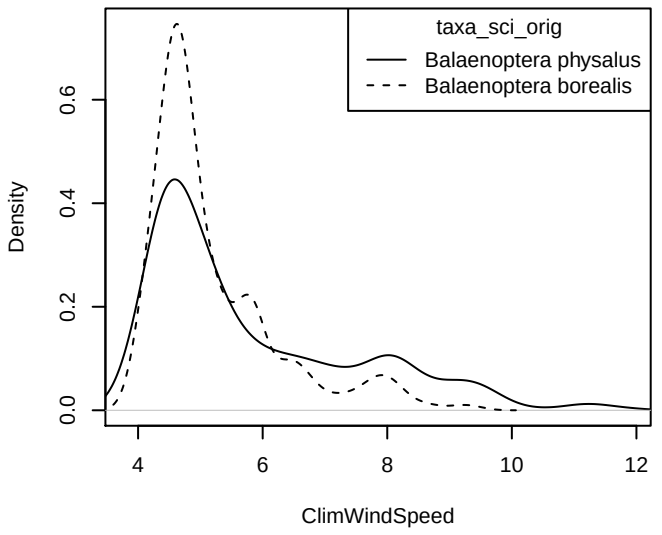
taxa_sci_orig
Balaenoptera physalus
Balaenoptera borealis
Density
0.0
0.2
0.4
0.6
4
6
8
10
12
ClimWindSpeed

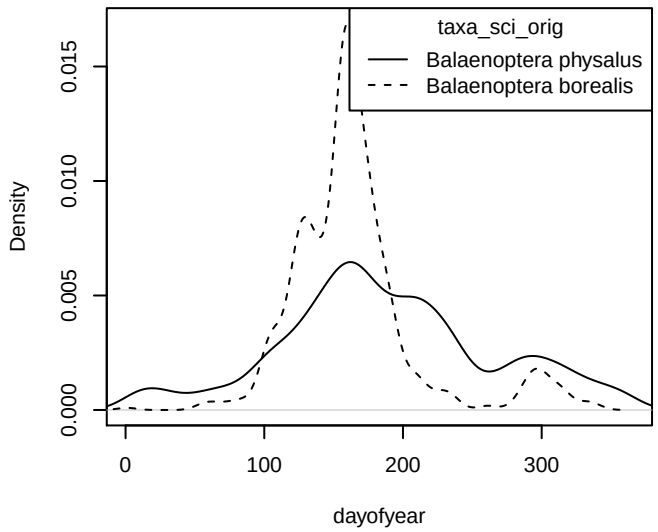

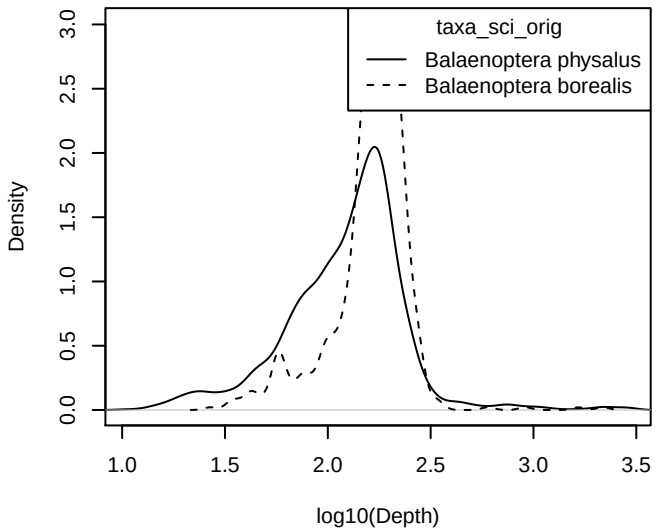

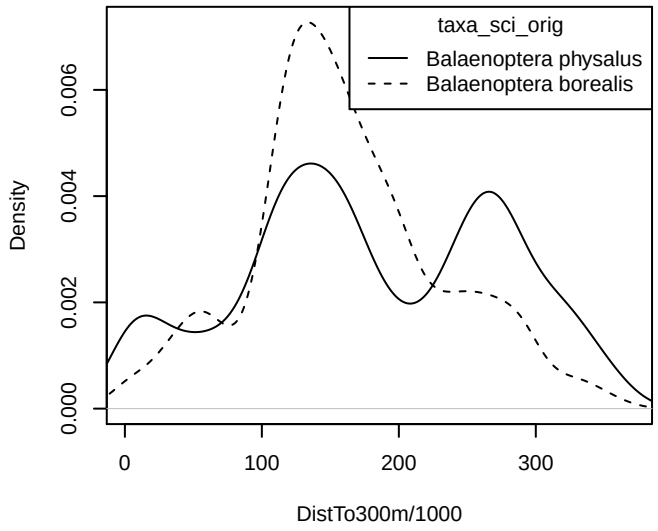

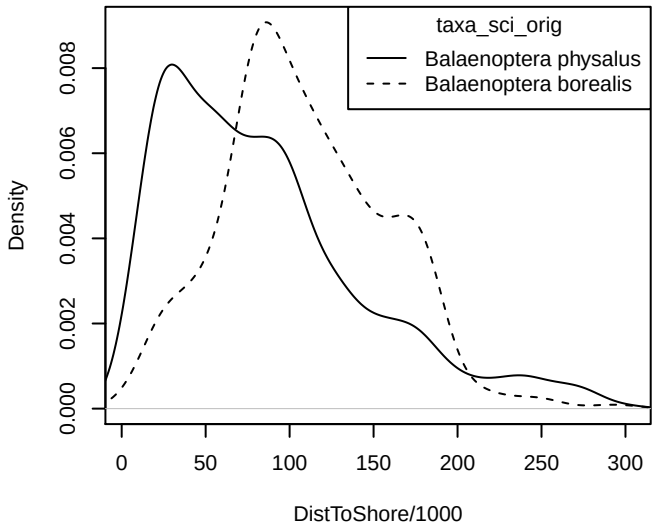

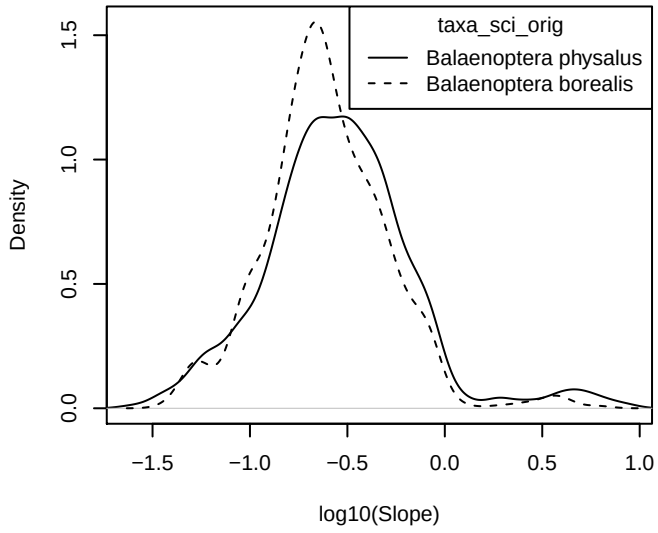

Statistical output

```
MODEL SUMMARY:
==============
```

```
     Random Forest using Conditional Inference Trees

Number of trees:  1000

Response:  factor(taxa_sci_orig)
Inputs:  dayofyear, Depth, Slope, DistToShore, DistTo300m, ClimSST, ClimDistToFront1, ClimChl1, ClimTKE, ClimE
Number of observations:  2458

Number of variables tried at each split: 5

Estimated predictor variable importance (conditional = FALSE):

                 Importance
ClimCumVGPM180      0.03383
ClimEKE             0.01948
ClimWindSpeed       0.01803
Depth               0.01777
DistToShore         0.01762
ClimVGPM            0.01171
DistTo300m          0.01154
dayofyear           0.01125
ClimChl1            0.00968
ClimSST             0.00920
Slope               0.00759
ClimTKE             0.00618
ClimDistToFront1    0.00512

MODEL PERFORMANCE SUMMARY:
==========================

Statistics calculated from the training data.

Area under the ROC curve (auc)           = 0.940
Mean cross-entropy (mxe)                 = 0.282
Precision-recall break-even point (prbe) = 0.915
Root-mean square error (rmse)            = 0.297

Cutoff selected by maximizing the Youden index = 0.721

Confusion matrix for that cutoff:

                                Actual Balaenoptera physalus  Actual Balaenoptera borealis  Total
Predicted Balaenoptera physalus                         1587                            92   1679
Predicted Balaenoptera borealis                          255                           524    779
Total                                                   1842                           616   2458

Model performance statistics for that cutoff:

Accuracy (acc)                              = 0.859
Error rate (err)                            = 0.141
Rate of positive predictions (rpp)          = 0.683
Rate of negative predictions (rnp)          = 0.317

True positive rate (tpr, or sensitivity)    = 0.862
False positive rate (fpr, or fallout)       = 0.149
True negative rate (tnr, or specificity)    = 0.851
False negative rate (fnr, or miss)          = 0.138
```

```
Positive prediction value (ppv, or precision) = 0.945
Negative prediction value (npv)               = 0.673
Prediction-conditioned fallout (pcfall)       = 0.055
Prediction-conditioned miss (pcmiss)          = 0.327

Matthews correlation coefficient (mcc)        = 0.663
Odds ratio (odds)                             = 35.447
SAR                                           = 0.698

Cohen's kappa (K)                             = 0.655
```

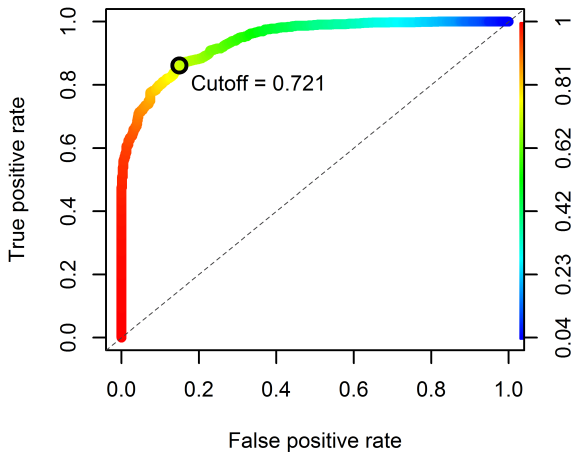

Figure 9: Receiver operating characteristic (ROC) curve illustrating the predictive performance of the model used to reclassify "Balaenoptera borealis/physalus" sightings into one species or the other.

Reclassifications Performed

Survey	Definitive B. borealis Sightings	Definitive B. physalus Sightings	Ambiguous Sightings	Reclassed to B. borealis	Reclassed to B. physalus
NEFSC Aerial Surveys	8	210	27	6	21
NEFSC NARWSS Harbor Porpoise Survey	0	16	0	0	0
NEFSC North Atlantic Right Whale Sighting Survey	603	1455	546	231	315
NEFSC Shipboard Surveys	6	138	100	0	100
NJDEP Aerial Surveys	0	1	0	0	0
NJDEP Shipboard Surveys	0	27	0	0	0
SEFSC Atlantic Shipboard Surveys	0	11	0	0	0
SEFSC Mid Atlantic Tursiops Aerial Surveys	0	6	0	0	0
UNCW Cape Hatteras Navy Surveys	0	5	0	0	0
UNCW Early Marine Mammal Surveys	0	2	0	0	0
UNCW Onslow Navy Surveys	0	1	0	0	0

UNCW Right Whale Surveys	0	12	0	0	0
Virginia Aquarium Aerial Surveys	0	14	0	0	0
Total	617	1898	673	237	436

Table 4: Counts of definitive sightings, ambiguous sightings, and what the ambiguous sightings were reclassified to. Note that this analysis was performed on all on-effort sightings, not just those in the focal study area. These counts may therefore be larger than those presented in the Survey Data section of this report, which are restricted to the focal study area.

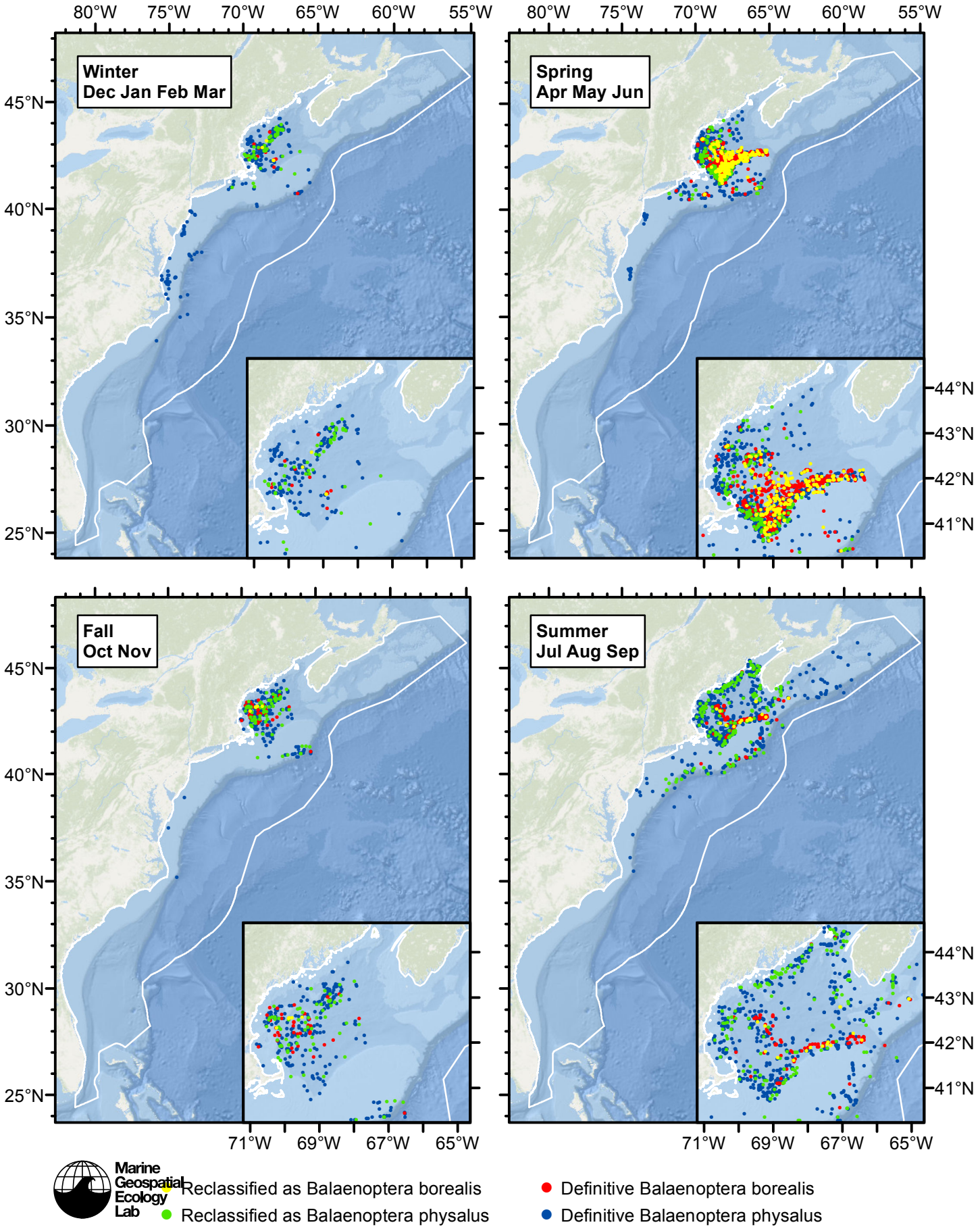

Figure 10: Definitive sightings used to train the model and ambiguous sightings reclassified by the model, by season.

Detection Functions

The detection hierarchy figures below show how sightings from multiple surveys were pooled to try to achieve Buckland et. al's (2001) recommendation that at least 60-80 sightings be used to fit a detection function. Leaf nodes, on the right, usually represent individual surveys, while the hierarchy to the left shows how they have been grouped according to how similar we believed the surveys were to each other in their detection performance.

At each node, the red or green number indicates the total number of sightings below that node in the hierarchy, and is colored green if 70 or more sightings were available, and red otherwise. If a grouping node has zero sightings–i.e. all of the surveys within it had zero sightings–it may be collapsed and shown as a leaf to save space.

Each histogram in the figure indicates a node where a detection function was fitted. The actual detection functions do not appear in this figure; they are presented in subsequent sections. The histogram shows the frequency of sightings by perpendicular sighting distance for all surveys contained by that node. Each survey (leaf node) recieves the detection function that is closest to it up the hierarchy. Thus, for common species, sufficient sightings may be available to fit detection functions deep in the hierarchy, with each function applying to only a few surveys, thereby allowing variability in detection performance between surveys to be addressed relatively finely. For rare species, so few sightings may be available that we have to pool many surveys together to try to meet Buckland's recommendation, and fit only a few coarse detection functions high in the hierarchy.

A blue Proxy Species tag indicates that so few sightings were available that, rather than ascend higher in the hierarchy to a point that we would pool grossly-incompatible surveys together, (e.g. shipboard surveys that used big-eye binoculars with those that used only naked eyes) we pooled sightings of similar species together instead. The list of species pooled is given in following sections.

Shipboard Surveys

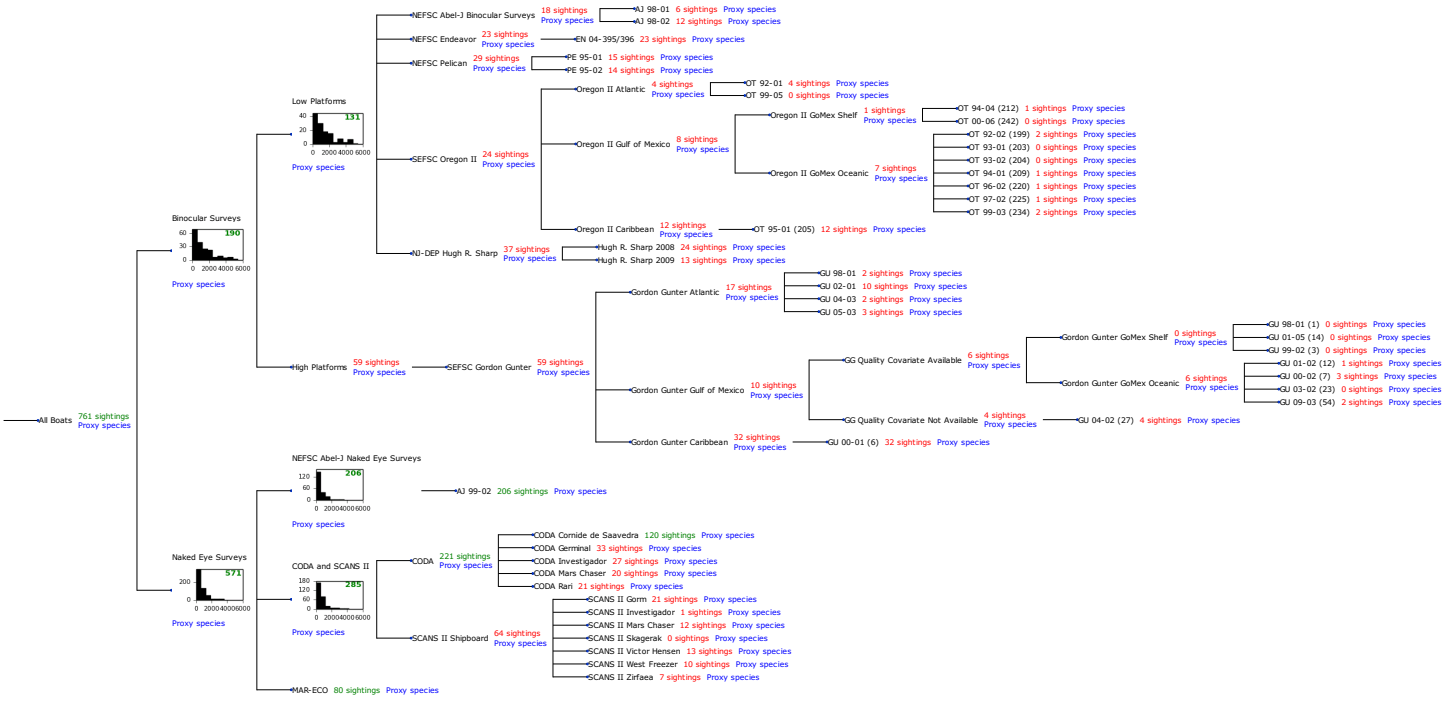

Figure 11: Detection hierarchy for shipboard surveys

Binocular Surveys

Because this taxon was sighted too infrequently to fit a detection function to its sightings alone, we fit a detection function to the pooled sightings of several other species that we believed would exhibit similar detectability. These "proxy species" are listed below.

Reported By Observer	Common Name	n
Balaenoptera	Balaenopterid sp.	8
Balaenoptera acutorostrata	Minke whale	4
Balaenoptera borealis	Sei whale	4
Balaenoptera borealis/edeni	Sei or Bryde's whale	6
Balaenoptera borealis/physalus	Fin or Sei whale	0
Balaenoptera edeni	Bryde's whale	21
Balaenoptera musculus	Blue whale	0
Balaenoptera physalus	Fin whale	98
Eubalaena glacialis	North Atlantic right whale	4
Eubalaena glacialis/Megaptera novaeangliae	Right or humpback whale	0
Megaptera novaeangliae	Humpback whale	46
Total		191

Table 5: Proxy species used to fit detection functions for Binocular Surveys. The number of sightings, n, is before truncation.

The sightings were right truncated at 5500m.

Covariate	Description
beaufort	Beaufort sea state.
size	Estimated size (number of individuals) of the sighted group.
vessel	Vessel from which the observation was made. This covariate allows the detection function to account for vessel-specific biases, such as the height of the survey platform.

Table 6: Covariates tested in candidate "multi-covariate distance sampling" (MCDS) detection functions.

Key	Adjustment	Order	Covariates	Succeeded	Δ AIC	Mean ESHW (m)
hr	poly	2		Yes	0.00	1309
hr	poly	4		Yes	0.47	1353
hr			size	Yes	0.78	1757
hr				Yes	0.80	1542
hn	cos	2		Yes	1.99	1802
hr			beaufort, size	Yes	2.64	1780
hr			beaufort	Yes	2.71	1553
hr			vessel, size	Yes	6.31	1920
hr			vessel	Yes	6.89	1605
hr			beaufort, vessel, size	Yes	8.03	1952

hr			beaufort, vessel	Yes	8.50	1675
hn	cos	3		Yes	9.91	1787
hn			size	Yes	11.86	2317
hn			beaufort, size	Yes	13.68	2319
hn			vessel, size	Yes	15.29	2299
hn			vessel	Yes	17.57	2301
hn				Yes	17.60	2311
hn			beaufort	Yes	19.19	2310
hn	herm	4		No		
hn			beaufort, vessel	No		
hn			beaufort, vessel, size	No		

Table 7: Candidate detection functions for Binocular Surveys. The first one listed was selected for the density model.

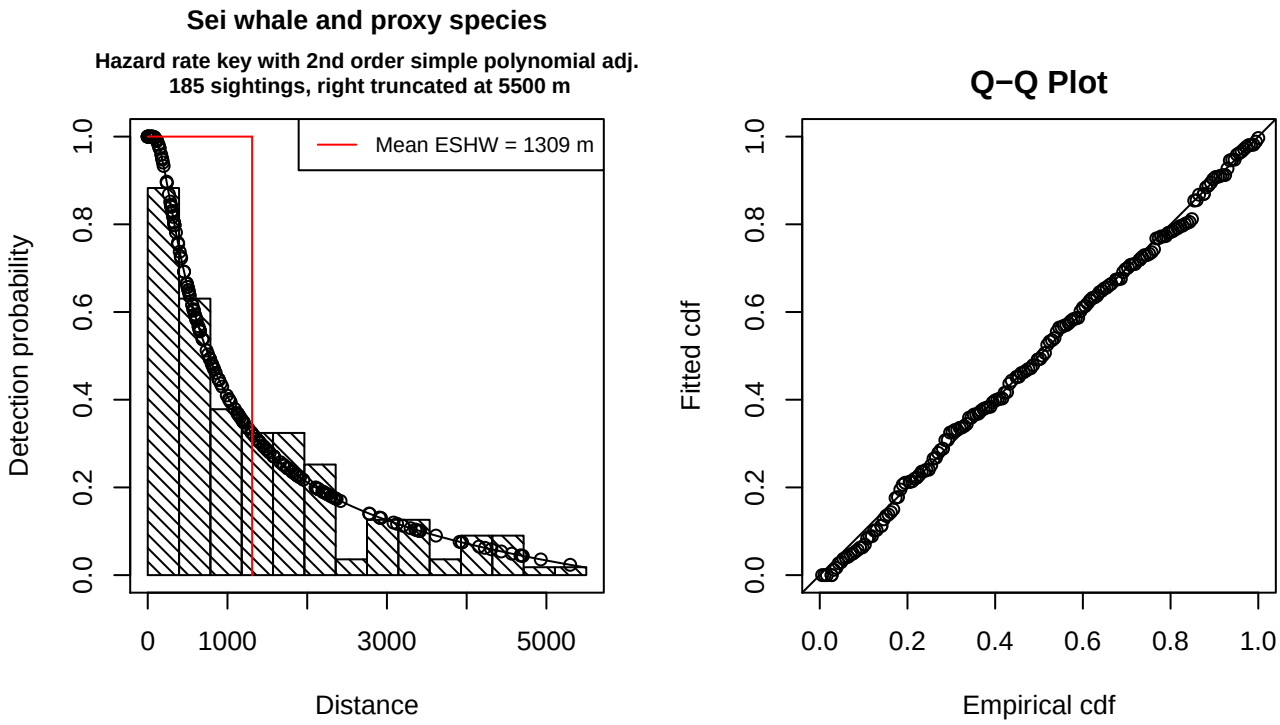

Figure 12: Detection function for Binocular Surveys that was selected for the density model

Statistical output for this detection function:

```
Summary for ds object
Number of observations :  185
Distance range         :  0  -  5500
AIC                    :  3029.944

Detection function:
 Hazard-rate key function with simple polynomial adjustment term of order 2
```

```
Detection function parameters
Scale Coefficients:
            estimate        se
(Intercept) 6.295212 0.4058184

Shape parameters:
                estimate        se
(Intercept) 1.091342e-06 0.2305983

Adjustment term parameter(s):
                estimate        se
poly, order 2 -0.8163334 0.2362959


Monotonicity constraints were enforced.
                       Estimate           SE        CV
Average p             0.2380581   0.04195346 0.1762320
N in covered region 777.1212078 145.75183566 0.1875535

Monotonicity constraints were enforced.
```

Additional diagnostic plots:

Figure 13: Scatterplots showing the relationship between Beaufort sea state and perpendicular sighting distance, for all sightings (left) and only those not right truncated (right). The line is a simple linear regression.

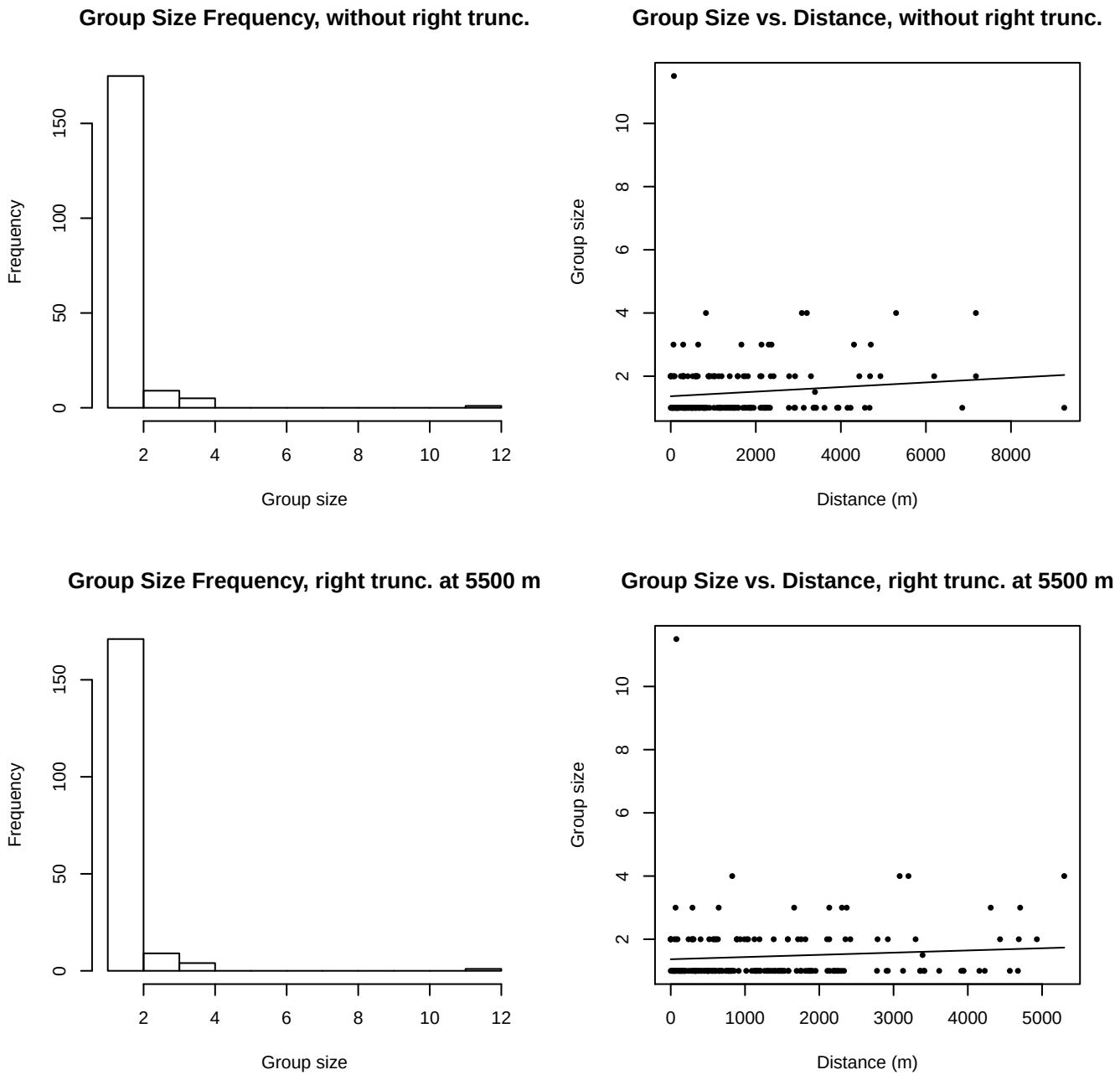

Figure 14: Histograms showing group size frequency and scatterplots showing the relationship between group size and perpendicular sighting distance, for all sightings (top row) and only those not right truncated (bottom row). In the scatterplot, the line is a simple linear regression.

Low Platforms

Because this taxon was sighted too infrequently to fit a detection function to its sightings alone, we fit a detection function to the pooled sightings of several other species that we believed would exhibit similar detectability. These "proxy species" are listed below.

Reported By Observer	Common Name	n
Balaenoptera	Balaenopterid sp.	1
Balaenoptera acutorostrata	Minke whale	3

Balaenoptera borealis	Sei whale	4
Balaenoptera borealis/edeni	Sei or Bryde's whale	5
Balaenoptera borealis/physalus	Fin or Sei whale	0
Balaenoptera edeni	Bryde's whale	7
Balaenoptera musculus	Blue whale	0
Balaenoptera physalus	Fin whale	86
Eubalaena glacialis	North Atlantic right whale	3
Eubalaena glacialis/Megaptera novaeangliae	Right or humpback whale	0
Megaptera novaeangliae	Humpback whale	23
Total		132

Table 8: Proxy species used to fit detection functions for Low Platforms. The number of sightings, n, is before truncation.

The sightings were right truncated at 5500m.

Covariate	Description
beaufort	Beaufort sea state.
size	Estimated size (number of individuals) of the sighted group.
vessel	Vessel from which the observation was made. This covariate allows the detection function to account for vessel-specific biases, such as the height of the survey platform.

Table 9: Covariates tested in candidate "multi-covariate distance sampling" (MCDS) detection functions.

Key	Adjustment	Order	Covariates	Succeeded	Δ AIC	Mean ESHW (m)
hr			size	Yes	0.00	1851
hn	cos	2		Yes	1.87	1764
hr				Yes	1.95	1652
hr			beaufort, size	Yes	1.99	1858
hr			vessel, size	Yes	2.55	2107
hr	poly	4		Yes	3.84	1634
hr	poly	2		Yes	3.89	1635
hr			beaufort, vessel, size	Yes	4.48	2116
hr			vessel	Yes	5.62	1830
hn			size	Yes	6.79	2311
hr			beaufort, vessel	Yes	7.51	1860
hn			vessel, size	Yes	8.30	2288
hn			beaufort, size	Yes	8.64	2312
hn	cos	3		Yes	11.49	1819

hn			vessel	Yes	13.80	2330
hn				Yes	15.66	2345
hn			beaufort	Yes	17.02	2343
hn	herm	4		No		
hr			beaufort	No		
hn			beaufort, vessel	No		
hn			beaufort, vessel, size	No		

Table 10: Candidate detection functions for Low Platforms. The first one listed was selected for the density model.

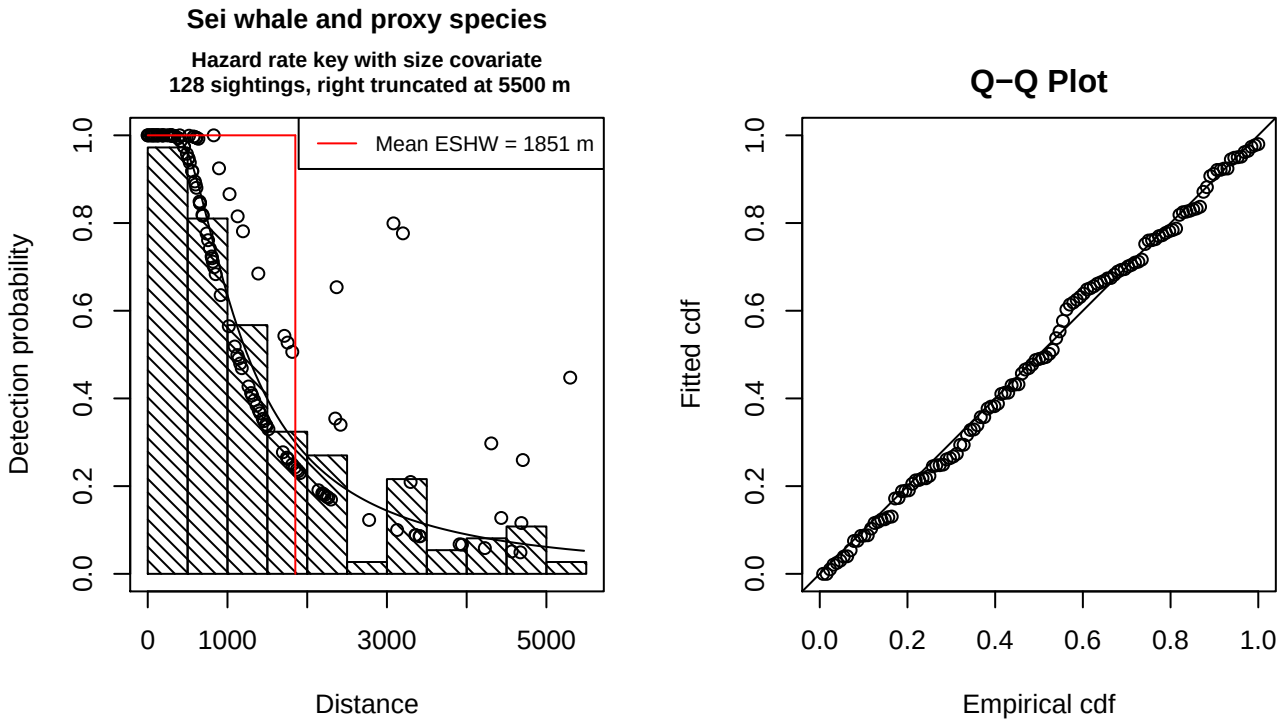

Figure 15: Detection function for Low Platforms that was selected for the density model

Statistical output for this detection function:

```
Summary for ds object
Number of observations :  128
Distance range         :  0  -  5500
AIC                    :  2096.769

Detection function:
 Hazard-rate key function

Detection function parameters
Scale Coefficients:
             estimate        se
(Intercept) 6.3348086 0.3715707
size        0.4890754 0.2062362
```

```
Shape parameters:
             estimate        se
(Intercept) 0.6087008 0.1772532

                       Estimate          SE        CV
Average p             0.3142815  0.03980905 0.1266668
N in covered region 407.2782102 59.82362021 0.1468864
```

Additional diagnostic plots:

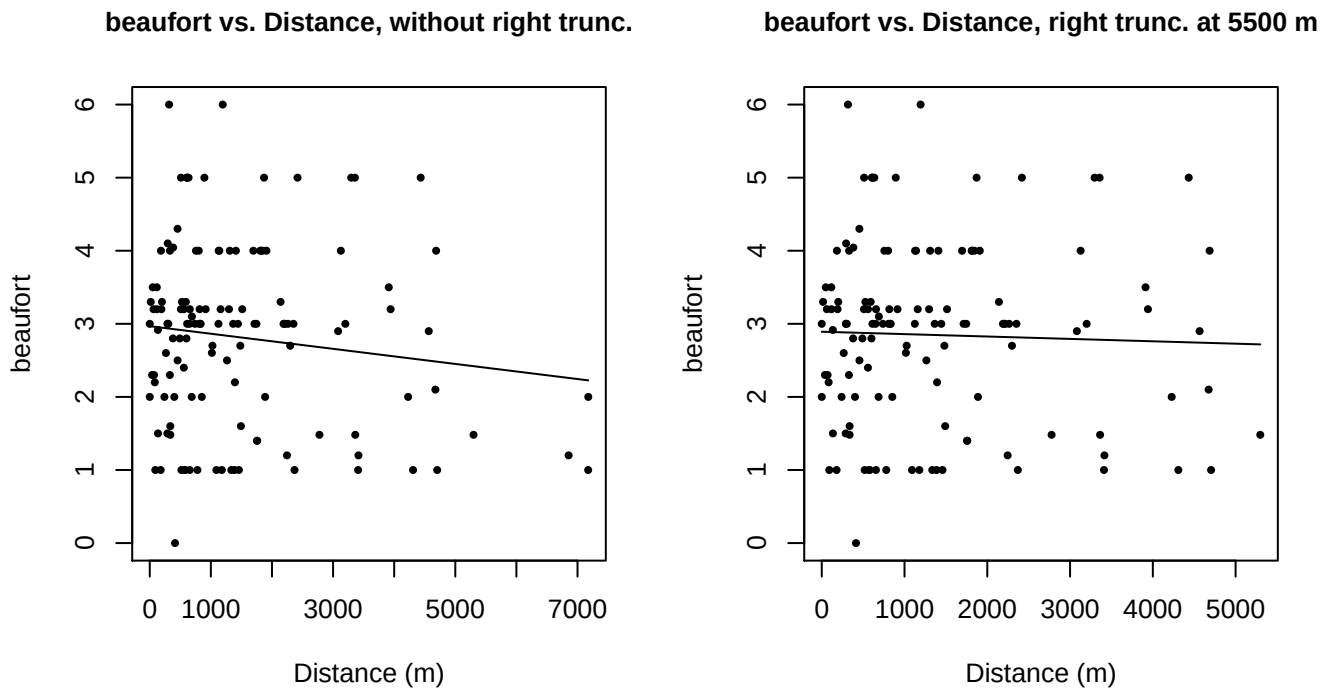

Figure 16: Scatterplots showing the relationship between Beaufort sea state and perpendicular sighting distance, for all sightings (left) and only those not right truncated (right). The line is a simple linear regression.

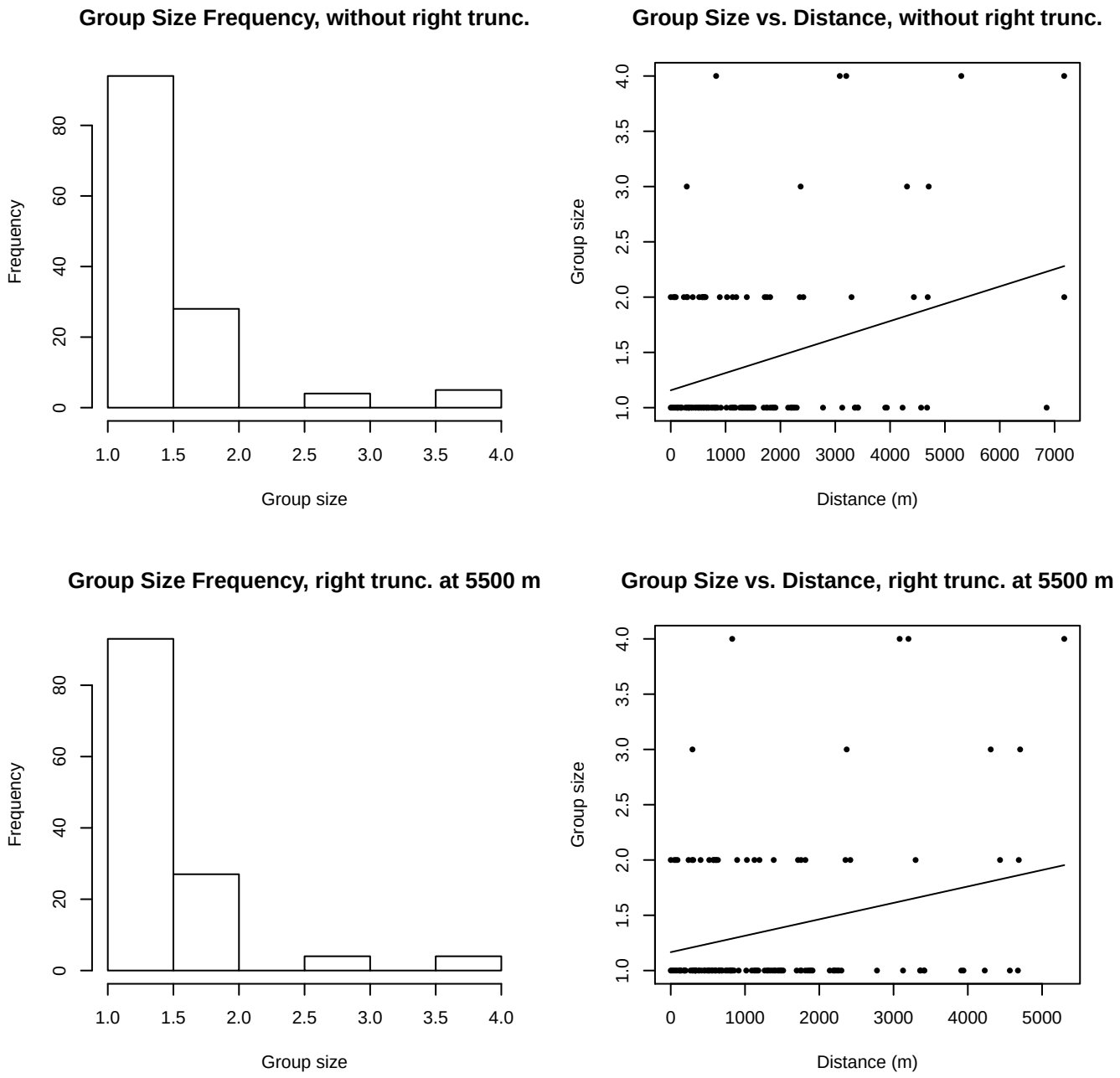

Figure 17: Histograms showing group size frequency and scatterplots showing the relationship between group size and perpendicular sighting distance, for all sightings (top row) and only those not right truncated (bottom row). In the scatterplot, the line is a simple linear regression.

Naked Eye Surveys

Because this taxon was sighted too infrequently to fit a detection function to its sightings alone, we fit a detection function to the pooled sightings of several other species that we believed would exhibit similar detectability. These "proxy species" are listed below.

Reported By Observer	Common Name	n
Balaenoptera	Balaenopterid sp.	7
Balaenoptera acutorostrata	Minke whale	177

Balaenoptera borealis	Sei whale	68
Balaenoptera borealis/edeni	Sei or Bryde's whale	0
Balaenoptera borealis/physalus	Fin or Sei whale	4
Balaenoptera edeni	Bryde's whale	1
Balaenoptera musculus	Blue whale	5
Balaenoptera physalus	Fin whale	261
Eubalaena glacialis	North Atlantic right whale	10
Eubalaena glacialis/Megaptera novaeangliae	Right or humpback whale	0
Megaptera novaeangliae	Humpback whale	38
Total		571

Table 11: Proxy species used to fit detection functions for Naked Eye Surveys. The number of sightings, n, is before truncation.

The sightings were right truncated at 2500m.

Covariate	Description
beaufort	Beaufort sea state.
size	Estimated size (number of individuals) of the sighted group.

Table 12: Covariates tested in candidate "multi-covariate distance sampling" (MCDS) detection functions.

Key	Adjustment	Order	Covariates	Succeeded	Δ AIC	Mean ESHW (m)
hn	cos	2		Yes	0.00	788
hr			size	Yes	0.23	881
hr	poly	2		Yes	4.00	802
hr	poly	4		Yes	4.09	816
hr				Yes	5.53	844
hn	cos	3		Yes	12.95	774
hn			size	Yes	17.09	953
hn			beaufort, size	Yes	19.06	953
hn				Yes	28.40	951
hn			beaufort	Yes	30.12	951
hn	herm	4		No		
hr			beaufort	No		
hr			beaufort, size	No		

Table 13: Candidate detection functions for Naked Eye Surveys. The first one listed was selected for the density model.

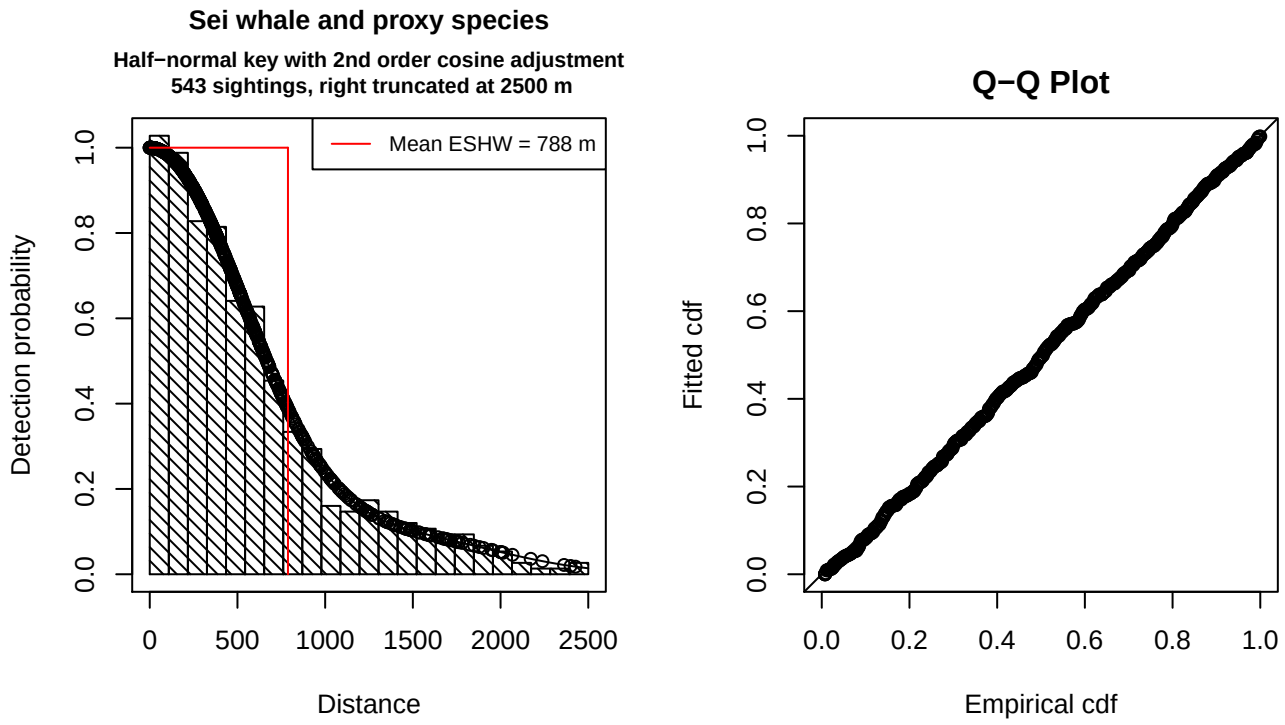

Figure 18: Detection function for Naked Eye Surveys that was selected for the density model

Statistical output for this detection function:

```
Summary for ds object
Number of observations :  543
Distance range         :  0  -  2500
AIC                    :  7957.87

Detection function:
 Half-normal key function with cosine adjustment term of order 2

Detection function parameters
Scale Coefficients:
            estimate         se
(Intercept) 6.752179 0.03907979

Adjustment term parameter(s):
             estimate         se
cos, order 2 0.410434 0.07032503


Monotonicity constraints were enforced.
                        Estimate          SE         CV
Average p              0.3152005  0.01193713 0.03787156
N in covered region 1722.7129496 89.43843095 0.05191720

Monotonicity constraints were enforced.
```

Additional diagnostic plots:

Figure 19: Scatterplots showing the relationship between Beaufort sea state and perpendicular sighting distance, for all sightings (left) and only those not right truncated (right). The line is a simple linear regression.

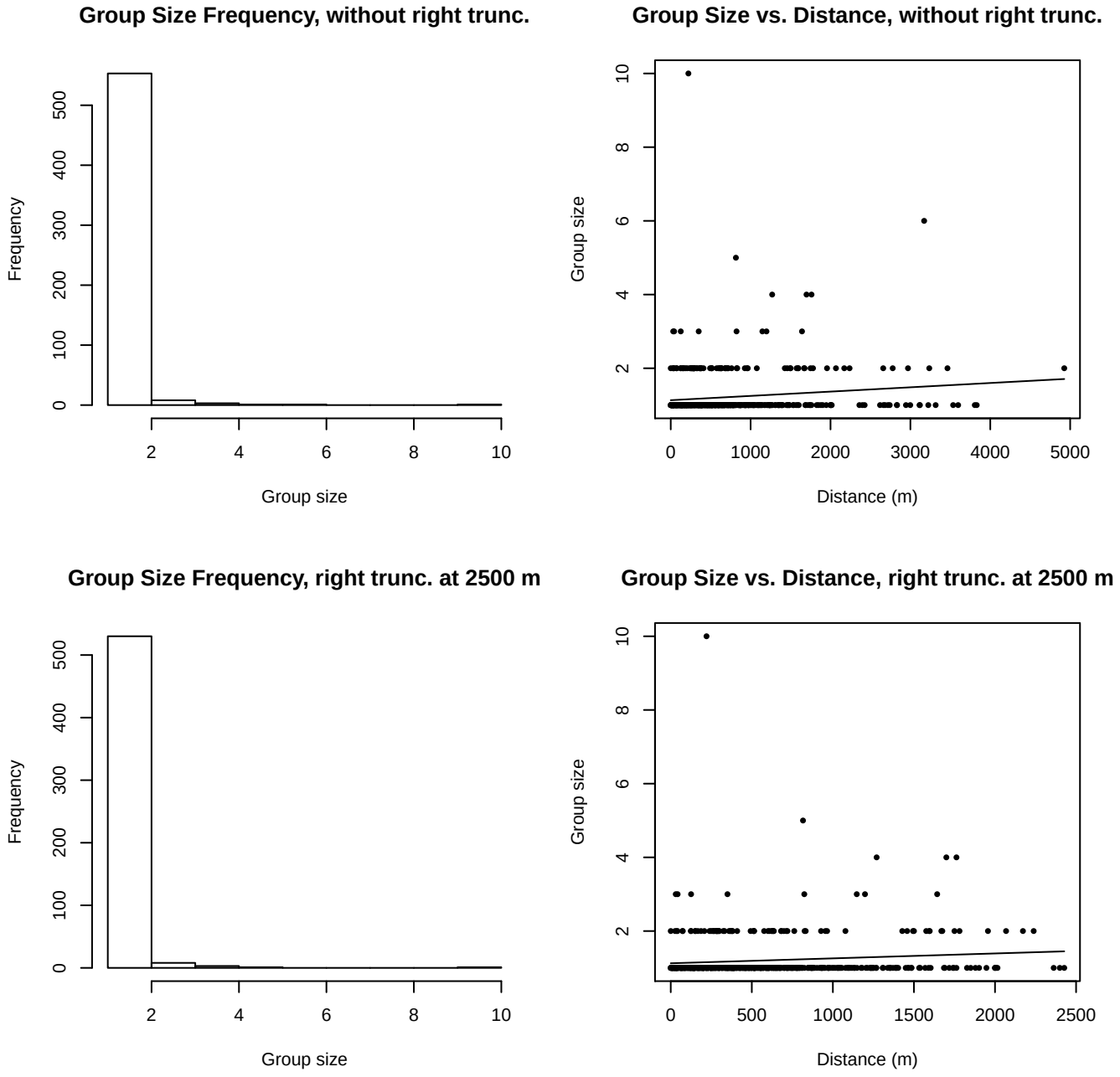

Figure 20: Histograms showing group size frequency and scatterplots showing the relationship between group size and perpendicular sighting distance, for all sightings (top row) and only those not right truncated (bottom row). In the scatterplot, the line is a simple linear regression.

NEFSC Abel-J Naked Eye Surveys

Because this taxon was sighted too infrequently to fit a detection function to its sightings alone, we fit a detection function to the pooled sightings of several other species that we believed would exhibit similar detectability. These "proxy species" are listed below.

Reported By Observer	Common Name	n
Balaenoptera	Balaenopterid sp.	0
Balaenoptera acutorostrata	Minke whale	100

Balaenoptera borealis	Sei whale	2
Balaenoptera borealis/edeni	Sei or Bryde's whale	0
Balaenoptera borealis/physalus	Fin or Sei whale	0
Balaenoptera edeni	Bryde's whale	0
Balaenoptera musculus	Blue whale	0
Balaenoptera physalus	Fin whale	57
Eubalaena glacialis	North Atlantic right whale	10
Eubalaena glacialis/Megaptera novaeangliae	Right or humpback whale	0
Megaptera novaeangliae	Humpback whale	37
Total		206

Table 14: Proxy species used to fit detection functions for NEFSC Abel-J Naked Eye Surveys. The number of sightings, n, is before truncation.

The sightings were right truncated at 2500m.

Covariate	Description
beaufort	Beaufort sea state.
quality	Survey-specific index of the quality of observation conditions, utilizing relevant factors other than Beaufort sea state (see methods).
size	Estimated size (number of individuals) of the sighted group.

Table 15: Covariates tested in candidate "multi-covariate distance sampling" (MCDS) detection functions.

Key	Adjustment	Order	Covariates	Succeeded	Δ AIC	Mean ESHW (m)
hn	cos	2		Yes	0.00	714
hr			size	Yes	0.04	799
hr				Yes	0.63	760
hr	poly	4		Yes	0.75	741
hr	poly	2		Yes	1.11	728
hn	cos	3		Yes	2.84	669
hn			size	Yes	5.20	855
hn			quality, size	Yes	6.85	854
hn				Yes	10.43	845
hn			quality	Yes	12.24	845
hn	herm	4		No		
hn			beaufort	No		
hr			beaufort	No		
hr			quality	No		
hn			beaufort, quality	No		

hr	beaufort, quality	No
hn	beaufort, size	No
hr	beaufort, size	No
hr	quality, size	No
hn	beaufort, quality, size	No
hr	beaufort, quality, size	No

Table 16: Candidate detection functions for NEFSC Abel-J Naked Eye Surveys. The first one listed was selected for the density model.

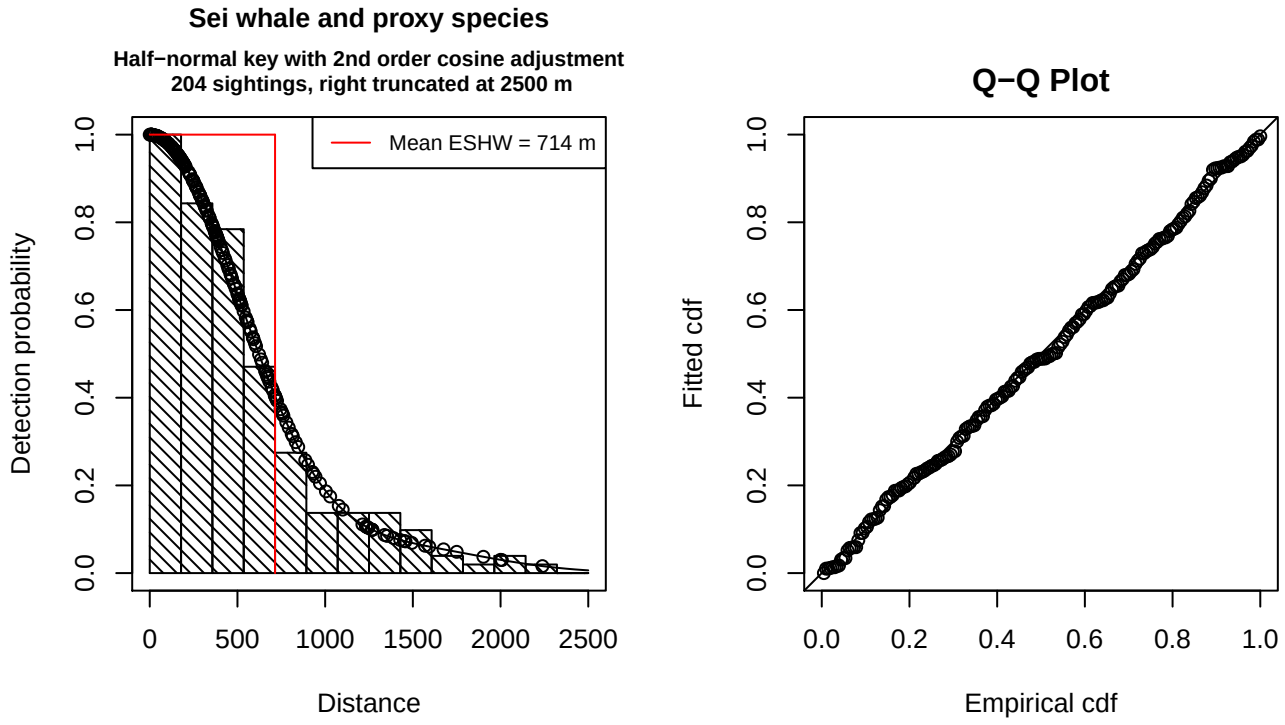

Figure 21: Detection function for NEFSC Abel-J Naked Eye Surveys that was selected for the density model

Statistical output for this detection function:

```
Summary for ds object
Number of observations :  204
Distance range         :  0  -  2500
AIC                    :  2944.665

Detection function:
 Half-normal key function with cosine adjustment term of order 2

Detection function parameters
Scale Coefficients:
            estimate         se
(Intercept) 6.665111 0.06962658

Adjustment term parameter(s):
```

```
              estimate        se
cos, order 2 0.4654073 0.1236342


Monotonicity constraints were enforced.
                        Estimate          SE         CV
Average p             0.2857526  0.01551915 0.05430975
N in covered region 713.9042245 57.33838382 0.08031663

Monotonicity constraints were enforced.
```

Additional diagnostic plots:

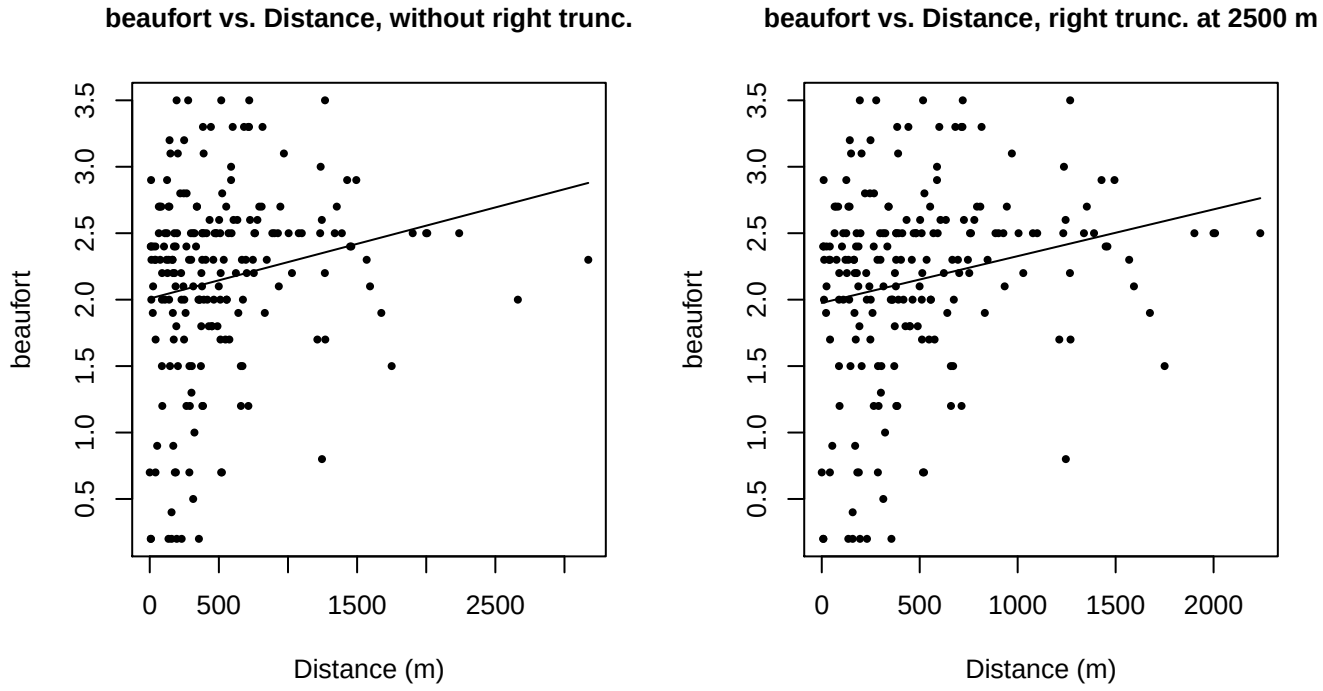

Figure 22: Scatterplots showing the relationship between Beaufort sea state and perpendicular sighting distance, for all sightings (left) and only those not right truncated (right). The line is a simple linear regression.

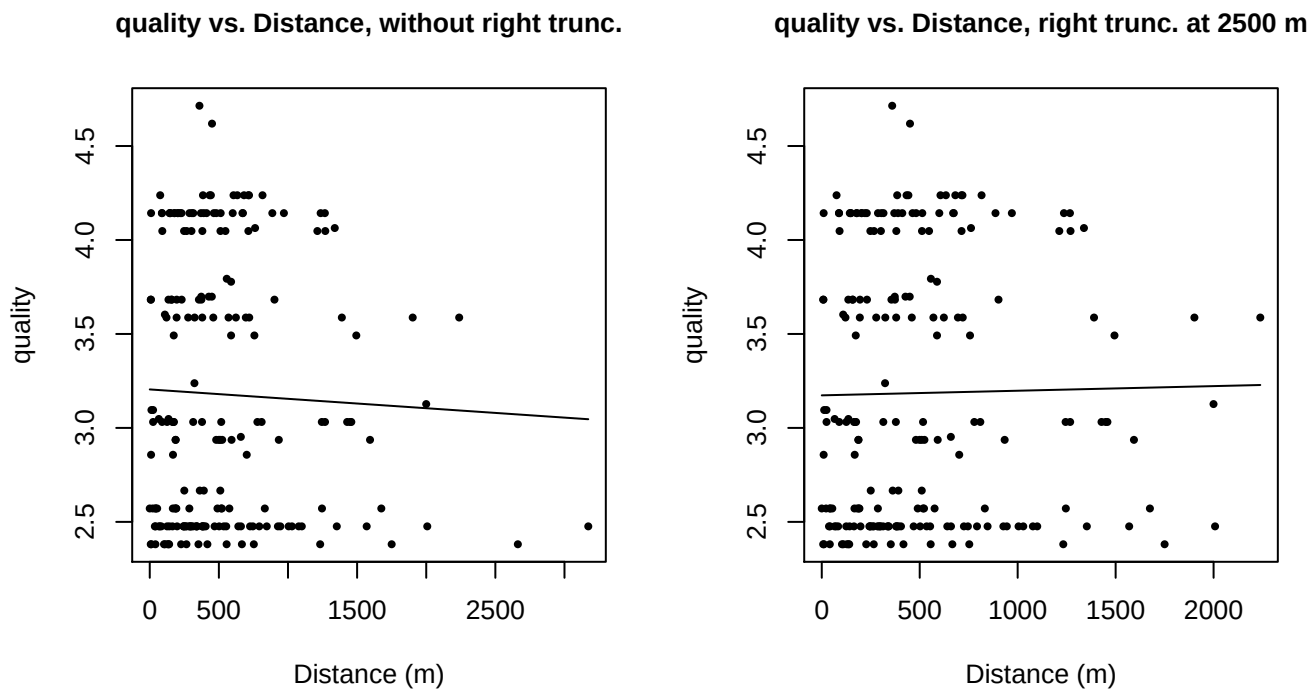

Figure 23: Scatterplots showing the relationship between the survey-specific index of the quality of observation conditions and perpendicular sighting distance, for all sightings (left) and only those not right truncated (right). Low values of the quality index correspond to better observation conditions. The line is a simple linear regression.

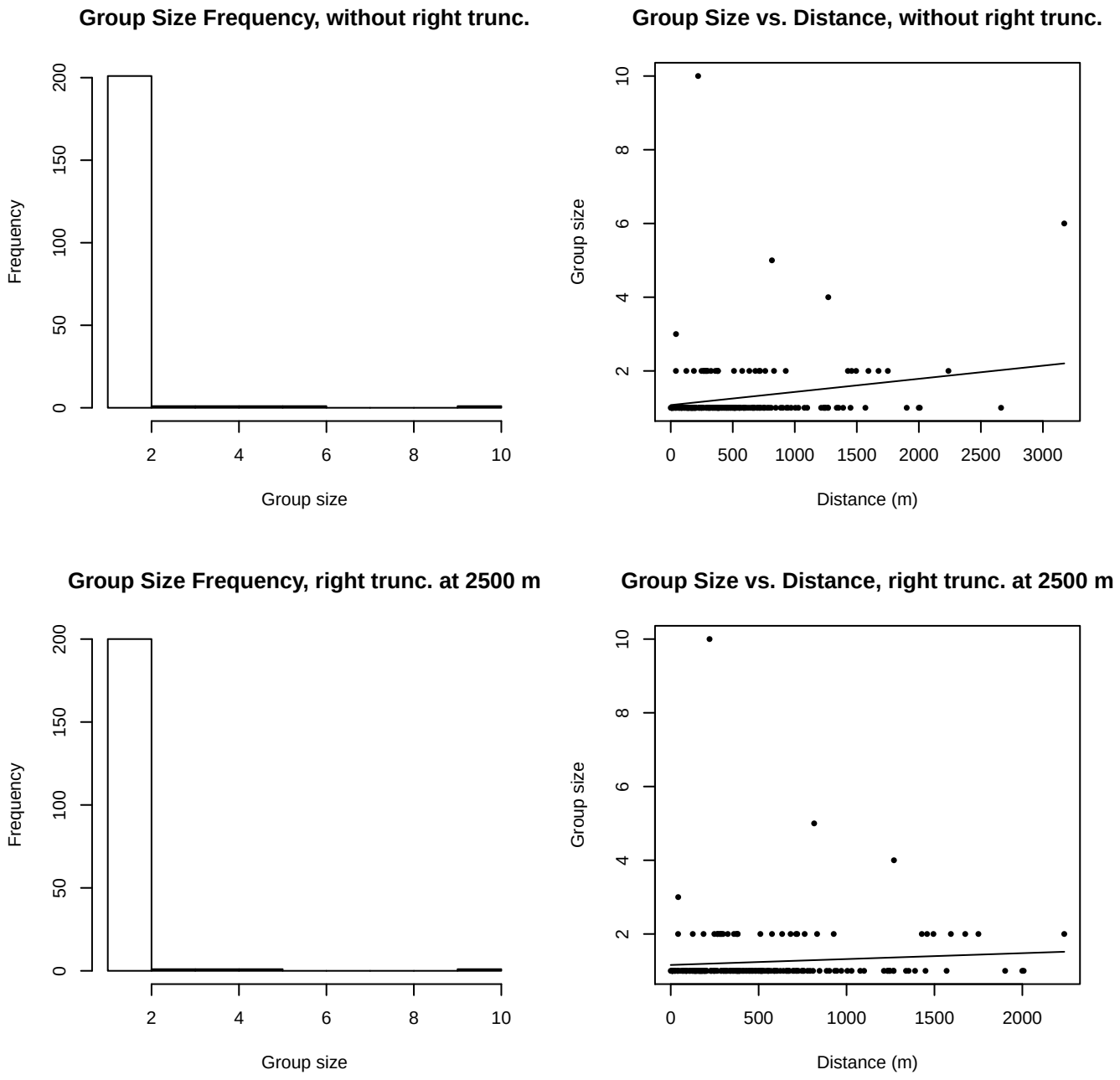

Figure 24: Histograms showing group size frequency and scatterplots showing the relationship between group size and perpendicular sighting distance, for all sightings (top row) and only those not right truncated (bottom row). In the scatterplot, the line is a simple linear regression.

CODA and SCANS II

Because this taxon was sighted too infrequently to fit a detection function to its sightings alone, we fit a detection function to the pooled sightings of several other species that we believed would exhibit similar detectability. These "proxy species" are listed below.

Reported By Observer	Common Name	n
Balaenoptera	Balaenopterid sp.	0
Balaenoptera acutorostrata	Minke whale	76

Balaenoptera borealis	Sei whale	12
Balaenoptera borealis/edeni	Sei or Bryde's whale	0
Balaenoptera borealis/physalus	Fin or Sei whale	4
Balaenoptera edeni	Bryde's whale	0
Balaenoptera musculus	Blue whale	1
Balaenoptera physalus	Fin whale	192
Eubalaena glacialis	North Atlantic right whale	0
Eubalaena glacialis/Megaptera novaeangliae	Right or humpback whale	0
Megaptera novaeangliae	Humpback whale	0
Total		285

Table 17: Proxy species used to fit detection functions for CODA and SCANS II. The number of sightings, n, is before truncation.

The sightings were right truncated at 2500m.

Covariate	Description
beaufort	Beaufort sea state.
quality	Survey-specific index of the quality of observation conditions, utilizing relevant factors other than Beaufort sea state (see methods).
size	Estimated size (number of individuals) of the sighted group.

Table 18: Covariates tested in candidate "multi-covariate distance sampling" (MCDS) detection functions.

Key	Adjustment	Order	Covariates	Succeeded	Δ AIC	Mean ESHW (m)
hn	cos	2		Yes	0.00	796
hn			size	Yes	3.86	900
hn				Yes	4.25	901
hn	cos	3		Yes	4.27	815
hr	poly	2		Yes	4.81	836
hr				Yes	5.06	929
hr	poly	4		Yes	5.80	872
hr			size	Yes	7.05	931
hn	herm	4		No		
hn			beaufort	No		
hr			beaufort	No		
hn			quality	No		
hr			quality	No		
hn			beaufort, quality	No		
hr			beaufort, quality	No		

hn	beaufort, size	No
hr	beaufort, size	No
hn	quality, size	No
hr	quality, size	No
hn	beaufort, quality, size	No
hr	beaufort, quality, size	No

Table 19: Candidate detection functions for CODA and SCANS II. The first one listed was selected for the density model.

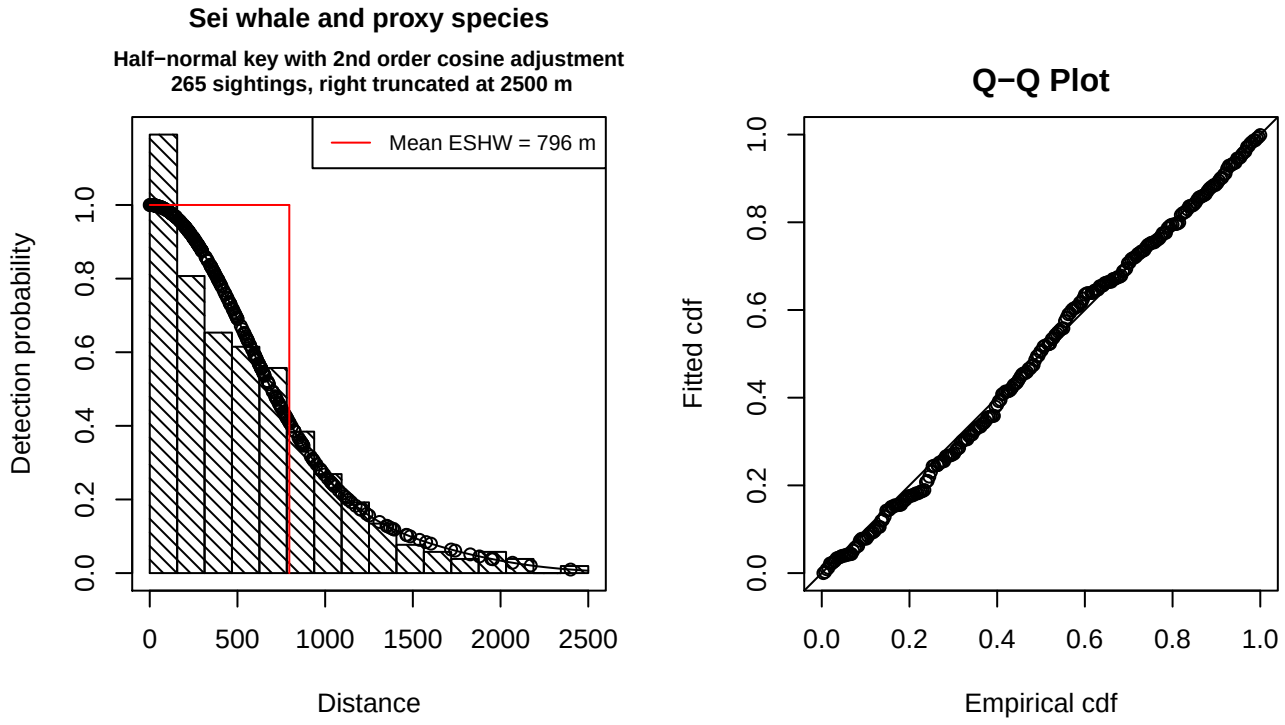

Figure 25: Detection function for CODA and SCANS II that was selected for the density model

Statistical output for this detection function:

```
Summary for ds object
Number of observations :  265
Distance range         :  0  -  2500
AIC                    :  3866.705

Detection function:
 Half-normal key function with cosine adjustment term of order 2

Detection function parameters
Scale Coefficients:
            estimate         se
(Intercept) 6.669743 0.05443104

Adjustment term parameter(s):
```

```
              estimate        se
cos, order 2 0.2900288 0.1074259


Monotonicity constraints were enforced.
                        Estimate          SE         CV
Average p              0.3182232  0.01860504 0.05846537
N in covered region 832.7488120 64.45573830 0.07740118

Monotonicity constraints were enforced.
```

Additional diagnostic plots:

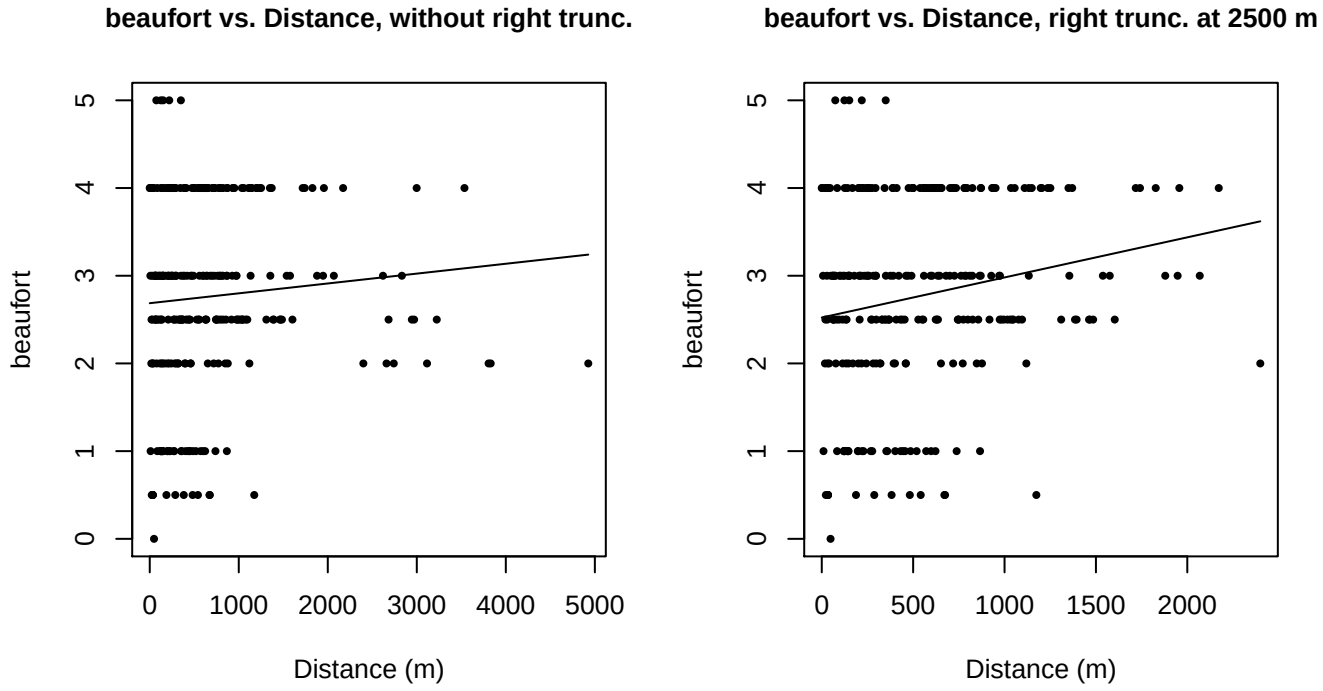

Figure 26: Scatterplots showing the relationship between Beaufort sea state and perpendicular sighting distance, for all sightings (left) and only those not right truncated (right). The line is a simple linear regression.

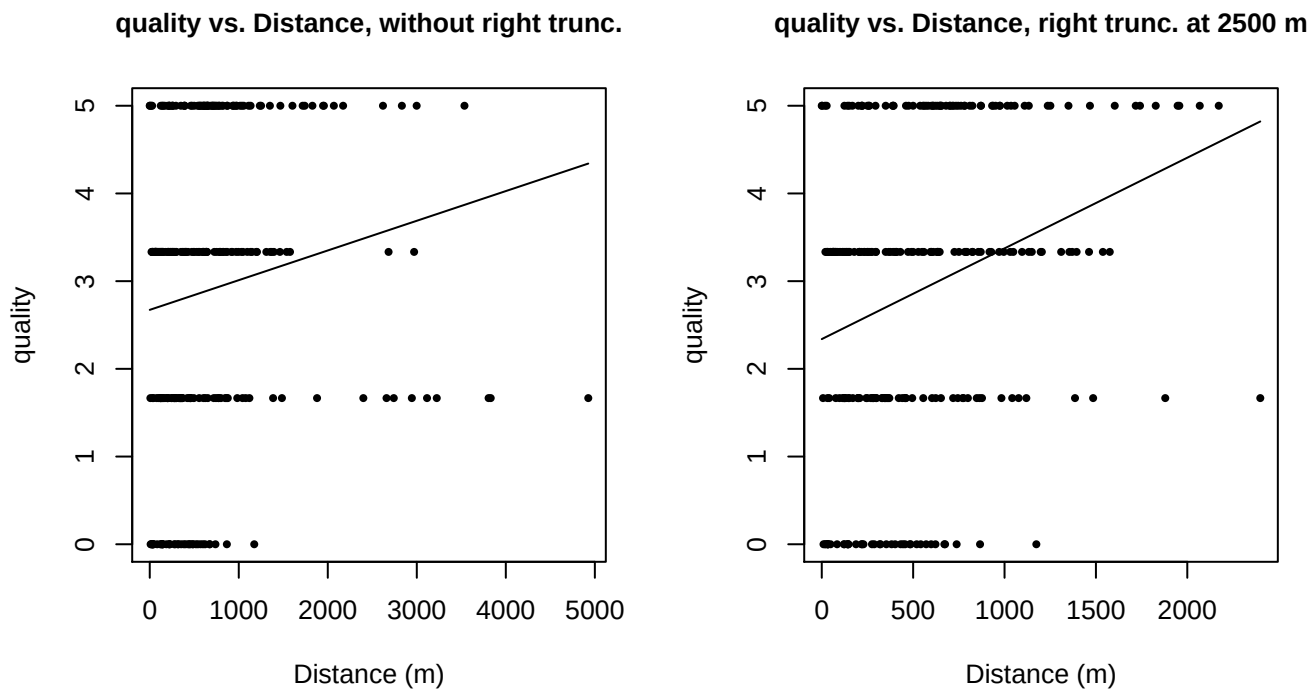

Figure 27: Scatterplots showing the relationship between the survey-specific index of the quality of observation conditions and perpendicular sighting distance, for all sightings (left) and only those not right truncated (right). Low values of the quality index correspond to better observation conditions. The line is a simple linear regression.

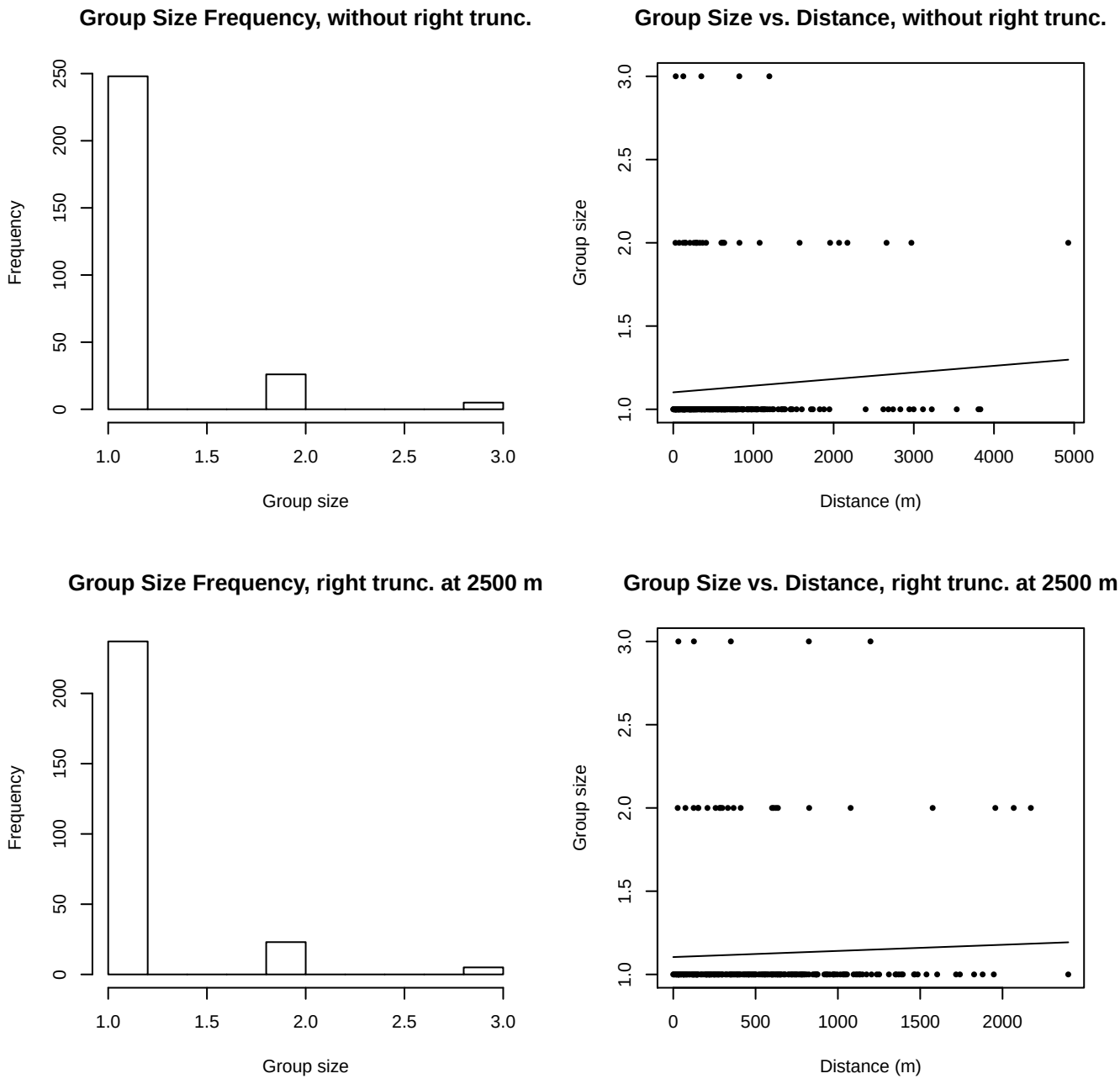

Figure 28: Histograms showing group size frequency and scatterplots showing the relationship between group size and perpendicular sighting distance, for all sightings (top row) and only those not right truncated (bottom row). In the scatterplot, the line is a simple linear regression.

Aerial Surveys

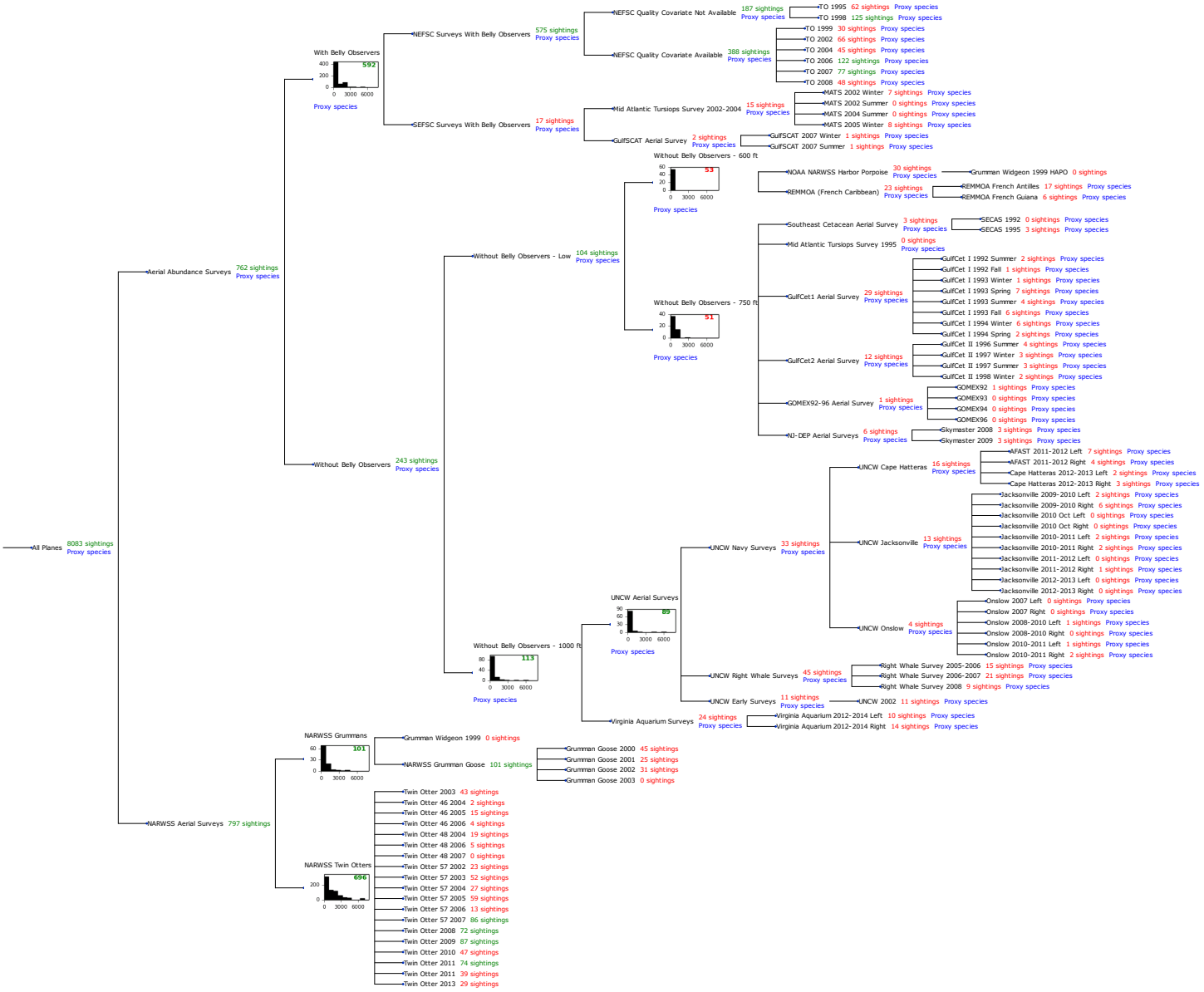

Figure 29: Detection hierarchy for aerial surveys

With Belly Observers

Because this taxon was sighted too infrequently to fit a detection function to its sightings alone, we fit a detection function to the pooled sightings of several other species that we believed would exhibit similar detectability. These "proxy species" are listed below.

Reported By Observer	Common Name	n
Balaenoptera	Balaenopterid sp.	2
Balaenoptera acutorostrata	Minke whale	97
Balaenoptera borealis	Sei whale	14
Balaenoptera borealis/edeni	Sei or Bryde's whale	0
Balaenoptera borealis/physalus	Fin or Sei whale	0

Balaenoptera edeni	Bryde's whale	2
Balaenoptera musculus	Blue whale	1
Balaenoptera physalus	Fin whale	235
Eubalaena glacialis	North Atlantic right whale	43
Eubalaena glacialis/Megaptera novaeangliae	Right or humpback whale	0
Megaptera novaeangliae	Humpback whale	198
Total		592

Table 20: Proxy species used to fit detection functions for With Belly Observers. The number of sightings, n, is before truncation.

The sightings were right truncated at 2000m.

Covariate	Description
beaufort	Beaufort sea state.
size	Estimated size (number of individuals) of the sighted group.

Table 21: Covariates tested in candidate "multi-covariate distance sampling" (MCDS) detection functions.

Key	Adjustment	Order	Covariates	Succeeded	Δ AIC	Mean ESHW (m)
hn	cos	2		Yes	0.00	594
hr	poly	2		Yes	1.71	598
hr	poly	4		Yes	1.86	609
hr			size	Yes	6.10	632
hr				Yes	7.37	627
hn	cos	3		Yes	11.15	585
hn			size	Yes	22.91	705
hn				Yes	23.39	703
hn	herm	4		No		
hn			beaufort	No		
hr			beaufort	No		
hn			beaufort, size	No		
hr			beaufort, size	No		

Table 22: Candidate detection functions for With Belly Observers. The first one listed was selected for the density model.

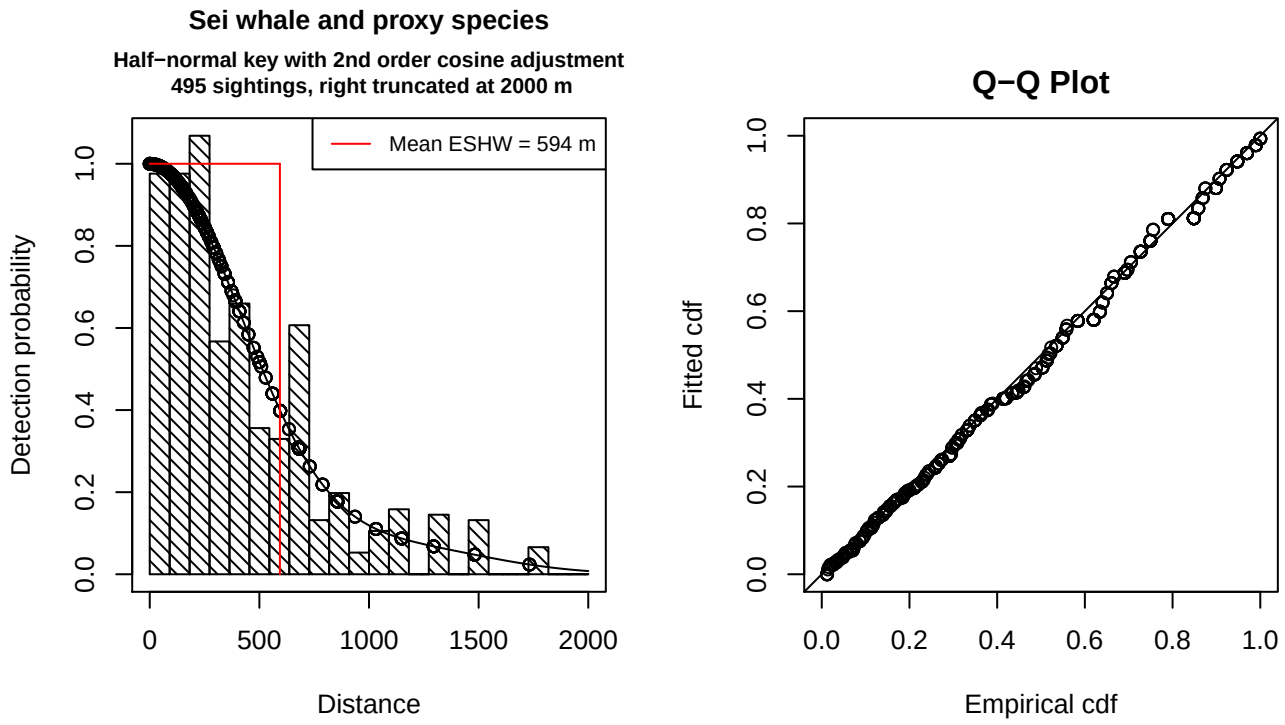

Figure 30: Detection function for With Belly Observers that was selected for the density model

Statistical output for this detection function:

```
Summary for ds object
Number of observations :  495
Distance range         :  0  -  2000
AIC                    :  6960.823

Detection function:
 Half-normal key function with cosine adjustment term of order 2

Detection function parameters
Scale Coefficients:
            estimate         se
(Intercept) 6.464817 0.04316341

Adjustment term parameter(s):
              estimate         se
cos, order 2 0.4286649 0.07975251


Monotonicity constraints were enforced.
                        Estimate          SE         CV
Average p              0.2967565  0.01131844 0.03814049
N in covered region 1668.0341879 89.44444950 0.05362267

Monotonicity constraints were enforced.
```

Additional diagnostic plots:

Figure 31: Scatterplots showing the relationship between Beaufort sea state and perpendicular sighting distance, for all sightings (left) and only those not right truncated (right). The line is a simple linear regression.

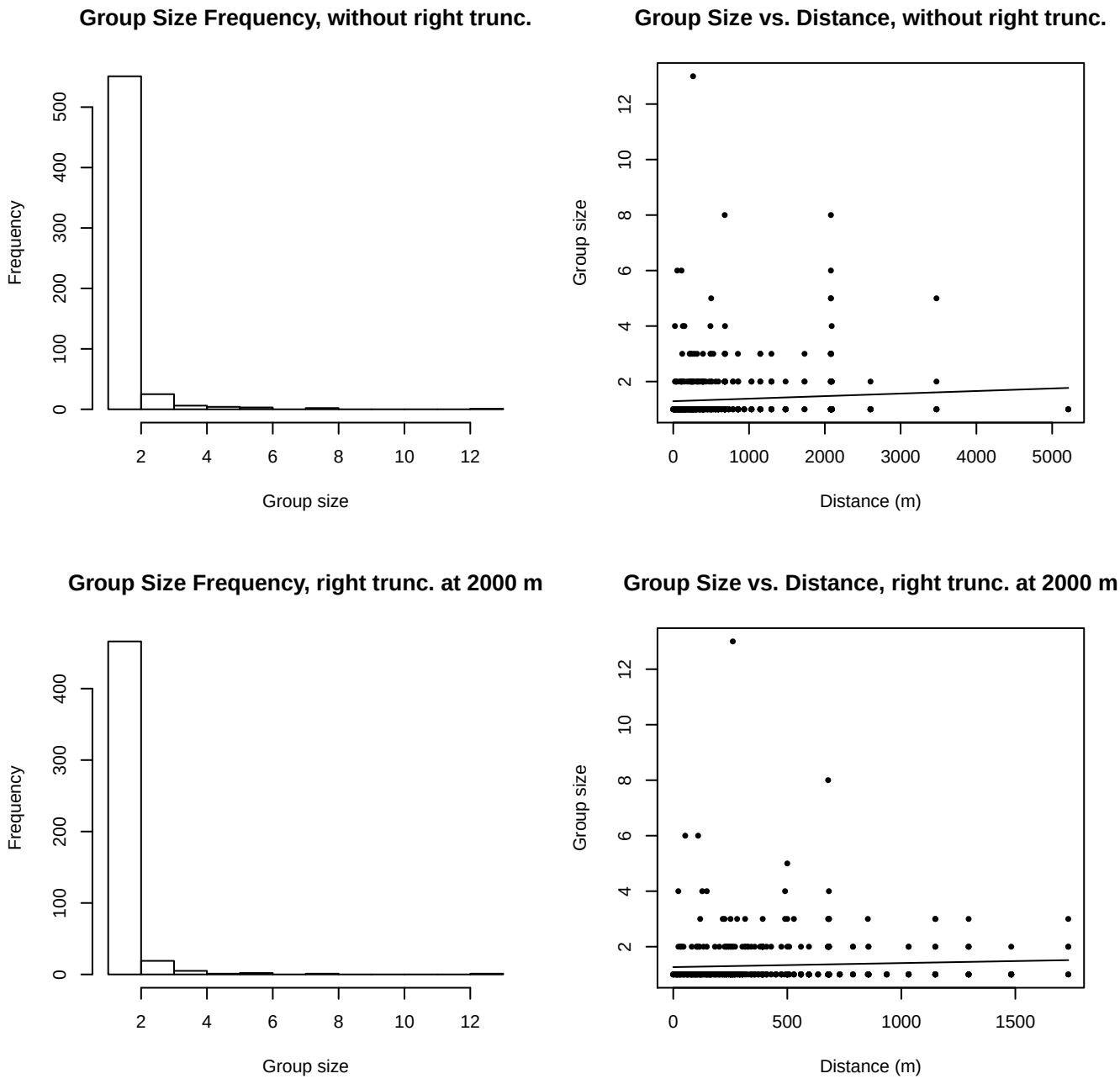

Figure 32: Histograms showing group size frequency and scatterplots showing the relationship between group size and perpendicular sighting distance, for all sightings (top row) and only those not right truncated (bottom row). In the scatterplot, the line is a simple linear regression.

Without Belly Observers - 600 ft

Because this taxon was sighted too infrequently to fit a detection function to its sightings alone, we fit a detection function to the pooled sightings of several other species that we believed would exhibit similar detectability. These "proxy species" are listed below.

Reported By Observer	Common Name	n
Balaenoptera	Balaenopterid sp.	2
Balaenoptera acutorostrata	Minke whale	8

Balaenoptera borealis	Sei whale	0
Balaenoptera borealis/edeni	Sei or Bryde's whale	0
Balaenoptera borealis/physalus	Fin or Sei whale	0
Balaenoptera edeni	Bryde's whale	0
Balaenoptera musculus	Blue whale	0
Balaenoptera physalus	Fin whale	15
Eubalaena glacialis	North Atlantic right whale	2
Eubalaena glacialis/Megaptera novaeangliae	Right or humpback whale	0
Megaptera novaeangliae	Humpback whale	16
Physeter macrocephalus	Sperm whale	10
Total		53

Table 23: Proxy species used to fit detection functions for Without Belly Observers - 600 ft. The number of sightings, n, is before truncation.

The sightings were right truncated at 600m. Due to a reduced frequency of sightings close to the trackline that plausibly resulted from the behavior of the observers and/or the configuration of the survey platform, the sightings were left truncted as well. Sightings closer than 32 m to the trackline were omitted from the analysis, and it was assumed that the the area closer to the trackline than this was not surveyed. This distance was estimated by inspecting histograms of perpendicular sighting distances.

Covariate	Description
beaufort	Beaufort sea state.
size	Estimated size (number of individuals) of the sighted group.

Table 24: Covariates tested in candidate "multi-covariate distance sampling" (MCDS) detection functions.

Key	Adjustment	Order	Covariates	Succeeded	Δ AIC	Mean ESHW (m)
hn				Yes	0.00	293
hr				Yes	1.14	318
hn			beaufort	Yes	1.57	293
hn	cos	3		Yes	1.65	311
hn	herm	4		Yes	1.93	291
hr			beaufort	Yes	1.97	326
hn	cos	2		Yes	1.97	283
hr	poly	2		Yes	3.14	318
hr	poly	4		Yes	3.14	318
hn			size	No		
hr			size	No		
hn			beaufort, size	No		
hr			beaufort, size	No		

Table 25: Candidate detection functions for Without Belly Observers - 600 ft. The first one listed was selected for the density model.

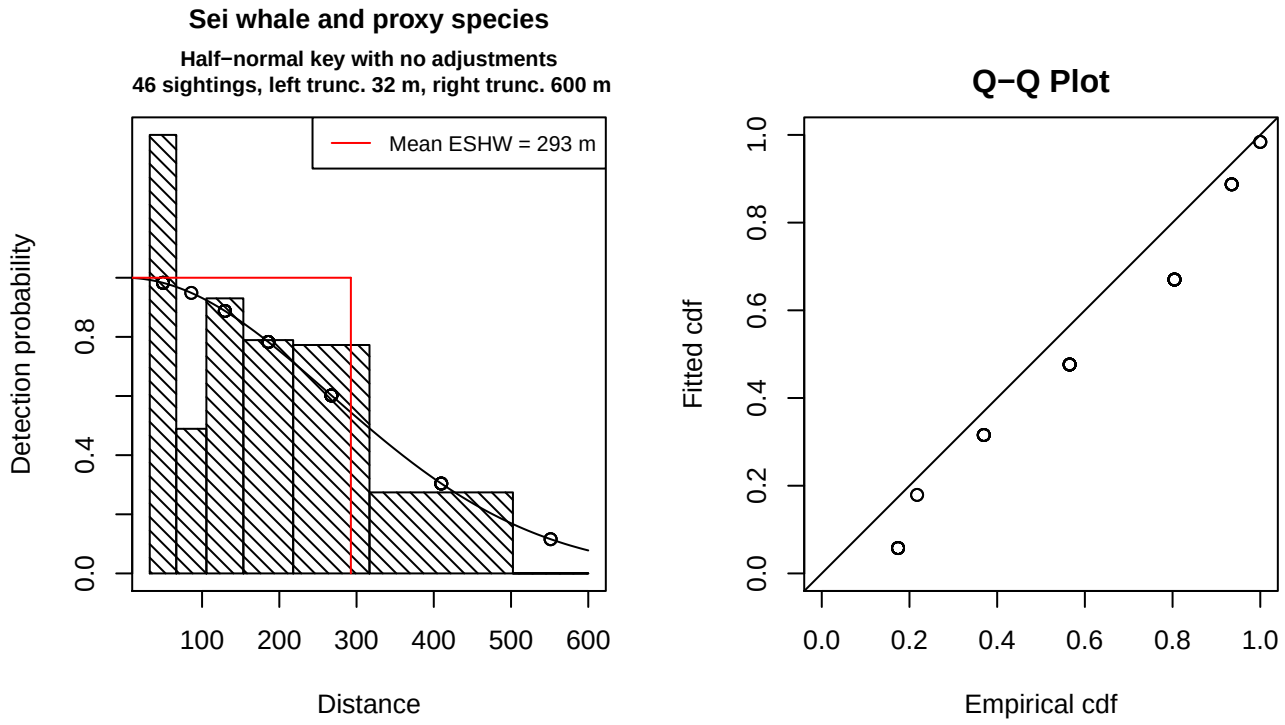

Figure 33: Detection function for Without Belly Observers - 600 ft that was selected for the density model

Statistical output for this detection function:

```
Summary for ds object
Number of observations :  46
Distance range         :  32.24668  -  600
AIC                    :  177.4011

Detection function:
 Half-normal key function

Detection function parameters
Scale Coefficients:
            estimate        se
(Intercept) 5.581559 0.1339955

                     Estimate          SE        CV
Average p            0.487738  0.06208134 0.1272842
N in covered region 94.312922 15.59372100 0.1653402
```

Additional diagnostic plots:

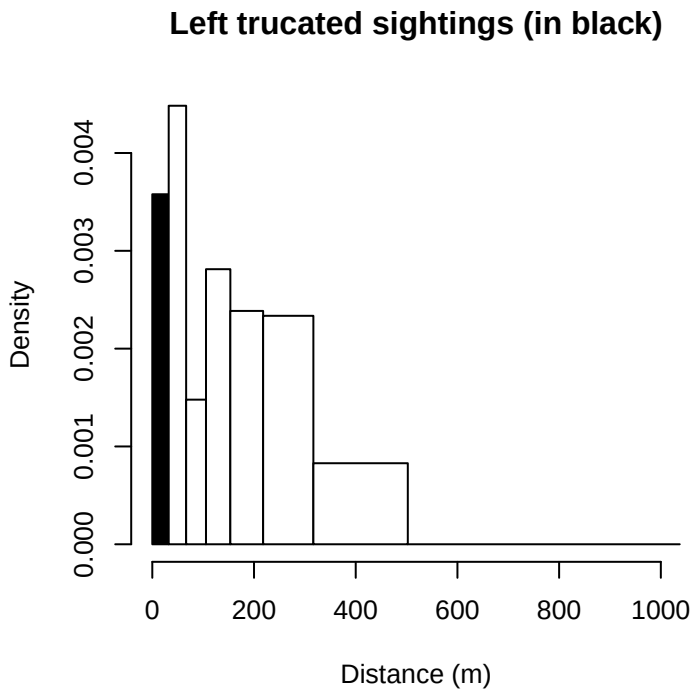

Figure 34: Density of sightings by perpendicular distance for Without Belly Observers - 600 ft. Black bars on the left show sightings that were left truncated.

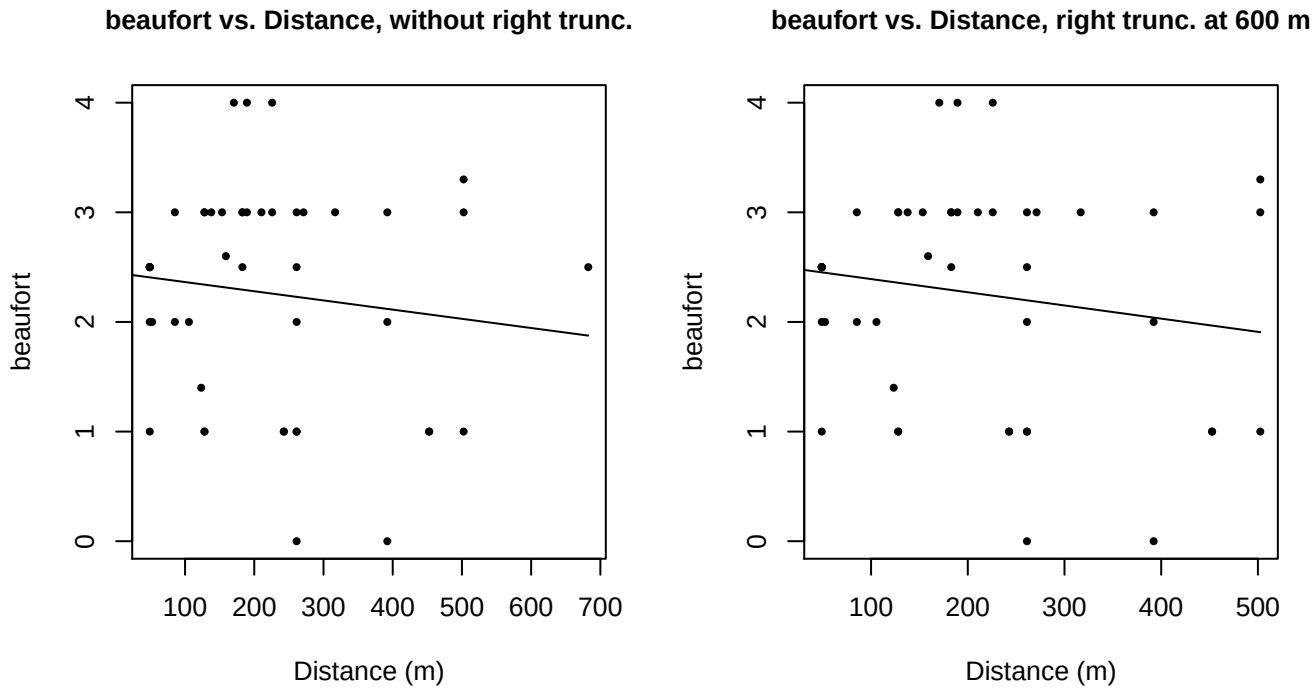

Figure 35: Scatterplots showing the relationship between Beaufort sea state and perpendicular sighting distance, for all sightings (left) and only those not right truncated (right). The line is a simple linear regression.

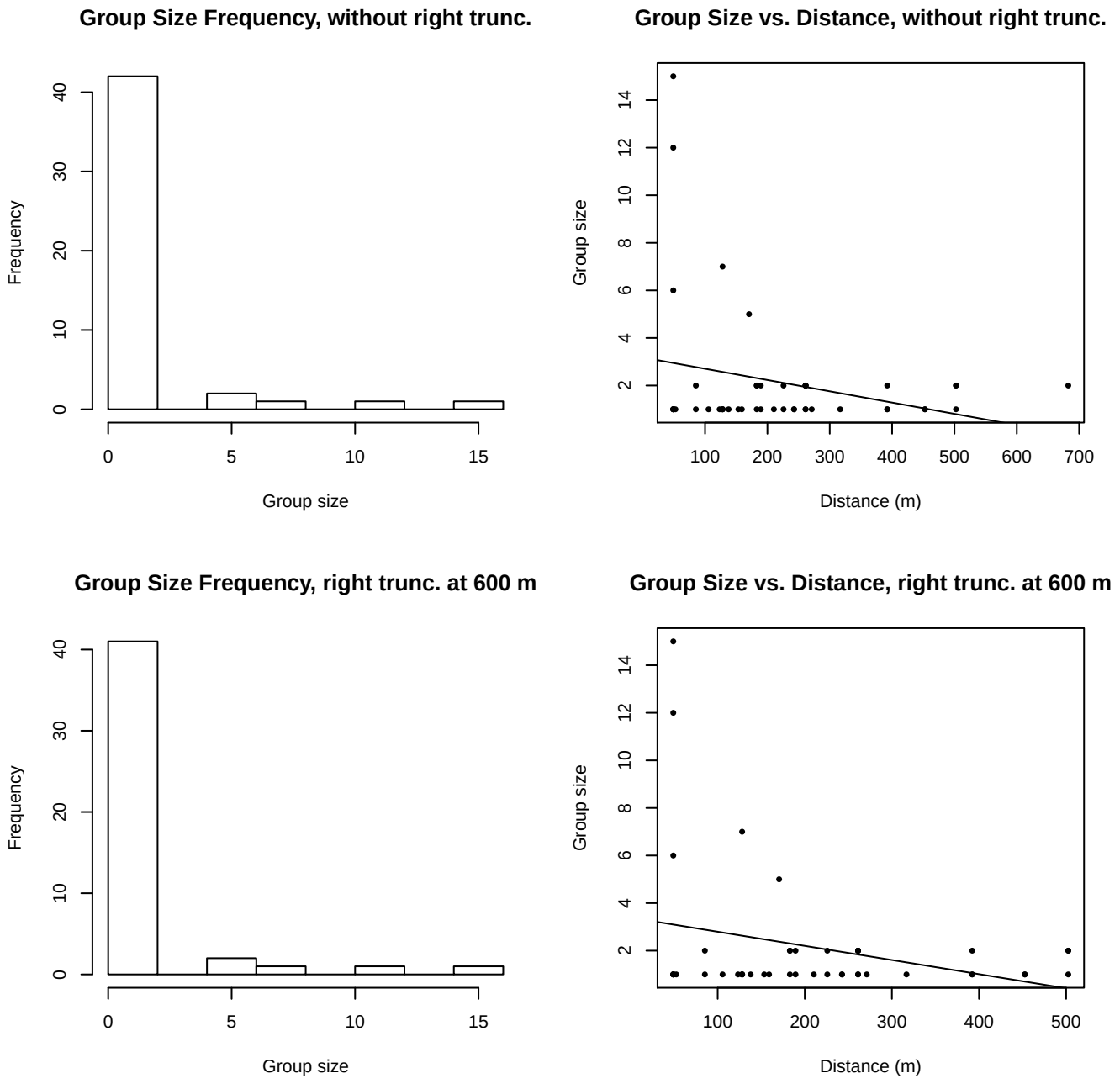

Figure 36: Histograms showing group size frequency and scatterplots showing the relationship between group size and perpendicular sighting distance, for all sightings (top row) and only those not right truncated (bottom row). In the scatterplot, the line is a simple linear regression.

Without Belly Observers - 750 ft

Because this taxon was sighted too infrequently to fit a detection function to its sightings alone, we fit a detection function to the pooled sightings of several other species that we believed would exhibit similar detectability. These "proxy species" are listed below.

Reported By Observer	Common Name	n
Balaenoptera	Balaenopterid sp.	1
Balaenoptera acutorostrata	Minke whale	0

Balaenoptera borealis	Sei whale	0
Balaenoptera borealis/edeni	Sei or Bryde's whale	2
Balaenoptera borealis/physalus	Fin or Sei whale	0
Balaenoptera edeni	Bryde's whale	3
Balaenoptera musculus	Blue whale	0
Balaenoptera physalus	Fin whale	2
Eubalaena glacialis	North Atlantic right whale	0
Eubalaena glacialis/Megaptera novaeangliae	Right or humpback whale	0
Megaptera novaeangliae	Humpback whale	6
Physeter macrocephalus	Sperm whale	37
Total		51

Table 26: Proxy species used to fit detection functions for Without Belly Observers - 750 ft. The number of sightings, n, is before truncation.

The sightings were right truncated at 600m. Due to a reduced frequency of sightings close to the trackline that plausibly resulted from the behavior of the observers and/or the configuration of the survey platform, the sightings were left truncted as well. Sightings closer than 40 m to the trackline were omitted from the analysis, and it was assumed that the the area closer to the trackline than this was not surveyed. This distance was estimated by inspecting histograms of perpendicular sighting distances. The vertical sighting angles were heaped at 10 degree increments, so the candidate detection functions were fitted using linear bins scaled accordingly.

Key	Adjustment	Order	Covariates	Succeeded	Δ AIC	Mean ESHW (m)
hn	cos	2		Yes	0.00	216
hr				Yes	0.59	251
hn	cos	3		Yes	2.31	255
hn	herm	4		Yes	2.46	316
hr	poly	2		Yes	2.59	251
hr	poly	4		Yes	2.69	246
hn				No		

Table 27: Candidate detection functions for Without Belly Observers - 750 ft. The first one listed was selected for the density model.

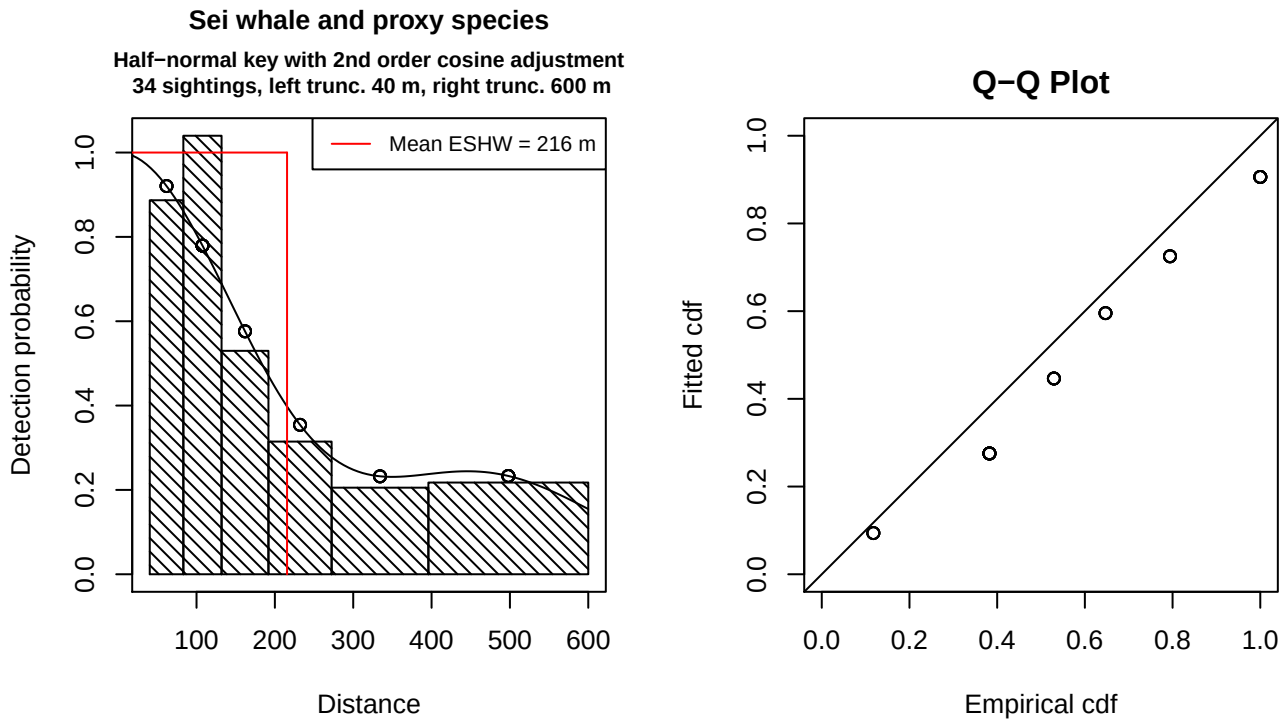

Figure 37: Detection function for Without Belly Observers - 750 ft that was selected for the density model

Statistical output for this detection function:

```
Summary for ds object
Number of observations :  34
Distance range         :  40.30835  -  600
AIC                    :  124.984

Detection function:
 Half-normal key function with cosine adjustment term of order 2

Detection function parameters
Scale Coefficients:
            estimate        se
(Intercept) 5.738324 0.1838281

Adjustment term parameter(s):
              estimate       se
cos, order 2 0.4333816 0.242253


Monotonicity constraints were enforced.
                     Estimate         SE        CV
Average p            0.3592782  0.0870934 0.2424122
N in covered region 94.6341973 26.3634679 0.2785829

Monotonicity constraints were enforced.
```

Additional diagnostic plots:

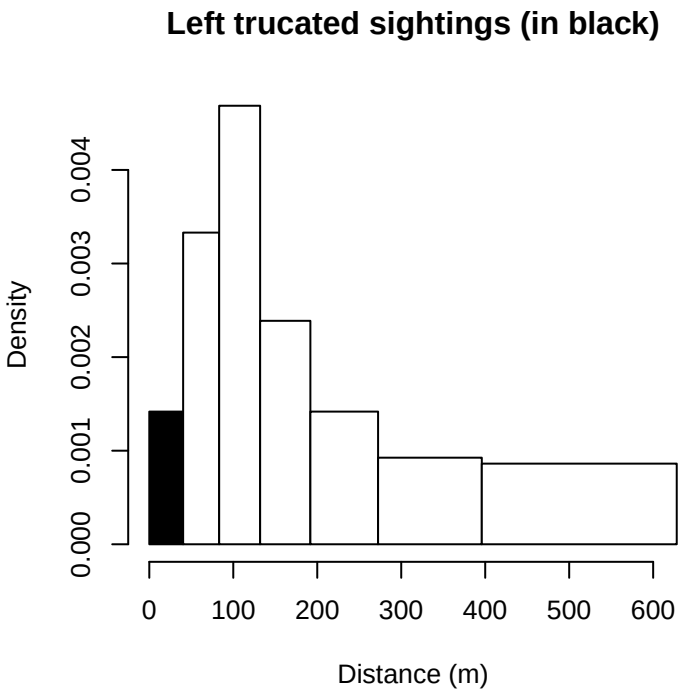

Figure 38: Density of sightings by perpendicular distance for Without Belly Observers - 750 ft. Black bars on the left show sightings that were left truncated.

Without Belly Observers - 1000 ft

Because this taxon was sighted too infrequently to fit a detection function to its sightings alone, we fit a detection function to the pooled sightings of several other species that we believed would exhibit similar detectability. These "proxy species" are listed below.

Reported By Observer	Common Name	n
Balaenoptera	Balaenopterid sp.	1
Balaenoptera acutorostrata	Minke whale	16
Balaenoptera borealis	Sei whale	0
Balaenoptera borealis/edeni	Sei or Bryde's whale	0
Balaenoptera borealis/physalus	Fin or Sei whale	0
Balaenoptera edeni	Bryde's whale	0
Balaenoptera musculus	Blue whale	0
Balaenoptera physalus	Fin whale	32
Eubalaena glacialis	North Atlantic right whale	34
Eubalaena glacialis/Megaptera novaeangliae	Right or humpback whale	0
Megaptera novaeangliae	Humpback whale	30
Total		113

Table 28: Proxy species used to fit detection functions for Without Belly Observers - 1000 ft. The number of sightings, n, is before truncation.

The sightings were right truncated at 1500m.

Covariate	Description
beaufort	Beaufort sea state.
quality	Survey-specific index of the quality of observation conditions, utilizing relevant factors other than Beaufort sea state (see methods).
size	Estimated size (number of individuals) of the sighted group.

Table 29: Covariates tested in candidate "multi-covariate distance sampling" (MCDS) detection functions.

Key	Adjustment	Order	Covariates	Succeeded	Δ AIC	Mean ESHW (m)
hr				Yes	0.00	434
hr	poly	4		Yes	1.58	424
hn	cos	2		Yes	1.71	462
hr	poly	2		Yes	1.92	427
hr			quality	Yes	1.96	433
hn	cos	3		Yes	3.64	418
hn				Yes	11.03	585
hn	herm	4		No		
hn			beaufort	No		
hr			beaufort	No		
hn			quality	No		
hn			size	No		
hr			size	No		
hn			beaufort, quality	No		
hr			beaufort, quality	No		
hn			beaufort, size	No		
hr			beaufort, size	No		
hn			quality, size	No		
hr			quality, size	No		
hn			beaufort, quality, size	No		
hr			beaufort, quality, size	No		

Table 30: Candidate detection functions for Without Belly Observers - 1000 ft. The first one listed was selected for the density model.

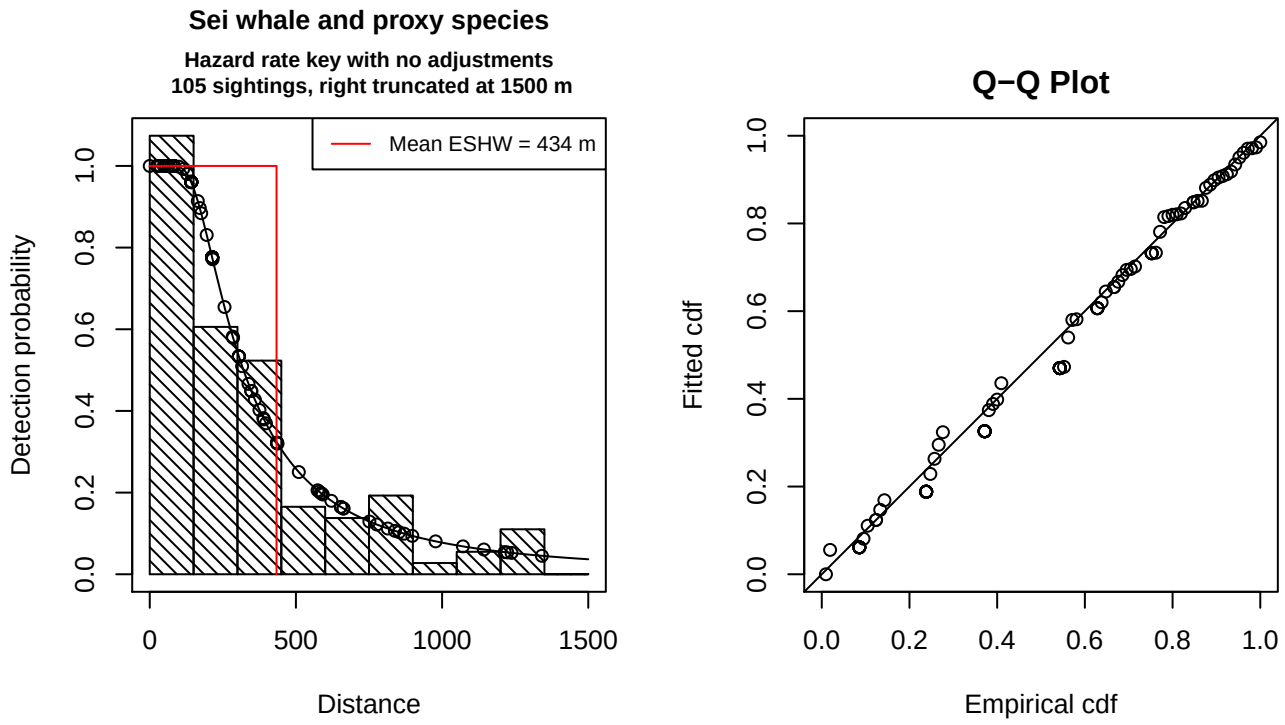

Figure 39: Detection function for Without Belly Observers - 1000 ft that was selected for the density model

Statistical output for this detection function:

```
Summary for ds object
Number of observations :  105
Distance range         :  0  -  1500
AIC                    :  1432.491

Detection function:
 Hazard-rate key function

Detection function parameters
Scale Coefficients:
            estimate        se
(Intercept) 5.576432 0.2232183

Shape parameters:
             estimate        se
(Intercept) 0.6374087 0.1752092

                       Estimate          SE        CV
Average p              0.2891295  0.03984493 0.1378100
N in covered region 363.1591175 58.28878285 0.1605048
```

Additional diagnostic plots:

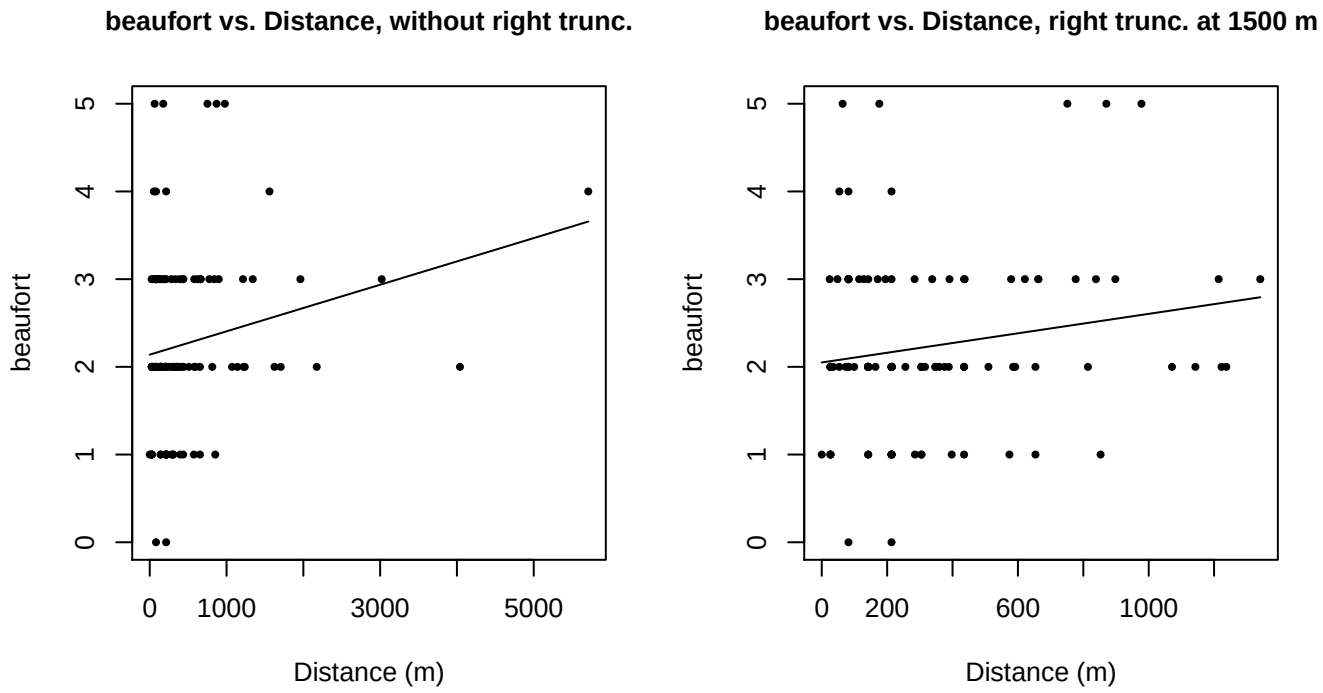

Figure 40: Scatterplots showing the relationship between Beaufort sea state and perpendicular sighting distance, for all sightings (left) and only those not right truncated (right). The line is a simple linear regression.

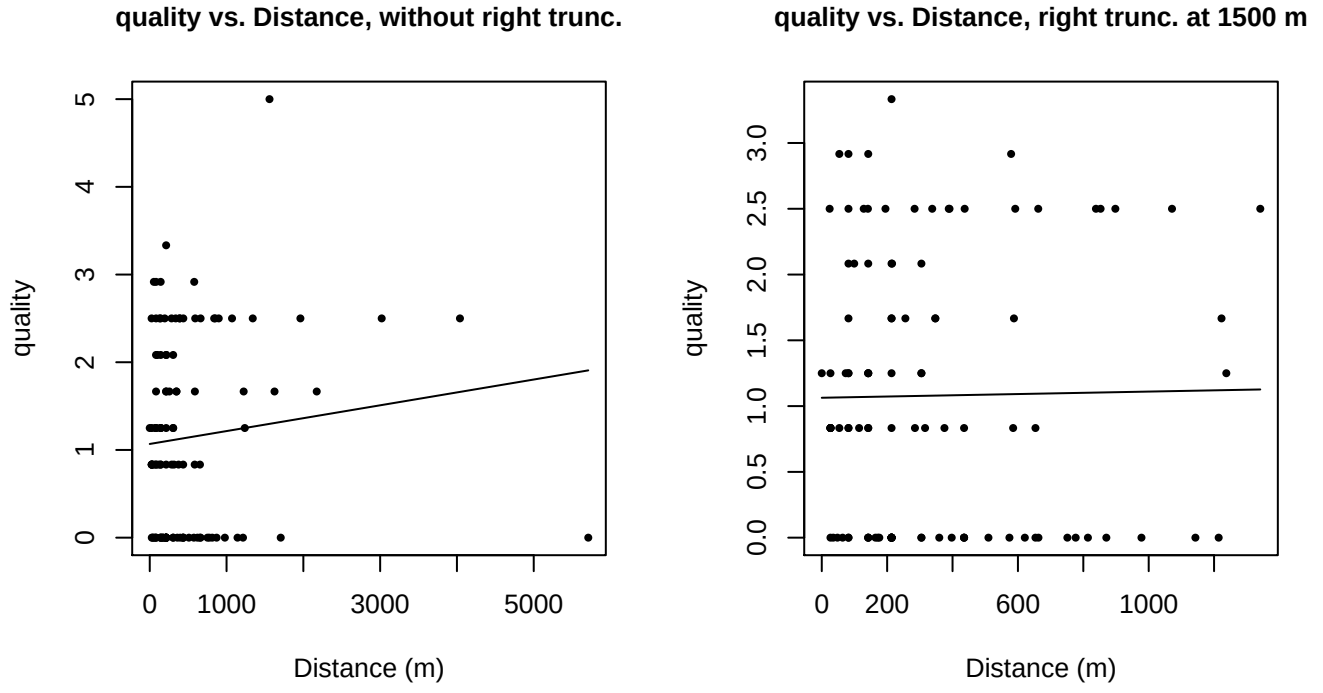

Figure 41: Scatterplots showing the relationship between the survey-specific index of the quality of observation conditions and perpendicular sighting distance, for all sightings (left) and only those not right truncated (right). Low values of the quality index correspond to better observation conditions. The line is a simple linear regression.

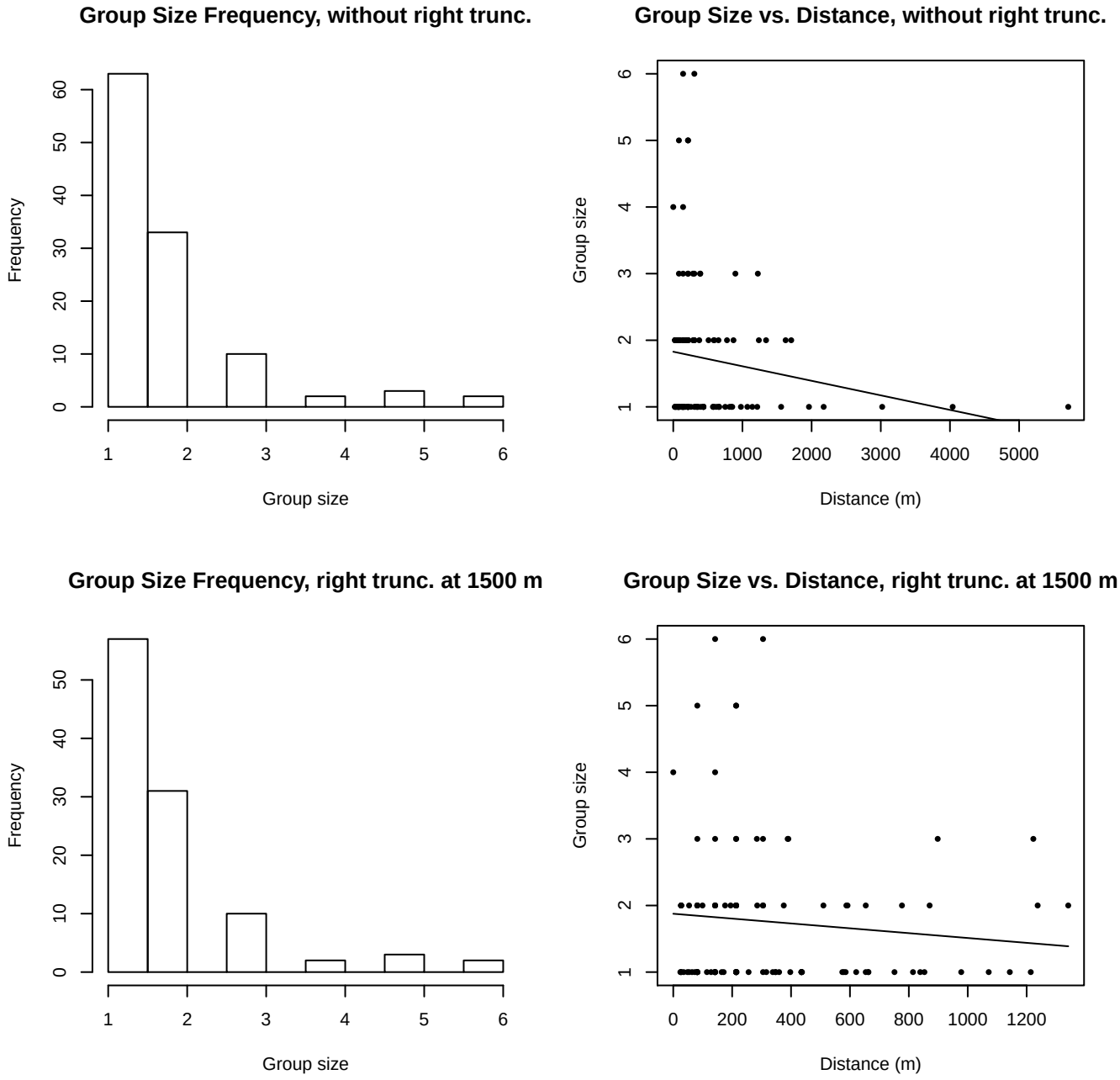

Figure 42: Histograms showing group size frequency and scatterplots showing the relationship between group size and perpendicular sighting distance, for all sightings (top row) and only those not right truncated (bottom row). In the scatterplot, the line is a simple linear regression.

UNCW Aerial Surveys

Because this taxon was sighted too infrequently to fit a detection function to its sightings alone, we fit a detection function to the pooled sightings of several other species that we believed would exhibit similar detectability. These "proxy species" are listed below.

Reported By Observer	Common Name	n
Balaenoptera	Balaenopterid sp.	1
Balaenoptera acutorostrata	Minke whale	15

Balaenoptera borealis	Sei whale	0
Balaenoptera borealis/edeni	Sei or Bryde's whale	0
Balaenoptera borealis/physalus	Fin or Sei whale	0
Balaenoptera edeni	Bryde's whale	0
Balaenoptera musculus	Blue whale	0
Balaenoptera physalus	Fin whale	19
Eubalaena glacialis	North Atlantic right whale	31
Eubalaena glacialis/Megaptera novaeangliae	Right or humpback whale	0
Megaptera novaeangliae	Humpback whale	23
Total		89

Table 31: Proxy species used to fit detection functions for UNCW Aerial Surveys. The number of sightings, n, is before truncation.

The sightings were right truncated at 1500m.

Covariate	Description
beaufort	Beaufort sea state.
quality	Survey-specific index of the quality of observation conditions, utilizing relevant factors other than Beaufort sea state (see methods).
size	Estimated size (number of individuals) of the sighted group.

Table 32: Covariates tested in candidate "multi-covariate distance sampling" (MCDS) detection functions.

Key	Adjustment	Order	Covariates	Succeeded	Δ AIC	Mean ESHW (m)
hn	cos	3		Yes	0.00	358
hr				Yes	0.01	397
hr	poly	4		Yes	0.85	391
hr	poly	2		Yes	1.03	386
hn	cos	2		Yes	1.24	409
hr			quality	Yes	1.55	396
hn				Yes	5.53	480
hn			quality	Yes	7.53	480
hn	herm	4		No		
hn			beaufort	No		
hr			beaufort	No		
hn			size	No		
hr			size	No		
hn			beaufort, quality	No		
hr			beaufort, quality	No		

hn	beaufort, size	No
hr	beaufort, size	No
hn	quality, size	No
hr	quality, size	No
hn	beaufort, quality, size	No
hr	beaufort, quality, size	No

Table 33: Candidate detection functions for UNCW Aerial Surveys. The first one listed was selected for the density model.

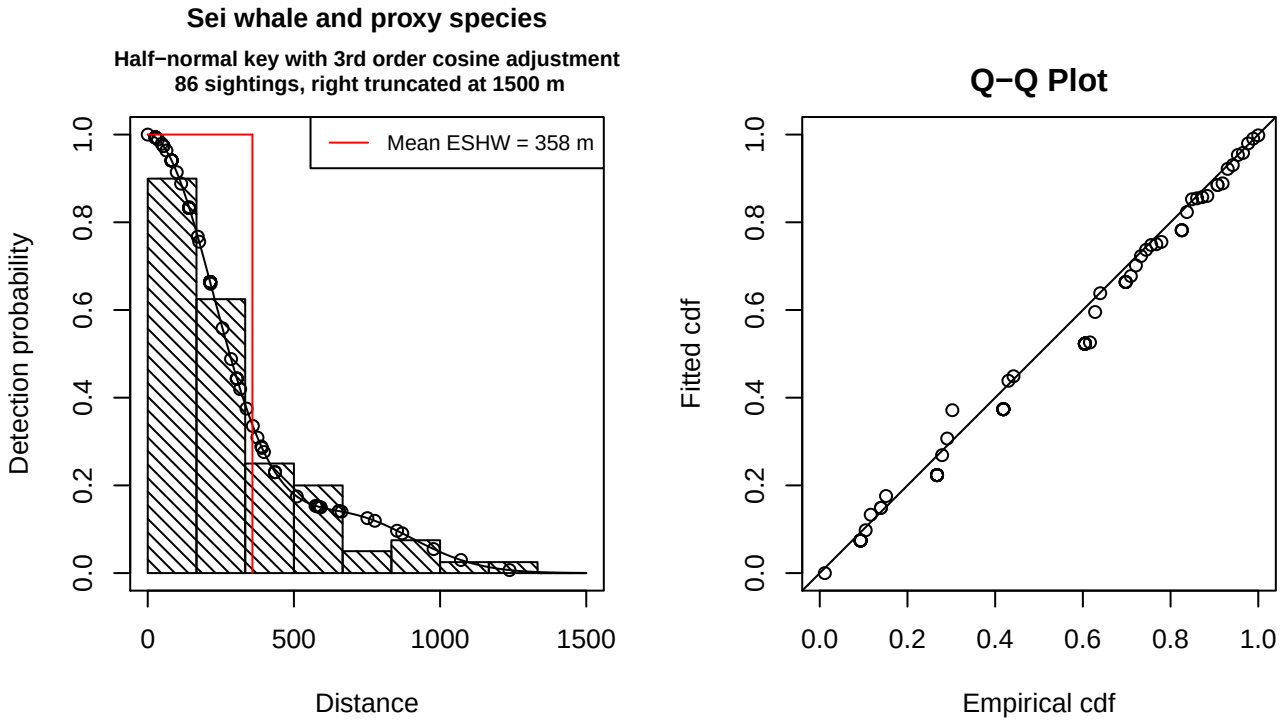

Figure 43: Detection function for UNCW Aerial Surveys that was selected for the density model

Statistical output for this detection function:

```
Summary for ds object
Number of observations :  86
Distance range         :  0  -  1500
AIC                    :  1144.166

Detection function:
 Half-normal key function with cosine adjustment term of order 3

Detection function parameters
Scale Coefficients:
            estimate         se
(Intercept) 6.006457 0.06897785

Adjustment term parameter(s):
```

```
              estimate        se
cos, order 3 0.4451316 0.1512901


Monotonicity constraints were enforced.
                        Estimate          SE        CV
Average p              0.2387636  0.02505434 0.1049337
N in covered region 360.1889048 50.76321102 0.1409350

Monotonicity constraints were enforced.
```

Additional diagnostic plots:

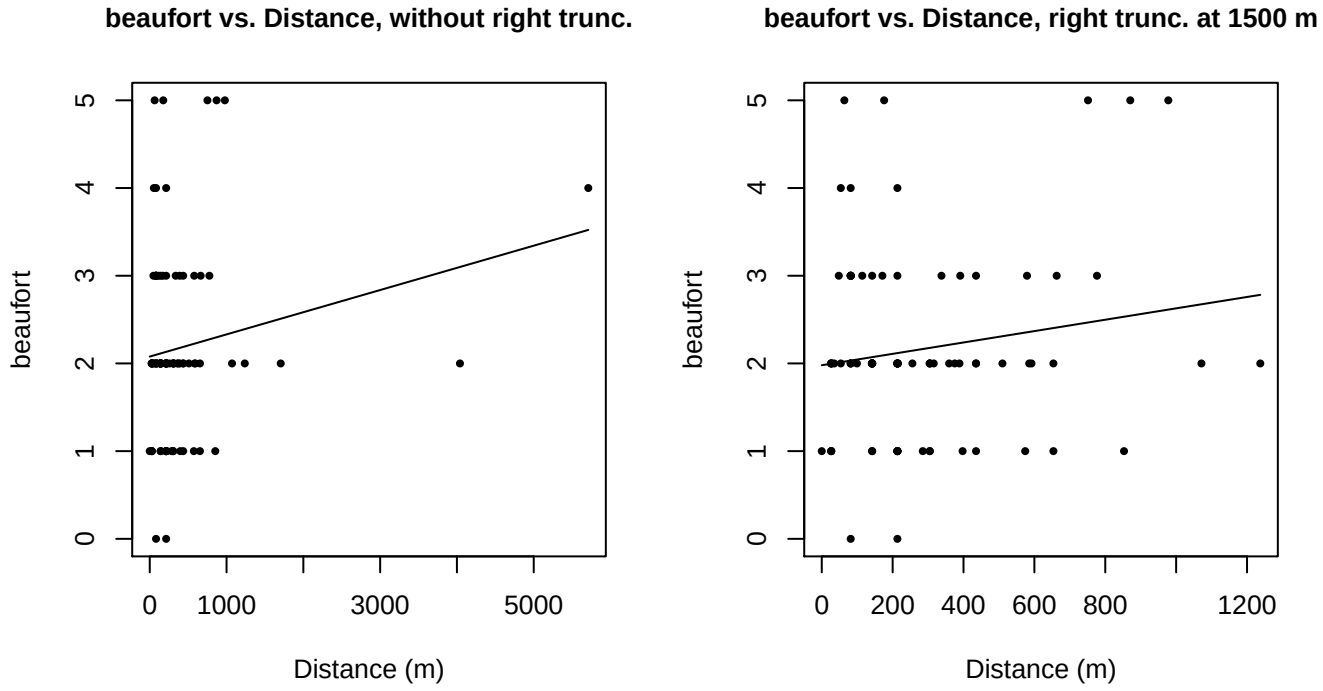

Figure 44: Scatterplots showing the relationship between Beaufort sea state and perpendicular sighting distance, for all sightings (left) and only those not right truncated (right). The line is a simple linear regression.

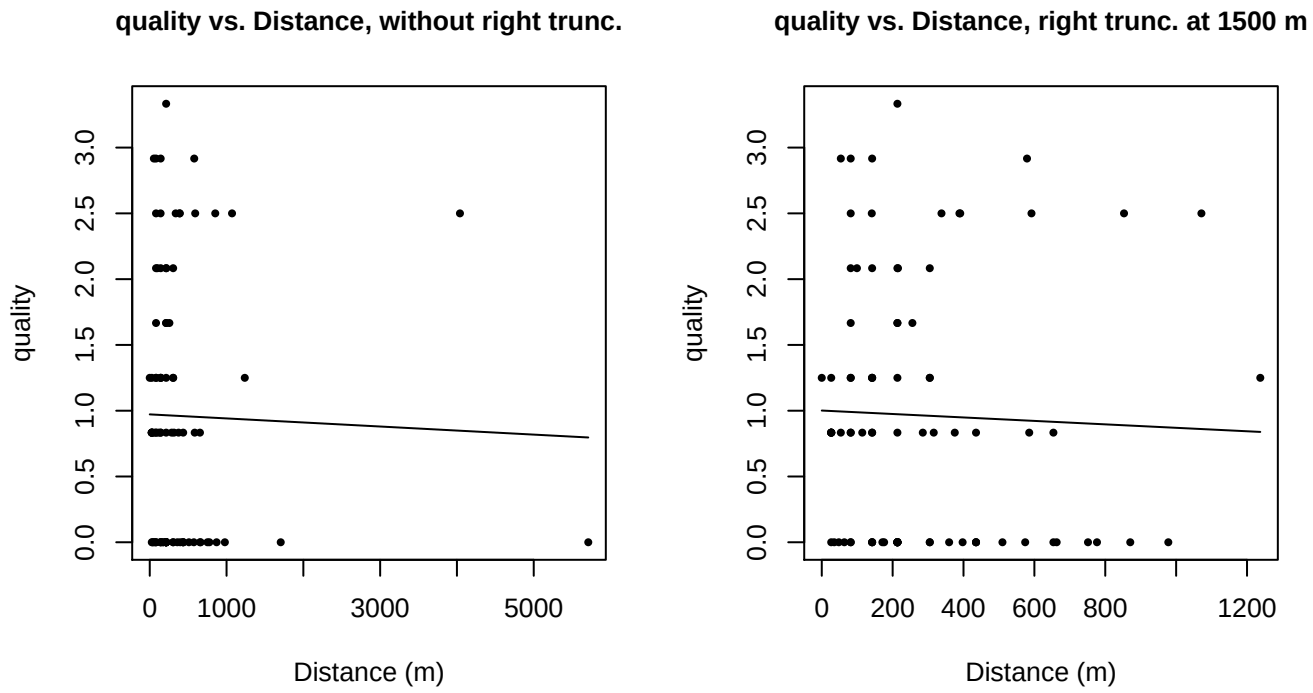

Figure 45: Scatterplots showing the relationship between the survey-specific index of the quality of observation conditions and perpendicular sighting distance, for all sightings (left) and only those not right truncated (right). Low values of the quality index correspond to better observation conditions. The line is a simple linear regression.

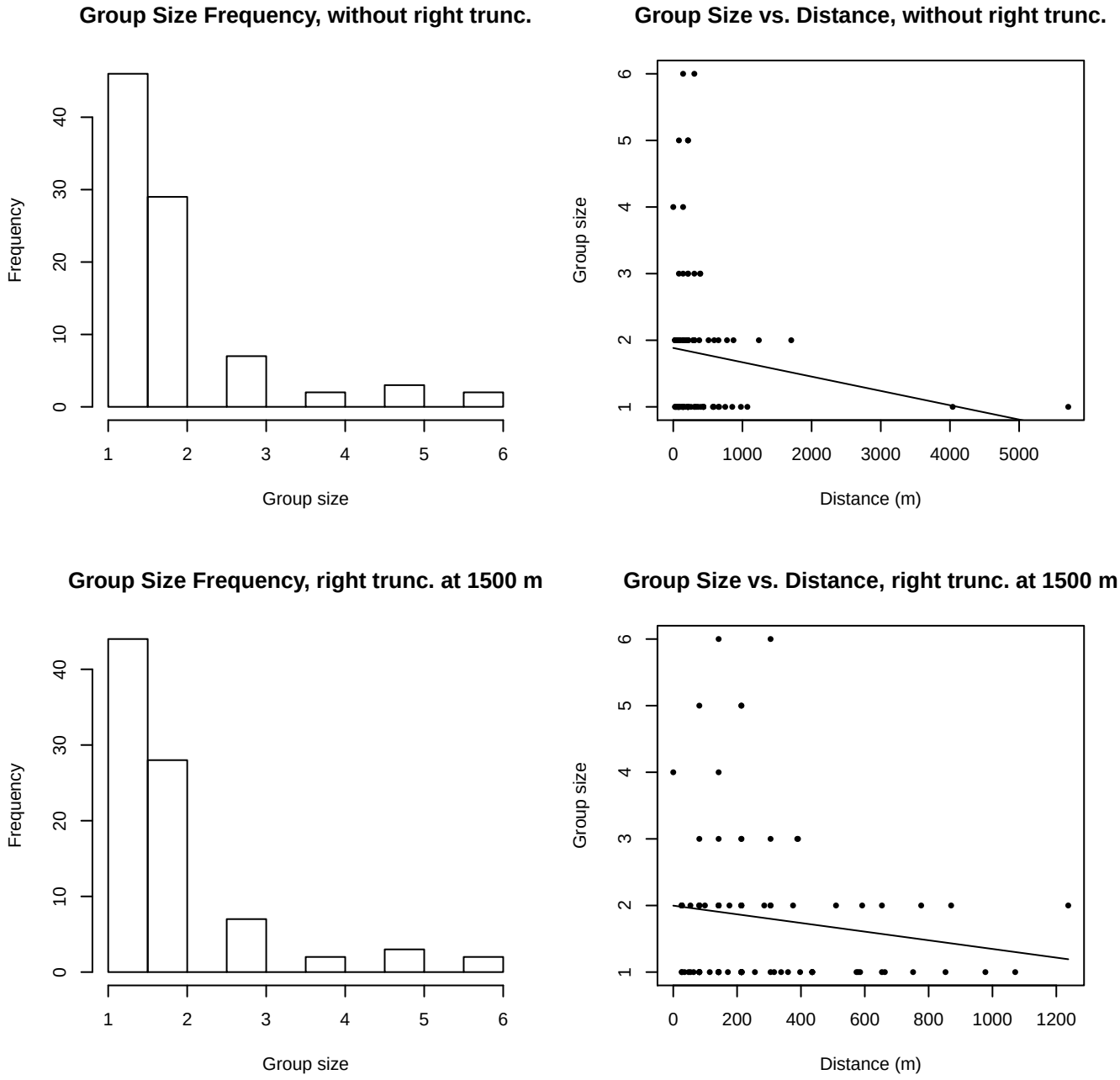

Figure 46: Histograms showing group size frequency and scatterplots showing the relationship between group size and perpendicular sighting distance, for all sightings (top row) and only those not right truncated (bottom row). In the scatterplot, the line is a simple linear regression.

NARWSS Grummans

The sightings were right truncated at 3000m. Due to a reduced frequency of sightings close to the trackline that plausibly resulted from the behavior of the observers and/or the configuration of the survey platform, the sightings were left truncted as well. Sightings closer than 107 m to the trackline were omitted from the analysis, and it was assumed that the the area closer to the trackline than this was not surveyed. This distance was estimated by inspecting histograms of perpendicular sighting distances.

Covariate	Description

beaufort	Beaufort sea state.
quality	Survey-specific index of the quality of observation conditions, utilizing relevant factors other than Beaufort sea state (see methods).
size	Estimated size (number of individuals) of the sighted group.

Table 34: Covariates tested in candidate "multi-covariate distance sampling" (MCDS) detection functions.

Key	Adjustment	Order	Covariates	Succeeded	Δ AIC	Mean ESHW (m)
hr			quality, size	Yes	0.00	873
hr			beaufort, size	Yes	1.43	838
hr			beaufort, quality, size	Yes	1.83	869
hr			size	Yes	2.00	829
hn			quality, size	Yes	7.08	833
hn			size	Yes	7.74	834
hr			beaufort	Yes	9.45	679
hr				Yes	9.58	671
hn			beaufort, size	Yes	9.71	833
hr			quality	Yes	10.52	695
hr	poly	4		Yes	11.35	669
hr	poly	2		Yes	11.37	667
hr			beaufort, quality	Yes	11.44	681
hn	cos	2		Yes	13.10	696
hn	cos	3		Yes	15.69	634
hn				Yes	18.43	837
hn			quality	Yes	19.69	837
hn	herm	4		No		
hn			beaufort	No		
hn			beaufort, quality	No		
hn			beaufort, quality, size	No		

Table 35: Candidate detection functions for NARWSS Grummans. The first one listed was selected for the density model.

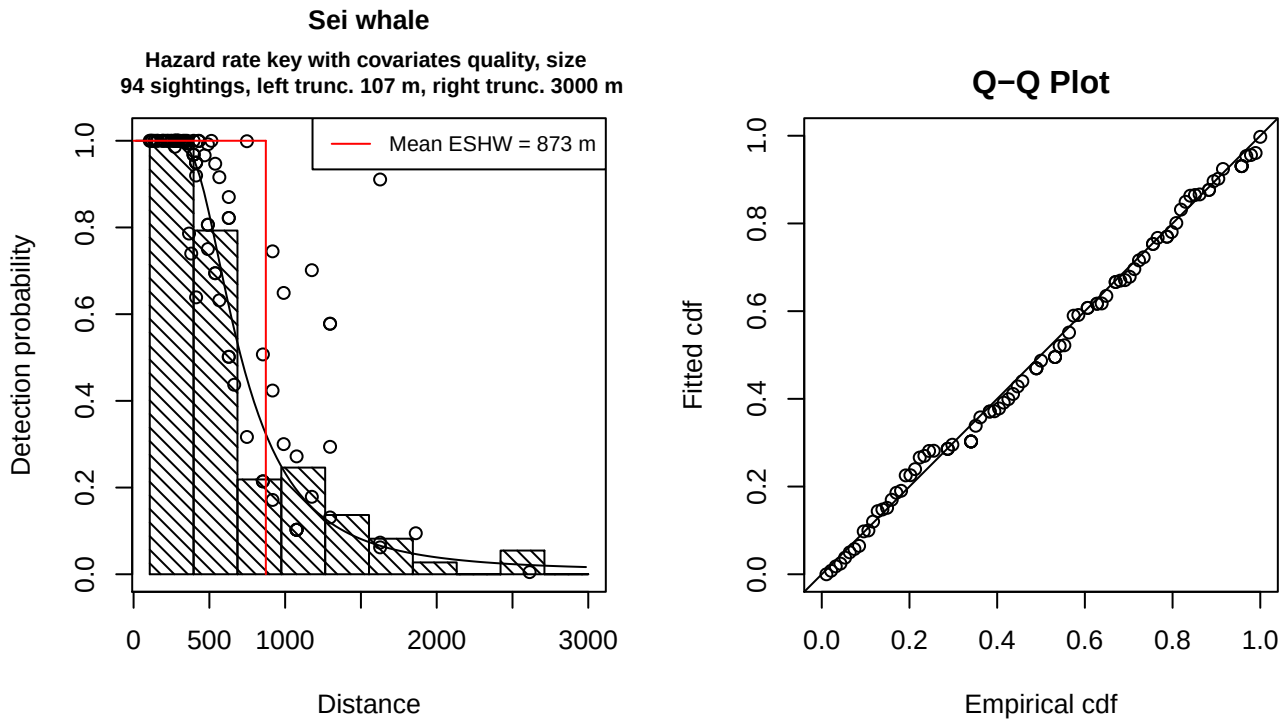

Figure 47: Detection function for NARWSS Grummans that was selected for the density model

Statistical output for this detection function:

```
Summary for ds object
Number of observations :  94
Distance range         :  106.5979  -  3000
AIC                    :  1354.44

Detection function:
 Hazard-rate key function

Detection function parameters
Scale Coefficients:
             estimate        se
(Intercept)  6.3867737 0.2444911
quality     -0.2486634 0.1649471
size         0.2621943 0.1022377

Shape parameters:
            estimate       se
(Intercept) 1.241471 0.175651

                       Estimate          SE        CV
Average p              0.2478645  0.02862242 0.1154761
N in covered region 379.2395126 55.98596360 0.1476269
```

Additional diagnostic plots:

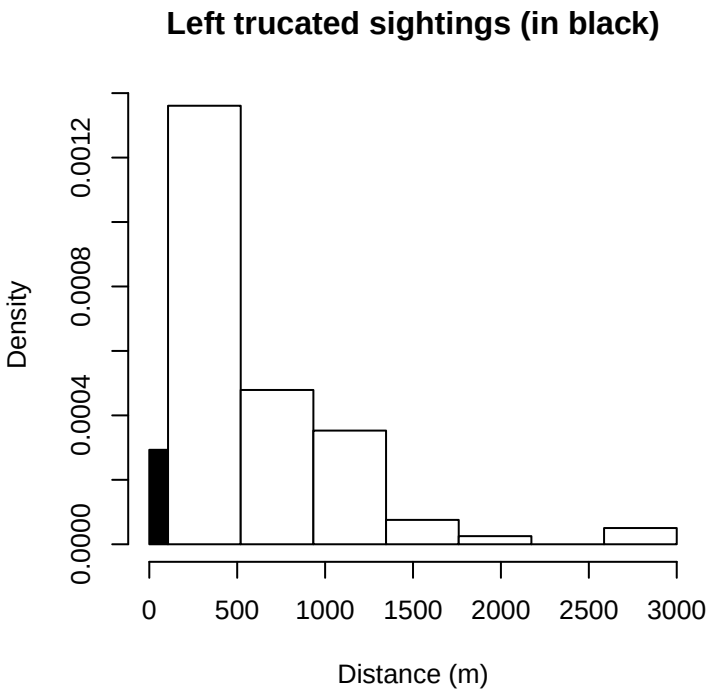

Figure 48: Density of sightings by perpendicular distance for NARWSS Grummans. Black bars on the left show sightings that were left truncated.

Figure 49: Scatterplots showing the relationship between Beaufort sea state and perpendicular sighting distance, for all sightings (left) and only those not right truncated (right). The line is a simple linear regression.

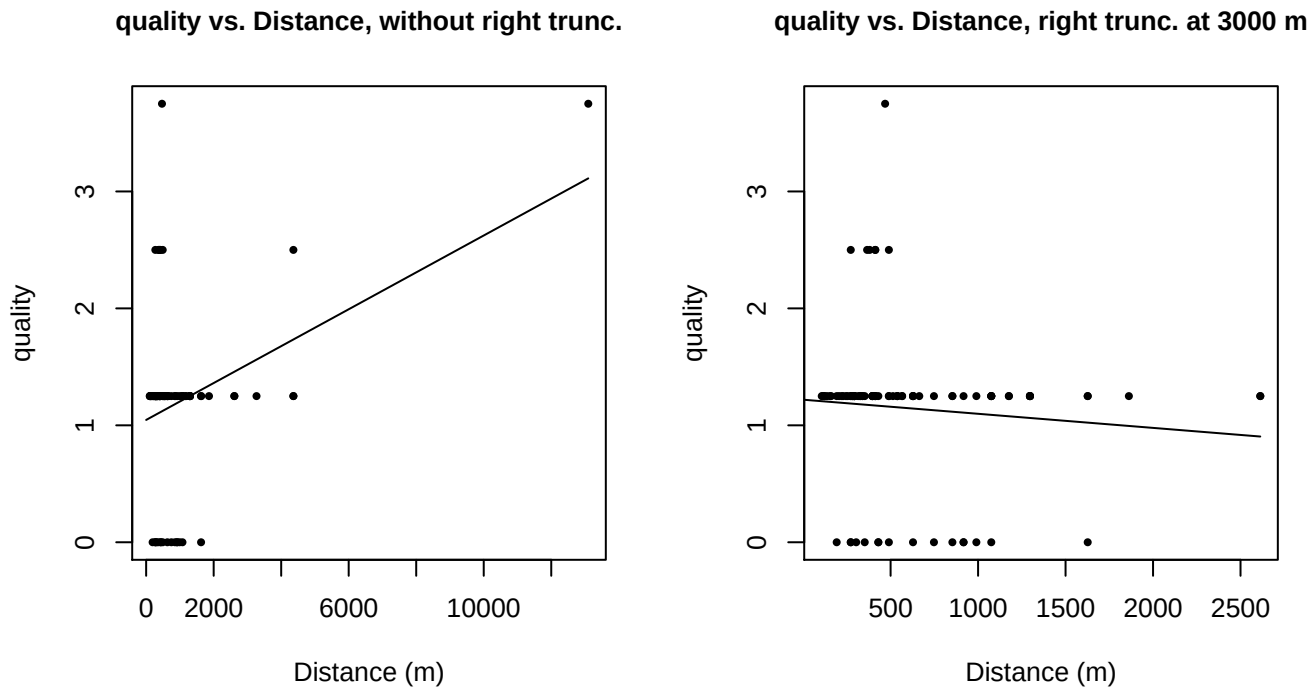

Figure 50: Scatterplots showing the relationship between the survey-specific index of the quality of observation conditions and perpendicular sighting distance, for all sightings (left) and only those not right truncated (right). Low values of the quality index correspond to better observation conditions. The line is a simple linear regression.

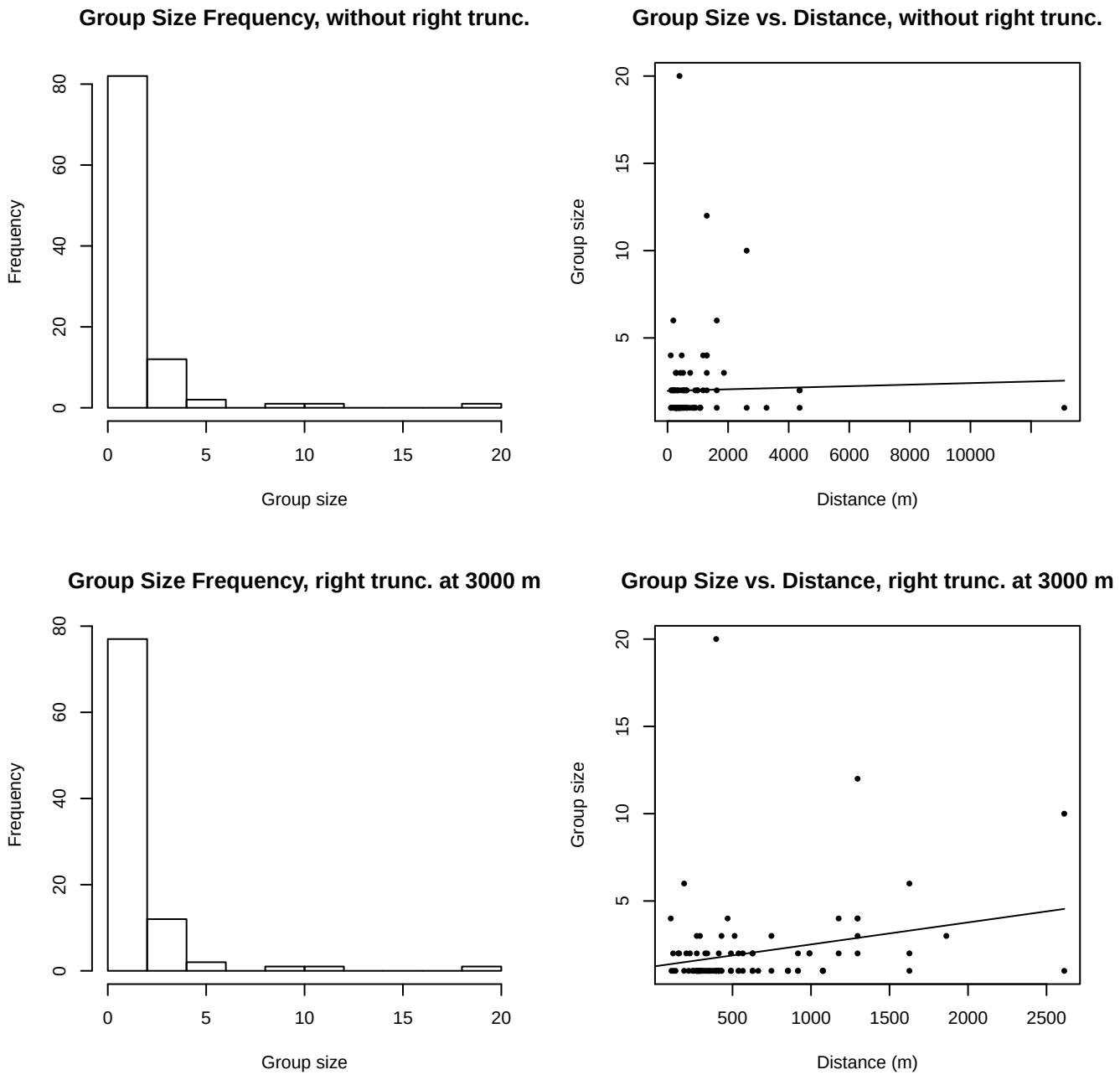

Figure 51: Histograms showing group size frequency and scatterplots showing the relationship between group size and perpendicular sighting distance, for all sightings (top row) and only those not right truncated (bottom row). In the scatterplot, the line is a simple linear regression.

NARWSS Twin Otters

The sightings were right truncated at 5000m. Due to a reduced frequency of sightings close to the trackline that plausibly resulted from the behavior of the observers and/or the configuration of the survey platform, the sightings were left truncted as well. Sightings closer than 107 m to the trackline were omitted from the analysis, and it was assumed that the the area closer to the trackline than this was not surveyed. This distance was estimated by inspecting histograms of perpendicular sighting distances. The vertical sighting angles were heaped at 10 degree increments up to 80 degrees and 1 degree increments thereafter, so the candidate detection functions were fitted using linear bins scaled accordingly.

Covariate	Description

beaufort	Beaufort sea state.
quality	Survey-specific index of the quality of observation conditions, utilizing relevant factors other than Beaufort sea state (see methods).
size	Estimated size (number of individuals) of the sighted group.

Table 36: Covariates tested in candidate "multi-covariate distance sampling" (MCDS) detection functions.

Key	Adjustment	Order	Covariates	Succeeded	Δ AIC	Mean ESHW (m)
hr	poly	2		Yes	0.00	1206
hr	poly	4		Yes	1.30	1208
hr			size	Yes	4.22	1424
hr				Yes	14.56	1375
hn	cos	3		Yes	15.96	1544
hn	cos	2		Yes	16.25	1682
hn				Yes	38.63	2014
hn	herm	4		Yes	39.90	2010
hn			beaufort	No		
hr			beaufort	No		
hn			quality	No		
hr			quality	No		
hn			size	No		
hn			beaufort, quality	No		
hr			beaufort, quality	No		
hn			beaufort, size	No		
hr			beaufort, size	No		
hn			quality, size	No		
hr			quality, size	No		
hn			beaufort, quality, size	No		
hr			beaufort, quality, size	No		

Table 37: Candidate detection functions for NARWSS Twin Otters. The first one listed was selected for the density model.

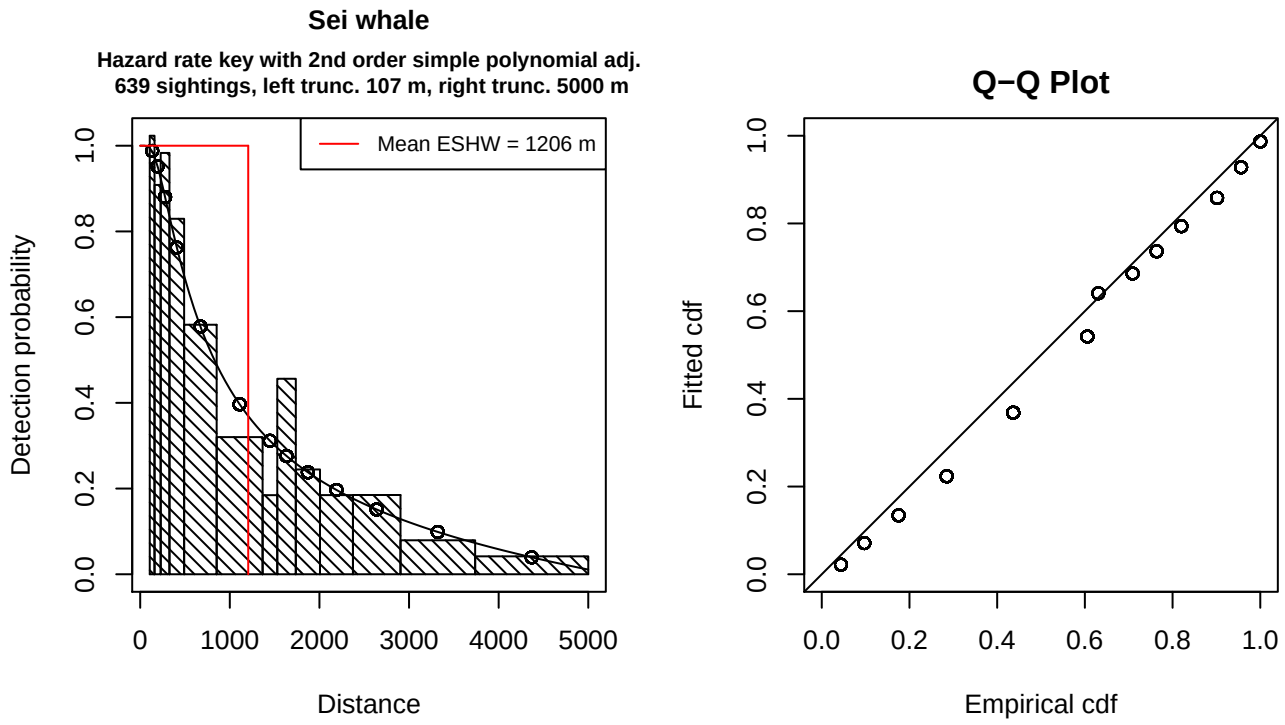

Figure 52: Detection function for NARWSS Twin Otters that was selected for the density model

Statistical output for this detection function:

```
Summary for ds object
Number of observations :  639
Distance range         :  106.5979  -  5000
AIC                    :  3140.146

Detection function:
 Hazard-rate key function with simple polynomial adjustment term of order 2

Detection function parameters
Scale Coefficients:
            estimate        se
(Intercept) 6.388861 0.3167177

Shape parameters:
                estimate        se
(Intercept) 1.340636e-08 0.1624549

Adjustment term parameter(s):
                estimate        se
poly, order 2 -0.9027297 0.1190062


Monotonicity constraints were enforced.
                        Estimate          SE        CV
Average p              0.2411157   0.03584093 0.1486462
N in covered region 2650.1795207 404.38726948 0.1525886

Monotonicity constraints were enforced.
```

Additional diagnostic plots:

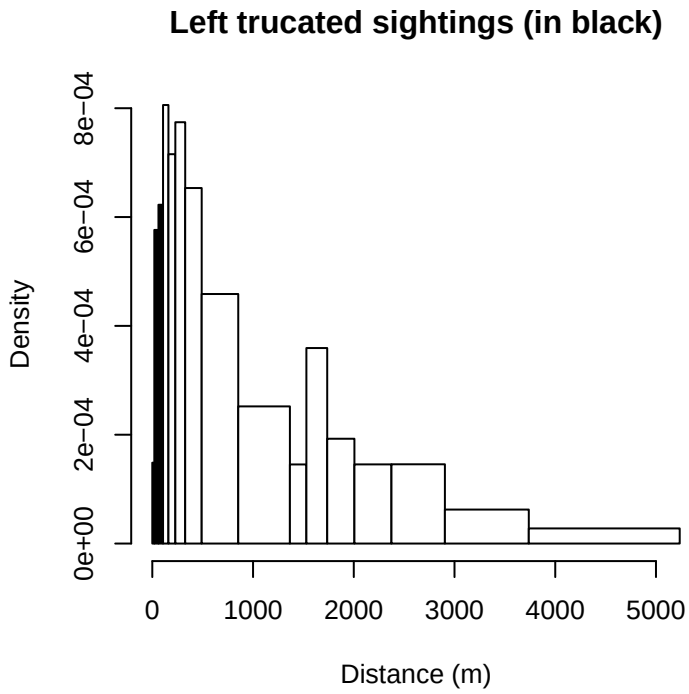

Figure 53: Density of sightings by perpendicular distance for NARWSS Twin Otters. Black bars on the left show sightings that were left truncated.

Figure 54: Scatterplots showing the relationship between Beaufort sea state and perpendicular sighting distance, for all sightings (left) and only those not right truncated (right). The line is a simple linear regression.

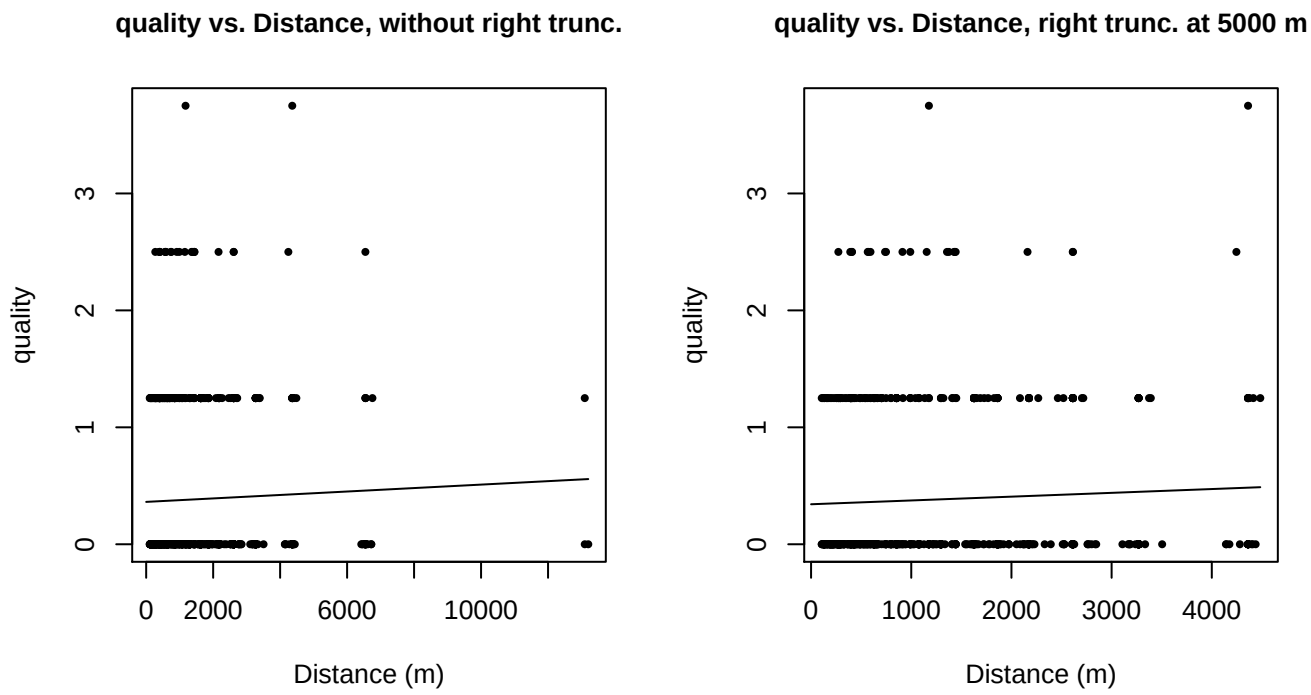

Figure 55: Scatterplots showing the relationship between the survey-specific index of the quality of observation conditions and perpendicular sighting distance, for all sightings (left) and only those not right truncated (right). Low values of the quality index correspond to better observation conditions. The line is a simple linear regression.

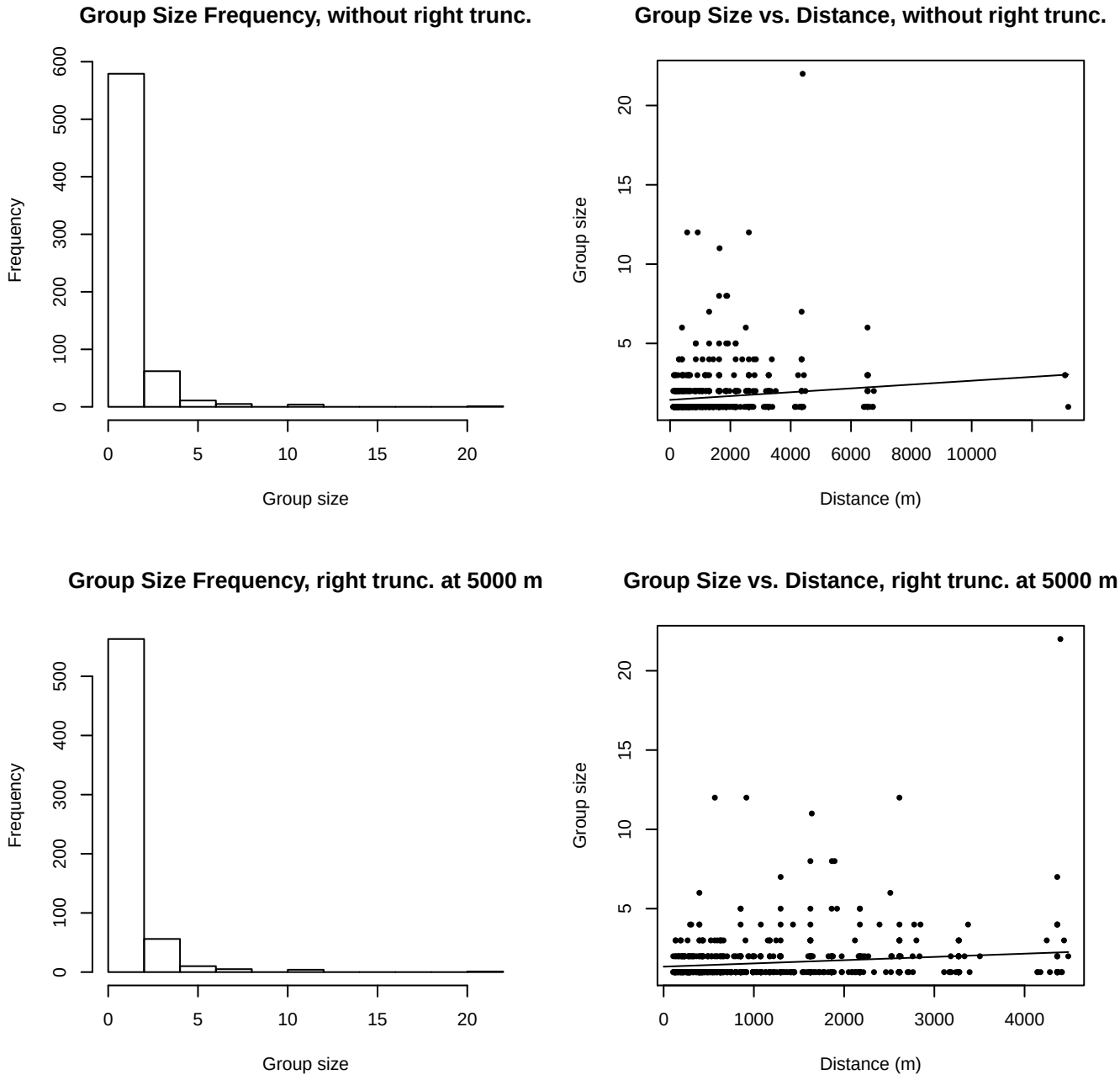

Figure 56: Histograms showing group size frequency and scatterplots showing the relationship between group size and perpendicular sighting distance, for all sightings (top row) and only those not right truncated (bottom row). In the scatterplot, the line is a simple linear regression.

g(0) Estimates

Platform	Surveys	Group Size	*g(0)*	Biases Addressed	Source
Shipboard	All	Any	0.63	Perception	Palka (2006)
Shipboard	NEFSC Abel-J Binocular Surveys	Any	0.32	Perception	Palka (2006)
Shipboard	NEFSC Endeavor	Any	0.94	Perception	Palka (2006)
Shipboard	Naked Eye Surveys	Any	0.48	Perception	Palka (2006)
Aerial	All	1-5	0.53	Both	Palka (2006)
		>5	1.00	Both	Palka (2006)

Table 38: Estimates of *g(0)* used in this density model.

Palka (2006) provided survey-specific g(0) estimates for fin and sei whales (pooled together) for two NOAA NEFSC shipboard surveys that used bigeye binoculars: the 1998 Abel-J survey (g(0)=0.32) and the 2004 Endeavor survey (g(0)=0.94). We used the estimates for the lower team, which was the primary team and the one for which we had sightings. All other binocular surveys did not estimate g(0); for these we used the simple mean (g(0)=0.68) of Palka's two estimates. These estimates accounted for perception bias but not availability bias (Palka 2005b).

As above, Palka (2006) provided a survey-specific, pooled fin and sei whale estimate of g(0) for the NOAA NEFSC Abel-J 1999 naked eye shipboard survey. We used the estimate for the upper team, which was the primary team and the one for which we have sightings. We also used this estimate with the European naked eye surveys, which did not publish g(0) estimates. (The European surveys were not used in the East Coast model documented here, but may have been used in the AFTT model. Please consult the AFTT model documentation for more information.)

Our literature review did not yield any aerial g(0) estimates specific to sei whales, nor any diving data from which availability bias could be estimated. For small groups, defined here as 1-5 individuals, we used Palka's (2006) estimate of g(0) for groups of 1-5 large whales, estimated from two years of aerial surveys using the Hiby (1999) circle-back method. This estimate accounted for both availability and perception bias, but pooled sightings of several species together to provide a generic estimate for all large whales, due to sample-size limitations. For large groups, defined as greater than 5 individuals, Palka (2006) assumed that g(0) was 1.

R. Prieto advised us against using dive data for another species as a proxy for sei whales. He planned a sei whale dive behavior study for summer 2014 but the project was delayed. Independently, M. Baumgartner intended to complete a similar study in summer 2014 but his project was also delayed. If either project succeeds in 2015, it may be possible to update our model with a species-specific estimate of availability bias.

Density Models

Deemed the "forgotten whale" by a recent review paper, sei whales have received relatively little scientific study compared to the other baleen whales present in the western North Atlantic. Over the last two decades, the number of papers published about sei whales was only 15-35% of the number of papers published about each of those other species (Prieto et al. 2012). Much of the knowledge of sei whale distribution and movements is still based on whaling records (Prieto et al. 2012) although NOAA has published abundance estimates based on line-transect surveys (Waring et al. 2014). (Many of NOAA's surveys, as well as those from other organizations, are incorporated into the density models presented in this report.)

Sei whales are thought to follow a typical baleen whale migration pattern, moving to high latitudes in summer to feed and low latitudes in winter to breed or calve. The breeding and calving grounds for whales that feed in the western North Atlantic are still unknown. The surveys used in the model presented here reported sightings in the Gulf of Maine feeding grounds every month of the year. Sightings were very rare in winter, increased substantially in April, peaked in June, and fell markedly over the remaining summer months, with only 2 sightings reported in September. A small resurgence occurred in October and November and fell again with only 1 sighting reported in December.

An analysis of whaling records from the Blandford, Nova Scotia whaling station reported two "runs" of sei whales, in June-July and September-October, and speculated that sei whales migrate northward from Cape Cod along the Scotian Shelf in June and July, and return again in September and October (Mitchell 1975, as summarized by Waring et al. 2014). Although the sightings utilized here are consistent with this hypothesis, at least when not corrected for surveying effort, a direct investigation of this hypothesis was beyond the scope of our project. Nevertheless, the pattern is distinct enough that we opted to fit a four-season model, under the presumption that sei whales exhibit different relationships with the marine environment during different stages of this apparent multi-stage migratory pattern.

To determine the seasons, we first focused on May and June, the months that had the most sightings. To this we added April; although April had markedly fewer sightings than May, they were distributed in the same region and were substantially more numerous than March. We therefore fixed the winter/spring transition at March/April. In July, there were markedly fewer sightings in the Great South Channel than in June, and far fewer sightings in total, so we fixed the spring/summer transition at June/July. A small number of sightings were reported in October and November, and these were bookended by very sparse counts in September and December, so we fixed the summer/fall transition at September/October and the fall/winter transition at November/December.

The surveys used in our study, spanning 1992-2014, reported no definitive sightings of sei whales south of 40 N. NOAA surveys in 1992 and 1995 reported a total of four ambiguous "Bryde's or sei whale" sightings, all occurring in the month of January, between Florida and Cape Hatteras. Bryde's and sei whales are often confused with each other; disambiguating them can require careful counting of the number of head ridges (three in Bryde's whales, one in sei whales) that can be very difficult for distant sightings (Jefferson et al. 2008). Acoustic monitoring detected sei whales near Onslow Bay, North Carolina in October-March (Debich et al. 2014; Hodge and Read 2014) and near Jacksonville, Florida near the shelf break (Norris et al. 2014; Debich et al. 2013). Byrd et al. (2014) reported one sei whale stranding in North Carolina, in the month of February, and one Bryde's whale, in March. Rosel and Wilcox (2014) reported one Bryde's whale stranding in South Carolina (they did not specify the time of year).

Given the evidence that both sei whales and Bryde's whales occupy the Florida to Cape Hatteras portion of the U.S. exclusive economic zone in winter, that data on north Atlantic sei whale distributions are both scarce and sparse particularly for winter (Prieto et al. 2012), and that Bryde's whales in this region constitute a rare genetic unit that may eventually be considered one of the most endangered of the baleen whales (Rosel and Wilcox 2014), we included these four ambiguous sightings on both our sei whale and Bryde's whale density models. That is, in the sei whale model documented here, we counted these four sightings as sei whales, while in the Bryde's whale model documented elsewhere, we counted these four sightings as Bryde's whales. This is a precautionary decision that, in principle, may overestimate the density of one species or the other but recognizes that both are present in the area and allows ocean users and regulators to treat potentially harmful activities as having a non-zero impact on these species, rather than assuming a zero impact simply because the ambiguous sightings could not be resolved.

Winter

In this season, we lacked sufficient sightings to model density from environmental predictors and fitted a stratified model instead. Sightings were reported in both the northern and southern parts of the study area, both on and off the continental shelf. Given this wide albeit sparse distribution of sightings, we included the entire U.S. exclusive economic zone within the model's spatial domain. We excluded Canadian waters, as almost no survey effort occurred there in these months.

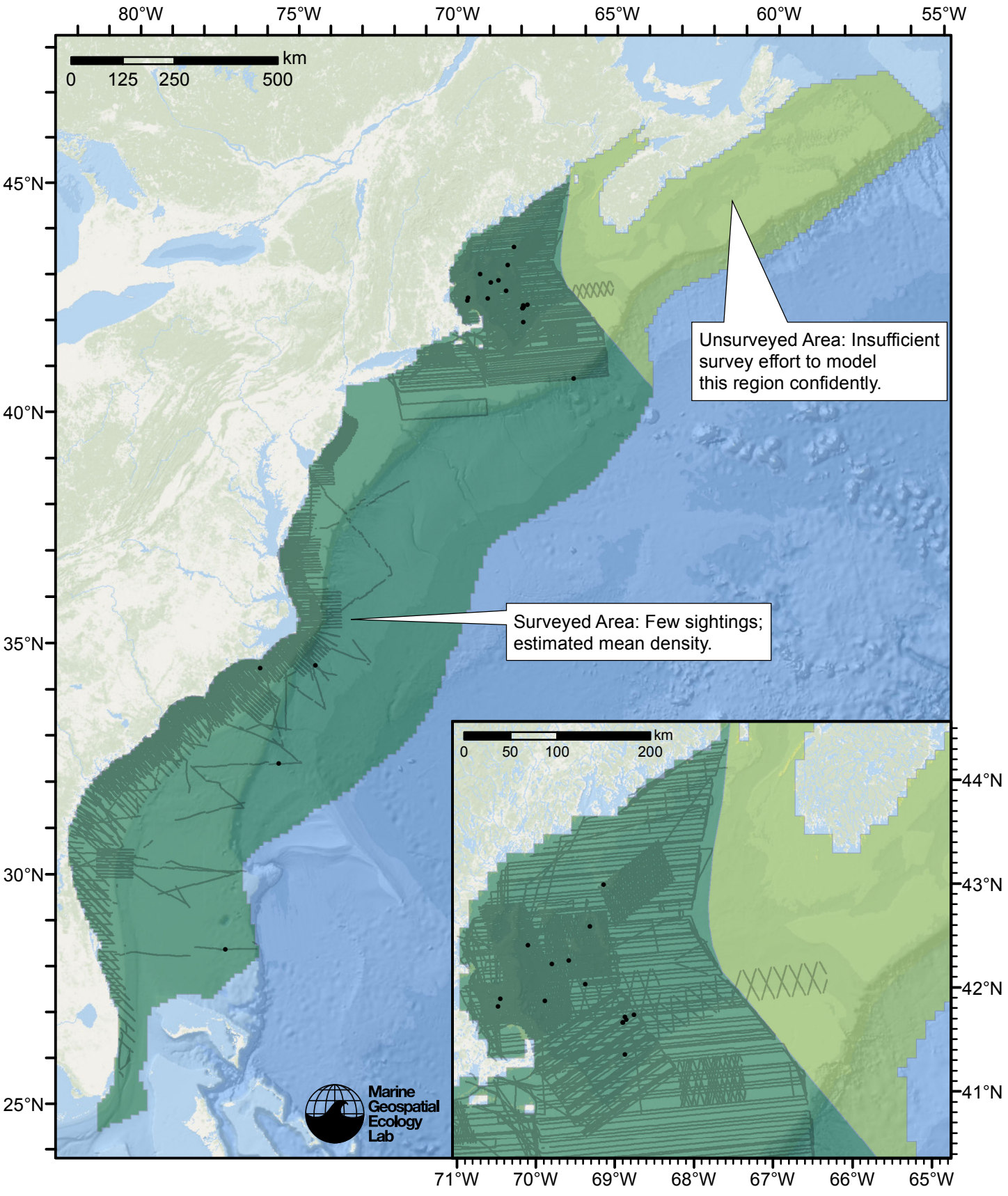

Figure 57: Sei whale density model schematic for Winter season. All on-effort sightings are shown, including those that were truncated when detection functions were fitted.

Climatological Model

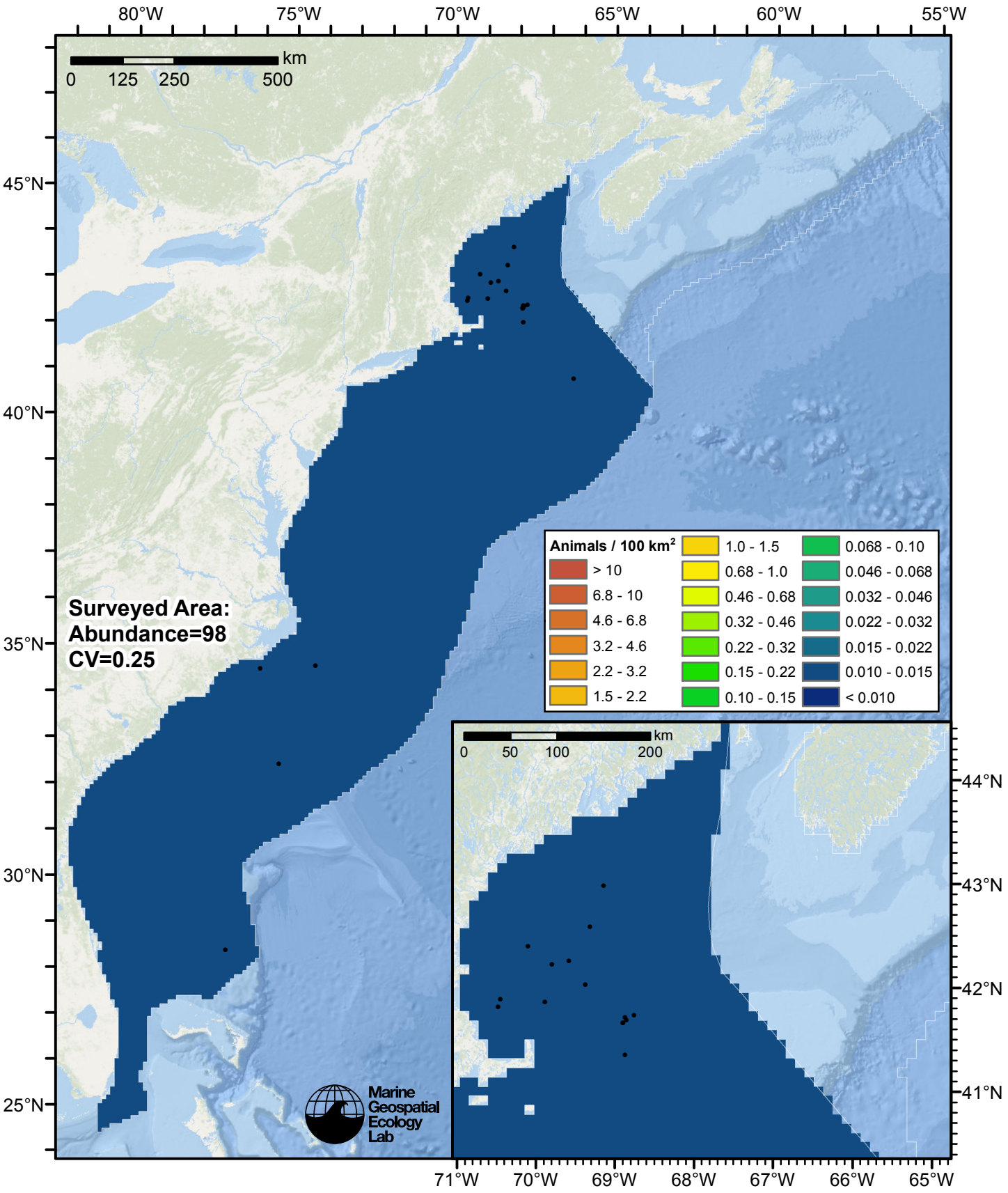

Figure 58: Sei whale density predicted by the Winter season climatological model that explained the most deviance. Pixels are 10x10 km. The legend gives the estimated individuals per pixel; breaks are logarithmic. The same scale is used for all seasons. Abundance for each region was computed by summing the density cells occuring in that region.

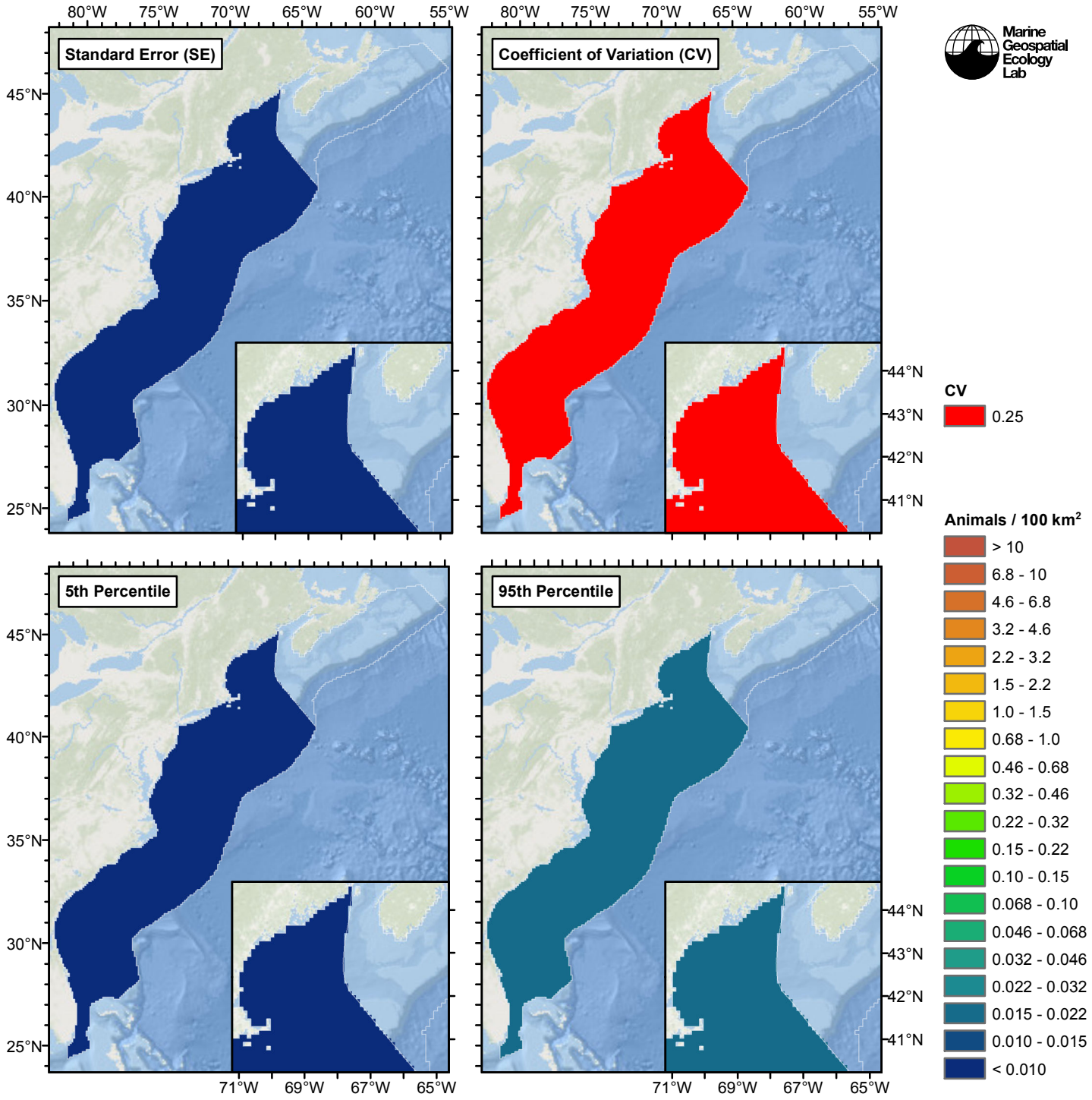

Figure 59: Estimated uncertainty for the Winter season climatological model that explained the most deviance. These estimates only incorporate the statistical uncertainty estimated for the spatial model (by the R mgcv package). They do not incorporate uncertainty in the detection functions, g(0) estimates, predictor variables, and so on.

Surveyed Area

A mean density estimate was made for this region. First, density (individuals per square kilometer) was calculated as the number of animals encountered divided by the area effectively surveyed, corrected by the detection functions and g(0) estimates. Then, density was multiplied by the size of each grid cell, in square kilometers, to obtain abundance (number of individuals) per grid cell. Finally, all grid cells in the region were assigned this abundance value.

Unsurveyed Area

Density was not modeled for this region.

Spring

In this season, the NOAA NARWSS program extensively surveyed the U.S. exclusive economic zone north of 40 N and reported many sightings of sei whales. No sei whales were reported south of this latitude. NOAA and UNCW performed substantial surveying along the continental shelf off North Carolina and Virginia, and spanning the shelf break at three U.S. Navy study sites off North Carolina and Florida. The remainder of the shelf was sparsely surveyed, and off-shelf surveying was very sparse. As with the winter model, we included the entire U.S. exclusive economic zone within the spring model's spatial domain, plus the portion of Canada's EEZ that encompasses Georges Bank, as NARWSS surveying in this season extended up the northern edge of Georges Bank.

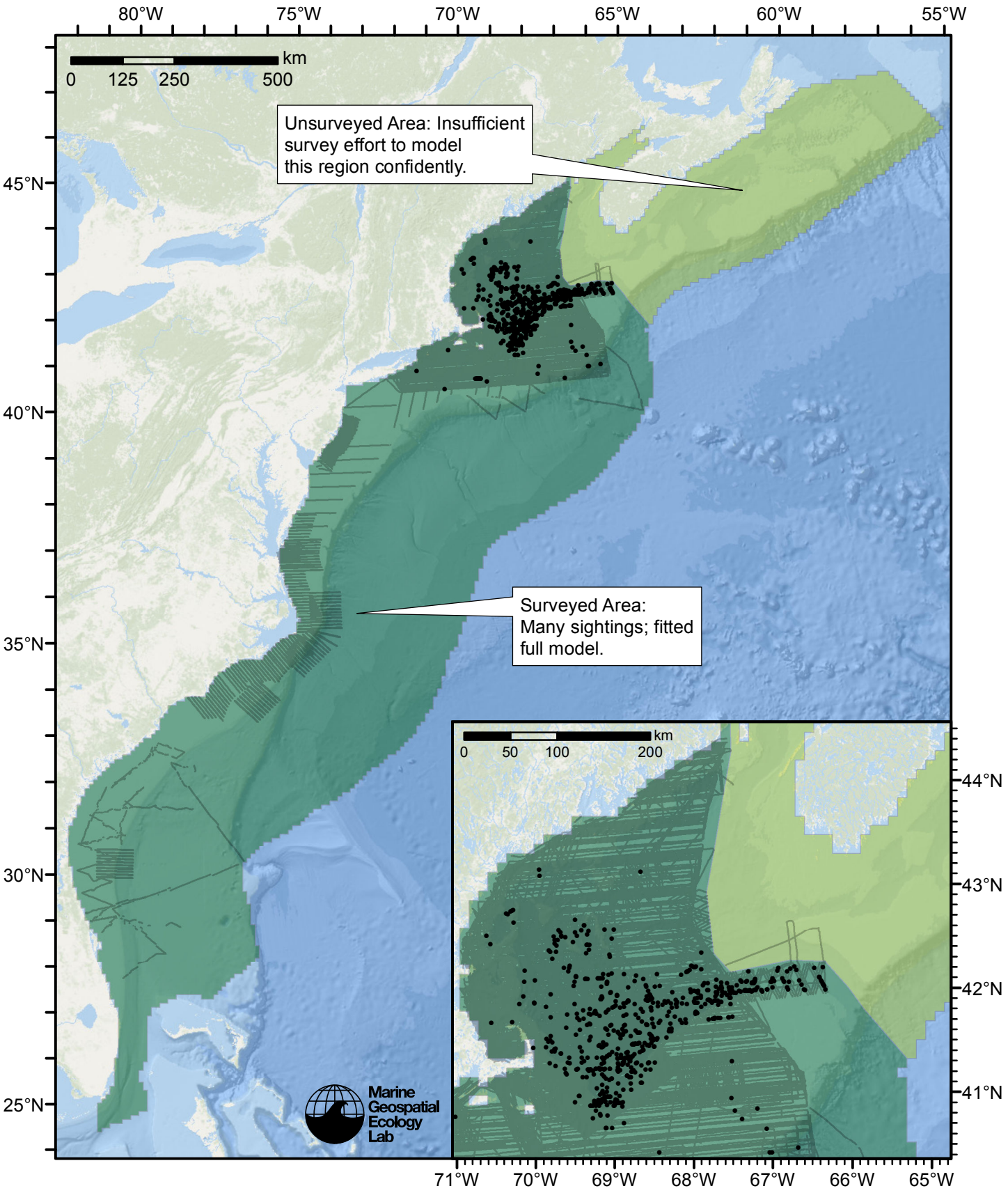

Figure 60: Sei whale density model schematic for Spring season. All on-effort sightings are shown, including those that were truncated when detection functions were fitted.

Climatological Model

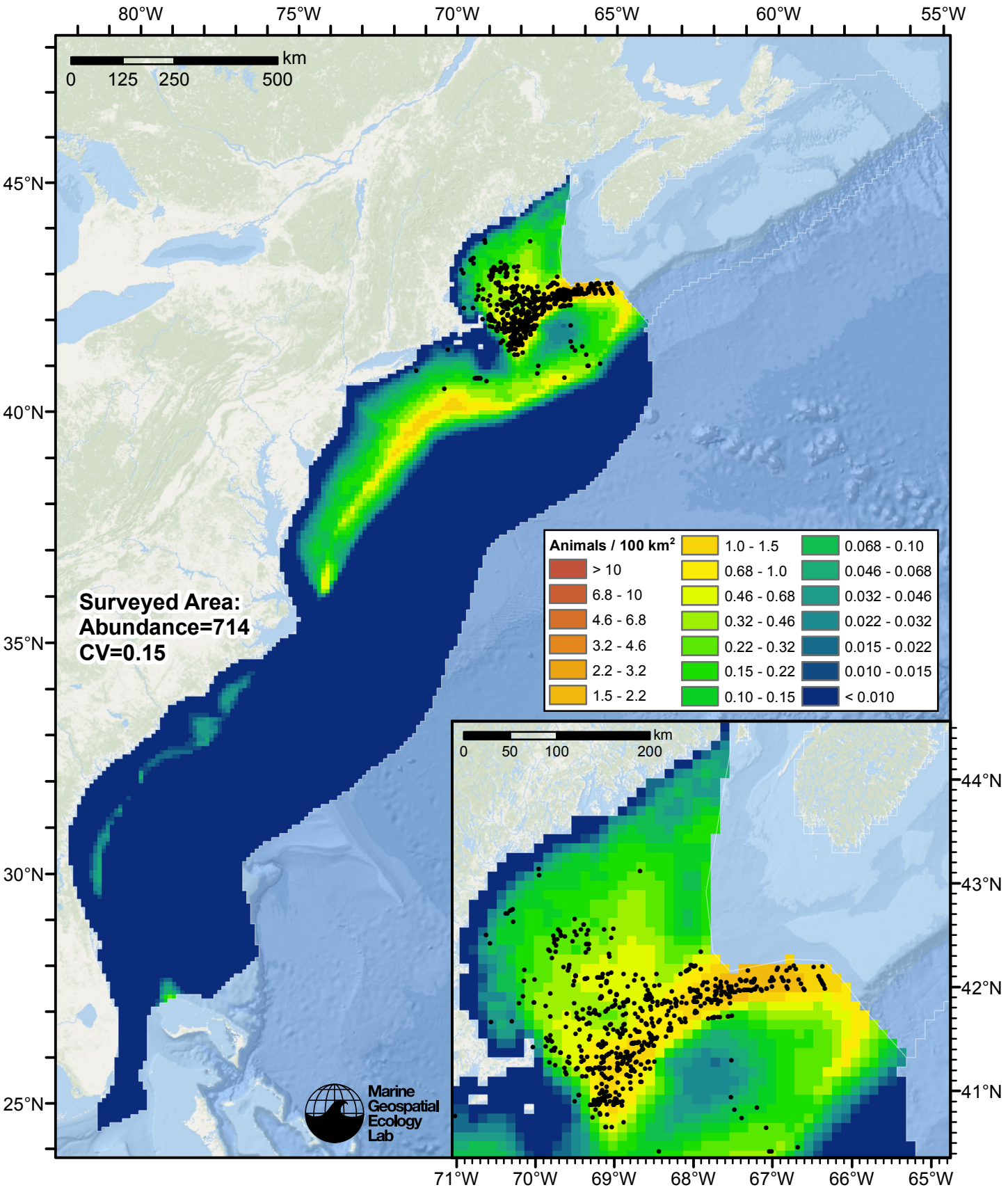

Figure 61: Sei whale density predicted by the Spring season climatological model that explained the most deviance. Pixels are 10x10 km. The legend gives the estimated individuals per pixel; breaks are logarithmic. The same scale is used for all seasons. Abundance for each region was computed by summing the density cells occuring in that region.

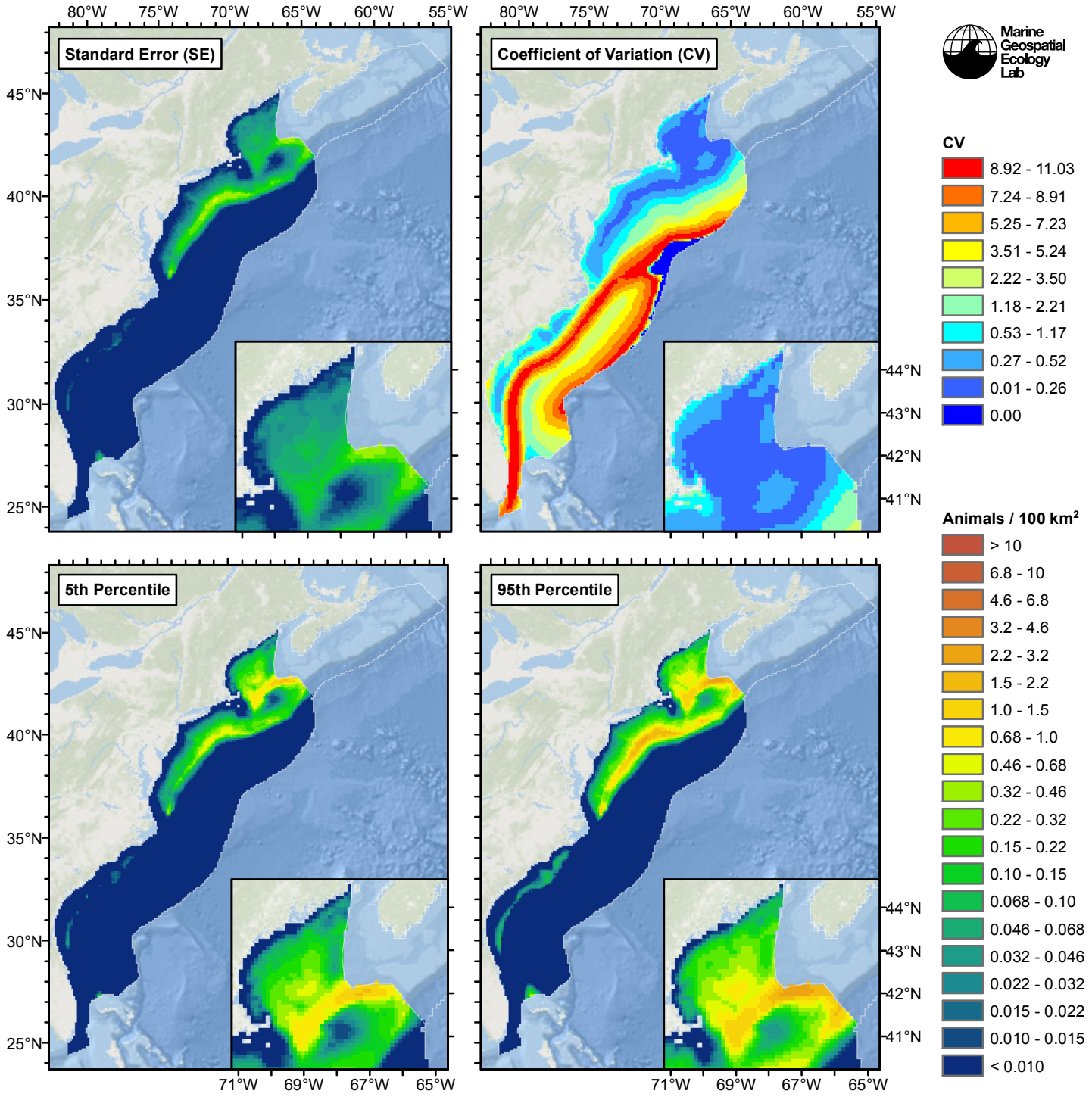

Figure 62: Estimated uncertainty for the Spring season climatological model that explained the most deviance. These estimates only incorporate the statistical uncertainty estimated for the spatial model (by the R mgcv package). They do not incorporate uncertainty in the detection functions, g(0) estimates, predictor variables, and so on.

Surveyed Area

Statistical output

```
Rscript.exe: This is mgcv 1.8-2. For overview type 'help("mgcv-package")'.


Family: Tweedie(p=1.26)
```

```
Link function: log

Formula:
abundance ~ offset(log(area_km2)) + s(log10(Depth), bs = "ts",
    k = 5) + s(I(DistTo125m/1000), bs = "ts", k = 5) + s(I(DistTo300m/1000),
    bs = "ts", k = 5) + s(I(ClimDistToFront2^(1/3)), bs = "ts",
    k = 5) + s(log10(pmax(ClimTKE, 1e-04)), bs = "ts", k = 5) +
    s(I(ClimCumVGPM90^(1/3)), bs = "ts", k = 5)

Parametric coefficients:
            Estimate Std. Error t value Pr(>|t|)
(Intercept)   -9.616      1.322  -7.275 3.54e-13 ***
---
Signif. codes:  0 '***' 0.001 '**' 0.01 '*' 0.05 '.' 0.1 ' ' 1

Approximate significance of smooth terms:
                                edf Ref.df      F  p-value
s(log10(Depth))               2.490      4  5.338 4.36e-06 ***
s(I(DistTo125m/1000))         2.954      4  6.858 6.56e-07 ***
s(I(DistTo300m/1000))         2.580      4 16.731  < 2e-16 ***
s(I(ClimDistToFront2^(1/3)))  3.136      4  5.477 2.03e-05 ***
s(log10(pmax(ClimTKE, 1e-04))) 2.144      4  5.005 1.59e-05 ***
s(I(ClimCumVGPM90^(1/3)))     2.795      4  7.167 3.28e-07 ***
---
Signif. codes:  0 '***' 0.001 '**' 0.01 '*' 0.05 '.' 0.1 ' ' 1

R-sq.(adj) =  0.0256   Deviance explained = 33.6%
-REML = 3519.5  Scale est. = 25.34     n = 33856

All predictors were significant. This is the final model.
Creating term plots.
Diagnostic output from gam.check():

Method: REML   Optimizer: outer newton
full convergence after 14 iterations.
Gradient range [-8.993162e-05,3.672071e-05]
(score 3519.45 & scale 25.34017).
Hessian positive definite, eigenvalue range [0.5941819,1884.96].
Model rank =  25 / 25

Basis dimension (k) checking results. Low p-value (k-index<1) may
indicate that k is too low, especially if edf is close to k'.

                                k'   edf k-index p-value
s(log10(Depth))               4.000 2.490   0.762    0.00
s(I(DistTo125m/1000))         4.000 2.954   0.813    0.01
s(I(DistTo300m/1000))         4.000 2.580   0.826    0.02
s(I(ClimDistToFront2^(1/3)))  4.000 3.136   0.847    0.35
s(log10(pmax(ClimTKE, 1e-04))) 4.000 2.144   0.786    0.00
s(I(ClimCumVGPM90^(1/3)))     4.000 2.795   0.812    0.00

Predictors retained during the model selection procedure: Depth, DistTo125m, DistTo300m,
ClimDistToFront2, ClimTKE, ClimCumVGPM90

Predictors dropped during the model selection procedure: Slope, ClimSST
```

Model term plots

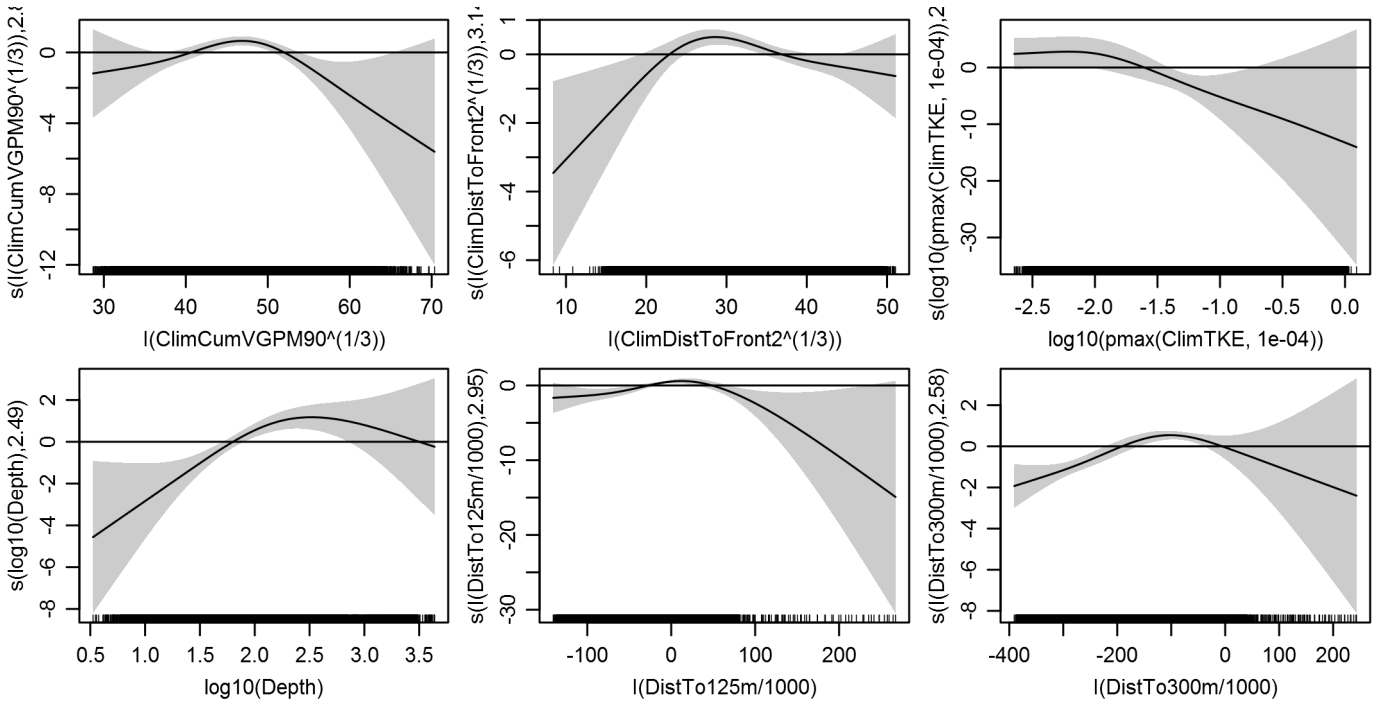

Diagnostic plots

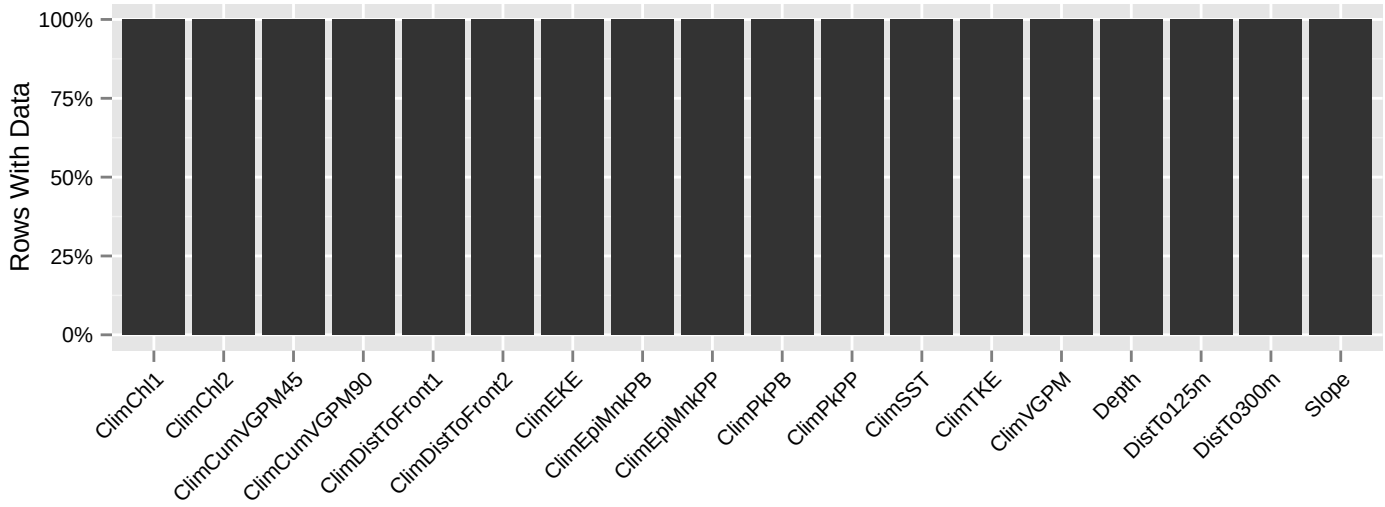

Figure 63: Segments with predictor values for the Sei whale Climatological model, Spring season, Surveyed Area. This plot is used to assess how many segments would be lost by including a given predictor in a model.

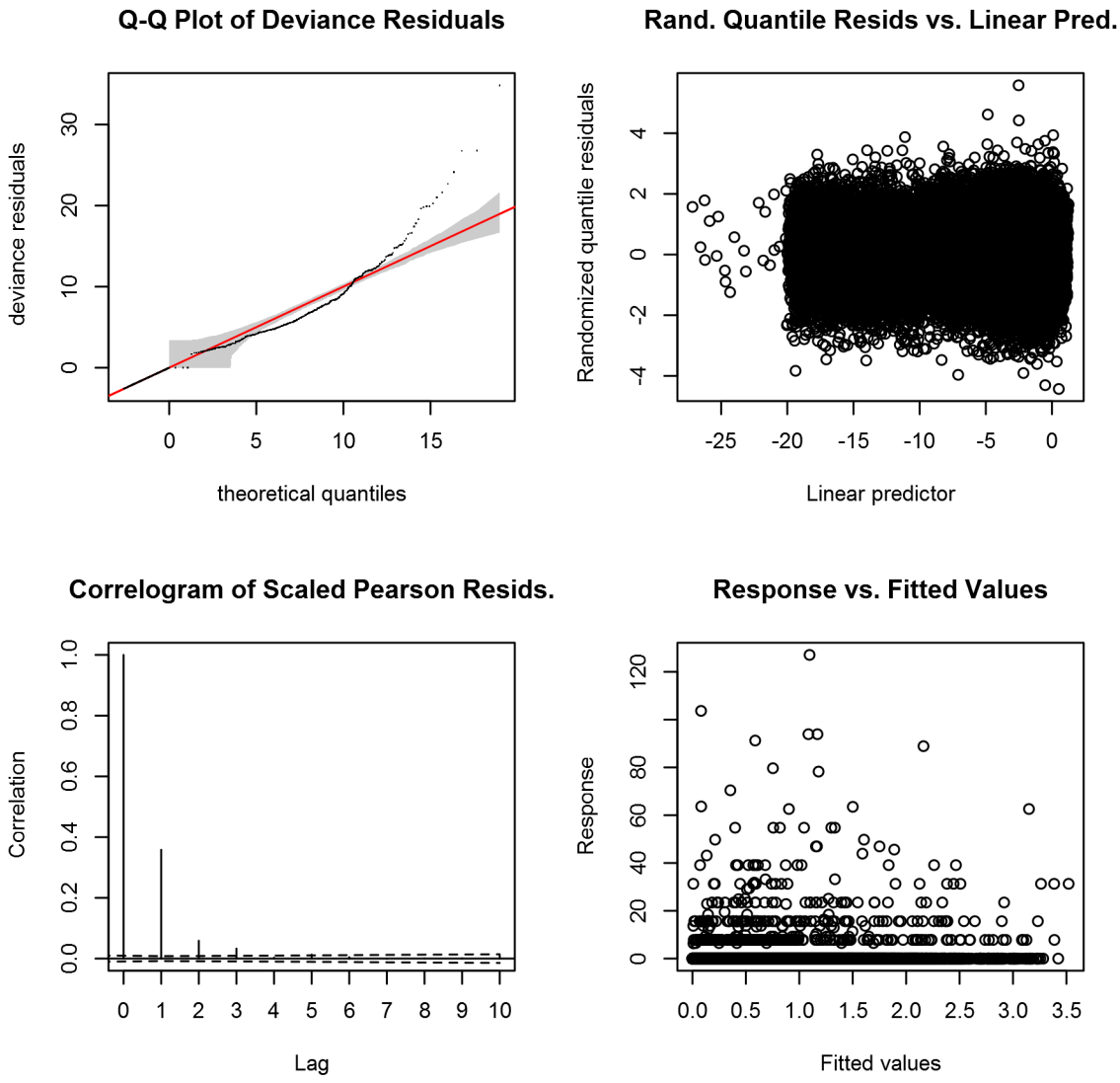

Figure 64: Statistical diagnostic plots for the Sei whale Climatological model, Spring season, Surveyed Area.

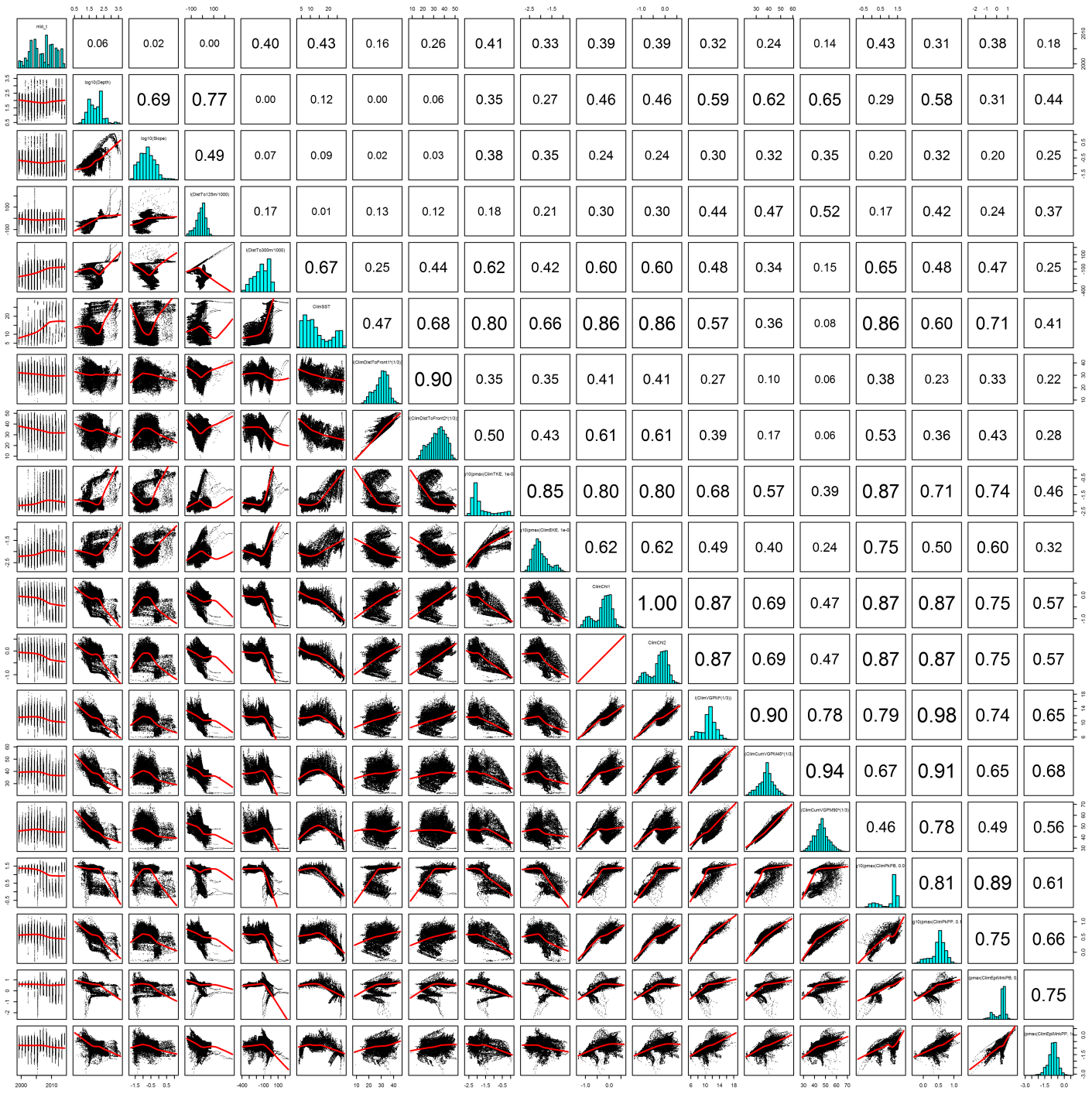

Figure 65: Scatterplot matrix for the Sei whale Climatological model, Spring season, Surveyed Area. This plot is used to inspect the distribution of predictors (via histograms along the diagonal), simple correlation between predictors (via pairwise Pearson coefficients above the diagonal), and linearity of predictor correlations (via scatterplots below the diagonal). This plot is best viewed at high magnification.

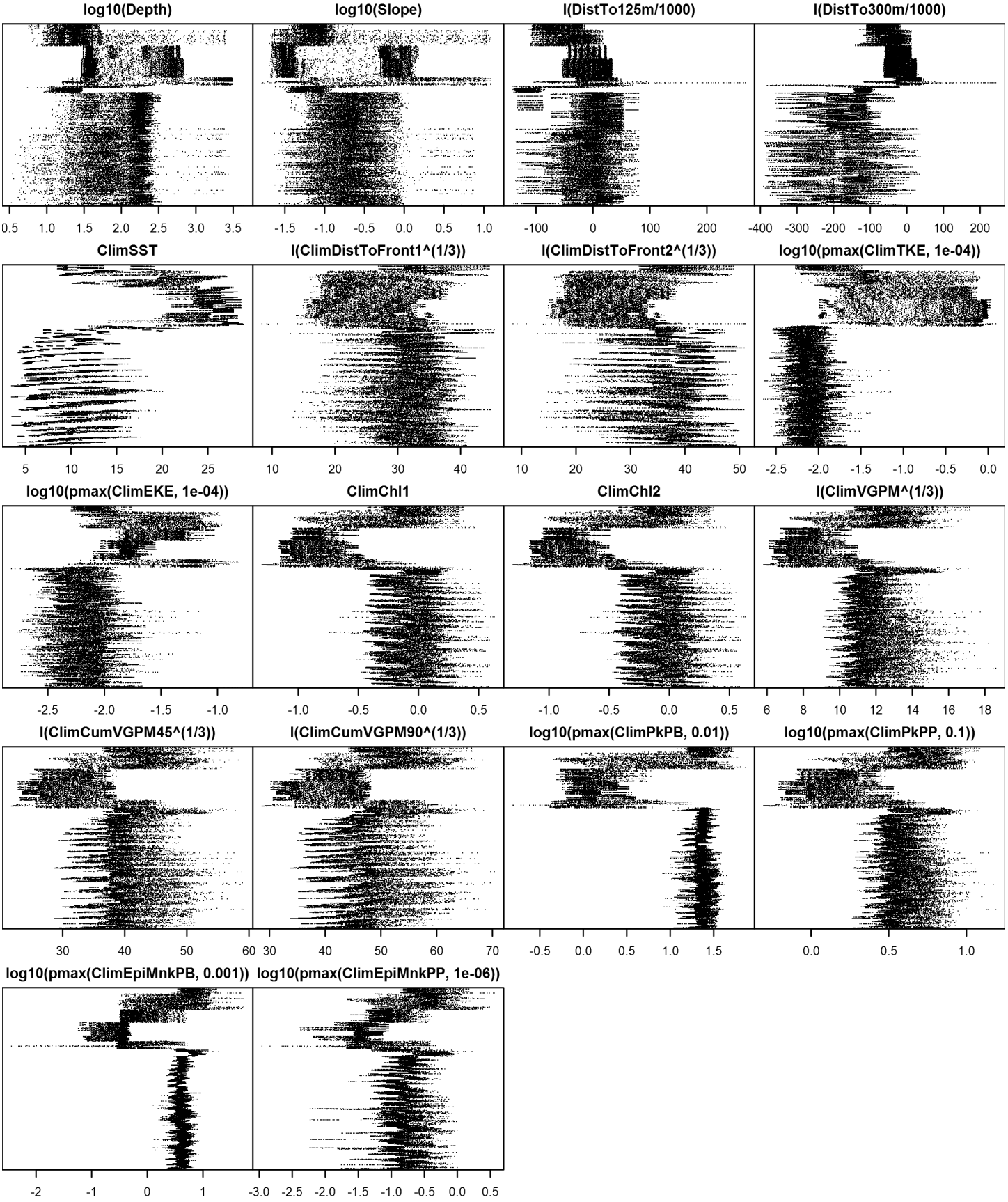

Figure 66: Dotplot for the Sei whale Climatological model, Spring season, Surveyed Area. This plot is used to check for suspicious patterns and outliers in the data. Points are ordered vertically by transect ID, sequentially in time.

Unsurveyed Area

Density was not modeled for this region.

Contemporaneous Model

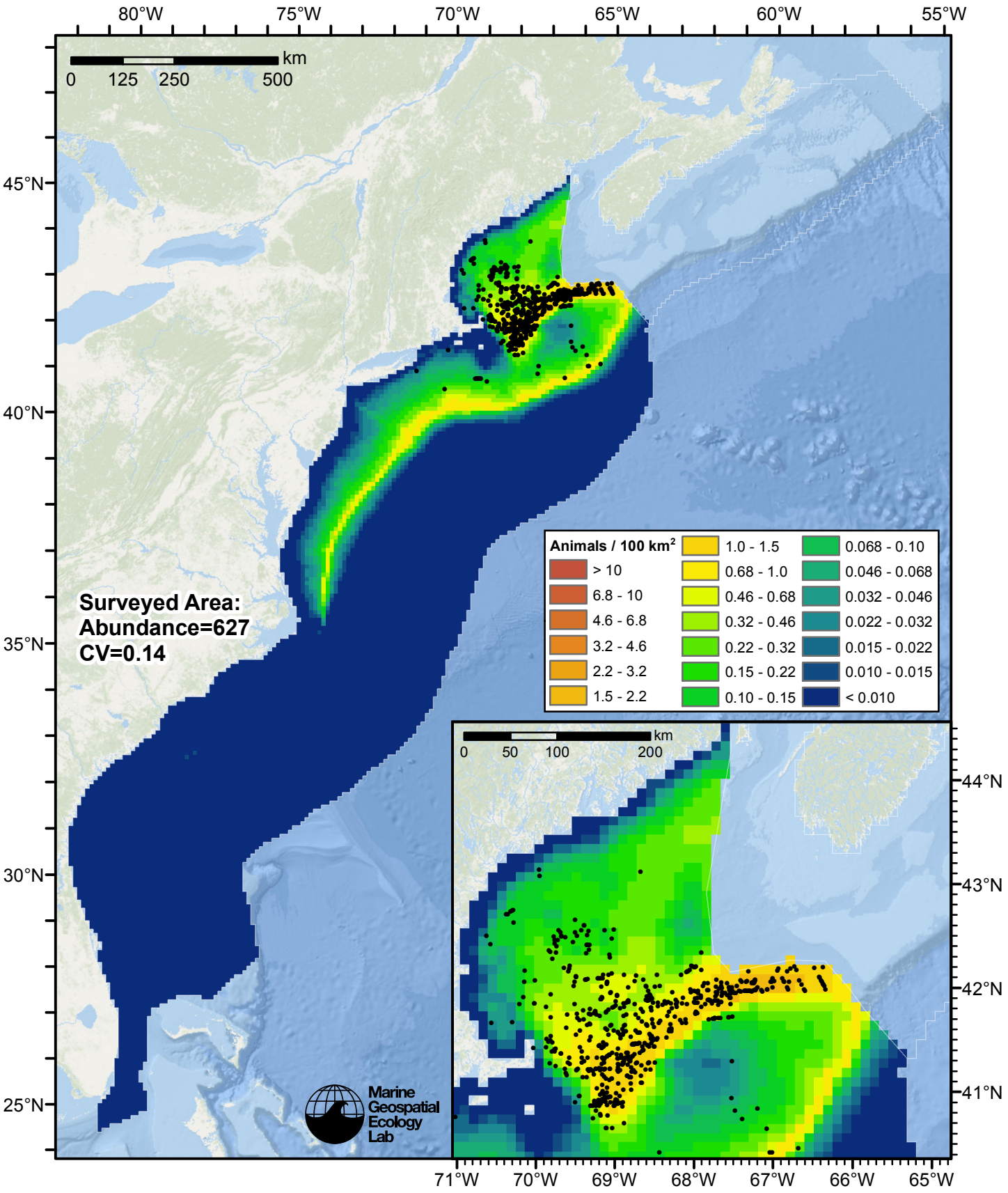

Figure 67: Sei whale density predicted by the Spring season contemporaneous model that explained the most deviance. Pixels are 10x10 km. The legend gives the estimated individuals per pixel; breaks are logarithmic. The same scale is used for all seasons. Abundance for each region was computed by summing the density cells occuring in that region.

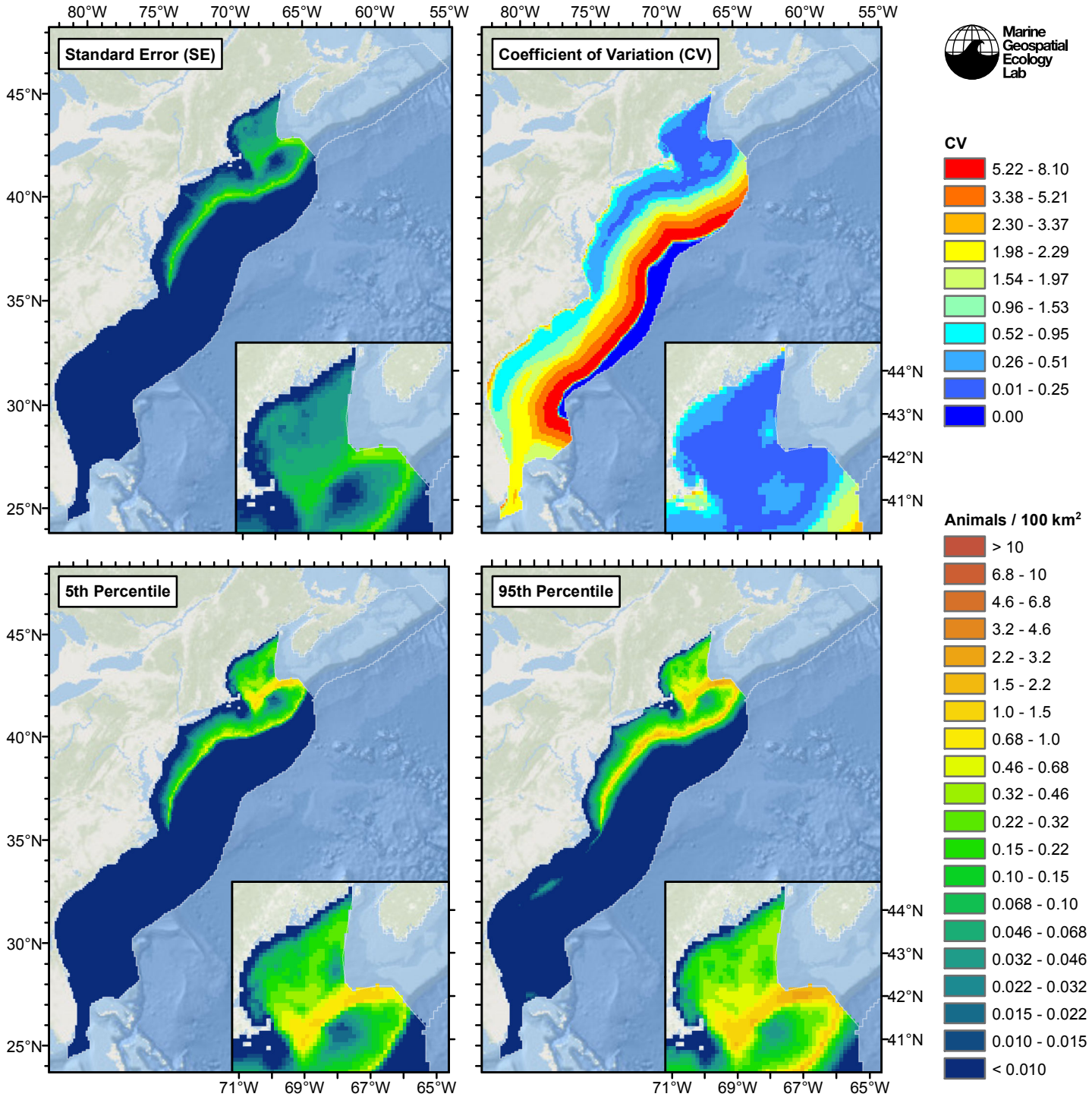

Figure 68: Estimated uncertainty for the Spring season contemporaneous model that explained the most deviance. These estimates only incorporate the statistical uncertainty estimated for the spatial model (by the R mgcv package). They do not incorporate uncertainty in the detection functions, g(0) estimates, predictor variables, and so on.

Surveyed Area

Statistical output

```
Rscript.exe: This is mgcv 1.8-2. For overview type 'help("mgcv-package")'.


Family: Tweedie(p=1.262)
```

```
Link function: log

Formula:
abundance ~ offset(log(area_km2)) + s(log10(Depth), bs = "ts",
    k = 5) + s(I(DistTo125m/1000), bs = "ts", k = 5) + s(I(DistTo300m/1000),
    bs = "ts", k = 5) + s(SST, bs = "ts", k = 5) + s(log10(pmax(TKE,
    1e-04)), bs = "ts", k = 5) + s(I(CumVGPM90^(1/3)), bs = "ts",
    k = 5)

Parametric coefficients:
            Estimate Std. Error t value Pr(>|t|)
(Intercept)  -8.6529     0.4228  -20.47   <2e-16 ***
---
Signif. codes:  0 '***' 0.001 '**' 0.01 '*' 0.05 '.' 0.1 ' ' 1

Approximate significance of smooth terms:
                             edf Ref.df      F  p-value
s(log10(Depth))            3.090      4  9.118 3.75e-09 ***
s(I(DistTo125m/1000))      3.291      4  6.713 2.06e-06 ***
s(I(DistTo300m/1000))      2.689      4 22.644  < 2e-16 ***
s(SST)                     2.944      4  8.586 2.44e-08 ***
s(log10(pmax(TKE, 1e-04))) 2.313      4  2.998  0.00185 **
s(I(CumVGPM90^(1/3)))      3.535      4 12.525 1.97e-11 ***
---
Signif. codes:  0 '***' 0.001 '**' 0.01 '*' 0.05 '.' 0.1 ' ' 1

R-sq.(adj) =  0.0254   Deviance explained = 34.2%
-REML = 3510.4  Scale est. = 25.23     n = 33367

All predictors were significant. This is the final model.
Creating term plots.
Diagnostic output from gam.check():

Method: REML   Optimizer: outer newton
full convergence after 11 iterations.
Gradient range [-1.274421e-06,3.848938e-07]
(score 3510.422 & scale 25.22958).
Hessian positive definite, eigenvalue range [0.4356145,1863.095].
Model rank =  25 / 25

Basis dimension (k) checking results. Low p-value (k-index<1) may
indicate that k is too low, especially if edf is close to k'.

                             k'   edf k-index p-value
s(log10(Depth))            4.000 3.090   0.838    0.01
s(I(DistTo125m/1000))      4.000 3.291   0.843    0.03
s(I(DistTo300m/1000))      4.000 2.689   0.848    0.06
s(SST)                     4.000 2.944   0.779    0.00
s(log10(pmax(TKE, 1e-04))) 4.000 2.313   0.852    0.07
s(I(CumVGPM90^(1/3)))      4.000 3.535   0.869    0.37

Predictors retained during the model selection procedure: Depth, DistTo125m, DistTo300m, SST, TKE,
CumVGPM90

Predictors dropped during the model selection procedure: Slope, DistToFront1
```

Model term plots

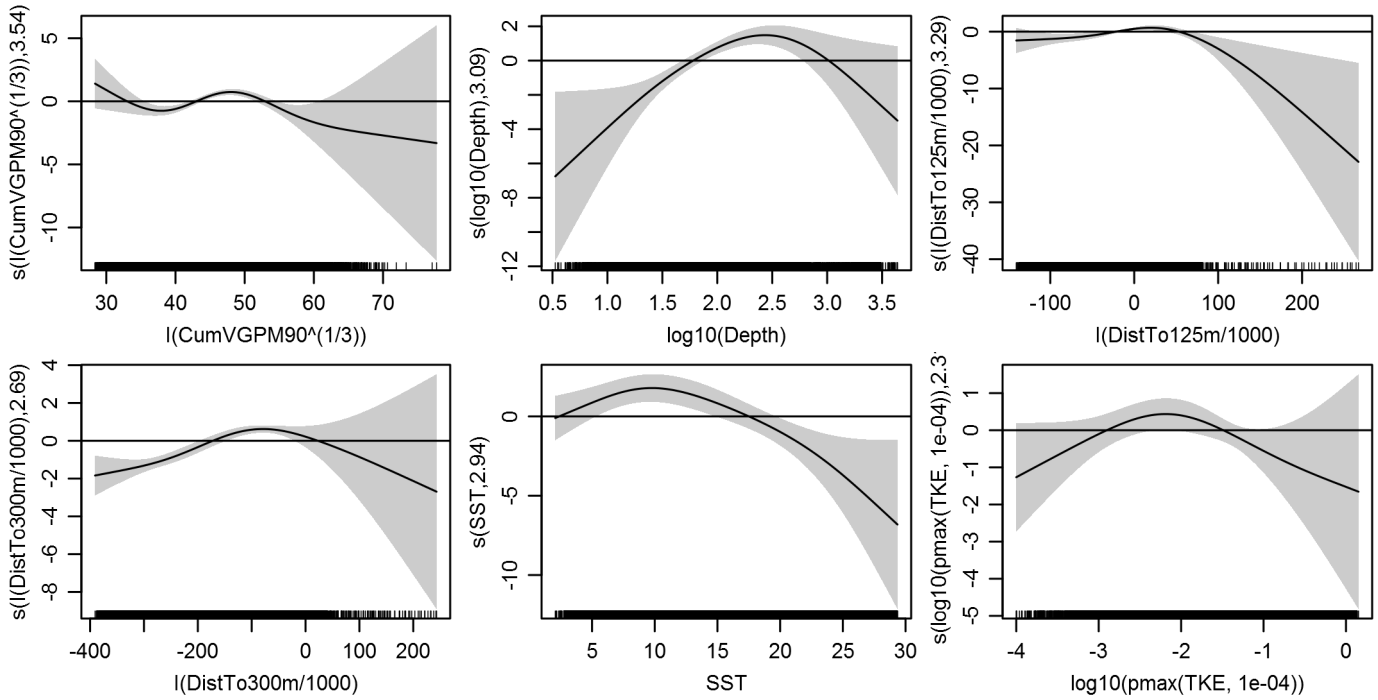

Diagnostic plots

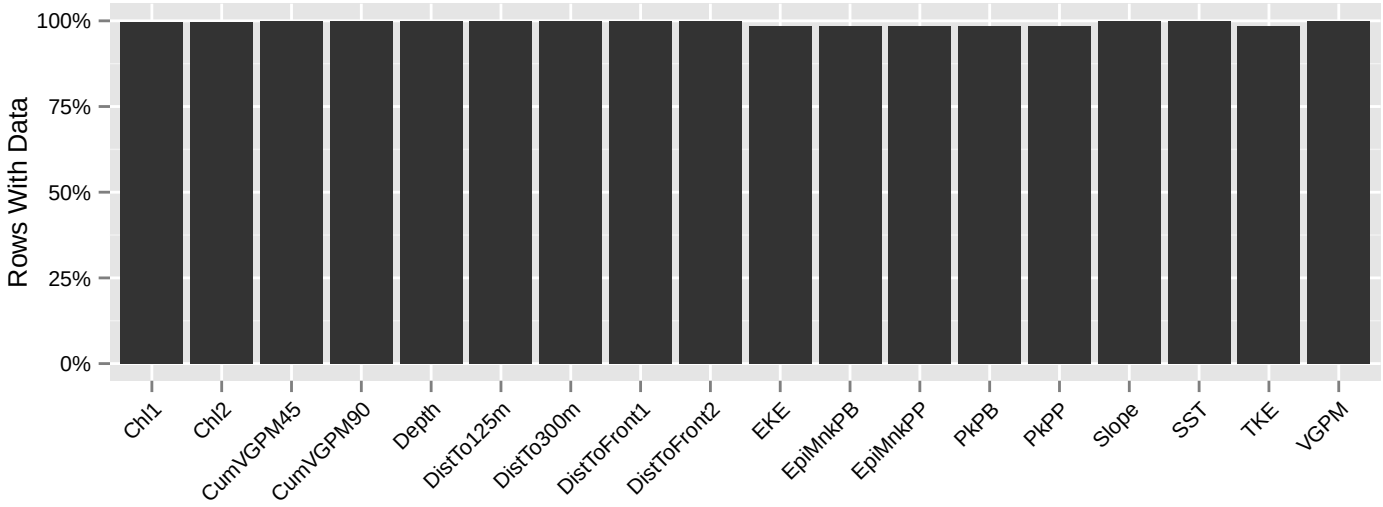

Figure 69: Segments with predictor values for the Sei whale Contemporaneous model, Spring season, Surveyed Area. This plot is used to assess how many segments would be lost by including a given predictor in a model.

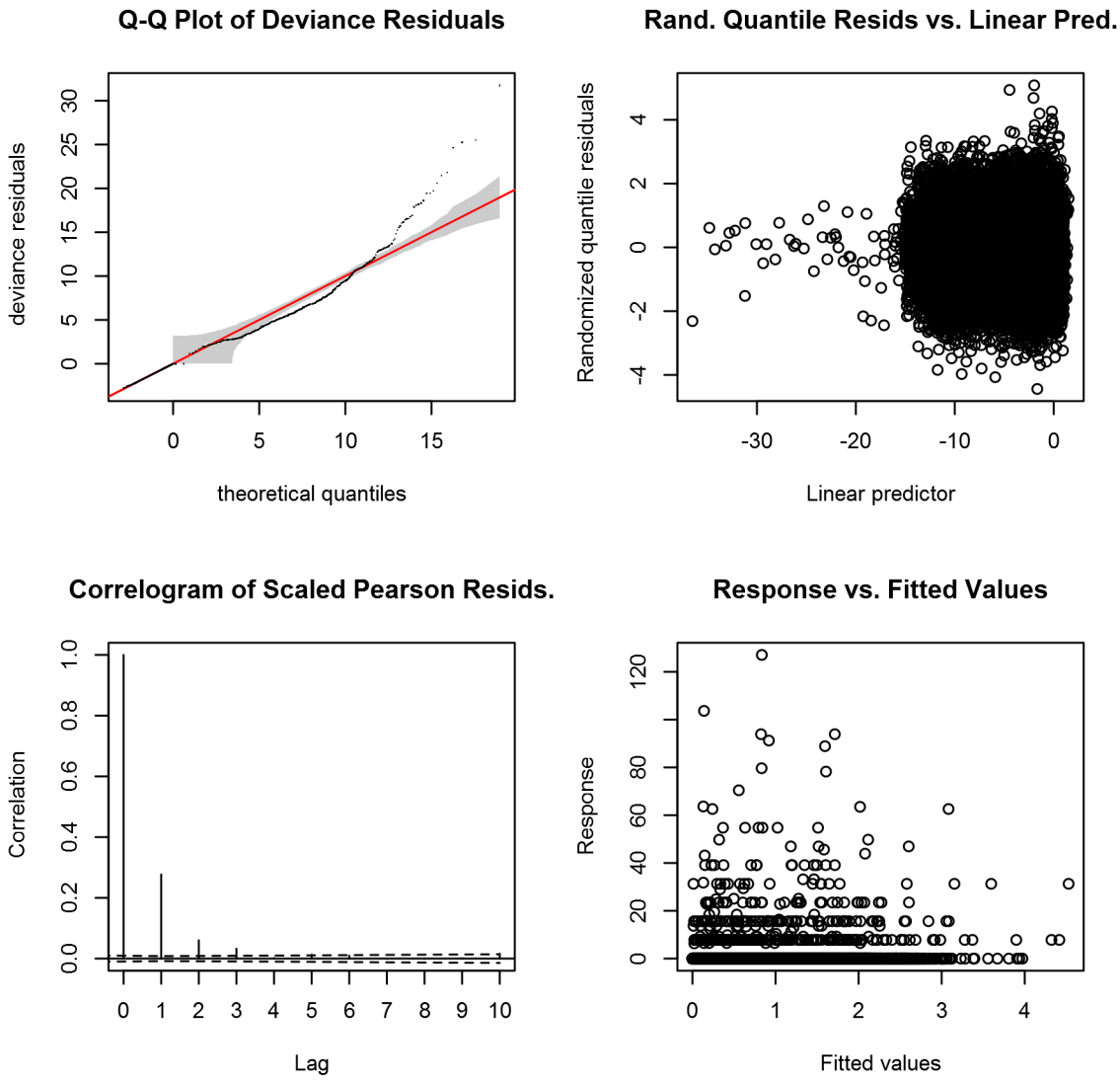

Figure 70: Statistical diagnostic plots for the Sei whale Contemporaneous model, Spring season, Surveyed Area.

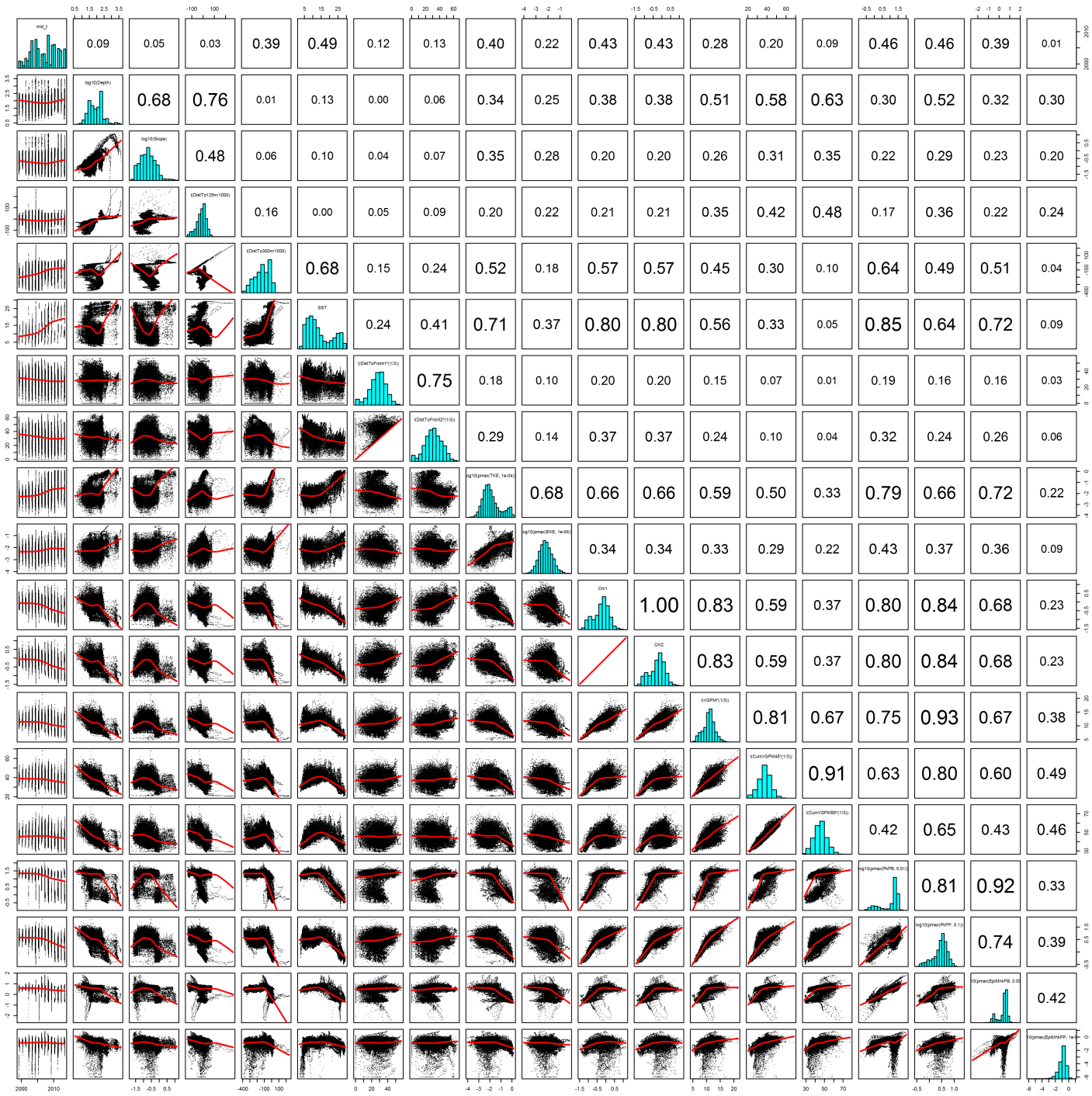

Figure 71: Scatterplot matrix for the Sei whale Contemporaneous model, Spring season, Surveyed Area. This plot is used to inspect the distribution of predictors (via histograms along the diagonal), simple correlation between predictors (via pairwise Pearson coefficients above the diagonal), and linearity of predictor correlations (via scatterplots below the diagonal). This plot is best viewed at high magnification.

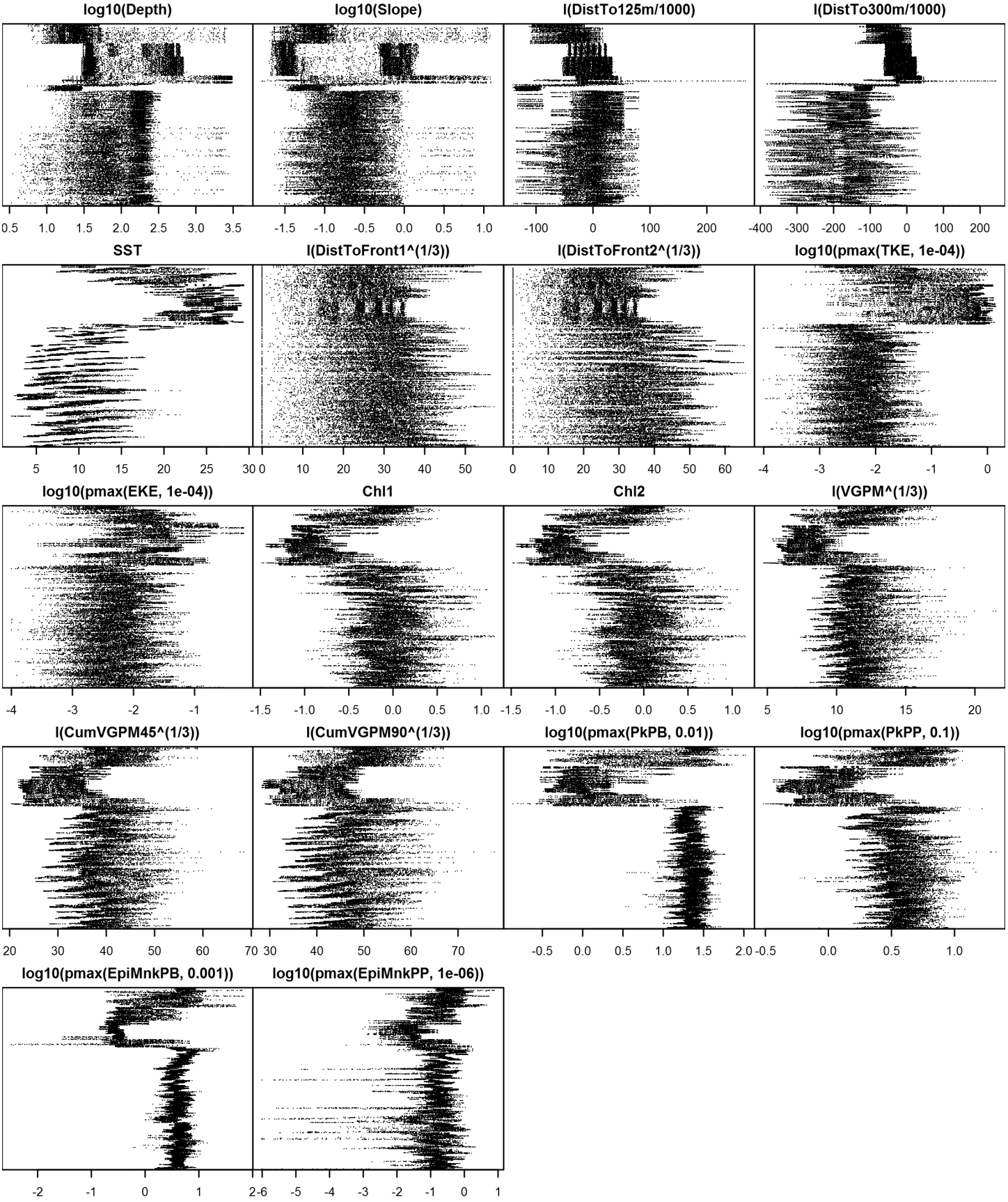

Figure 72: Dotplot for the Sei whale Contemporaneous model, Spring season, Surveyed Area. This plot is used to check for suspicious patterns and outliers in the data. Points are ordered vertically by transect ID, sequentially in time.

Unsurveyed Area

Density was not modeled for this region.

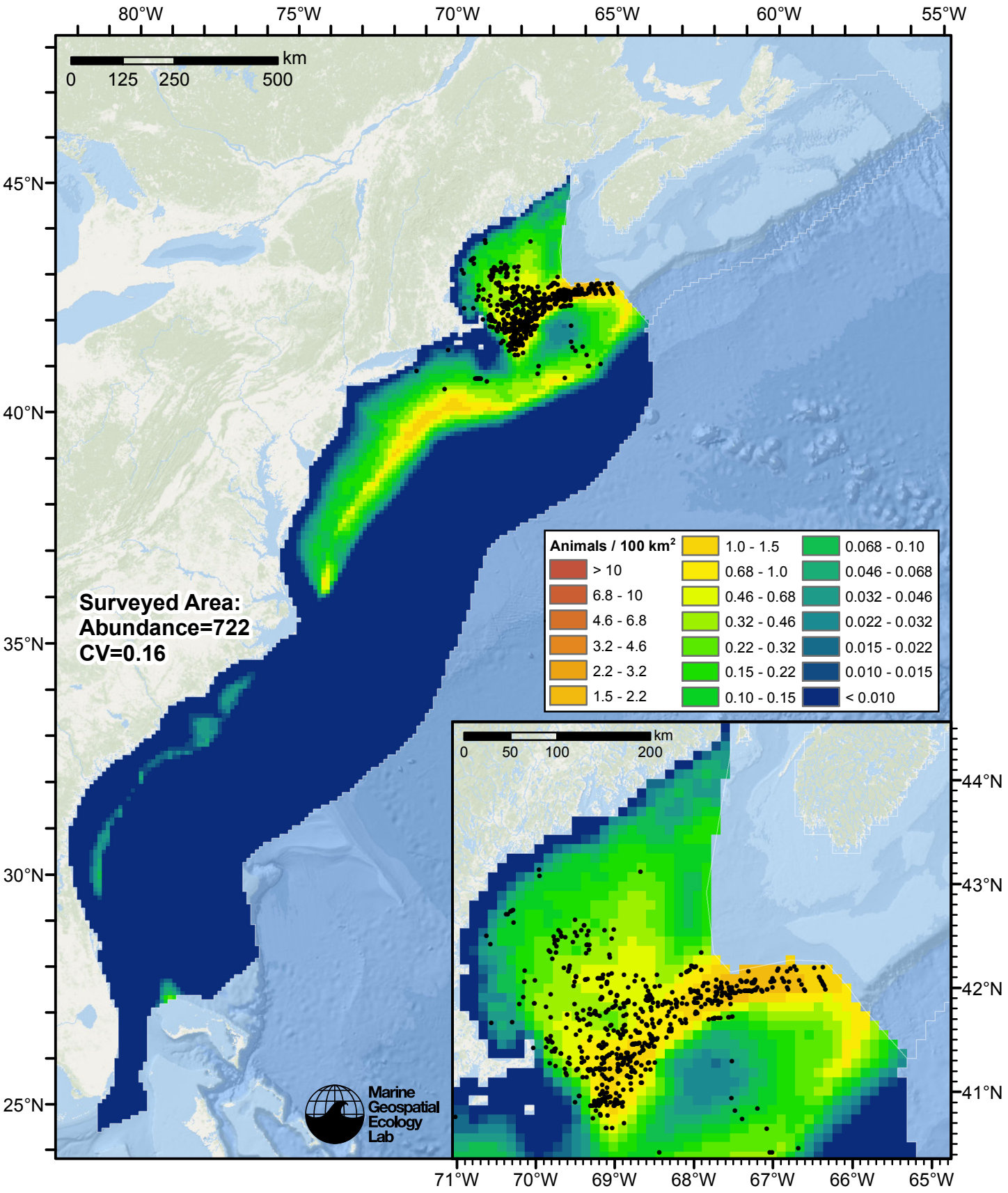

Figure 73: Sei whale density predicted by the Spring season climatological same segments model that explained the most deviance. Pixels are 10x10 km. The legend gives the estimated individuals per pixel; breaks are logarithmic. The same scale is used for all seasons. Abundance for each region was computed by summing the density cells occuring in that region.

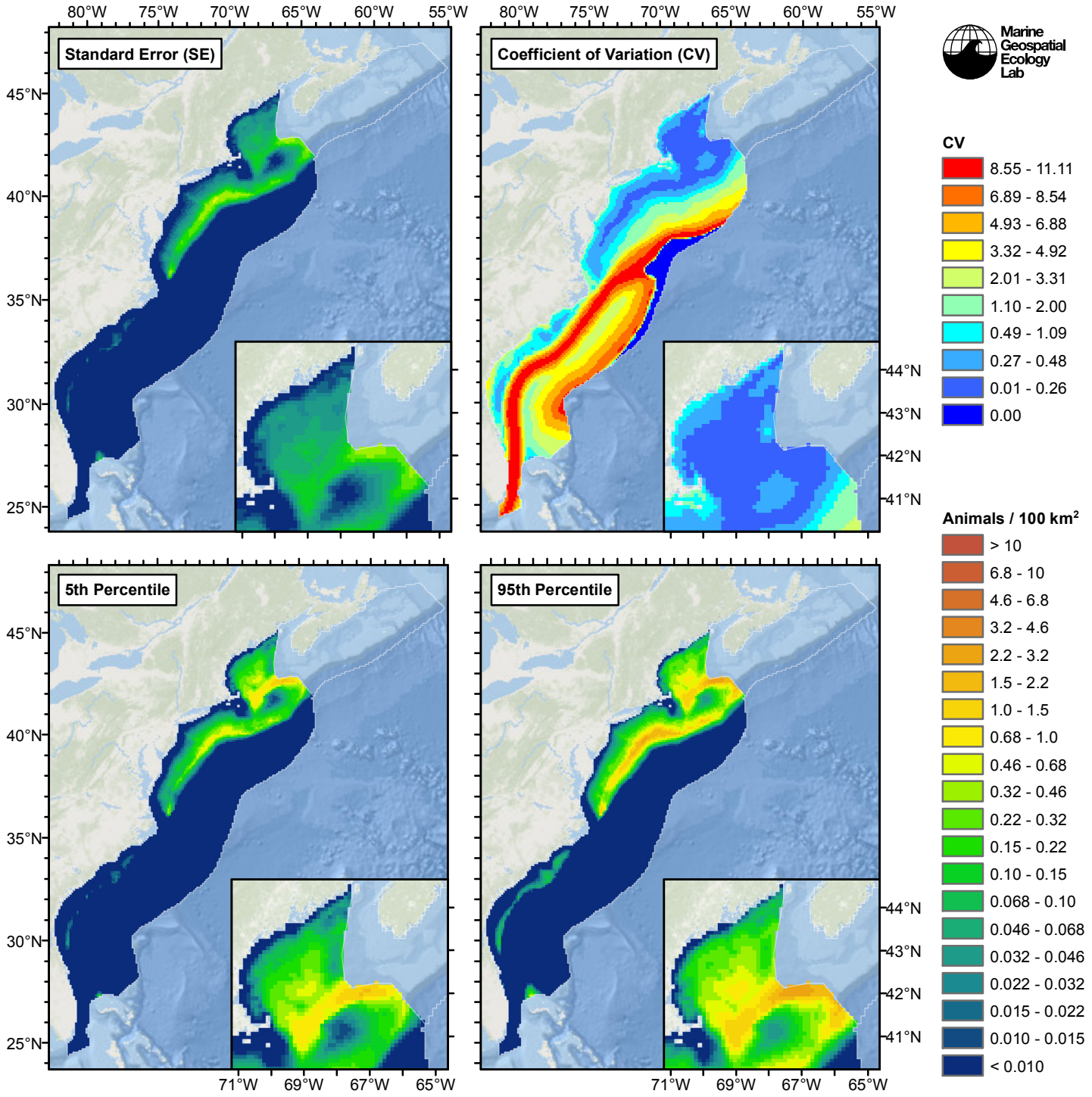

Figure 74: Estimated uncertainty for the Spring season climatological same segments model that explained the most deviance. These estimates only incorporate the statistical uncertainty estimated for the spatial model (by the R mgcv package). They do not incorporate uncertainty in the detection functions, g(0) estimates, predictor variables, and so on.

Surveyed Area

Statistical output

```
Rscript.exe: This is mgcv 1.8-2. For overview type 'help("mgcv-package")'.


Family: Tweedie(p=1.261)
```

```
Link function: log

Formula:
abundance ~ offset(log(area_km2)) + s(log10(Depth), bs = "ts",
    k = 5) + s(I(DistTo125m/1000), bs = "ts", k = 5) + s(I(DistTo300m/1000),
    bs = "ts", k = 5) + s(I(ClimDistToFront2^(1/3)), bs = "ts",
    k = 5) + s(log10(pmax(ClimTKE, 1e-04)), bs = "ts", k = 5) +
    s(I(ClimCumVGPM90^(1/3)), bs = "ts", k = 5)

Parametric coefficients:
            Estimate Std. Error t value Pr(>|t|)
(Intercept)   -9.628      1.348   -7.14  9.5e-13 ***
---
Signif. codes:  0 '***' 0.001 '**' 0.01 '*' 0.05 '.' 0.1 ' ' 1

Approximate significance of smooth terms:
                                edf Ref.df      F  p-value
s(log10(Depth))               2.478      4  5.005 9.39e-06 ***
s(I(DistTo125m/1000))         3.069      4  6.998 5.36e-07 ***
s(I(DistTo300m/1000))         2.553      4 16.665  < 2e-16 ***
s(I(ClimDistToFront2^(1/3)))  3.126      4  5.447 2.13e-05 ***
s(log10(pmax(ClimTKE, 1e-04))) 2.147      4  5.010 1.59e-05 ***
s(I(ClimCumVGPM90^(1/3)))     2.804      4  7.257 2.72e-07 ***
---
Signif. codes:  0 '***' 0.001 '**' 0.01 '*' 0.05 '.' 0.1 ' ' 1

R-sq.(adj) =  0.0254   Deviance explained = 33.3%
-REML = 3518.8  Scale est. = 25.349    n = 33367

All predictors were significant. This is the final model.
Creating term plots.
Diagnostic output from gam.check():

Method: REML   Optimizer: outer newton
full convergence after 15 iterations.
Gradient range [-0.0001279604,2.878234e-05]
(score 3518.759 & scale 25.34884).
Hessian positive definite, eigenvalue range [0.579078,1882.45].
Model rank =  25 / 25

Basis dimension (k) checking results. Low p-value (k-index<1) may
indicate that k is too low, especially if edf is close to k'.

                                k'   edf k-index p-value
s(log10(Depth))               4.000 2.478   0.776    0.00
s(I(DistTo125m/1000))         4.000 3.069   0.817    0.04
s(I(DistTo300m/1000))         4.000 2.553   0.789    0.00
s(I(ClimDistToFront2^(1/3)))  4.000 3.126   0.818    0.04
s(log10(pmax(ClimTKE, 1e-04))) 4.000 2.147   0.702    0.00
s(I(ClimCumVGPM90^(1/3)))     4.000 2.804   0.787    0.00

Predictors retained during the model selection procedure: Depth, DistTo125m, DistTo300m,
ClimDistToFront2, ClimTKE, ClimCumVGPM90

Predictors dropped during the model selection procedure: Slope, ClimSST
```

Model term plots

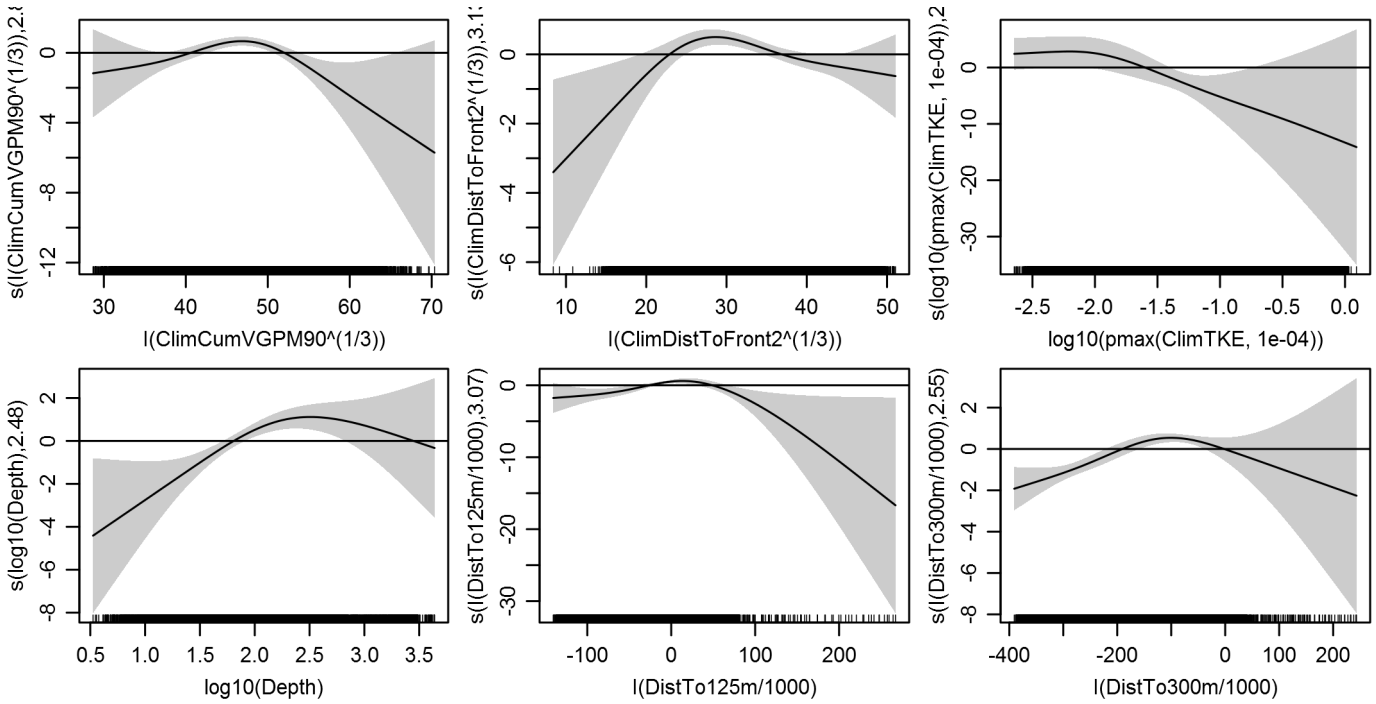

Diagnostic plots

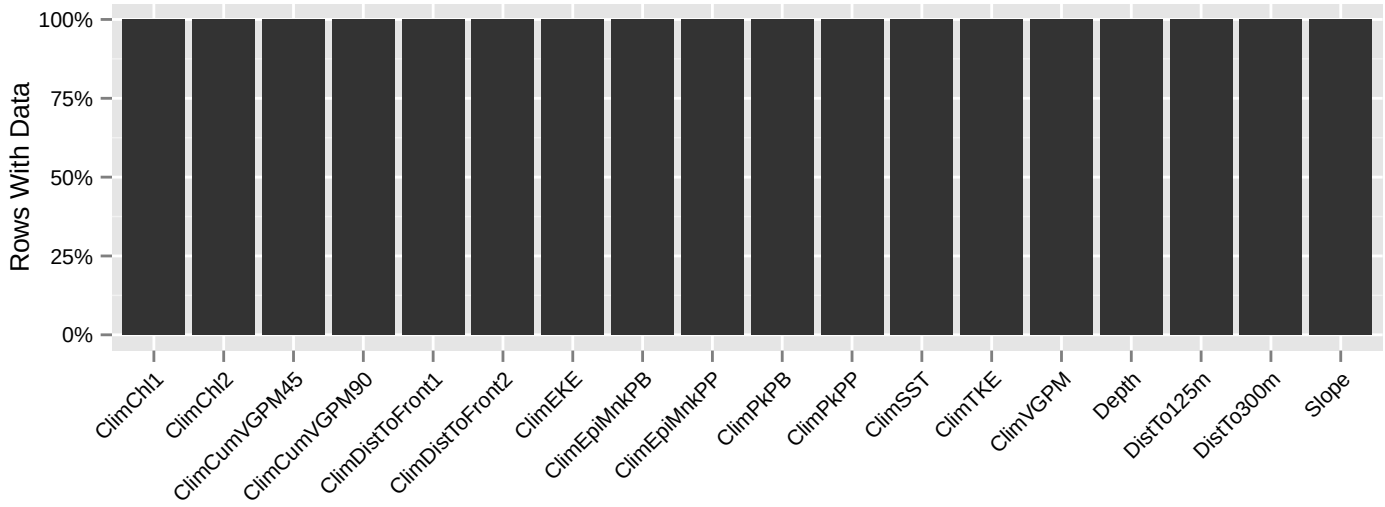

Figure 75: Segments with predictor values for the Sei whale Climatological model, Spring season, Surveyed Area. This plot is used to assess how many segments would be lost by including a given predictor in a model.

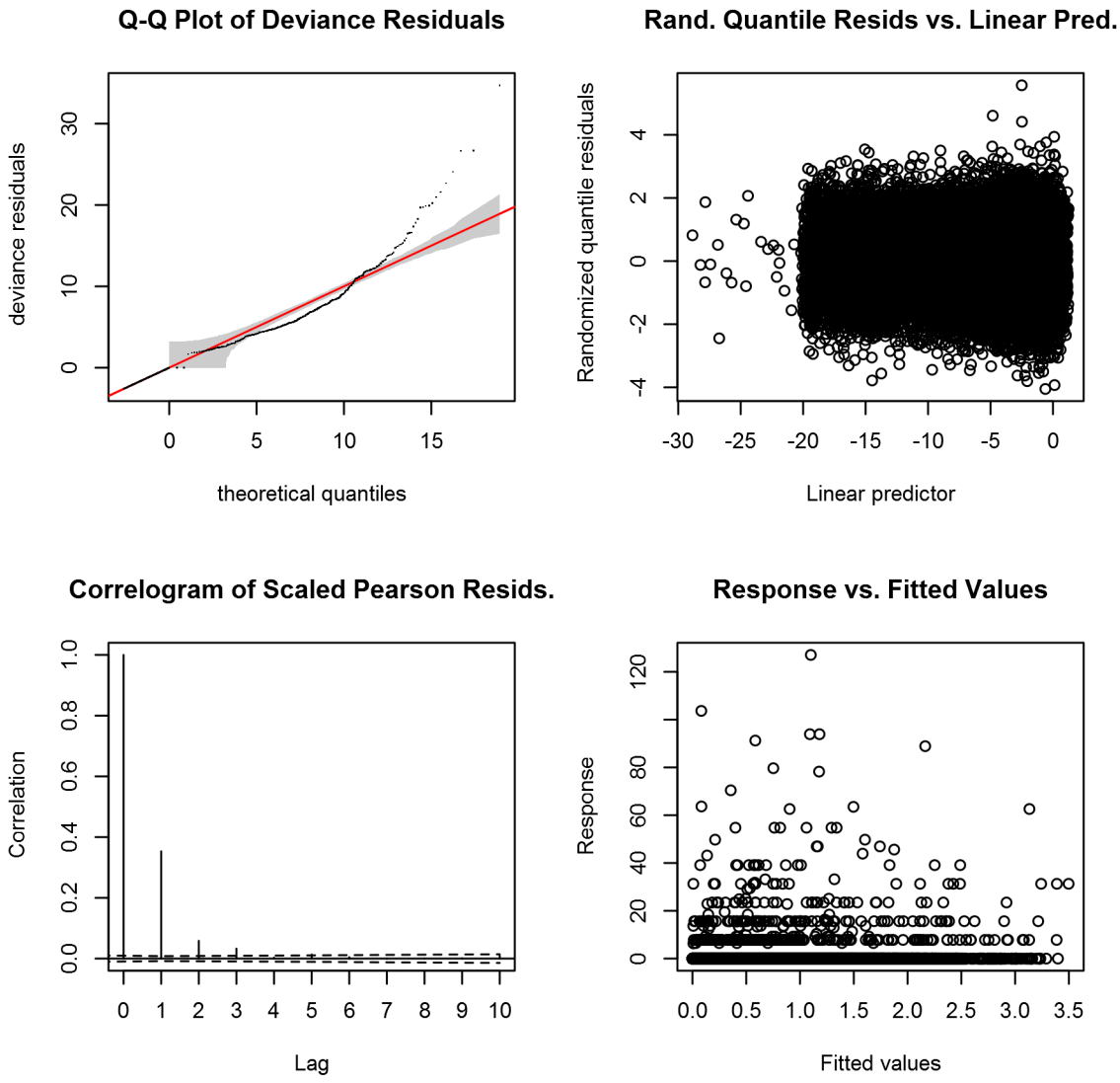

Figure 76: Statistical diagnostic plots for the Sei whale Climatological model, Spring season, Surveyed Area.

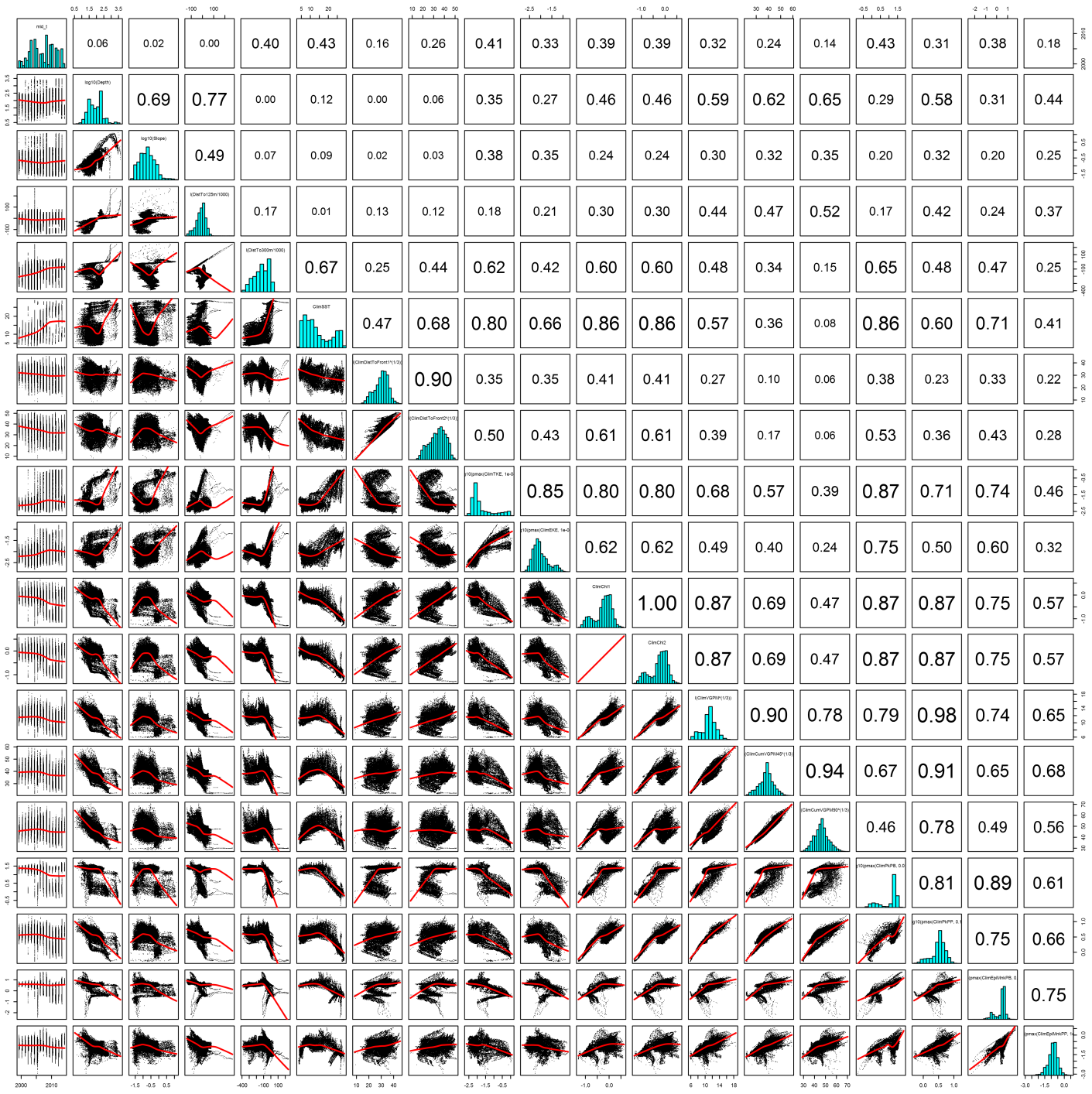

Figure 77: Scatterplot matrix for the Sei whale Climatological model, Spring season, Surveyed Area. This plot is used to inspect the distribution of predictors (via histograms along the diagonal), simple correlation between predictors (via pairwise Pearson coefficients above the diagonal), and linearity of predictor correlations (via scatterplots below the diagonal). This plot is best viewed at high magnification.

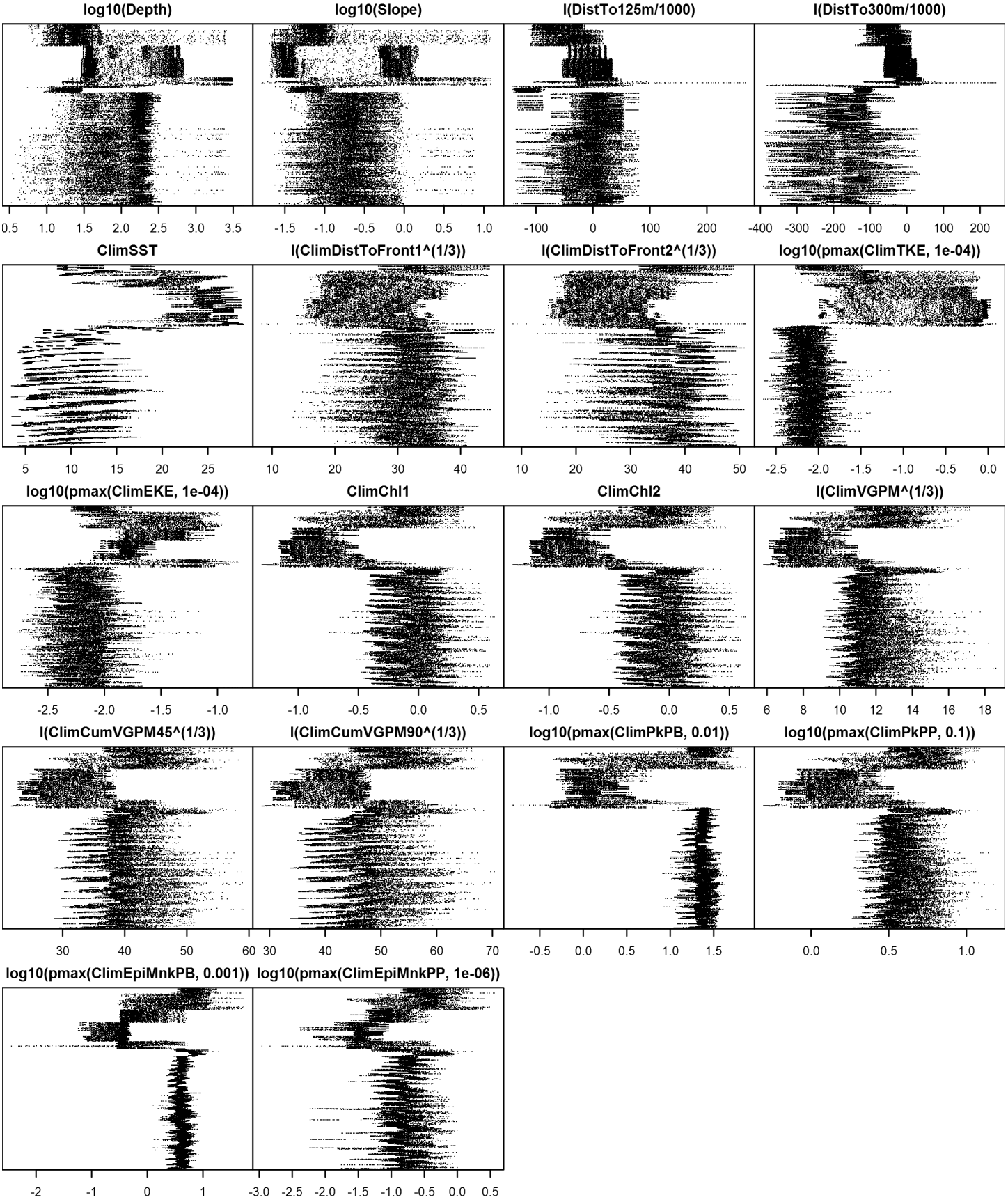

Figure 78: Dotplot for the Sei whale Climatological model, Spring season, Surveyed Area. This plot is used to check for suspicious patterns and outliers in the data. Points are ordered vertically by transect ID, sequentially in time.

Unsurveyed Area

Density was not modeled for this region.

Summer

The entire study area was surveyed extensively in this season but far fewer sightings were reported than in spring, suggestive of Mitchell's (1975) hypothesis that sei whales migrate northward from Cape Cod along the Scotian Shelf in June and July, exit the area, and return again in September and October (Mitchell 1975, as summarized by Waring et al. 2014). No sightings were reported south of the Gulf Stream. Under the assumption that sei whales would only occupy the productive waters north of the Gulf Stream during feeding season, we divided the study area at the north wall of the Gulf Stream, separating the highly productive northern region, representing possible feeding habitat, from the less productive southern region, which we assumed was unoccupied.

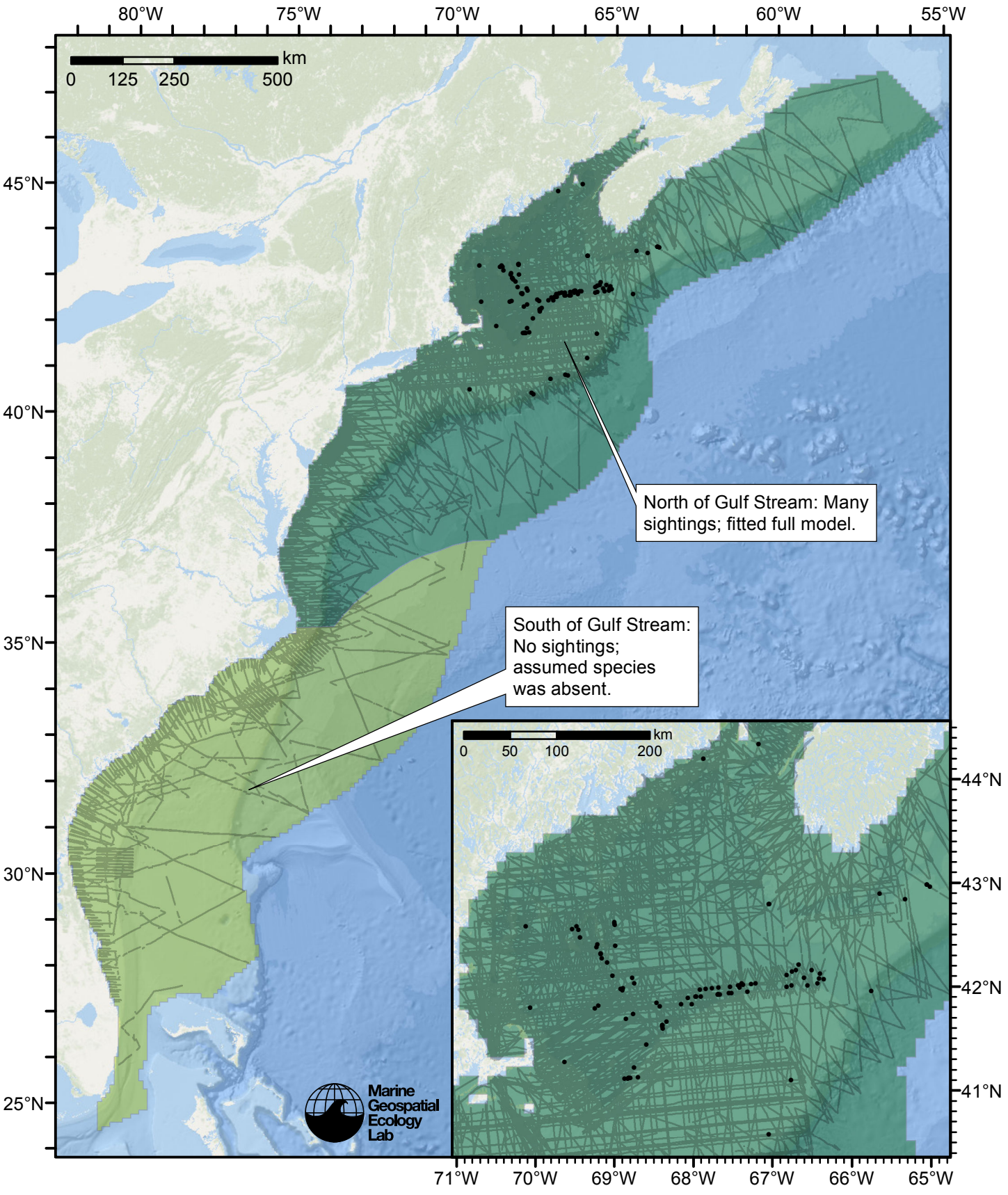

Figure 79: Sei whale density model schematic for Summer season. All on-effort sightings are shown, including those that were truncated when detection functions were fitted.

Climatological Model

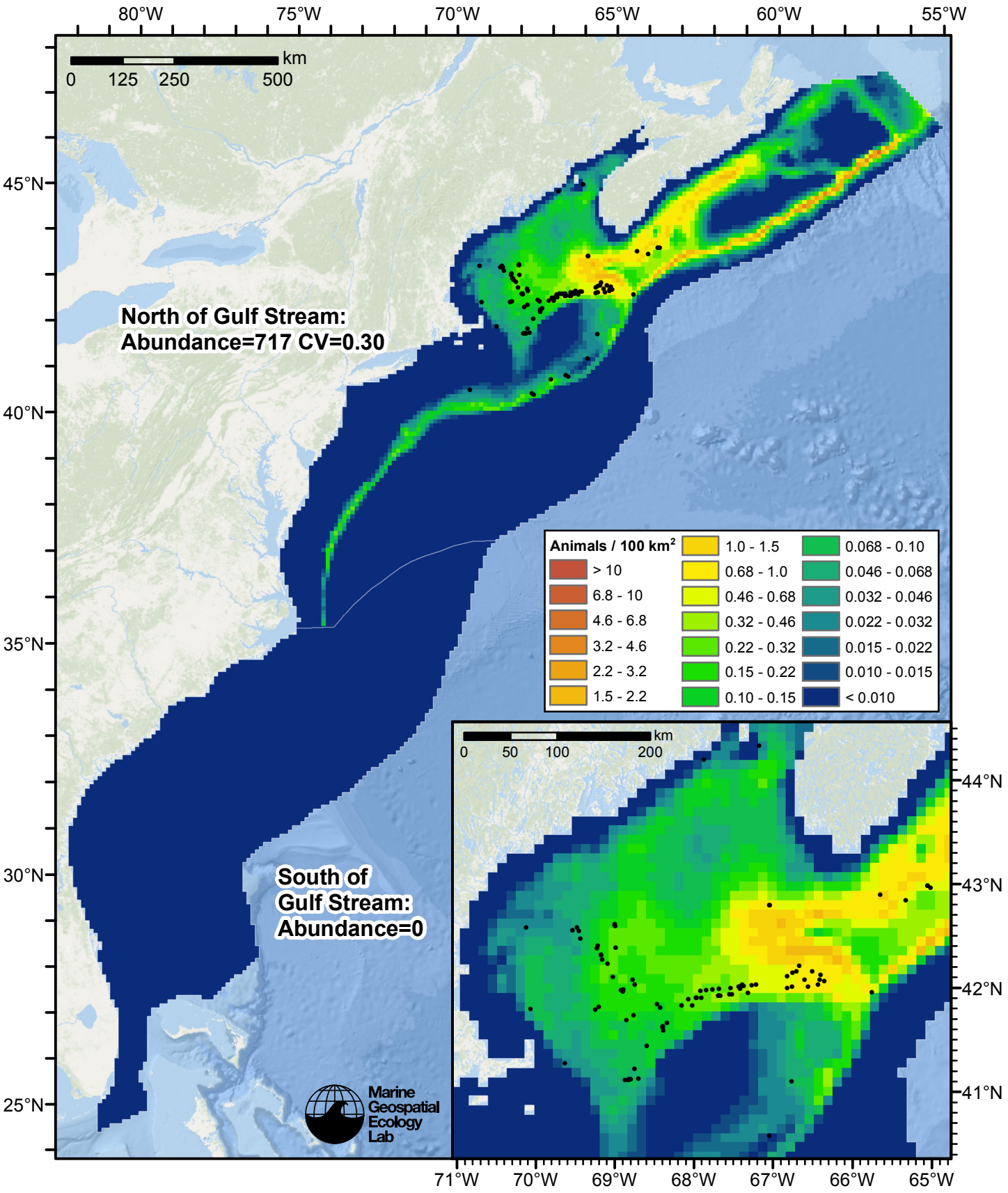

Figure 80: Sei whale density predicted by the Summer season climatological model that explained the most deviance. Pixels are 10x10 km. The legend gives the estimated individuals per pixel; breaks are logarithmic. The same scale is used for all seasons. Abundance for each region was computed by summing the density cells occuring in that region.

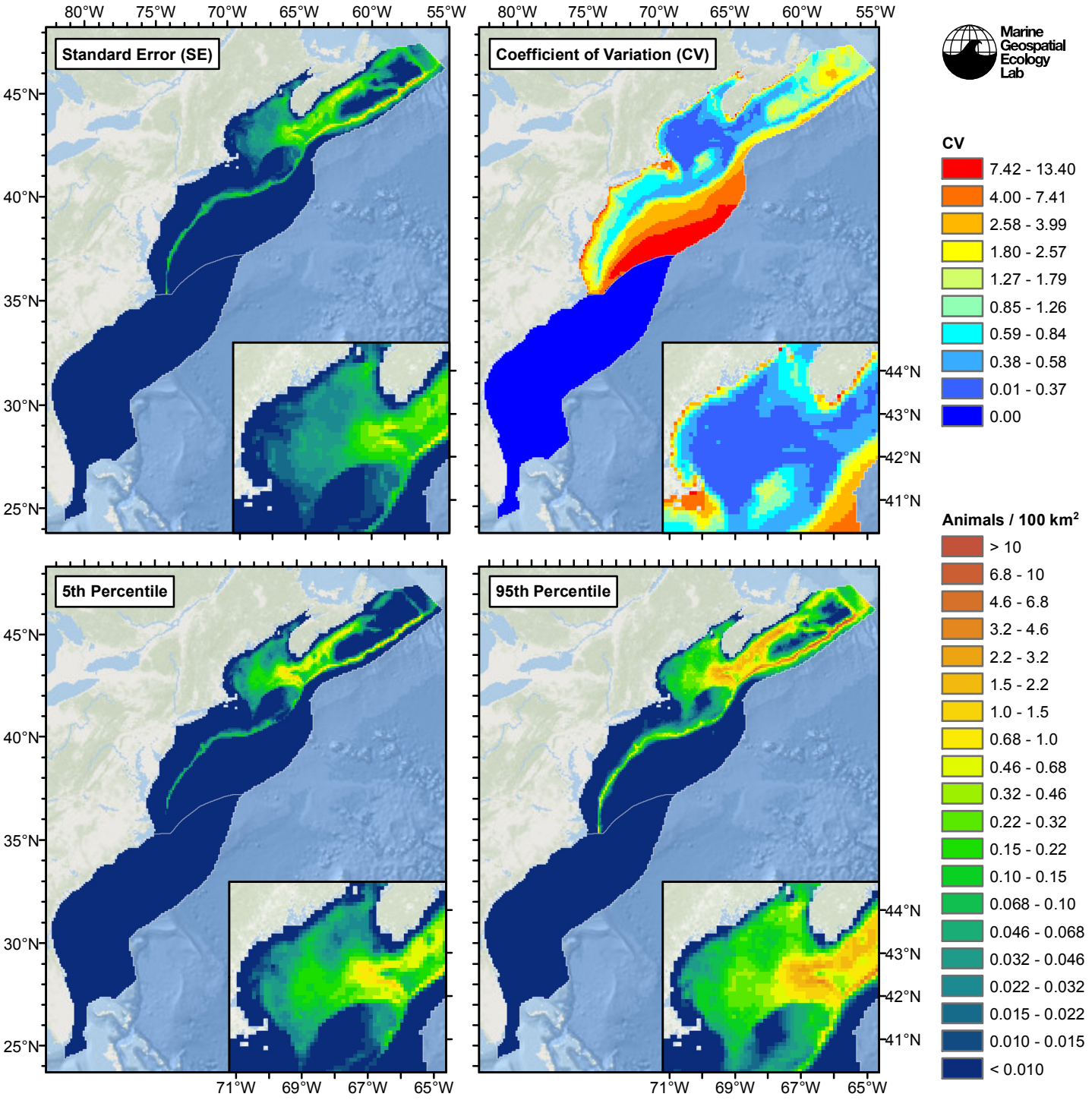

Figure 81: Estimated uncertainty for the Summer season climatological model that explained the most deviance. These estimates only incorporate the statistical uncertainty estimated for the spatial model (by the R mgcv package). They do not incorporate uncertainty in the detection functions, g(0) estimates, predictor variables, and so on.

North of Gulf Stream

Statistical output

```
Rscript.exe: This is mgcv 1.8-2. For overview type 'help("mgcv-package")'.


Family: Tweedie(p=1.223)
```

```
Link function: log

Formula:
abundance ~ offset(log(area_km2)) + s(log10(Depth), bs = "ts",
    k = 5) + s(log10(Slope), bs = "ts", k = 5) + s(ClimSST, bs = "ts",
    k = 5) + s(log10(pmax(ClimEKE, 1e-04)), bs = "ts", k = 5) +
    s(I(ClimCumVGPM90^(1/3)), bs = "ts", k = 5)

Parametric coefficients:
            Estimate Std. Error t value Pr(>|t|)
(Intercept) -10.3251     0.6938  -14.88   <2e-16 ***
---
Signif. codes:  0 '***' 0.001 '**' 0.01 '*' 0.05 '.' 0.1 ' ' 1

Approximate significance of smooth terms:
                                edf Ref.df     F  p-value
s(log10(Depth))               2.5607      4 5.364 1.14e-05 ***
s(log10(Slope))               0.8825      4 1.442  0.00885 **
s(ClimSST)                    1.1666      4 7.208 3.93e-08 ***
s(log10(pmax(ClimEKE, 1e-04))) 2.9455      4 6.170 5.27e-06 ***
s(I(ClimCumVGPM90^(1/3)))     0.9768      4 3.505 9.14e-05 ***
---
Signif. codes:  0 '***' 0.001 '**' 0.01 '*' 0.05 '.' 0.1 ' ' 1

R-sq.(adj) =  0.0287   Deviance explained = 39.4%
-REML = 630.78  Scale est. = 25.515    n = 16688

All predictors were significant. This is the final model.
Creating term plots.
Diagnostic output from gam.check():

Method: REML   Optimizer: outer newton
full convergence after 13 iterations.
Gradient range [-0.0001435394,0.0001988536]
(score 630.7755 & scale 25.51513).
Hessian positive definite, eigenvalue range [0.2991103,396.2843].
Model rank =  21 / 21

Basis dimension (k) checking results. Low p-value (k-index<1) may
indicate that k is too low, especially if edf is close to k'.

                                k'   edf k-index p-value
s(log10(Depth))               4.000 2.561   0.678    0.00
s(log10(Slope))               4.000 0.882   0.789    0.03
s(ClimSST)                    4.000 1.167   0.779    0.00
s(log10(pmax(ClimEKE, 1e-04))) 4.000 2.946   0.809    0.18
s(I(ClimCumVGPM90^(1/3)))     4.000 0.977   0.776    0.02

Predictors retained during the model selection procedure: Depth, Slope, ClimSST, ClimEKE,
ClimCumVGPM90

Predictors dropped during the model selection procedure: DistTo125m, DistTo300m, ClimDistToFront1
```

Model term plots

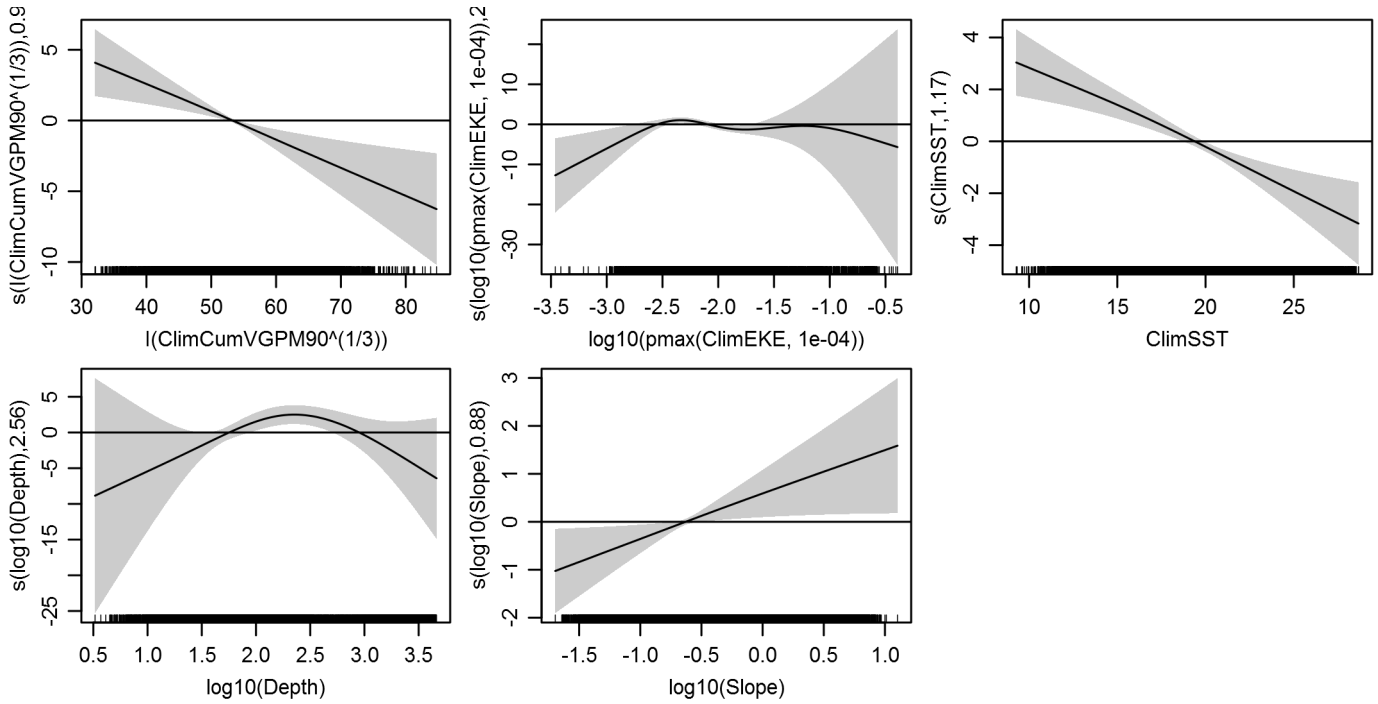

Diagnostic plots

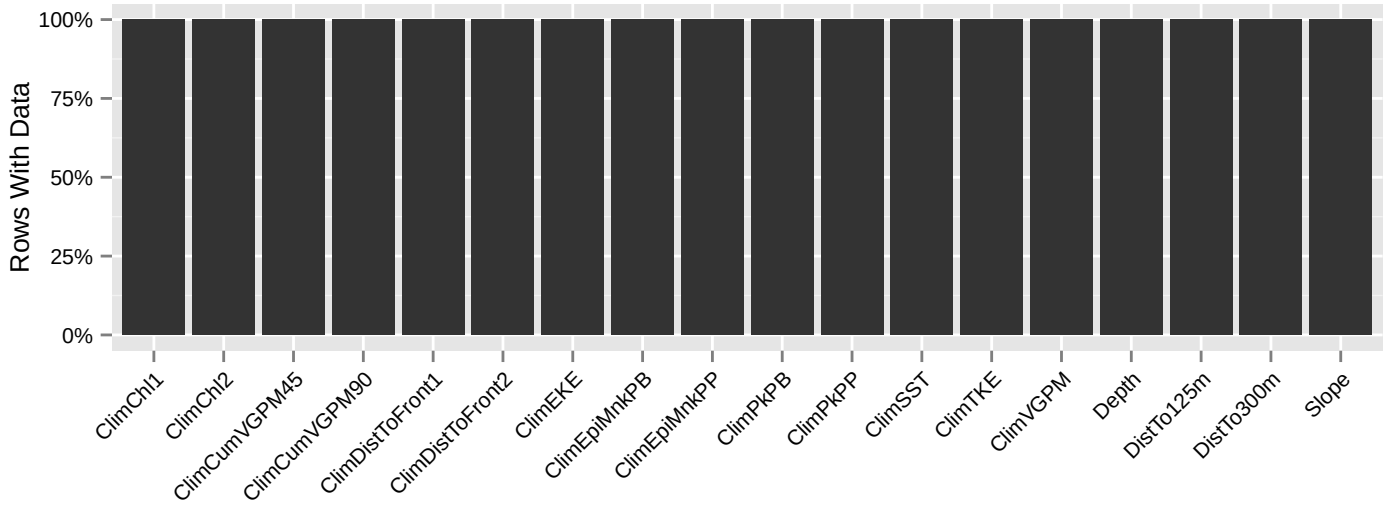

Figure 82: Segments with predictor values for the Sei whale Climatological model, Summer season, North of Gulf Stream. This plot is used to assess how many segments would be lost by including a given predictor in a model.

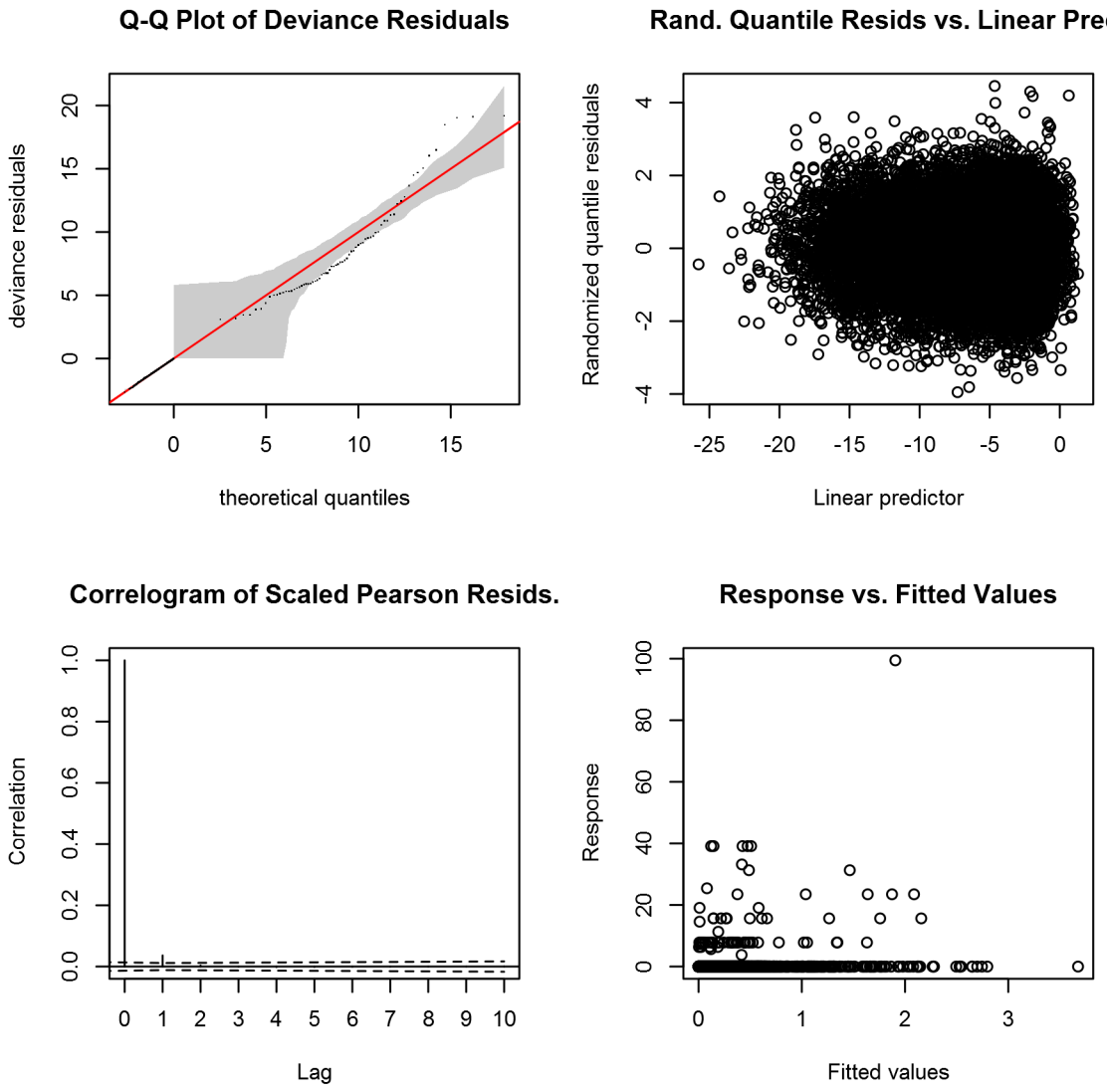

Figure 83: Statistical diagnostic plots for the Sei whale Climatological model, Summer season, North of Gulf Stream.

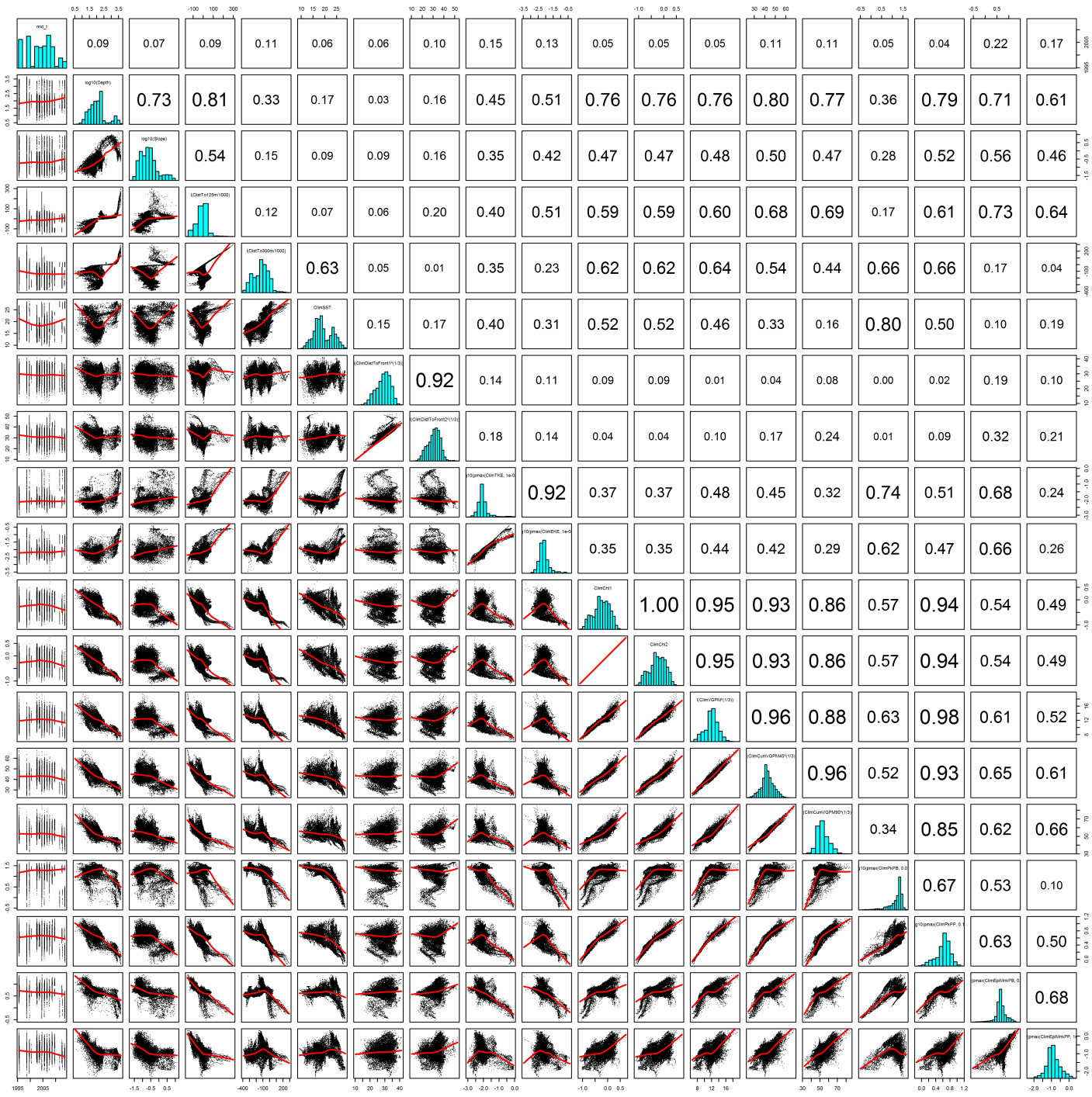

Figure 84: Scatterplot matrix for the Sei whale Climatological model, Summer season, North of Gulf Stream. This plot is used to inspect the distribution of predictors (via histograms along the diagonal), simple correlation between predictors (via pairwise Pearson coefficients above the diagonal), and linearity of predictor correlations (via scatterplots below the diagonal). This plot is best viewed at high magnification.

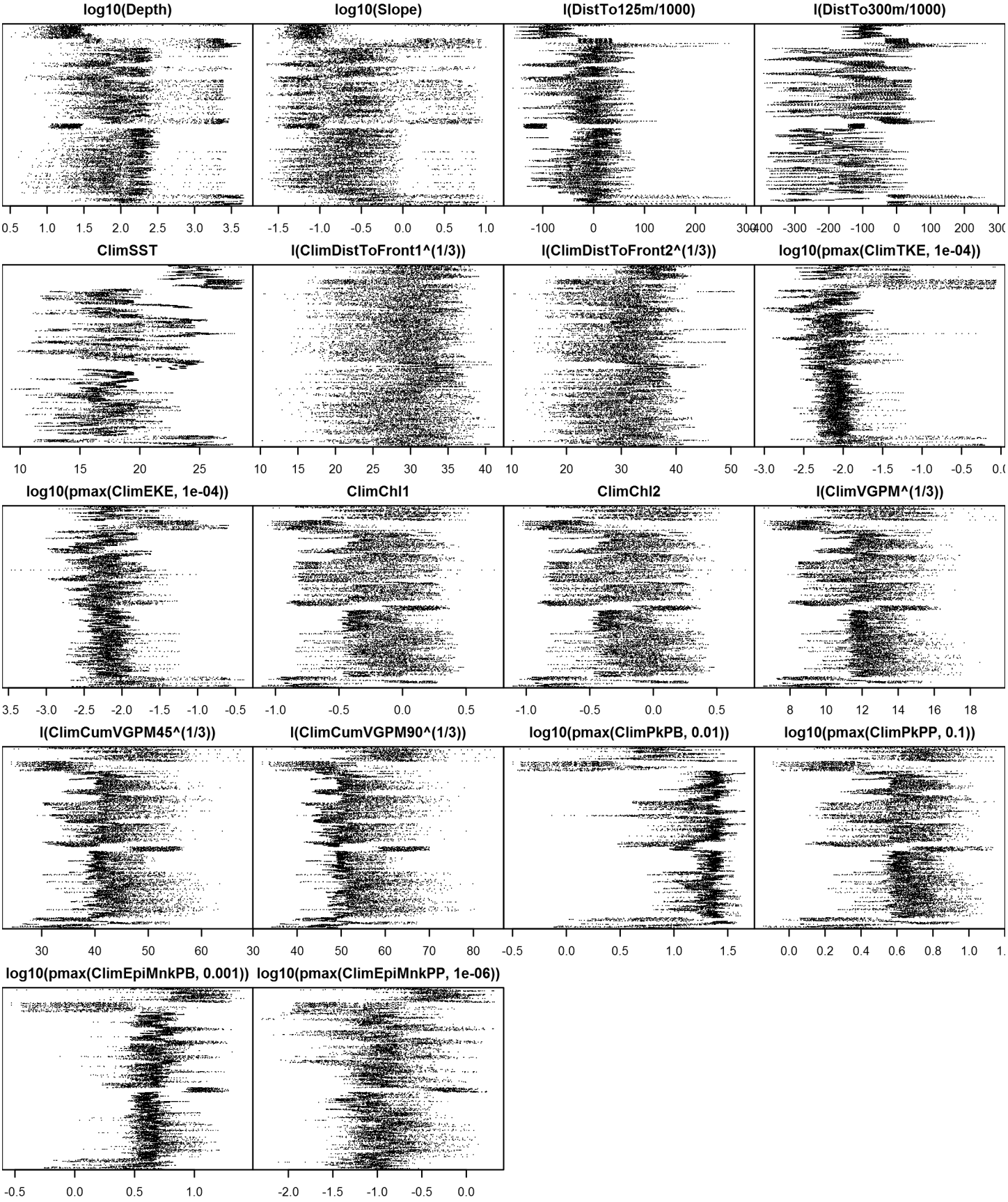

Figure 85: Dotplot for the Sei whale Climatological model, Summer season, North of Gulf Stream. This plot is used to check for suspicious patterns and outliers in the data. Points are ordered vertically by transect ID, sequentially in time.

South of Gulf Stream

Density assumed to be 0 in this region.

Contemporaneous Model

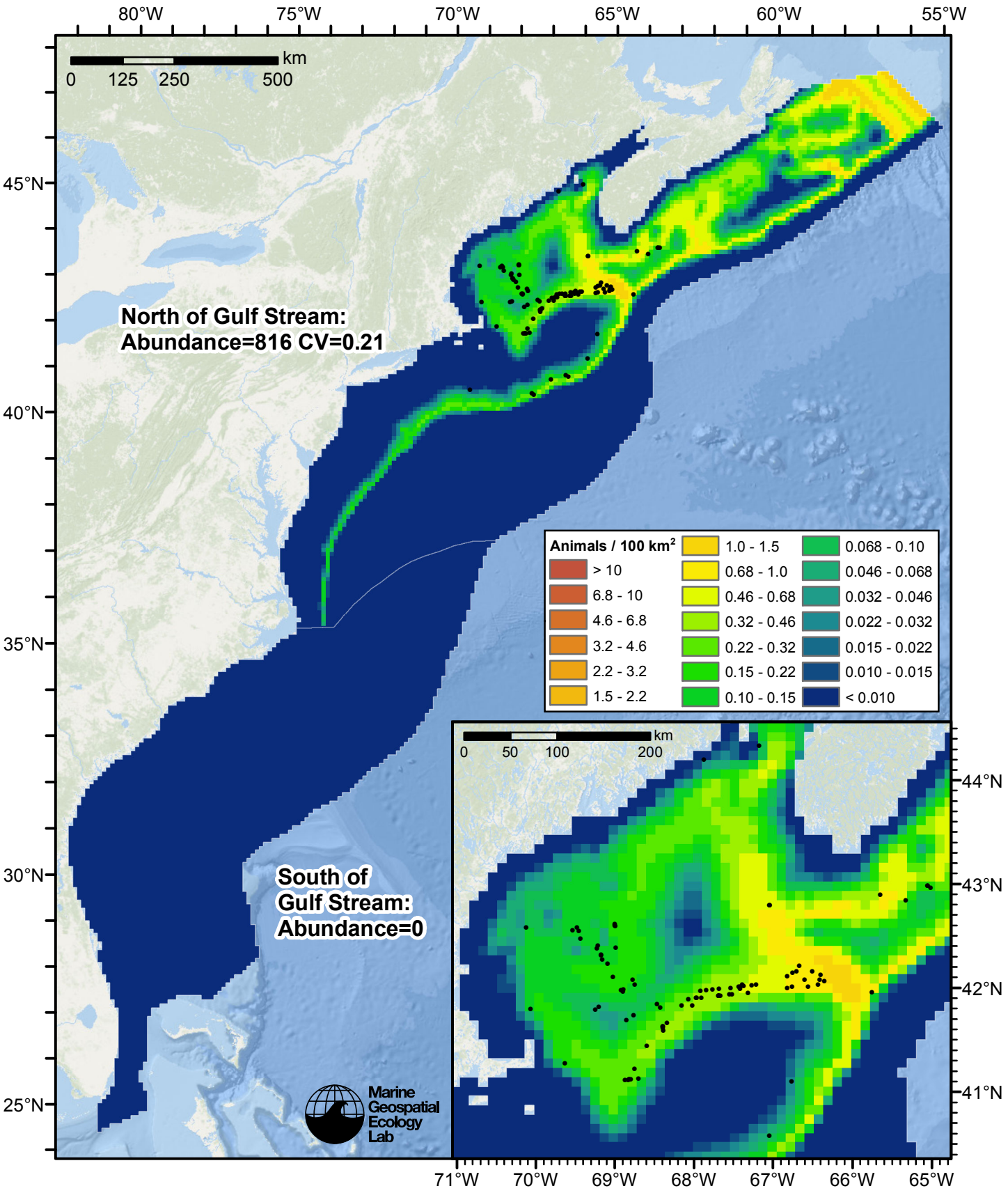

Figure 86: Sei whale density predicted by the Summer season contemporaneous model that explained the most deviance. Pixels are 10x10 km. The legend gives the estimated individuals per pixel; breaks are logarithmic. The same scale is used for all seasons. Abundance for each region was computed by summing the density cells occuring in that region.

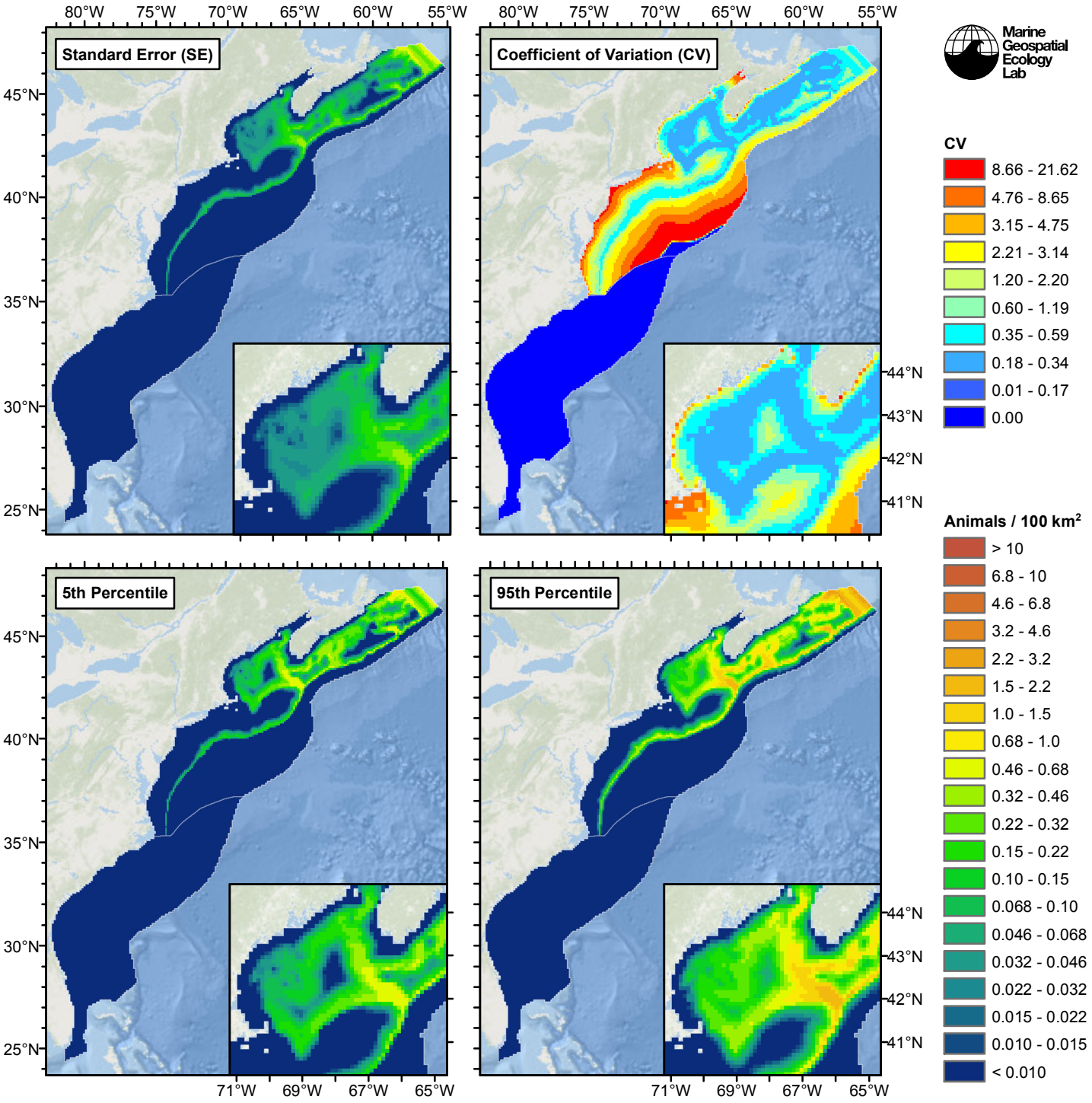

Figure 87: Estimated uncertainty for the Summer season contemporaneous model that explained the most deviance. These estimates only incorporate the statistical uncertainty estimated for the spatial model (by the R mgcv package). They do not incorporate uncertainty in the detection functions, g(0) estimates, predictor variables, and so on.

North of Gulf Stream

Statistical output

```
Rscript.exe: This is mgcv 1.8-2. For overview type 'help("mgcv-package")'.


Family: Tweedie(p=1.245)
```

```
Link function: log

Formula:
abundance ~ offset(log(area_km2)) + s(log10(Depth), bs = "ts",
    k = 5) + s(I(DistTo125m/1000), bs = "ts", k = 5) + s(I(DistTo300m/1000),
    bs = "ts", k = 5) + s(SST, bs = "ts", k = 5)

Parametric coefficients:
            Estimate Std. Error t value Pr(>|t|)
(Intercept)  -10.861      1.153  -9.424   <2e-16 ***
---
Signif. codes:  0 '***' 0.001 '**' 0.01 '*' 0.05 '.' 0.1 ' ' 1

Approximate significance of smooth terms:
                         edf Ref.df     F  p-value
s(log10(Depth))       2.5806      4 2.965  0.00229 **
s(I(DistTo125m/1000)) 2.1538      4 2.768  0.00235 **
s(I(DistTo300m/1000)) 0.9954      4 4.211 2.27e-05 ***
s(SST)                1.0955      4 4.815 7.44e-06 ***
---
Signif. codes:  0 '***' 0.001 '**' 0.01 '*' 0.05 '.' 0.1 ' ' 1

R-sq.(adj) =  0.0162   Deviance explained = 34.4%
-REML = 645.26  Scale est. = 29.017    n = 16688

All predictors were significant. This is the final model.
Creating term plots.
Diagnostic output from gam.check():

Method: REML   Optimizer: outer newton
full convergence after 14 iterations.
Gradient range [-3.92027e-05,4.224407e-05]
(score 645.2613 & scale 29.01737).
Hessian positive definite, eigenvalue range [0.264265,388.203].
Model rank =  17 / 17

Basis dimension (k) checking results. Low p-value (k-index<1) may
indicate that k is too low, especially if edf is close to k'.

                         k'   edf k-index p-value
s(log10(Depth))       4.000 2.581   0.771    0.00
s(I(DistTo125m/1000)) 4.000 2.154   0.768    0.00
s(I(DistTo300m/1000)) 4.000 0.995   0.814    0.03
s(SST)                4.000 1.096   0.809    0.02

Predictors retained during the model selection procedure: Depth, DistTo125m, DistTo300m, SST

Predictors dropped during the model selection procedure: Slope, DistToFront1
```

Model term plots

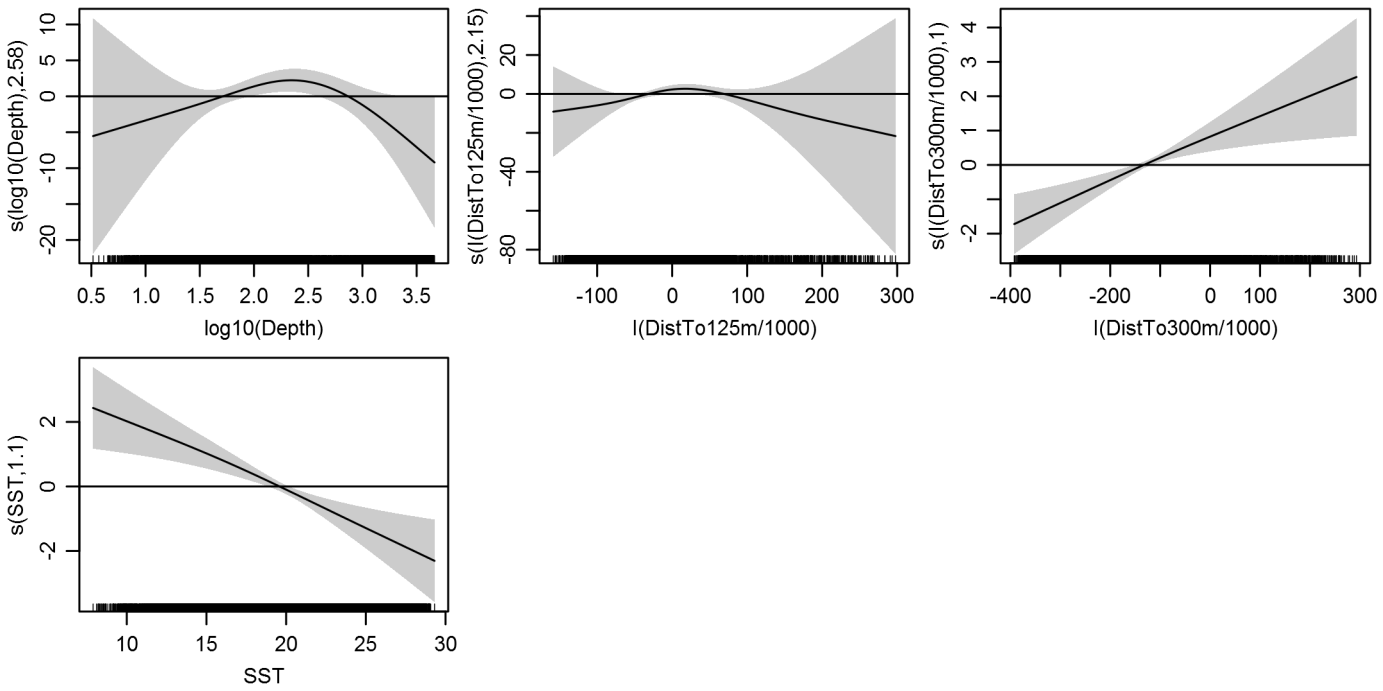

Diagnostic plots

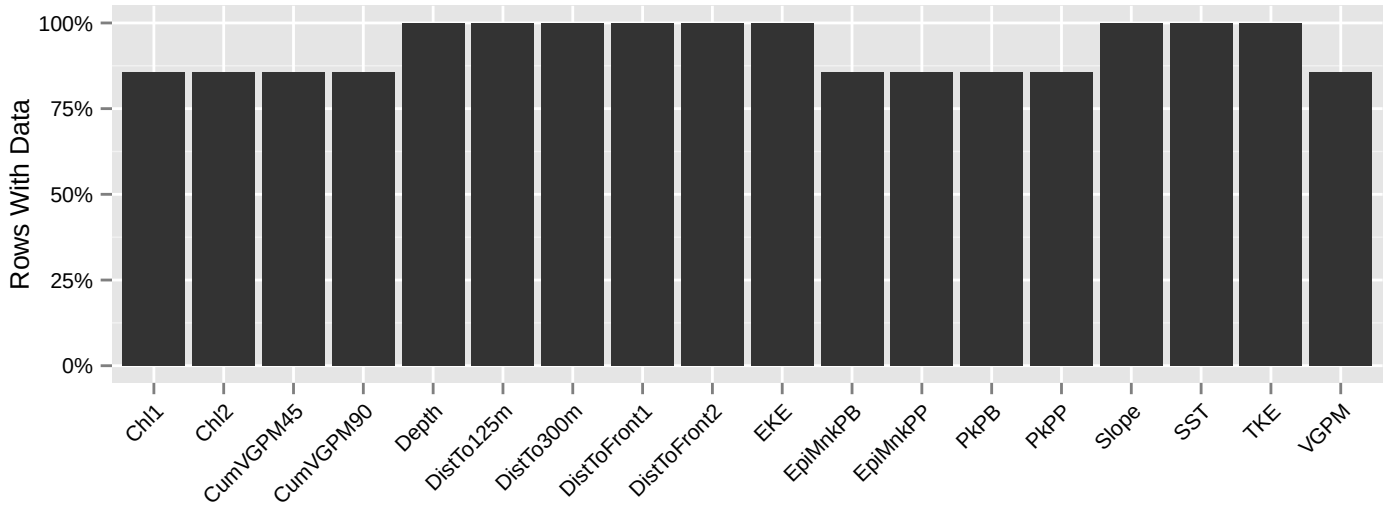

Figure 88: Segments with predictor values for the Sei whale Contemporaneous model, Summer season, North of Gulf Stream. This plot is used to assess how many segments would be lost by including a given predictor in a model.

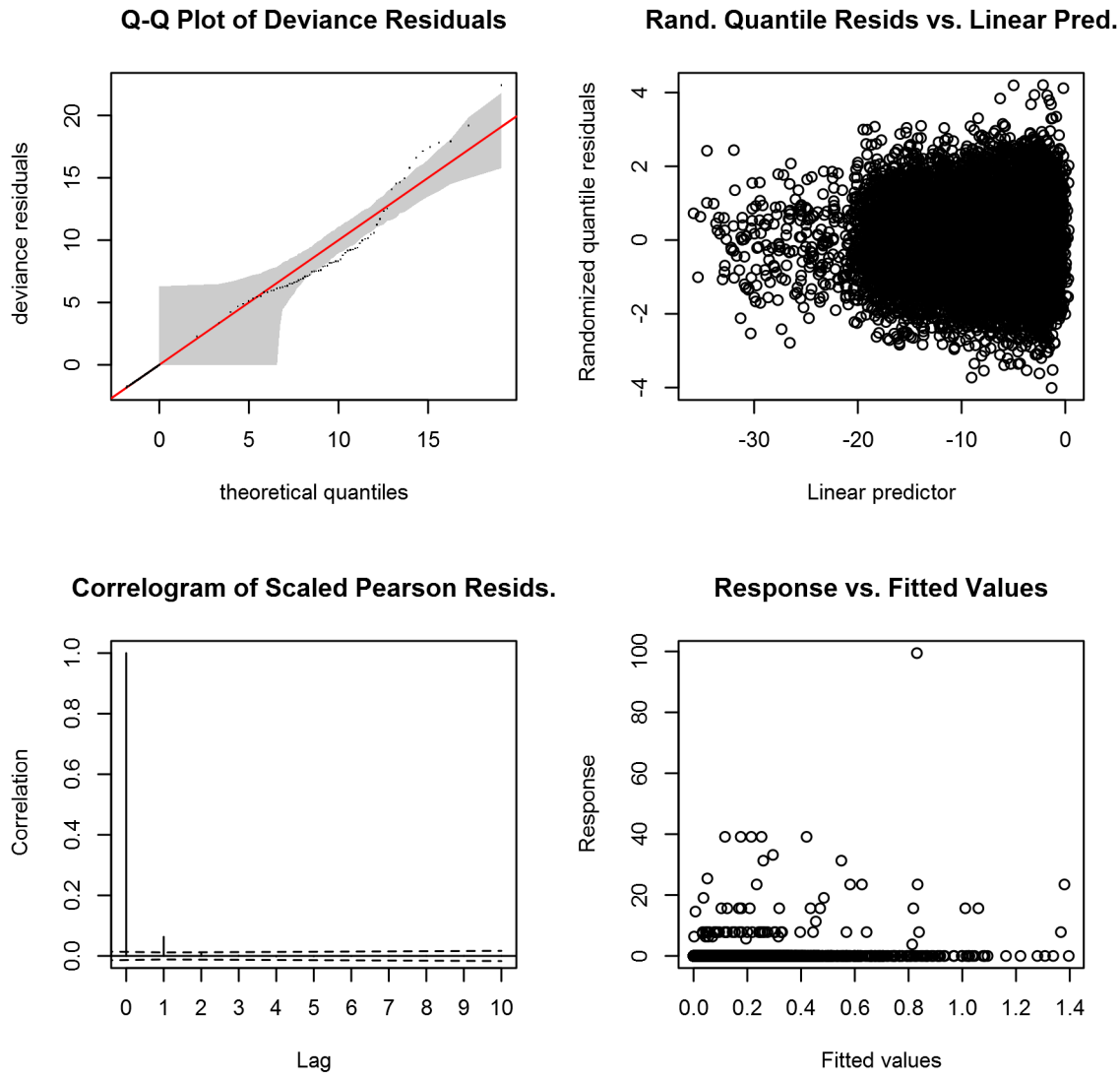

Figure 89: Statistical diagnostic plots for the Sei whale Contemporaneous model, Summer season, North of Gulf Stream.

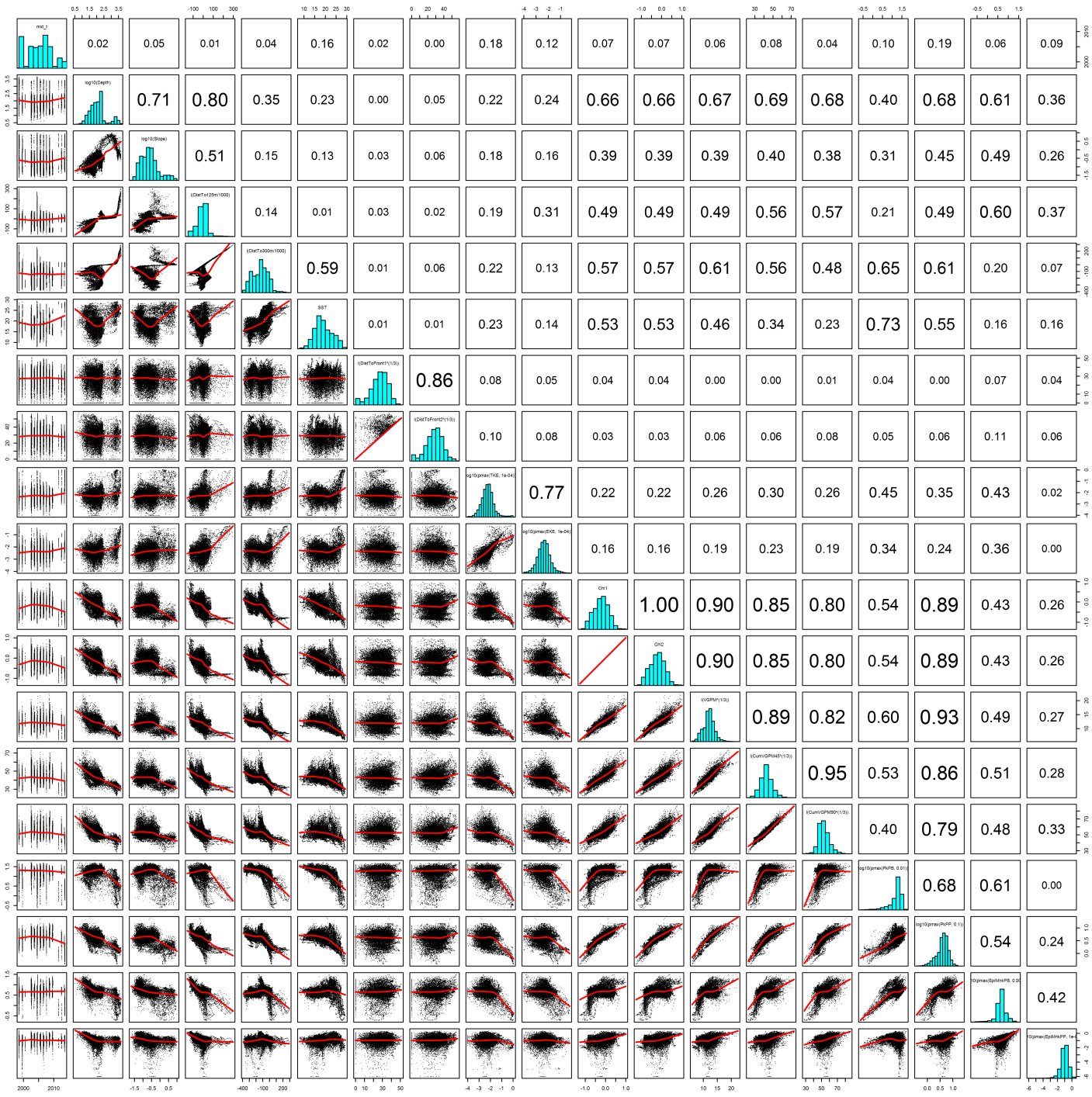

Figure 90: Scatterplot matrix for the Sei whale Contemporaneous model, Summer season, North of Gulf Stream. This plot is used to inspect the distribution of predictors (via histograms along the diagonal), simple correlation between predictors (via pairwise Pearson coefficients above the diagonal), and linearity of predictor correlations (via scatterplots below the diagonal). This plot is best viewed at high magnification.

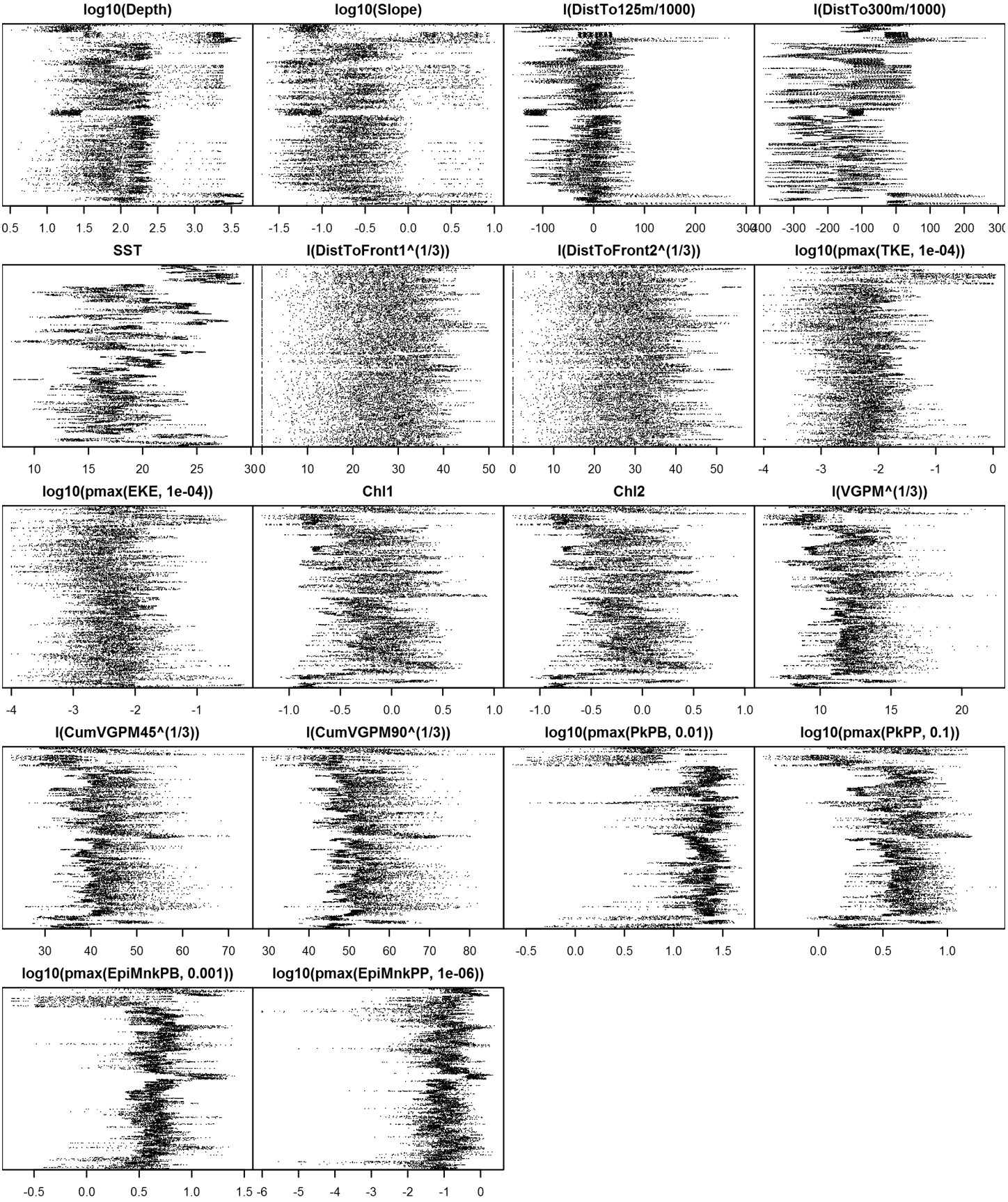

Figure 91: Dotplot for the Sei whale Contemporaneous model, Summer season, North of Gulf Stream. This plot is used to check for suspicious patterns and outliers in the data. Points are ordered vertically by transect ID, sequentially in time.

South of Gulf Stream

Density assumed to be 0 in this region.

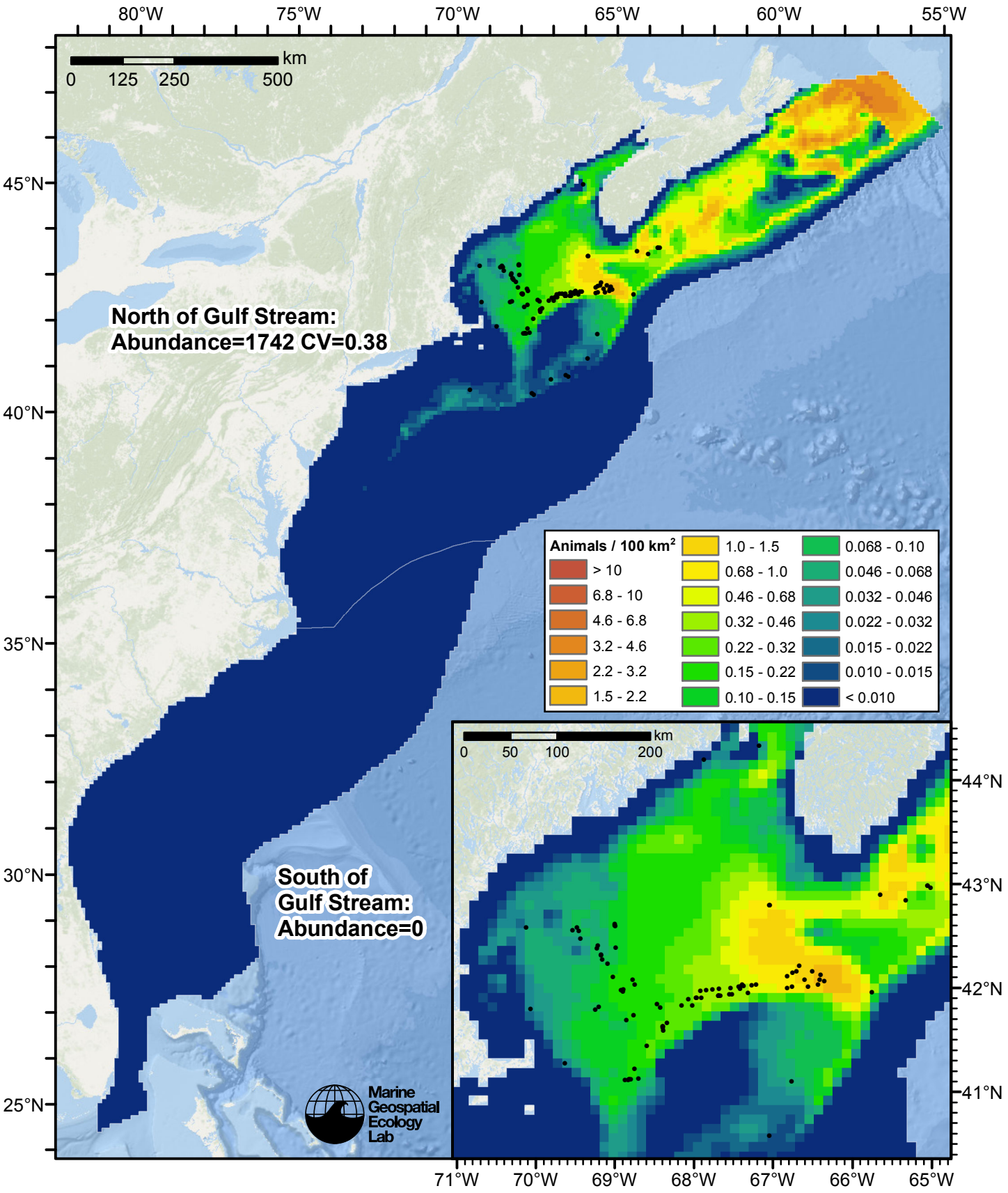

Figure 92: Sei whale density predicted by the Summer season climatological same segments model that explained the most deviance. Pixels are 10x10 km. The legend gives the estimated individuals per pixel; breaks are logarithmic. The same scale is used for all seasons. Abundance for each region was computed by summing the density cells occuring in that region.

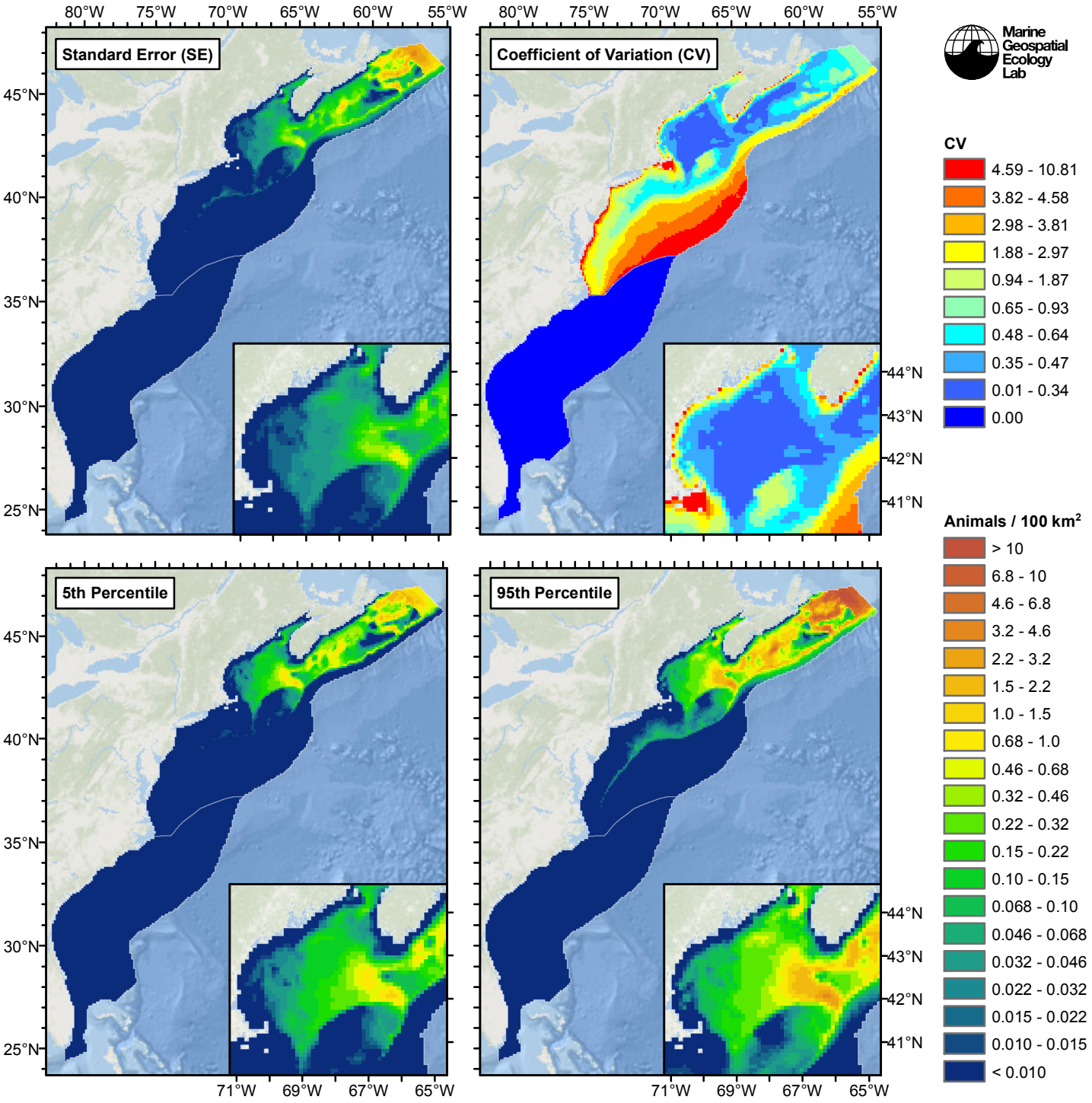

Figure 93: Estimated uncertainty for the Summer season climatological same segments model that explained the most deviance. These estimates only incorporate the statistical uncertainty estimated for the spatial model (by the R mgcv package). They do not incorporate uncertainty in the detection functions, g(0) estimates, predictor variables, and so on.

North of Gulf Stream

Statistical output

```
Rscript.exe: This is mgcv 1.8-2. For overview type 'help("mgcv-package")'.


Family: Tweedie(p=1.239)
```

```
Link function: log

Formula:
abundance ~ offset(log(area_km2)) + s(log10(Depth), bs = "ts",
    k = 5) + s(I(DistTo300m/1000), bs = "ts", k = 5) + s(ClimSST,
    bs = "ts", k = 5) + s(log10(pmax(ClimEKE, 1e-04)), bs = "ts",
    k = 5) + s(log10(pmax(ClimPkPB, 0.01)), bs = "ts", k = 5)

Parametric coefficients:
            Estimate Std. Error t value Pr(>|t|)
(Intercept) -10.2432     0.6644  -15.42   <2e-16 ***
---
Signif. codes:  0 '***' 0.001 '**' 0.01 '*' 0.05 '.' 0.1 ' ' 1

Approximate significance of smooth terms:
                                edf Ref.df      F  p-value
s(log10(Depth))               2.5429      4 10.064 3.52e-10 ***
s(I(DistTo300m/1000))         0.9710      4  3.124 0.000148 ***
s(ClimSST)                    0.9435      4  2.052 0.001929 **
s(log10(pmax(ClimEKE, 1e-04))) 0.8842      4  1.536 0.006512 **
s(log10(pmax(ClimPkPB, 0.01))) 0.9091      4  2.077 0.001742 **
---
Signif. codes:  0 '***' 0.001 '**' 0.01 '*' 0.05 '.' 0.1 ' ' 1

R-sq.(adj) =  0.0212   Deviance explained = 35.6%
-REML = 613.07  Scale est. = 27.575    n = 14272

All predictors were significant. This is the final model.
Creating term plots.
Diagnostic output from gam.check():

Method: REML   Optimizer: outer newton
full convergence after 11 iterations.
Gradient range [-2.190822e-07,1.178905e-07]
(score 613.0671 & scale 27.57505).
Hessian positive definite, eigenvalue range [0.2870762,371.3574].
Model rank =  21 / 21

Basis dimension (k) checking results. Low p-value (k-index<1) may
indicate that k is too low, especially if edf is close to k'.

                                k'   edf k-index p-value
s(log10(Depth))               4.000 2.543   0.764    0.00
s(I(DistTo300m/1000))         4.000 0.971   0.810    0.00
s(ClimSST)                    4.000 0.944   0.798    0.00
s(log10(pmax(ClimEKE, 1e-04))) 4.000 0.884   0.837    0.07
s(log10(pmax(ClimPkPB, 0.01))) 4.000 0.909   0.800    0.00

Predictors retained during the model selection procedure: Depth, DistTo300m, ClimSST, ClimEKE,
ClimPkPB

Predictors dropped during the model selection procedure: Slope, DistTo125m, ClimDistToFront1
```

Model term plots

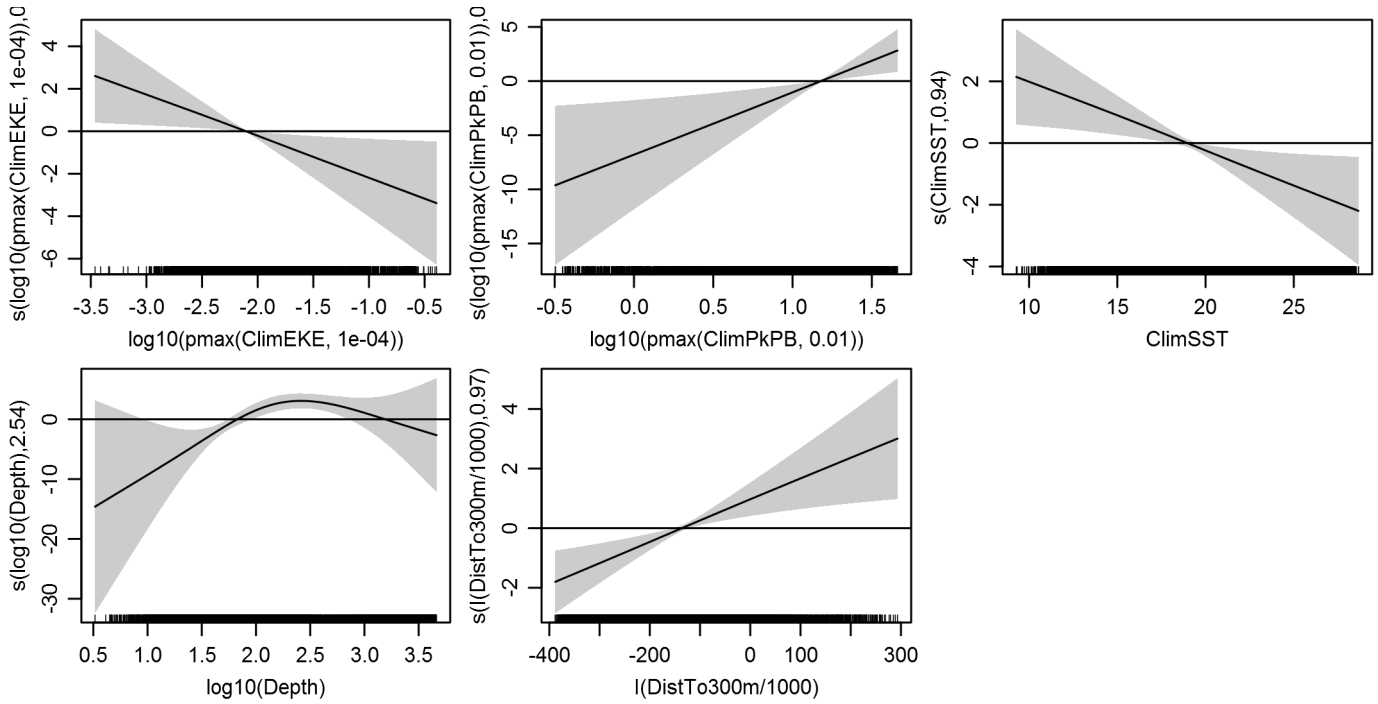

Diagnostic plots

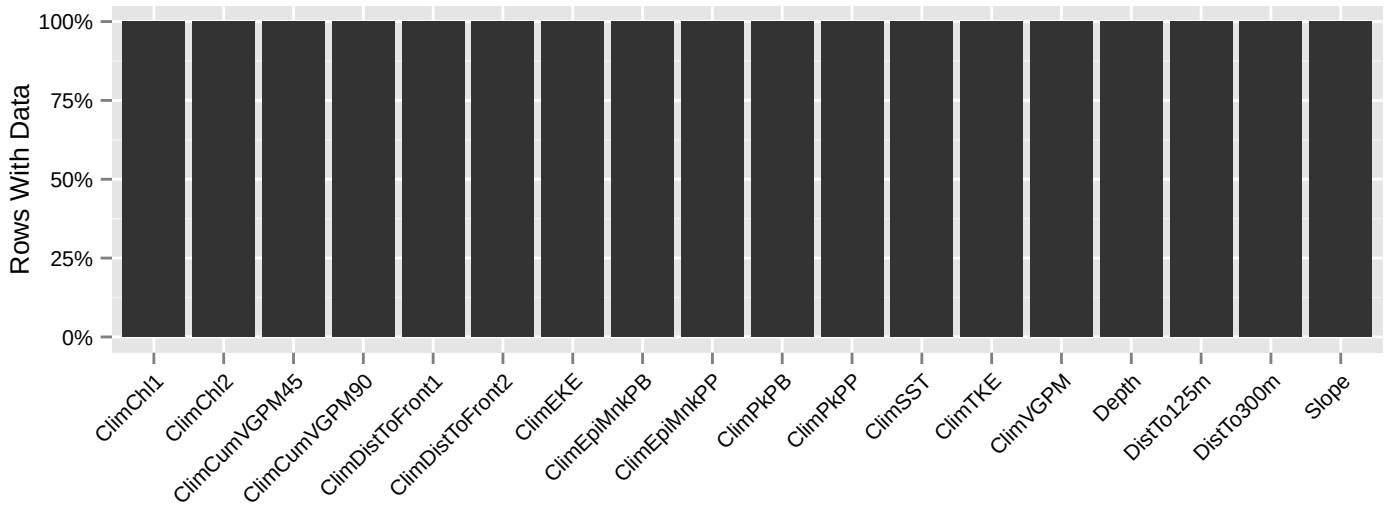

Figure 94: Segments with predictor values for the Sei whale Climatological model, Summer season, North of Gulf Stream. This plot is used to assess how many segments would be lost by including a given predictor in a model.

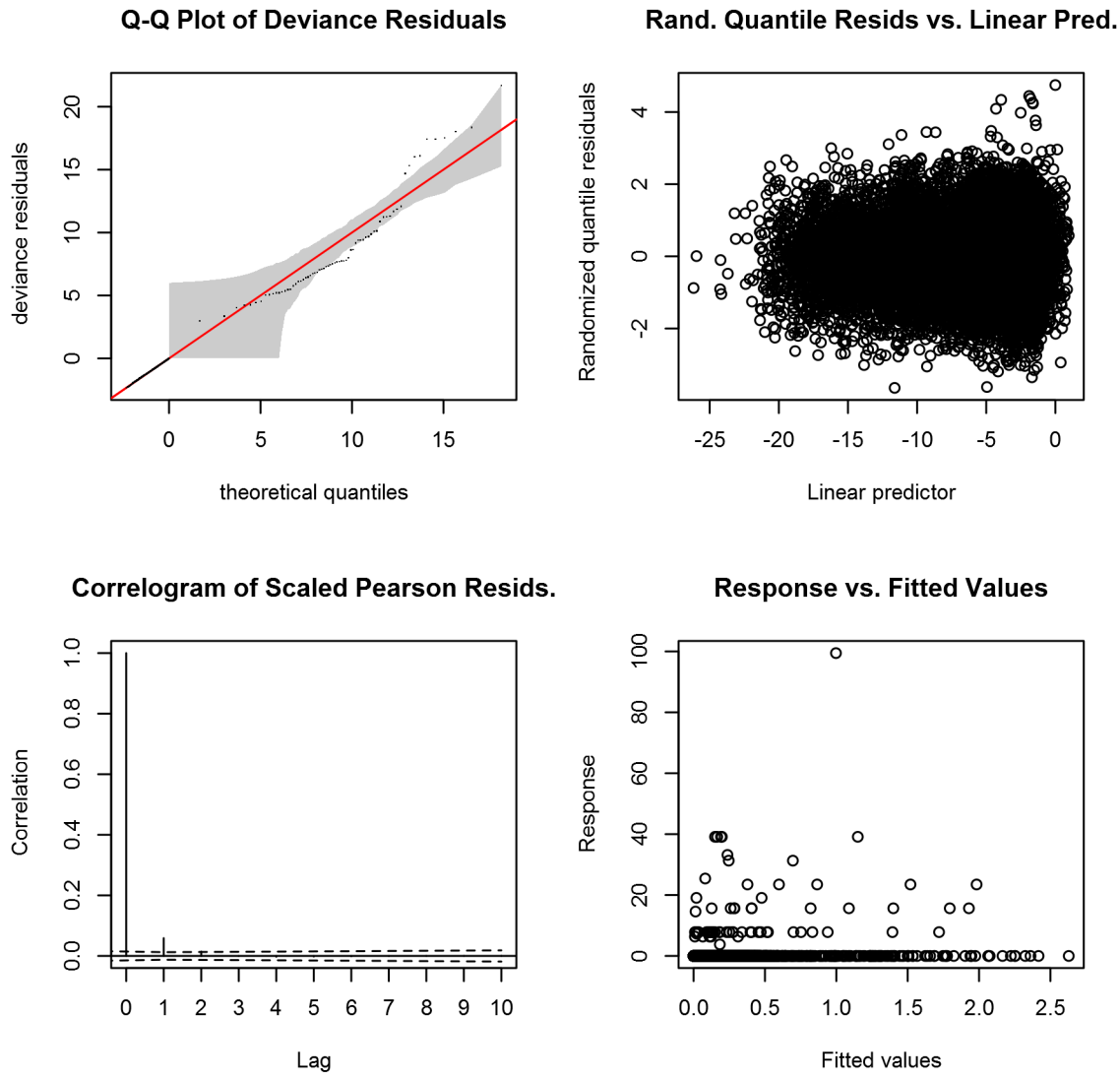

Figure 95: Statistical diagnostic plots for the Sei whale Climatological model, Summer season, North of Gulf Stream.

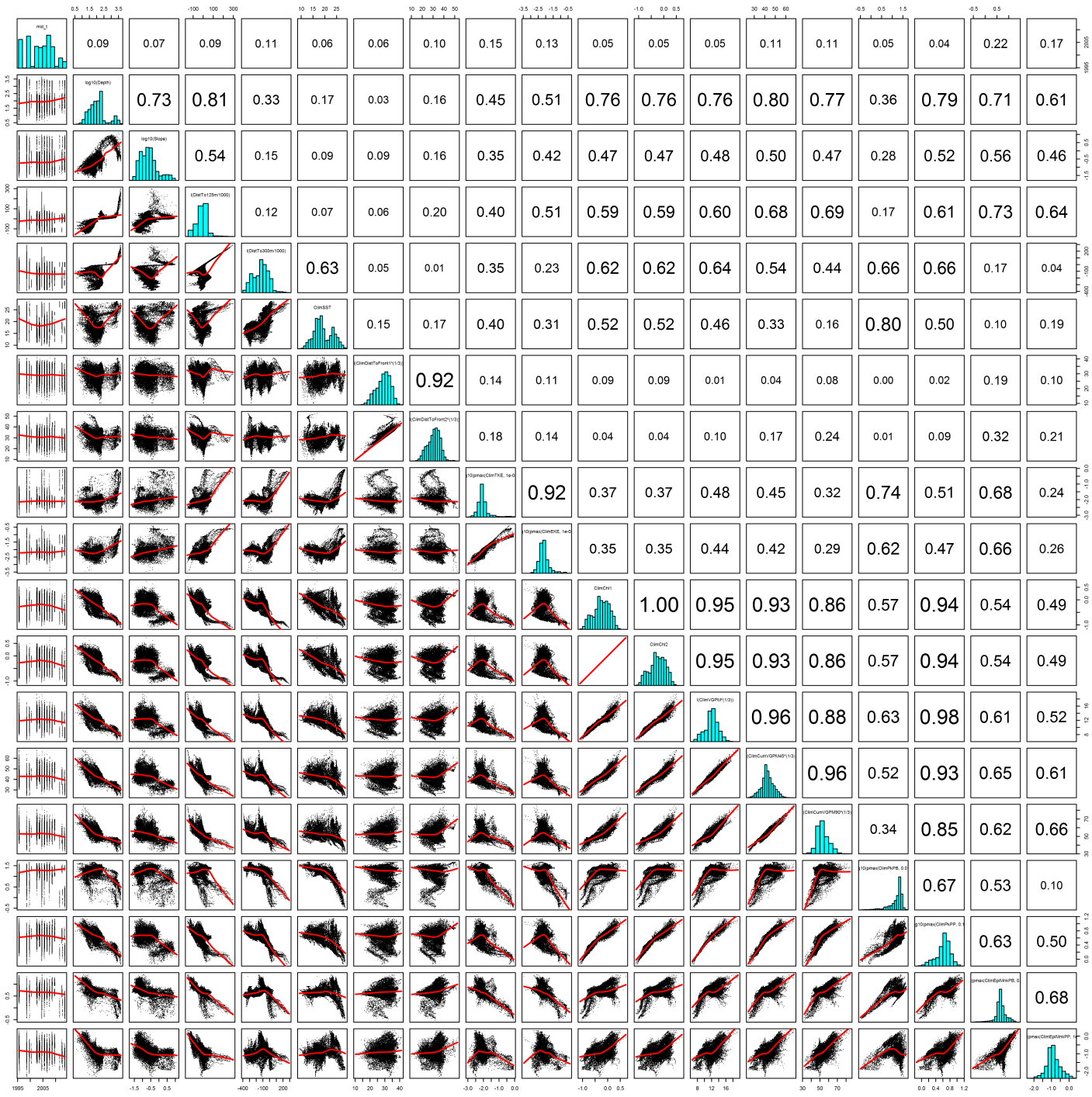

Figure 96: Scatterplot matrix for the Sei whale Climatological model, Summer season, North of Gulf Stream. This plot is used to inspect the distribution of predictors (via histograms along the diagonal), simple correlation between predictors (via pairwise Pearson coefficients above the diagonal), and linearity of predictor correlations (via scatterplots below the diagonal). This plot is best viewed at high magnification.

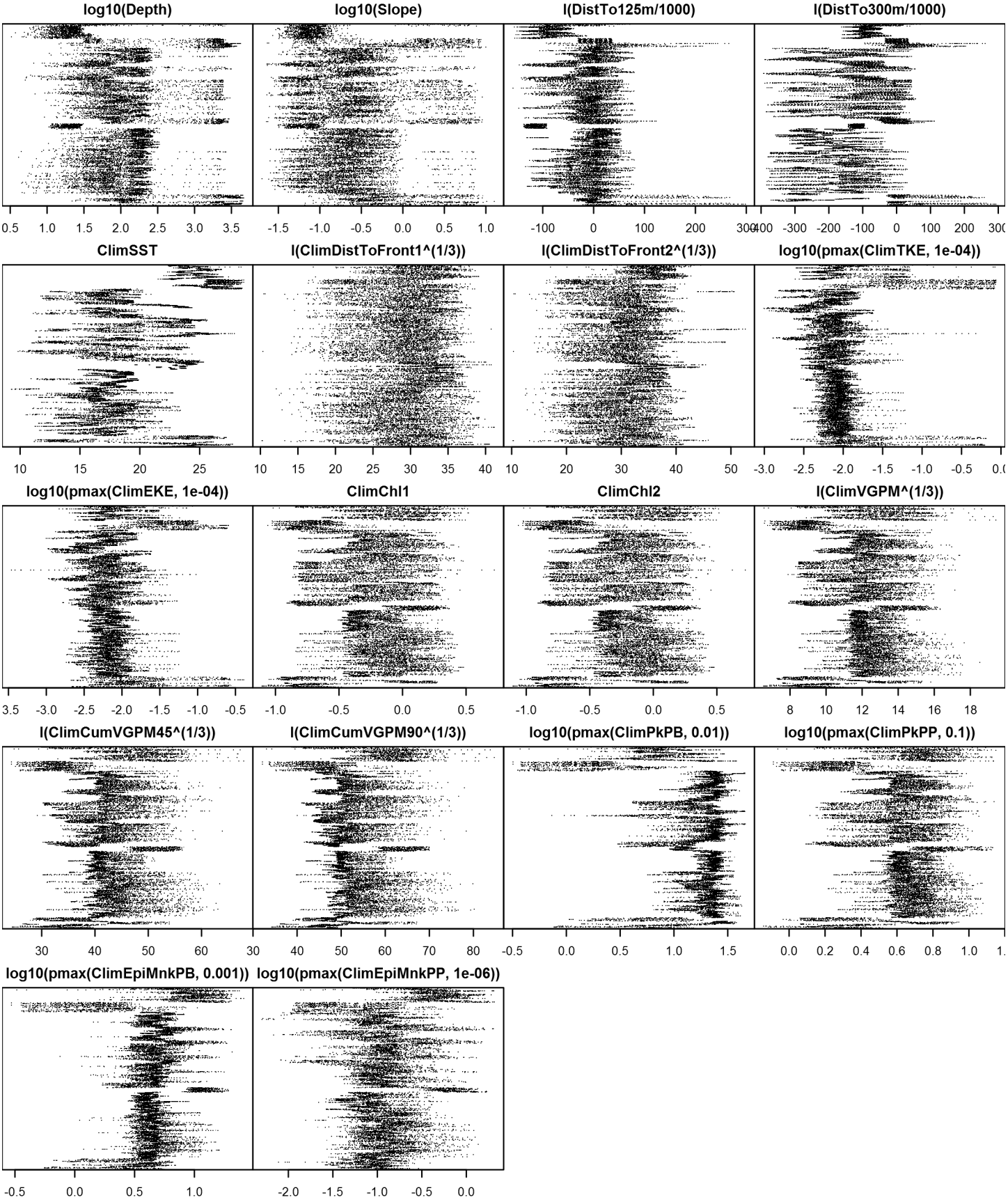

Figure 97: Dotplot for the Sei whale Climatological model, Summer season, North of Gulf Stream. This plot is used to check for suspicious patterns and outliers in the data. Points are ordered vertically by transect ID, sequentially in time.

South of Gulf Stream

Density assumed to be 0 in this region.

Fall

In this season, only 43 sightings were available, all reported by the NARWSS program north of 40 N. The only other areas with significant survey effort were three study areas in the southeast surveyed by UNCW, and the coastline of New Jersey, surveyed out to 37 km by NJ-DEP. Given the lack of spatial coverage, we could only confidently model sei whale density in the region surveyed by NARWSS.

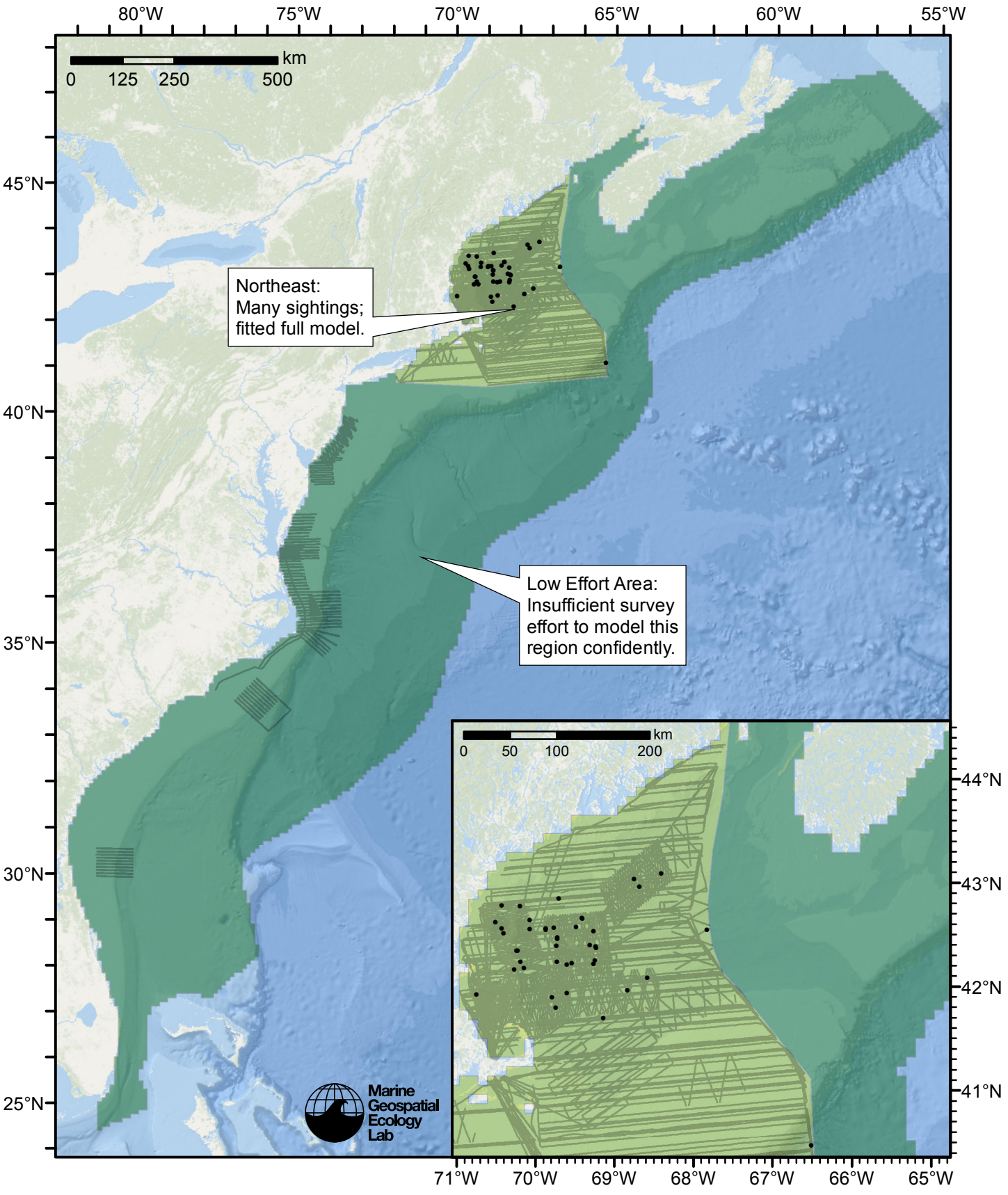

Figure 98: Sei whale density model schematic for Fall season. All on-effort sightings are shown, including those that were truncated when detection functions were fitted.

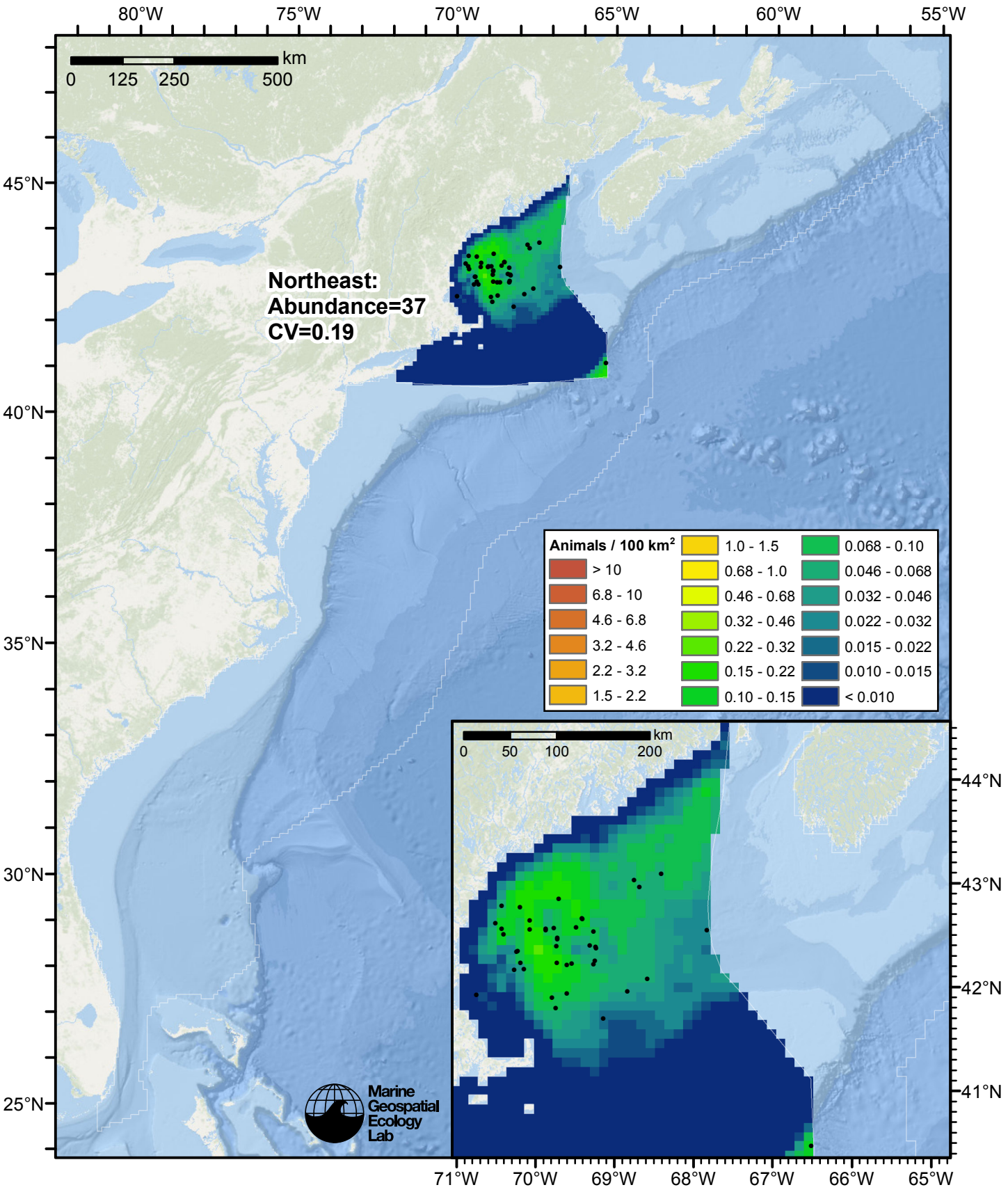

Figure 99: Sei whale density predicted by the Fall season climatological model that explained the most deviance. Pixels are 10x10 km. The legend gives the estimated individuals per pixel; breaks are logarithmic. The same scale is used for all seasons. Abundance for each region was computed by summing the density cells occuring in that region.

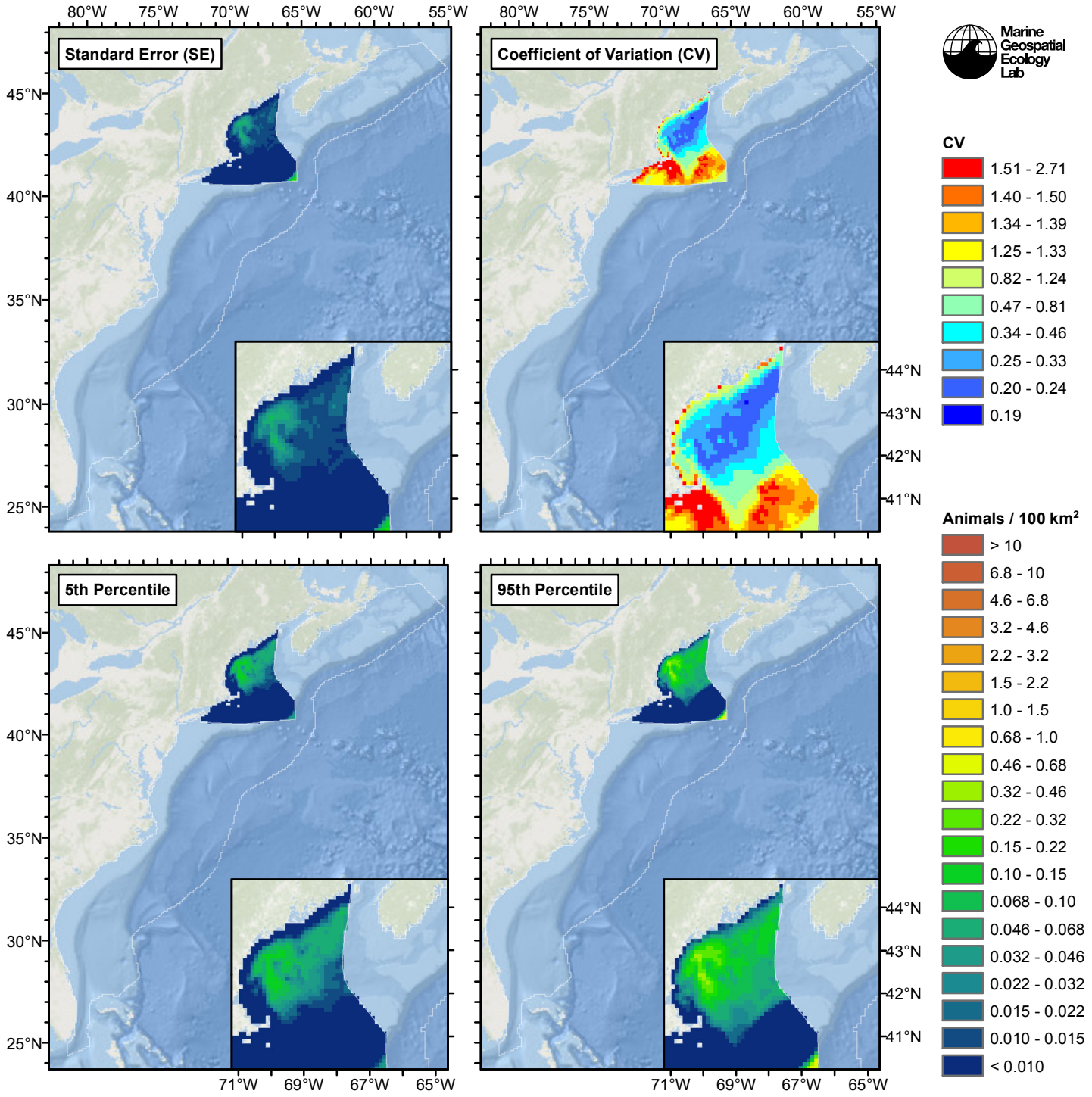

Figure 100: Estimated uncertainty for the Fall season climatological model that explained the most deviance. These estimates only incorporate the statistical uncertainty estimated for the spatial model (by the R mgcv package). They do not incorporate uncertainty in the detection functions, g(0) estimates, predictor variables, and so on.

Northeast

Statistical output

```
Rscript.exe: This is mgcv 1.8-2. For overview type 'help("mgcv-package")'.


Family: Tweedie(p=1.126)
```

```
Link function: log

Formula:
abundance ~ offset(log(area_km2)) + s(log10(Depth), bs = "ts",
    k = 5) + s(I(DistTo300m/1000), bs = "ts", k = 5)

Parametric coefficients:
            Estimate Std. Error t value Pr(>|t|)
(Intercept)  -8.9677     0.4849  -18.49   <2e-16 ***
---
Signif. codes:  0 '***' 0.001 '**' 0.01 '*' 0.05 '.' 0.1 ' ' 1

Approximate significance of smooth terms:
                         edf Ref.df     F  p-value
s(log10(Depth))        1.049      4 3.918 2.82e-05 ***
s(I(DistTo300m/1000)) 1.102      4 3.473 8.08e-05 ***
---
Signif. codes:  0 '***' 0.001 '**' 0.01 '*' 0.05 '.' 0.1 ' ' 1

R-sq.(adj) =  0.00296   Deviance explained = 14.2%
-REML = 279.77  Scale est. = 16.118    n = 6780

All predictors were significant. This is the final model.
Creating term plots.
Diagnostic output from gam.check():

Method: REML   Optimizer: outer newton
full convergence after 10 iterations.
Gradient range [-0.0006769701,0.0003121349]
(score 279.7695 & scale 16.11772).
Hessian positive definite, eigenvalue range [0.4170728,275.2486].
Model rank =  9 / 9

Basis dimension (k) checking results. Low p-value (k-index<1) may
indicate that k is too low, especially if edf is close to k'.

                          k'   edf k-index p-value
s(log10(Depth))       4.000 1.049   0.767    0.00
s(I(DistTo300m/1000)) 4.000 1.102   0.808    0.02

Predictors retained during the model selection procedure: Depth, DistTo300m

Predictors dropped during the model selection procedure: Slope, DistTo125m
```

Model term plots

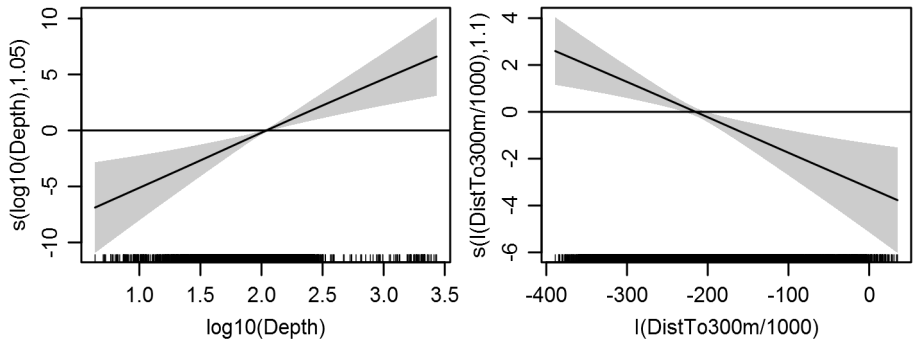

Diagnostic plots

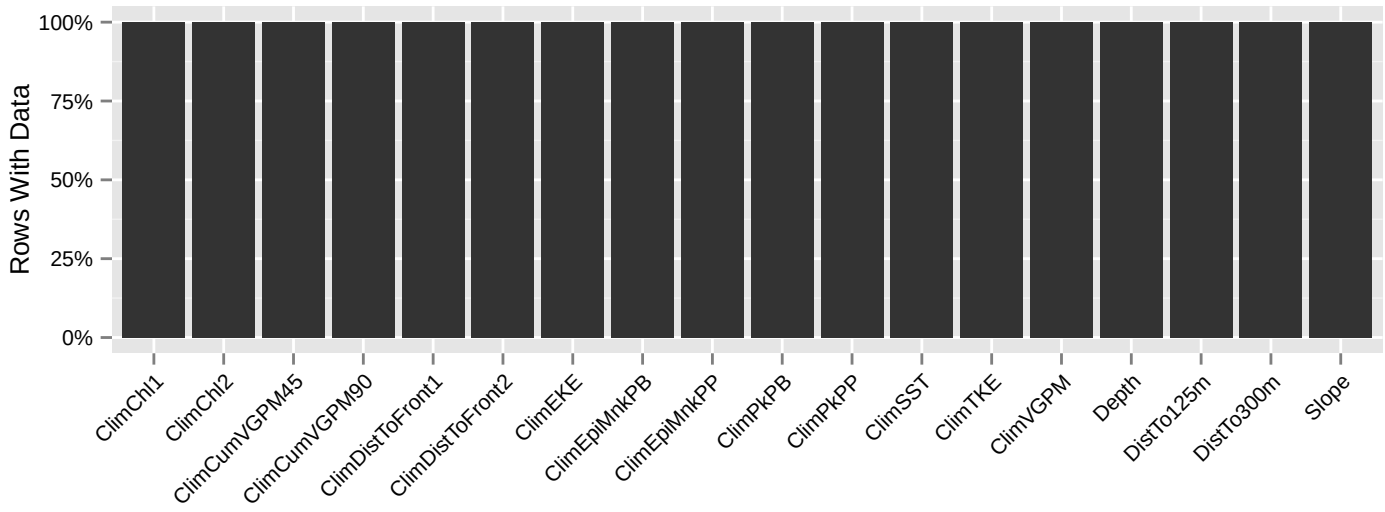

Figure 101: Segments with predictor values for the Sei whale Climatological model, Fall season, Northeast. This plot is used to assess how many segments would be lost by including a given predictor in a model.

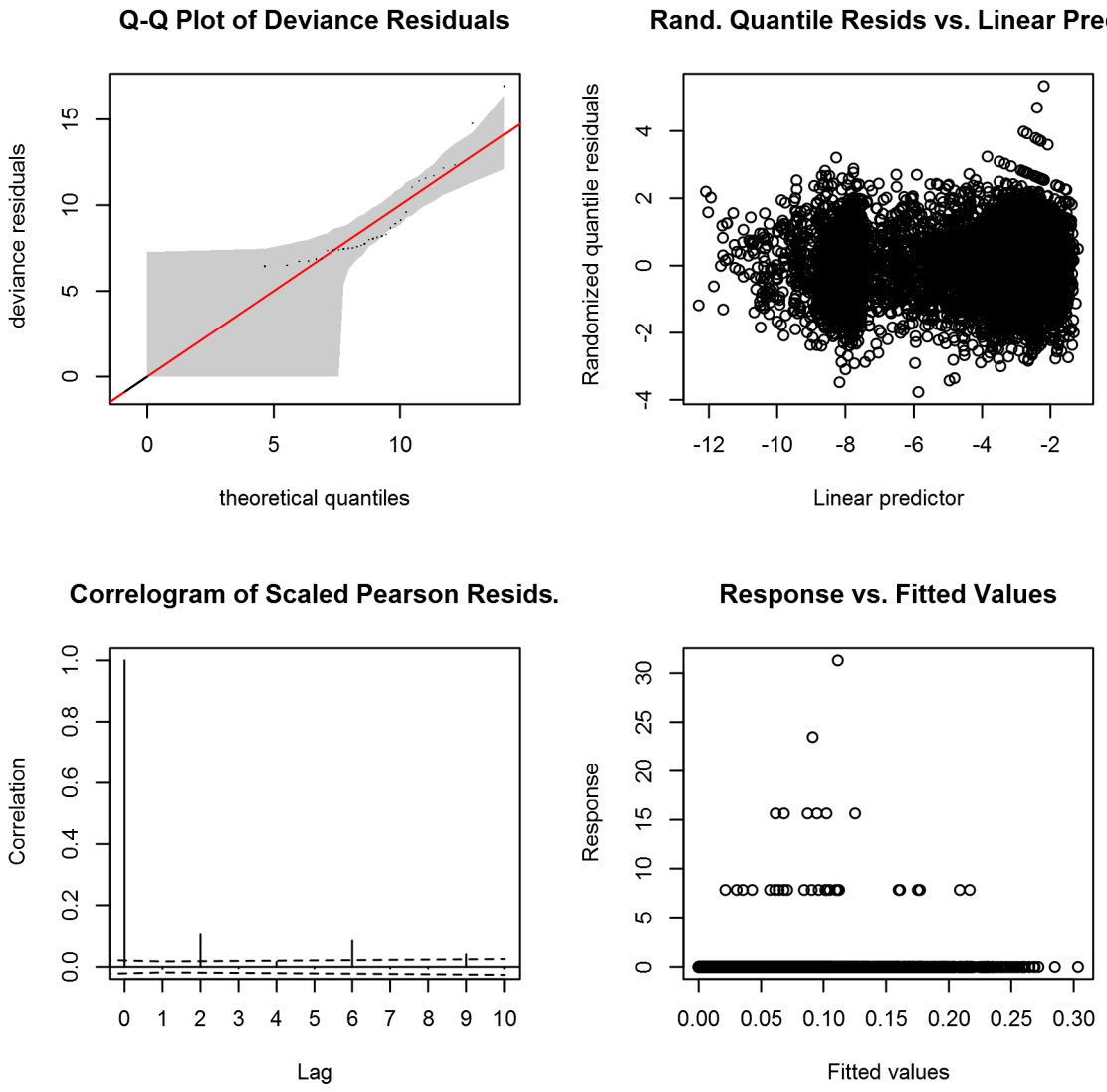

Figure 102: Statistical diagnostic plots for the Sei whale Climatological model, Fall season, Northeast.

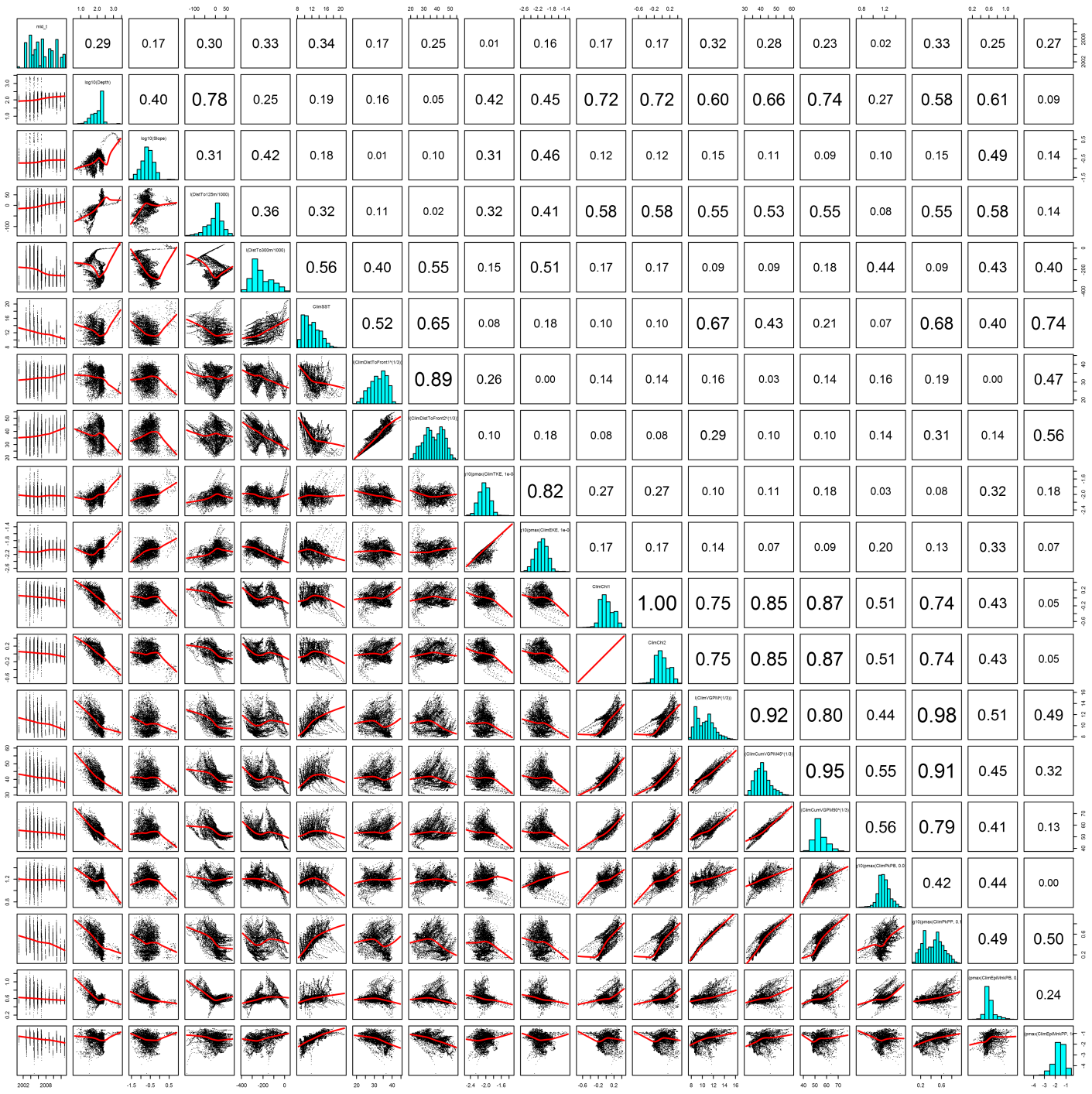

Figure 103: Scatterplot matrix for the Sei whale Climatological model, Fall season, Northeast. This plot is used to inspect the distribution of predictors (via histograms along the diagonal), simple correlation between predictors (via pairwise Pearson coefficients above the diagonal), and linearity of predictor correlations (via scatterplots below the diagonal). This plot is best viewed at high magnification.

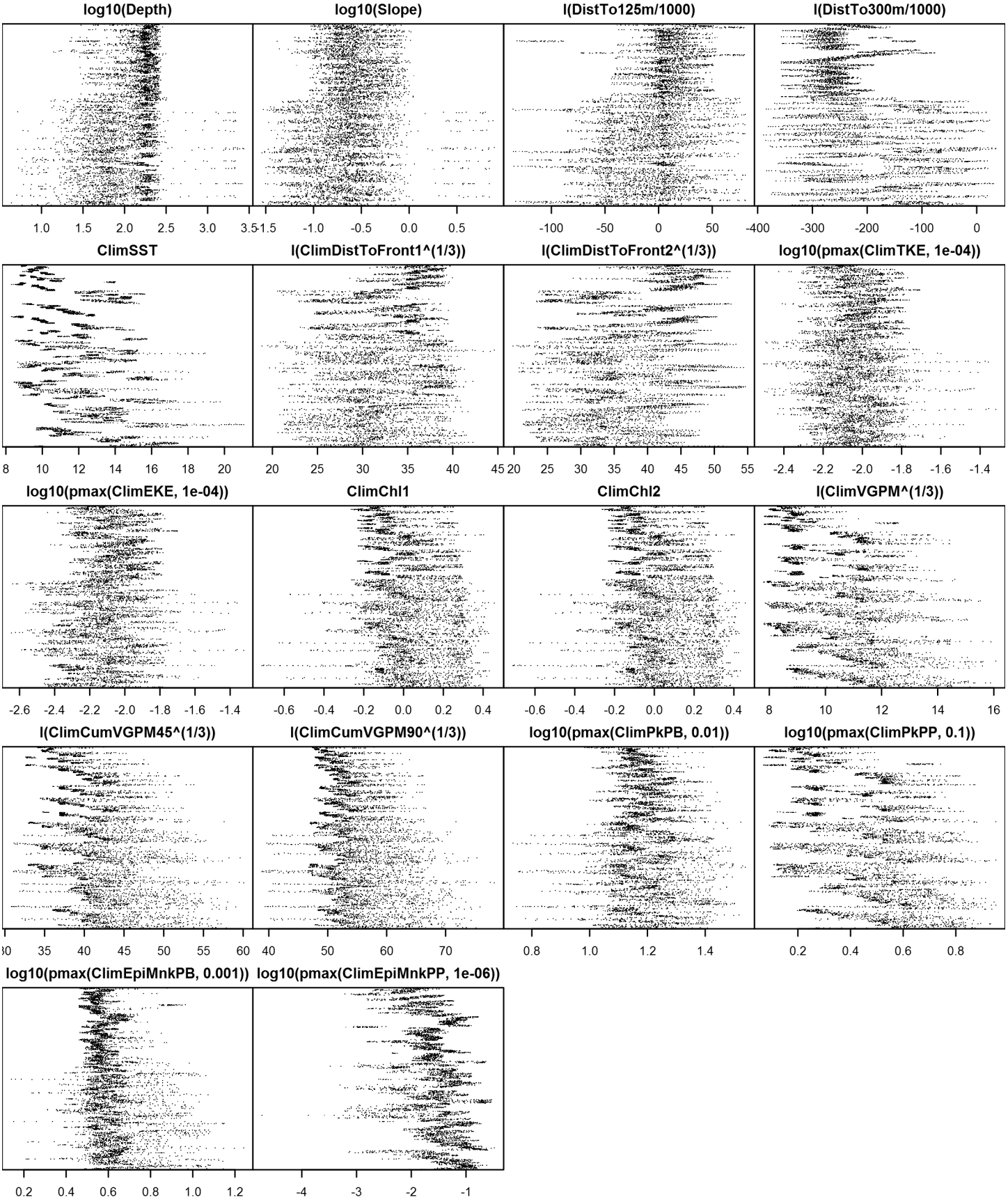

Figure 104: Dotplot for the Sei whale Climatological model, Fall season, Northeast. This plot is used to check for suspicious patterns and outliers in the data. Points are ordered vertically by transect ID, sequentially in time.

Low Effort Area

Density was not modeled for this region.

Contemporaneous Model

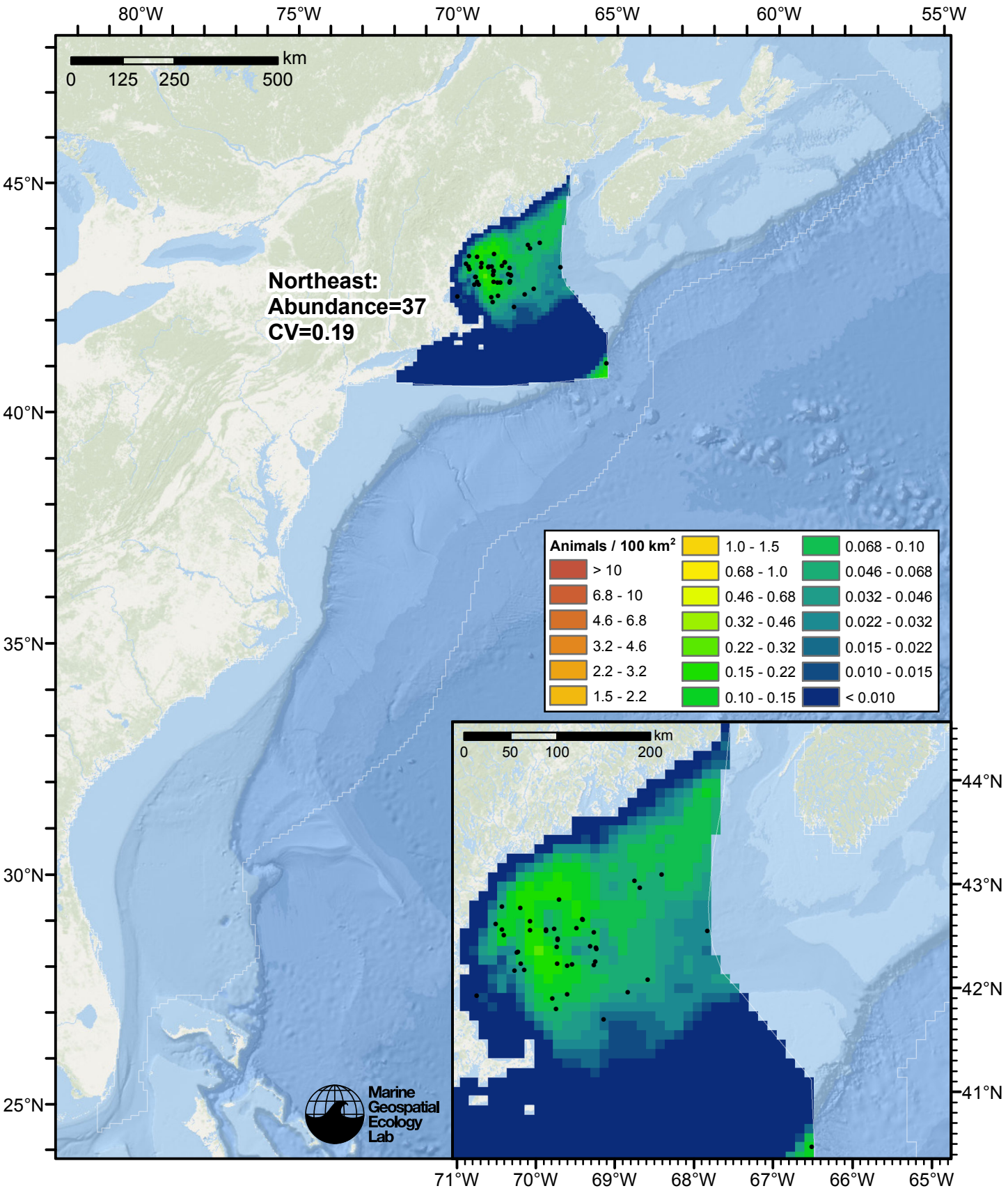

Figure 105: Sei whale density predicted by the Fall season contemporaneous model that explained the most deviance. Pixels are 10x10 km. The legend gives the estimated individuals per pixel; breaks are logarithmic. The same scale is used for all seasons. Abundance for each region was computed by summing the density cells occuring in that region.

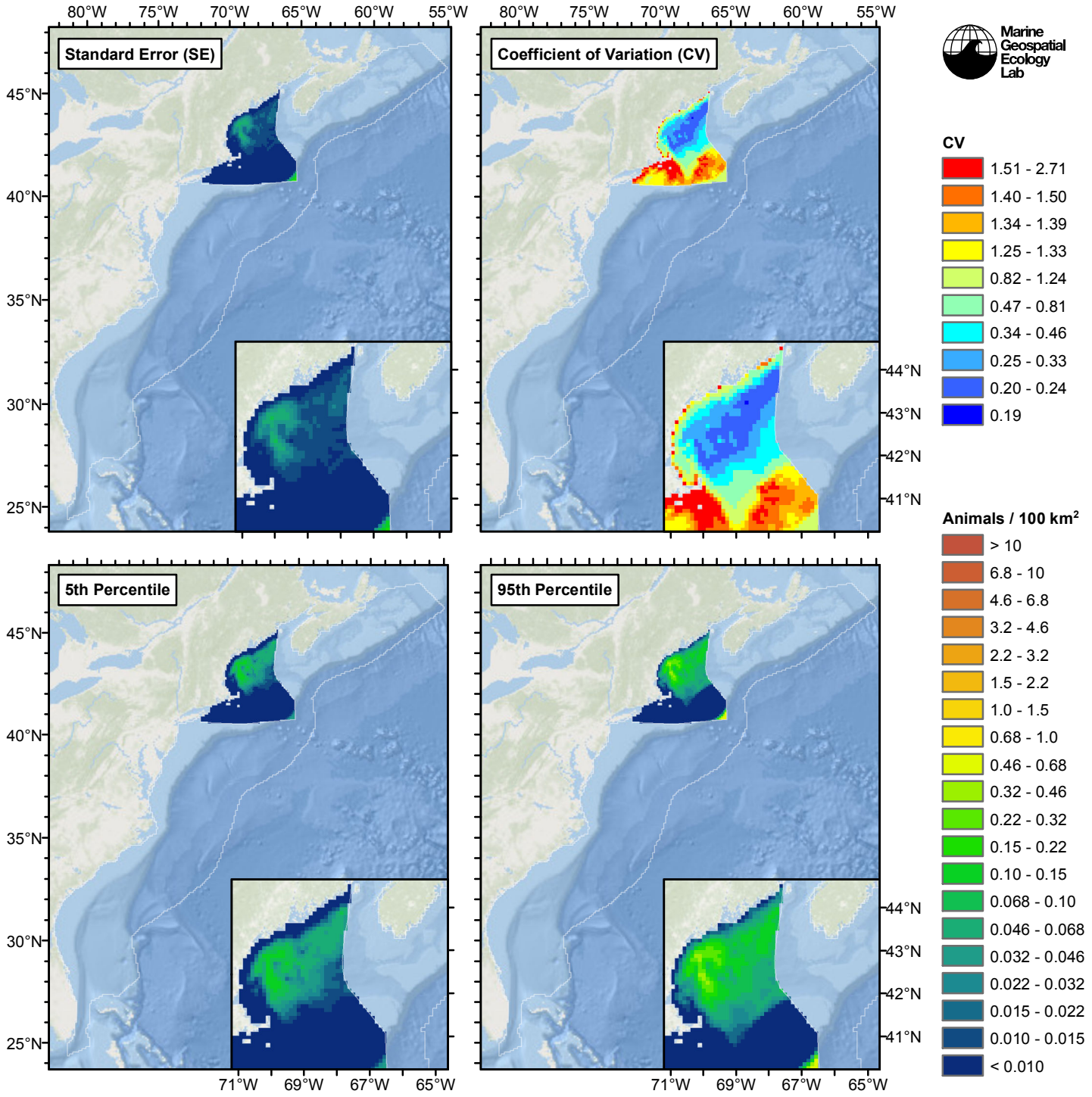

Figure 106: Estimated uncertainty for the Fall season contemporaneous model that explained the most deviance. These estimates only incorporate the statistical uncertainty estimated for the spatial model (by the R mgcv package). They do not incorporate uncertainty in the detection functions, g(0) estimates, predictor variables, and so on.

Northeast

Statistical output

```
Rscript.exe: This is mgcv 1.8-2. For overview type 'help("mgcv-package")'.


Family: Tweedie(p=1.126)
```

```
Link function: log

Formula:
abundance ~ offset(log(area_km2)) + s(log10(Depth), bs = "ts",
    k = 5) + s(I(DistTo300m/1000), bs = "ts", k = 5)

Parametric coefficients:
            Estimate Std. Error t value Pr(>|t|)
(Intercept)  -8.9677     0.4849  -18.49   <2e-16 ***
---
Signif. codes:  0 '***' 0.001 '**' 0.01 '*' 0.05 '.' 0.1 ' ' 1

Approximate significance of smooth terms:
                         edf Ref.df     F  p-value
s(log10(Depth))        1.049      4 3.918 2.82e-05 ***
s(I(DistTo300m/1000)) 1.102      4 3.473 8.08e-05 ***
---
Signif. codes:  0 '***' 0.001 '**' 0.01 '*' 0.05 '.' 0.1 ' ' 1

R-sq.(adj) =  0.00296   Deviance explained = 14.2%
-REML = 279.77  Scale est. = 16.118    n = 6780

All predictors were significant. This is the final model.
Creating term plots.
Diagnostic output from gam.check():

Method: REML   Optimizer: outer newton
full convergence after 10 iterations.
Gradient range [-0.0006769701,0.0003121349]
(score 279.7695 & scale 16.11772).
Hessian positive definite, eigenvalue range [0.4170728,275.2486].
Model rank =  9 / 9

Basis dimension (k) checking results. Low p-value (k-index<1) may
indicate that k is too low, especially if edf is close to k'.

                          k'   edf k-index p-value
s(log10(Depth))       4.000 1.049   0.792    0.02
s(I(DistTo300m/1000)) 4.000 1.102   0.790    0.02

Predictors retained during the model selection procedure: Depth, DistTo300m

Predictors dropped during the model selection procedure: Slope, DistTo125m, SST, DistToFront1
```

Model term plots

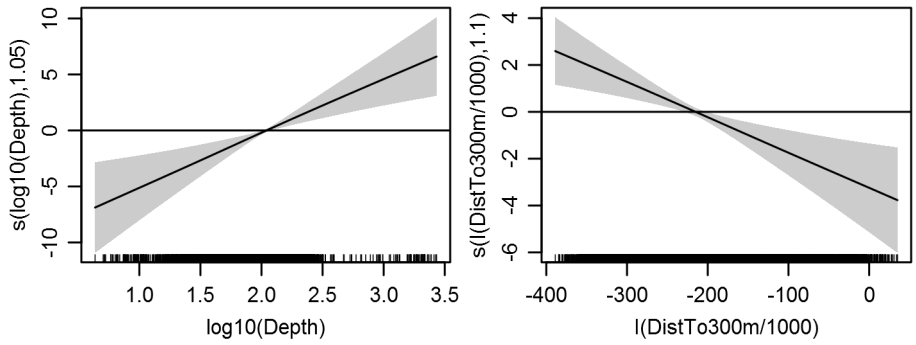

Diagnostic plots

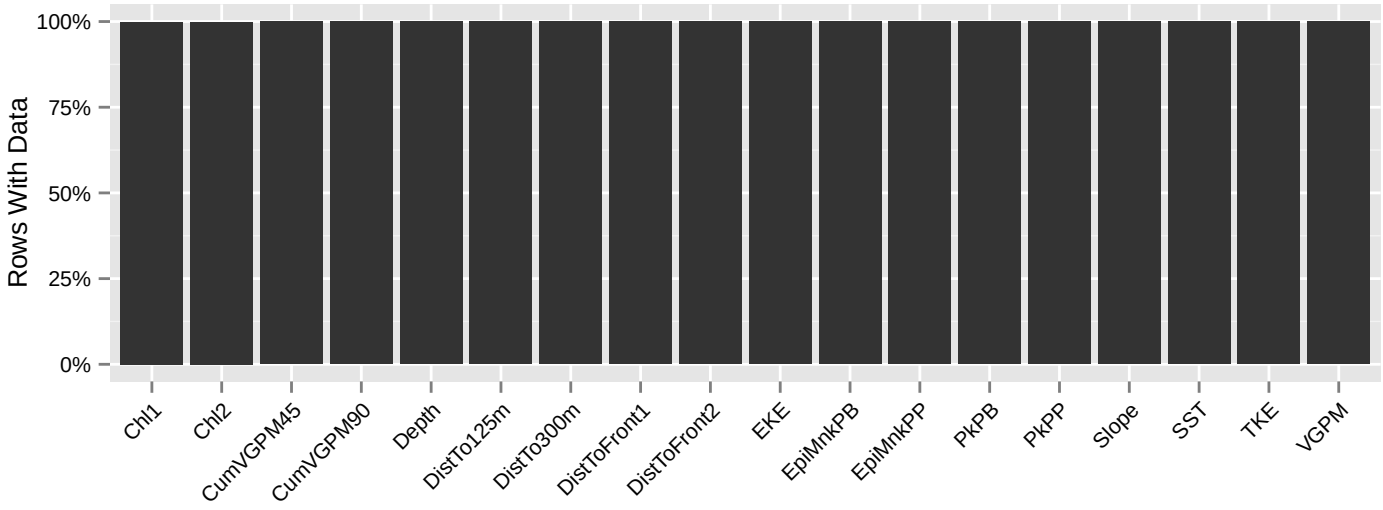

Figure 107: Segments with predictor values for the Sei whale Contemporaneous model, Fall season, Northeast. This plot is used to assess how many segments would be lost by including a given predictor in a model.

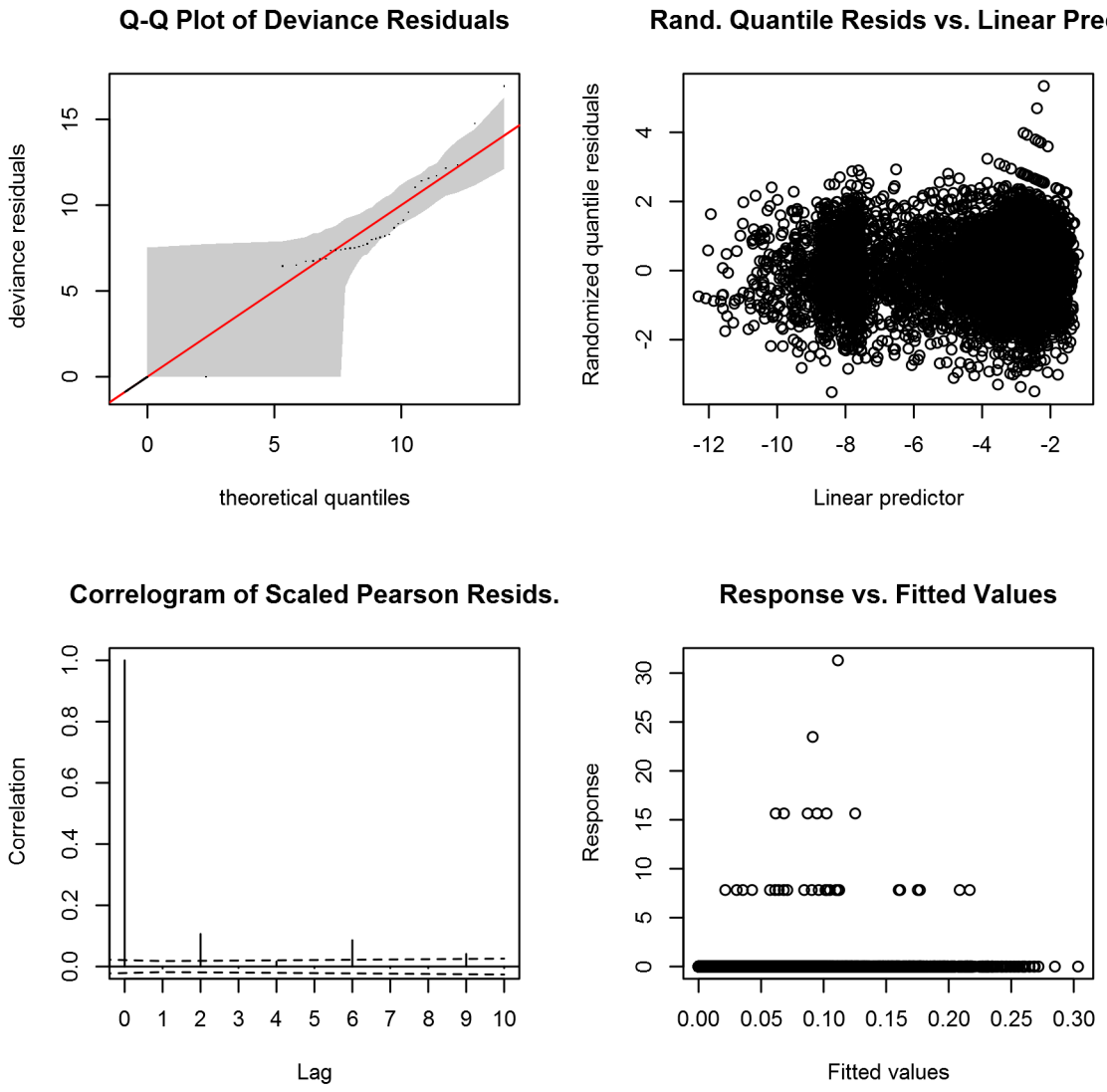

Figure 108: Statistical diagnostic plots for the Sei whale Contemporaneous model, Fall season, Northeast.

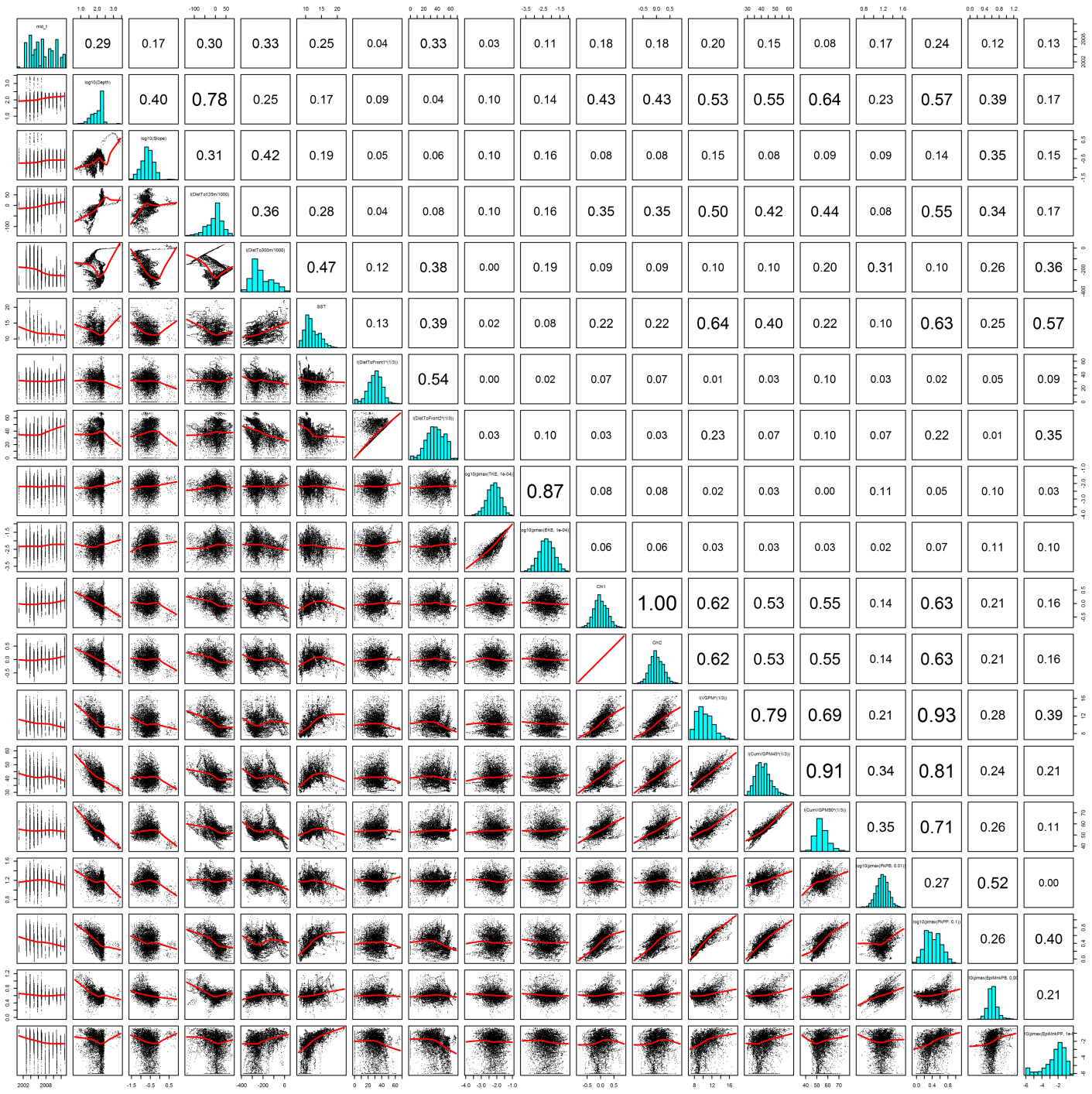

Figure 109: Scatterplot matrix for the Sei whale Contemporaneous model, Fall season, Northeast. This plot is used to inspect the distribution of predictors (via histograms along the diagonal), simple correlation between predictors (via pairwise Pearson coefficients above the diagonal), and linearity of predictor correlations (via scatterplots below the diagonal). This plot is best viewed at high magnification.

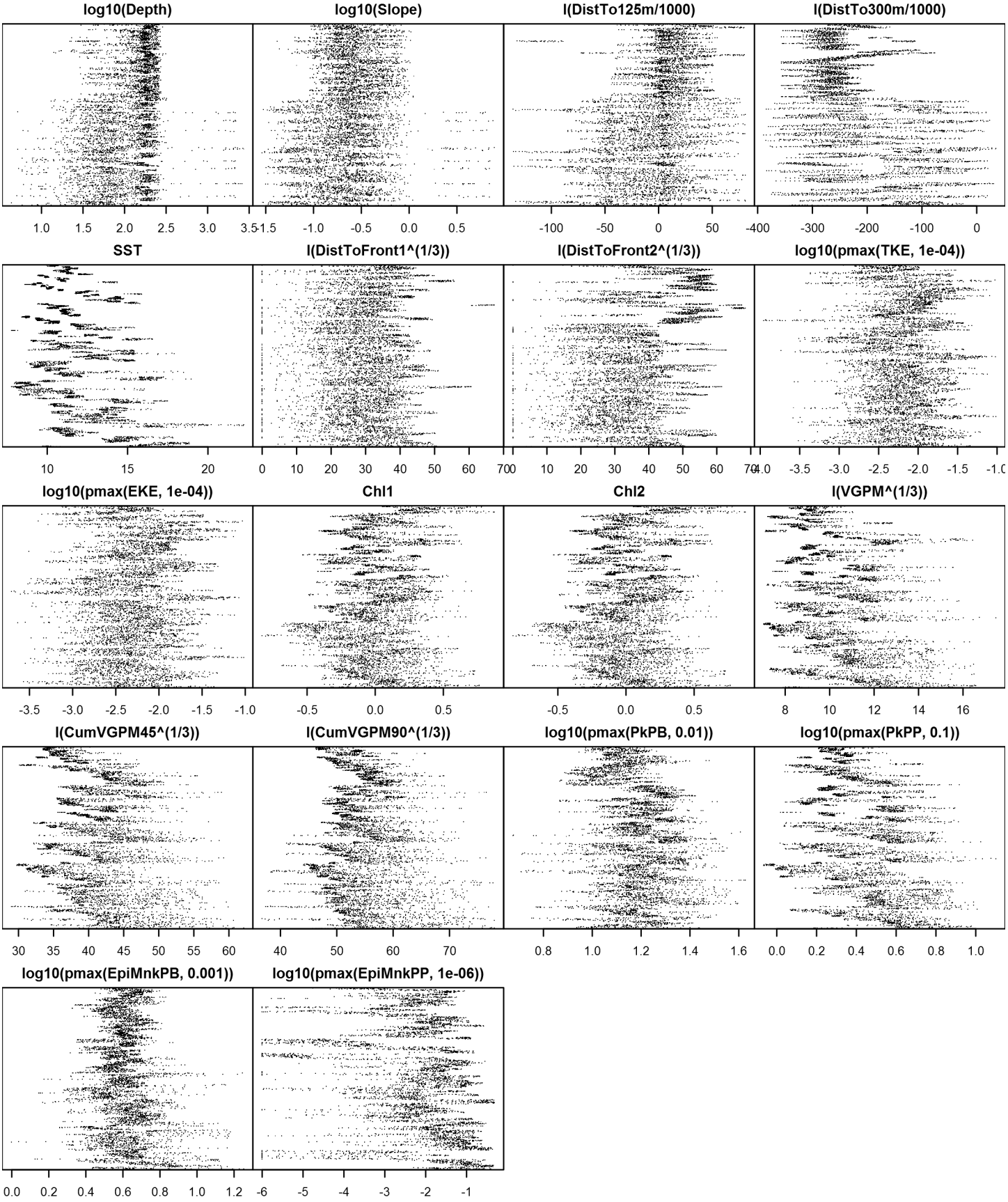

Figure 110: Dotplot for the Sei whale Contemporaneous model, Fall season, Northeast. This plot is used to check for suspicious patterns and outliers in the data. Points are ordered vertically by transect ID, sequentially in time.

Low Effort Area

Density was not modeled for this region.

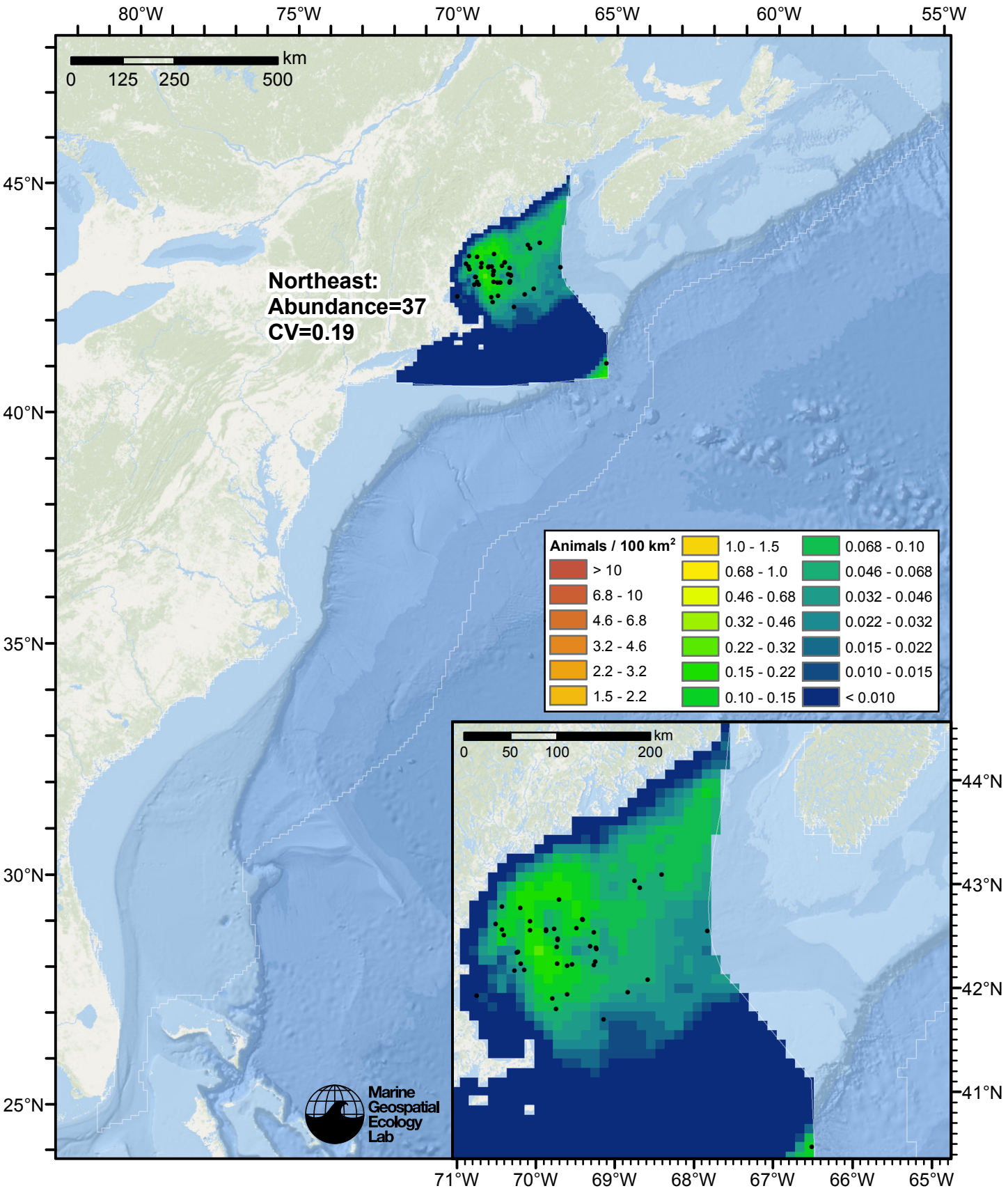

Figure 111: Sei whale density predicted by the Fall season climatological same segments model that explained the most deviance. Pixels are 10x10 km. The legend gives the estimated individuals per pixel; breaks are logarithmic. The same scale is used for all seasons. Abundance for each region was computed by summing the density cells occuring in that region.

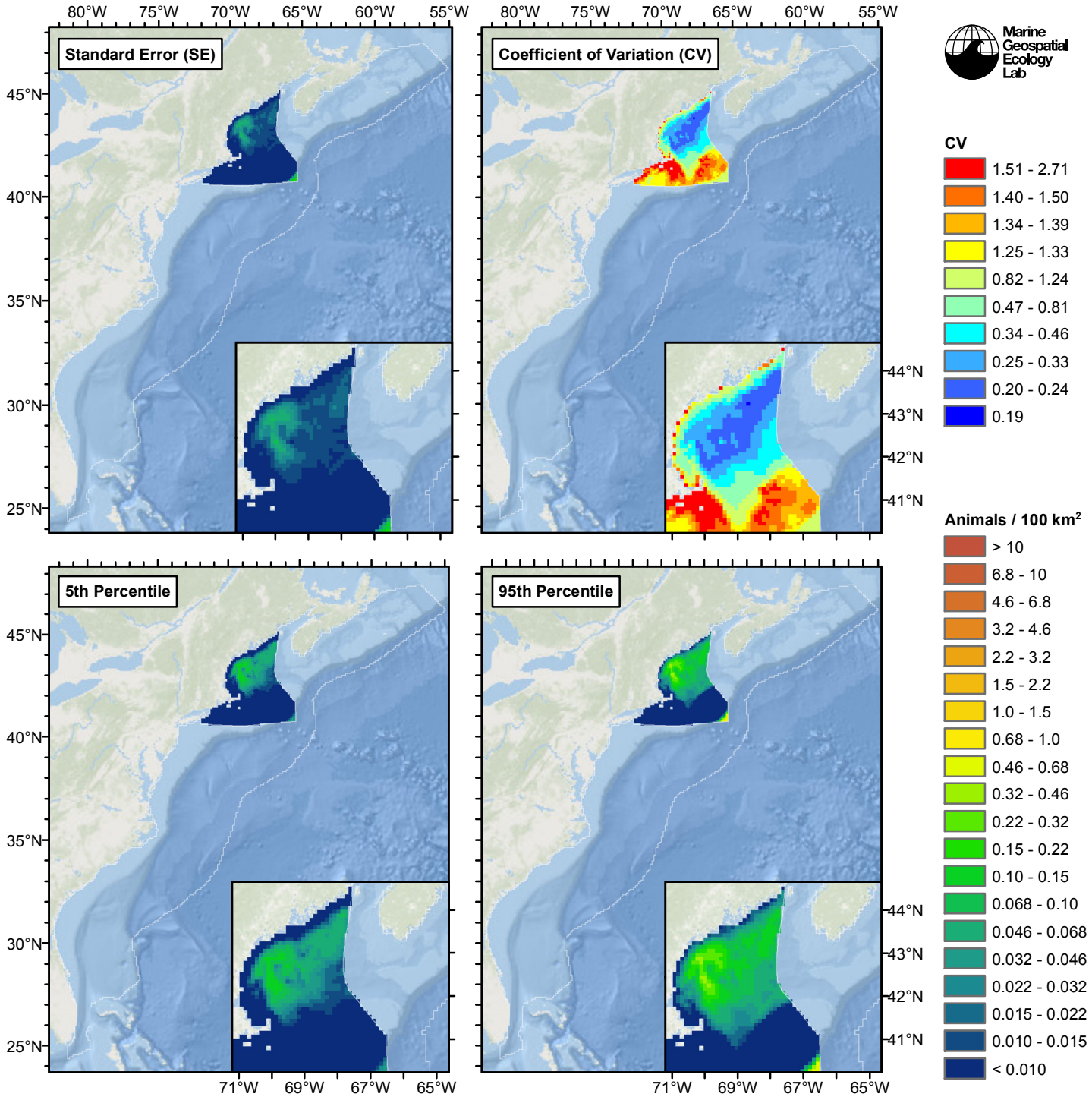

Figure 112: Estimated uncertainty for the Fall season climatological same segments model that explained the most deviance. These estimates only incorporate the statistical uncertainty estimated for the spatial model (by the R mgcv package). They do not incorporate uncertainty in the detection functions, g(0) estimates, predictor variables, and so on.

Northeast

Statistical output

```
Rscript.exe: This is mgcv 1.8-2. For overview type 'help("mgcv-package")'.


Family: Tweedie(p=1.126)
```

```
Link function: log

Formula:
abundance ~ offset(log(area_km2)) + s(log10(Depth), bs = "ts",
    k = 5) + s(I(DistTo300m/1000), bs = "ts", k = 5)

Parametric coefficients:
            Estimate Std. Error t value Pr(>|t|)
(Intercept)  -8.9677     0.4849  -18.49   <2e-16 ***
---
Signif. codes:  0 '***' 0.001 '**' 0.01 '*' 0.05 '.' 0.1 ' ' 1

Approximate significance of smooth terms:
                         edf Ref.df     F  p-value
s(log10(Depth))        1.049      4 3.918 2.82e-05 ***
s(I(DistTo300m/1000)) 1.102      4 3.473 8.08e-05 ***
---
Signif. codes:  0 '***' 0.001 '**' 0.01 '*' 0.05 '.' 0.1 ' ' 1

R-sq.(adj) =  0.00296   Deviance explained = 14.2%
-REML = 279.77  Scale est. = 16.118    n = 6780

All predictors were significant. This is the final model.
Creating term plots.
Diagnostic output from gam.check():

Method: REML   Optimizer: outer newton
full convergence after 10 iterations.
Gradient range [-0.0006769701,0.0003121349]
(score 279.7695 & scale 16.11772).
Hessian positive definite, eigenvalue range [0.4170728,275.2486].
Model rank =  9 / 9

Basis dimension (k) checking results. Low p-value (k-index<1) may
indicate that k is too low, especially if edf is close to k'.

                          k'   edf k-index p-value
s(log10(Depth))        4.000 1.049   0.804    0.01
s(I(DistTo300m/1000)) 4.000 1.102   0.831    0.04

Predictors retained during the model selection procedure: Depth, DistTo300m

Predictors dropped during the model selection procedure: Slope, DistTo125m, ClimSST,
ClimDistToFront1
```

Model term plots

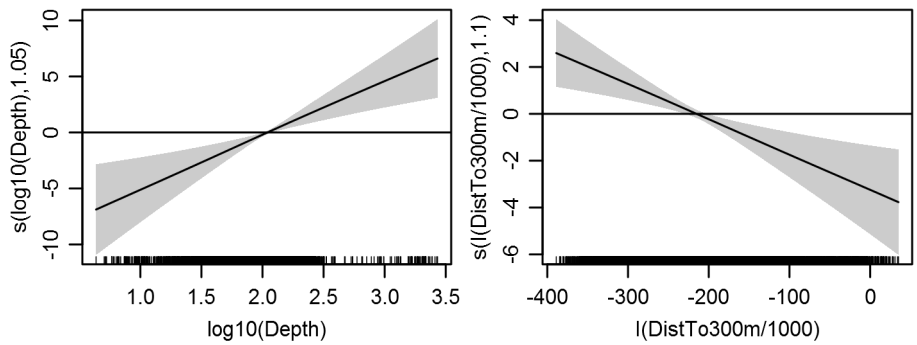

Diagnostic plots

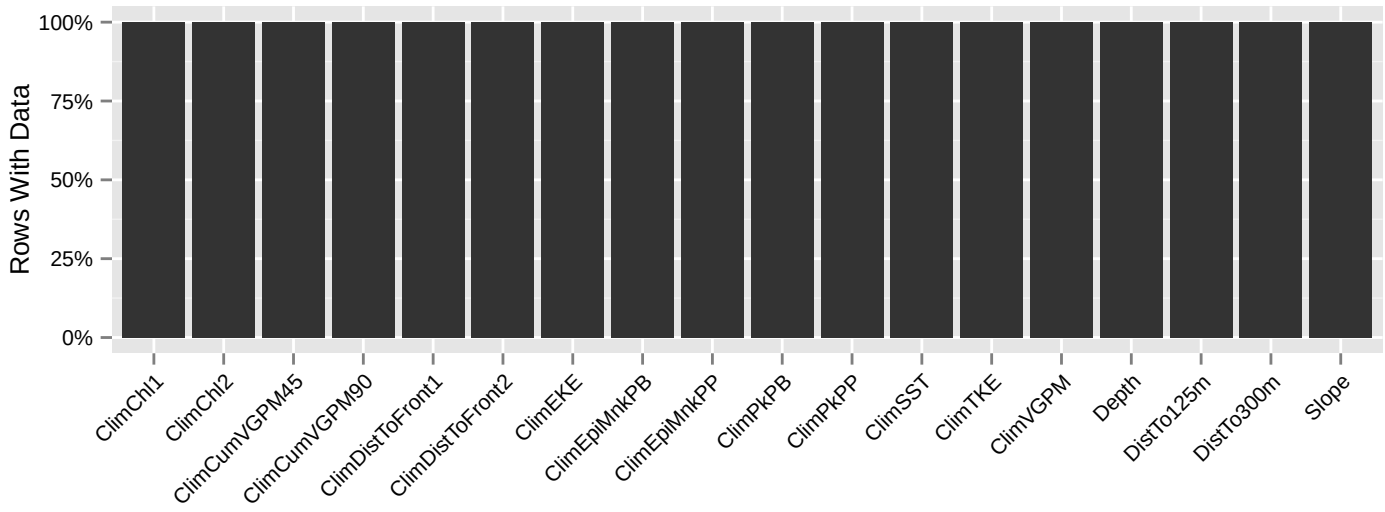

Figure 113: Segments with predictor values for the Sei whale Climatological model, Fall season, Northeast. This plot is used to assess how many segments would be lost by including a given predictor in a model.

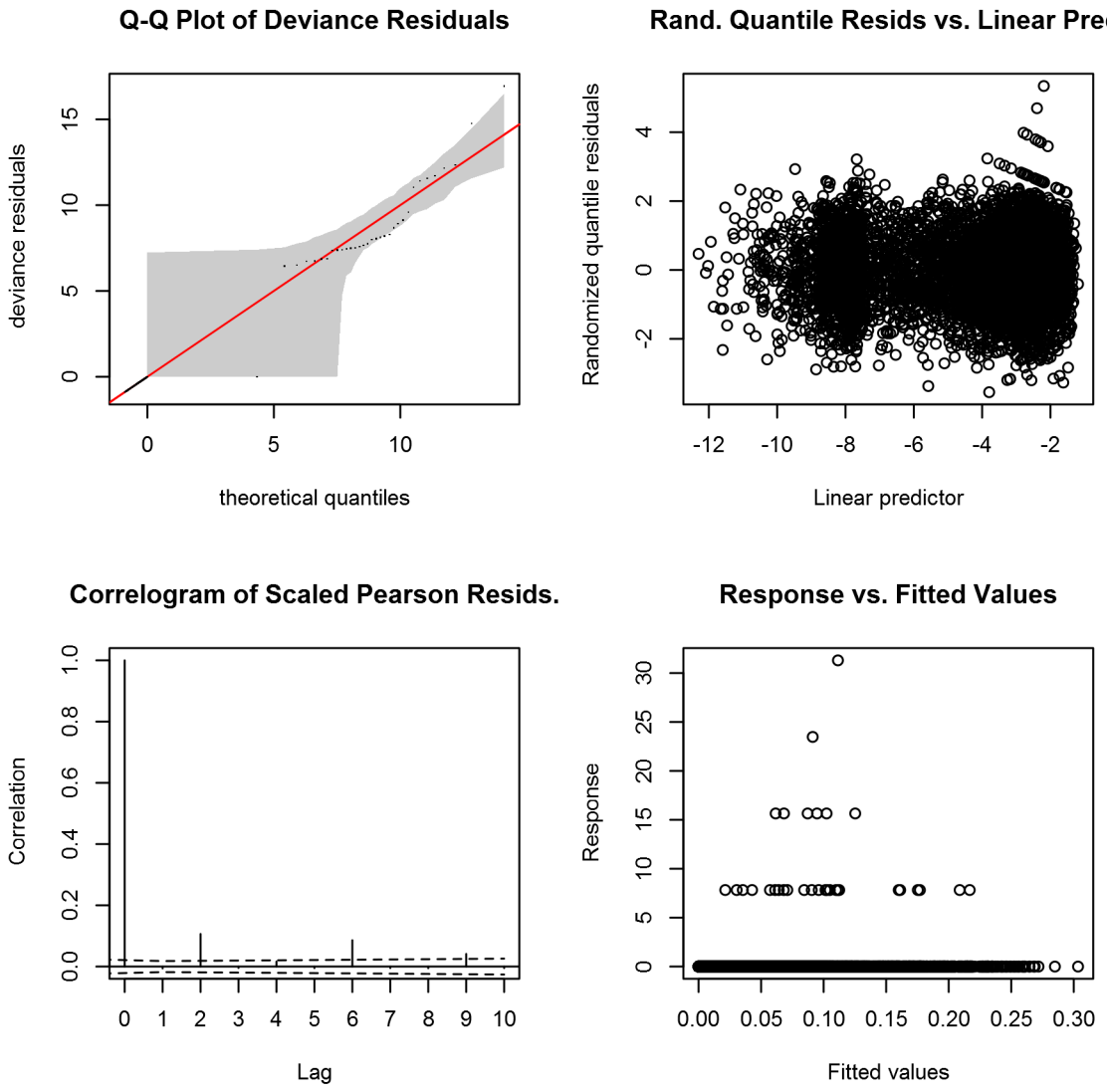

Figure 114: Statistical diagnostic plots for the Sei whale Climatological model, Fall season, Northeast.

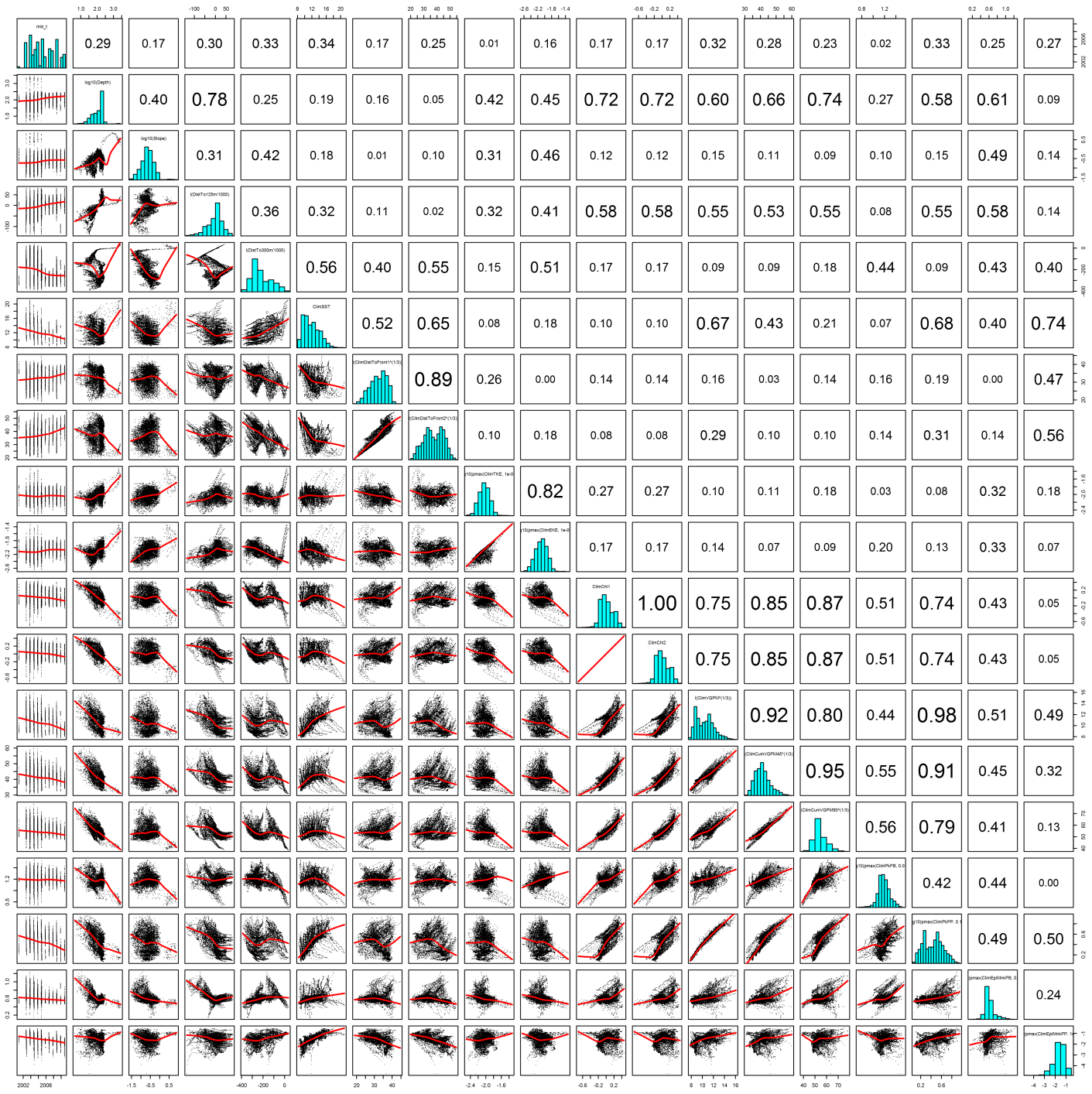

Figure 115: Scatterplot matrix for the Sei whale Climatological model, Fall season, Northeast. This plot is used to inspect the distribution of predictors (via histograms along the diagonal), simple correlation between predictors (via pairwise Pearson coefficients above the diagonal), and linearity of predictor correlations (via scatterplots below the diagonal). This plot is best viewed at high magnification.

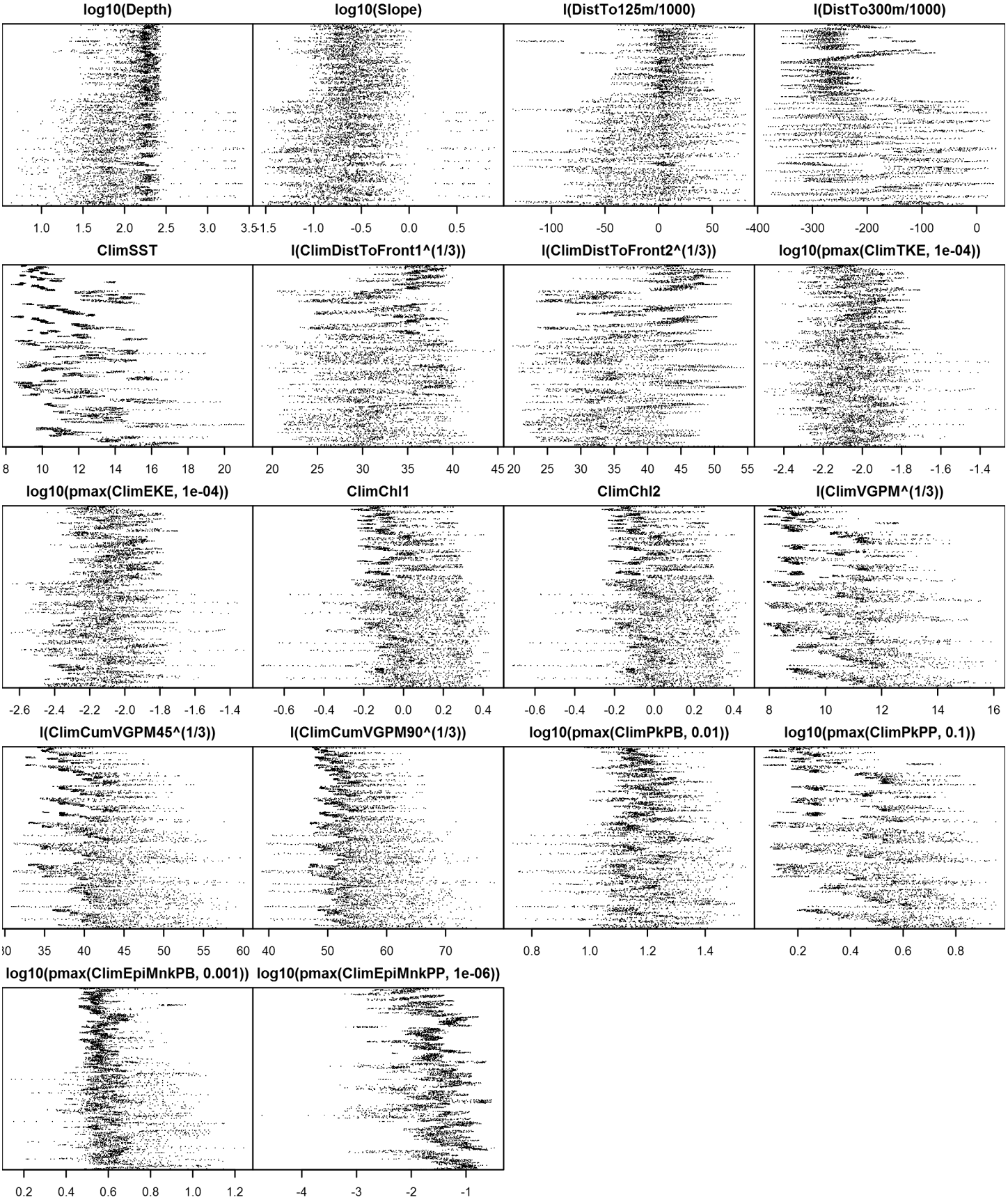

Figure 116: Dotplot for the Sei whale Climatological model, Fall season, Northeast. This plot is used to check for suspicious patterns and outliers in the data. Points are ordered vertically by transect ID, sequentially in time.

Low Effort Area

Density was not modeled for this region.

Model Comparison

Spatial Model Performance

The table below summarizes the performance of the candidate spatial models that were tested. For each season, the first model contained only physiographic predictors. Subsequent models added additional suites of predictors of based on when they became available via remote sensing.

For each model, three versions were fitted; the % Dev Expl columns give the % deviance explained by each one. The "climatological" models were fitted to 8-day climatologies of the environmental predictors. Because the environmental predictors were always available, no segments were lost, allowing these models to consider the maximal amount of survey data. The "contemporaneous" models were fitted to day-of-sighting images of the environmental predictors; these were smoothed to reduce data loss due to clouds, but some segments still failed to retrieve environmental values and were lost. Finally, the "climatological same segments" models fitted climatological predictors to the segments retained by the contemporaneous model, so that the explantory power of the two types of predictors could be directly compared. For each of the three models, predictors were selected independently via shrinkage smoothers; thus the three models did not necessarily utilize the same predictors.

Predictors derived from ocean currents first became available in January 1993 after the launch of the TOPEX/Poseidon satellite; productivity predictors first became available in September 1997 after the launch of the SeaWiFS sensor. Contemporaneous and climatological same segments models considering these predictors usually suffered data loss. Date Range shows the years spanned by the retained segments. The Segments column gives the number of segments retained; % Lost gives the percentage lost.

Season	Predictors	Climatol % Dev Expl	Contemp % Dev Expl	Climatol Same Segs % Dev Expl	Segments	% Lost	Date Range
Winter							
	None	10.8			31668		1992-2014
Spring							
	Phys	28.6			33856		1999-2014
	Phys+SST	32.1	32.5	32.1	33856	0.0	1999-2014
	Phys+SST+Curr	32.5	32.5	32.2	33367	1.4	1999-2013
	Phys+SST+Curr+Prod	33.6	34.2	33.3	33367	1.4	1999-2013
Summer							
	Phys	32.8			16688		1995-2013
	Phys+SST	33.8	34.4	33.8	16688	0.0	1995-2013
	Phys+SST+Curr	34.6	34.4	34.6	16688	0.0	1995-2013
	Phys+SST+Curr+Prod	39.4	33.8	35.6	14272	14.5	1998-2013
Fall							
	Phys	14.2			6780		2000-2012
	Phys+SST	14.2	14.2	14.2	6780	0.0	2000-2012
	Phys+SST+Curr	14.2	14.2	14.2	6780	0.0	2000-2012
	Phys+SST+Curr+Prod	14.2	14.2	14.2	6780	0.0	2000-2012

Table 39: Deviance explained by the candidate density models.

Abundance Estimates

The table below shows the estimated mean abundance (number of animals) within the study area, for the models that explained the most deviance for each model type. Mean abundance was calculated by first predicting density maps for a series of time steps, then computing the abundance for each map, and then averaging the abundances. For the climatological models, we used 8-day climatologies, resulting in 46 abundance maps. For the contemporaneous models, we used daily images, resulting in 365 predicted abundance maps per year that the prediction spanned. The Dates column gives the dates to which the estimates apply. For our models, these are the years for which both survey data and remote sensing data were available.

The Assumed g(0)=1 column specifies whether the abundance estimate assumed that detection was certain along the survey trackline. Studies that assumed this did not correct for availability or perception bias, and therefore underestimated abundance. The In our models column specifies whether the survey data from the study was also used in our models. If not, the study provides a completely independent estimate of abundance.

Season	Dates	Model or study	Estimated abundance	CV	Assumed g(0)=1	In our models
Winter						
	1992-2014	Climatological model*	98	0.25	No	
	1992-2014	Contemporaneous model	98	0.25	No	
	1992-2014	Climatological same segments model	98	0.25	No	
Spring						
	1999-2014	Climatological model	714	0.15	No	
	1999-2013	Contemporaneous model*	627	0.14	No	
	1999-2014	Climatological same segments model	722	0.16	No	
Summer						
	1995-2013	Climatological model*	717	0.30	No	
	1995-2013	Contemporaneous model	816	0.21	No	
	1995-2013	Climatological same segments model	1742	0.38	No	
	Jun-Aug 2011	Central Virginia to lower Bay of Fundy (Waring et al. 2014)	357	0.52	No	No
	August 2006	Southern Gulf of Maine to Bay of Fundy and Gulf of St. Lawrence (Waring et al. 2014)	207	0.62	No	Yes
	Jun-Aug 2004	Maryland to Bay of Fundy (Waring et al. 2007)	386	0.85	No	Yes
	Aug 2002	Southern Gulf of Maine to Maine (Palka 2006)	71	1.01	No	Yes
Fall						
	2000-2012	Climatological model*	37	0.19	No	
	2000-2012	Contemporaneous model	37	0.19	No	
	2000-2012	Climatological same segments model	37	0.19	No	

Table 40: Estimated mean abundance within the study area. We selected the model marked with * as our best estimate of the abundance and distribution of this taxon. For comparison, independent abundance estimates from NOAA technical reports and/or the scientific literature are shown. Please see the Discussion section below for our evaluation of our models compared to the other estimates. Our coefficients of variation (CVs) underestimate the true uncertainty in our estimates, as they only incorporated the uncertainty of the GAM stage of our models. Other sources of uncertainty include the detection functions and g(0) estimates. It was not possible to incorporate these into our CVs without undertaking a computationally-prohibitive bootstrap; we hope to attempt that in a future version of our models.

Density Maps

Climatological Model

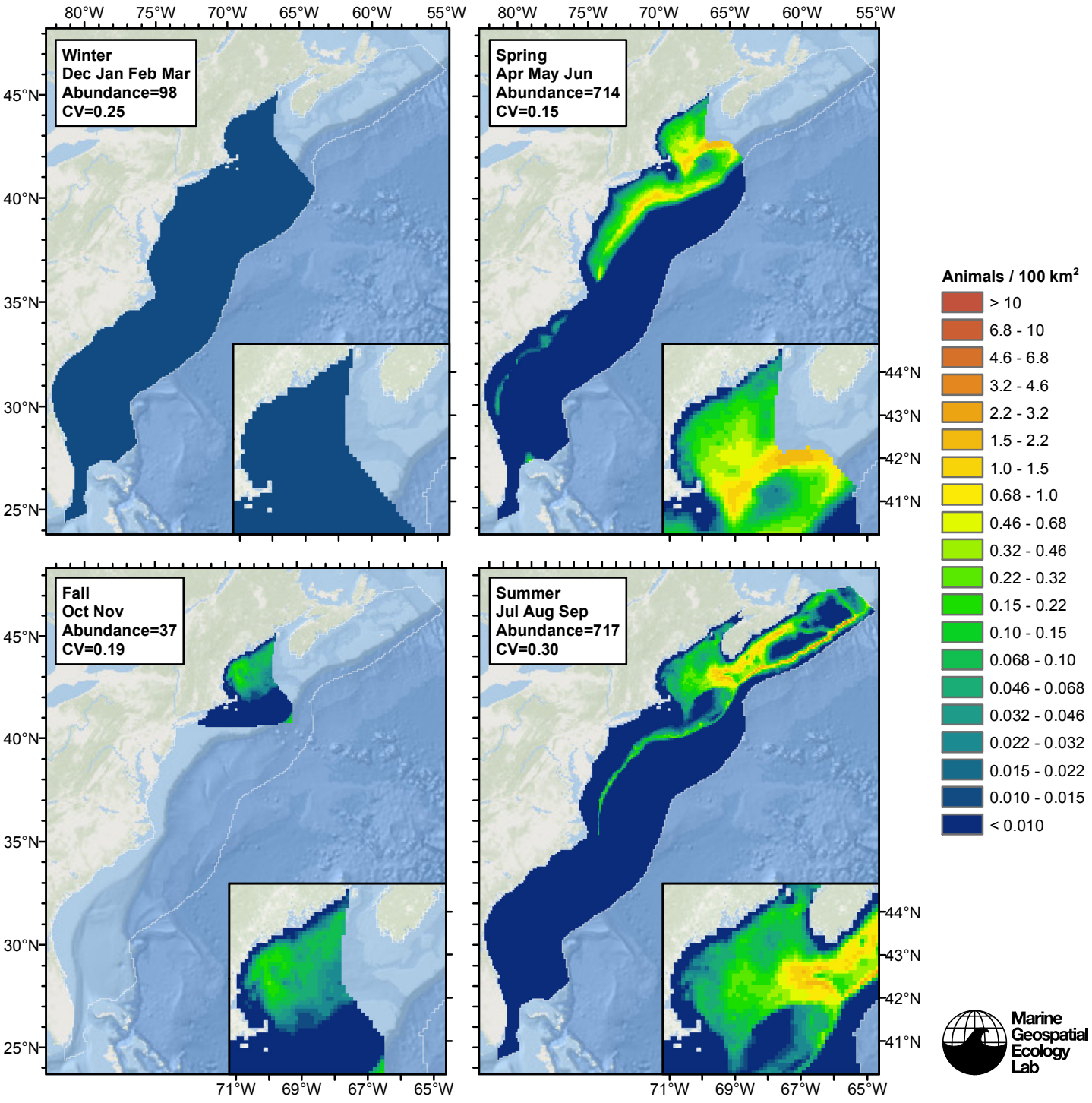

Figure 117: Sei whale density and abundance predicted by the climatological model that explained the most deviance. Regions inside the study area (white line) where the background map is visible are areas we did not model (see text).

Contemporaneous Model

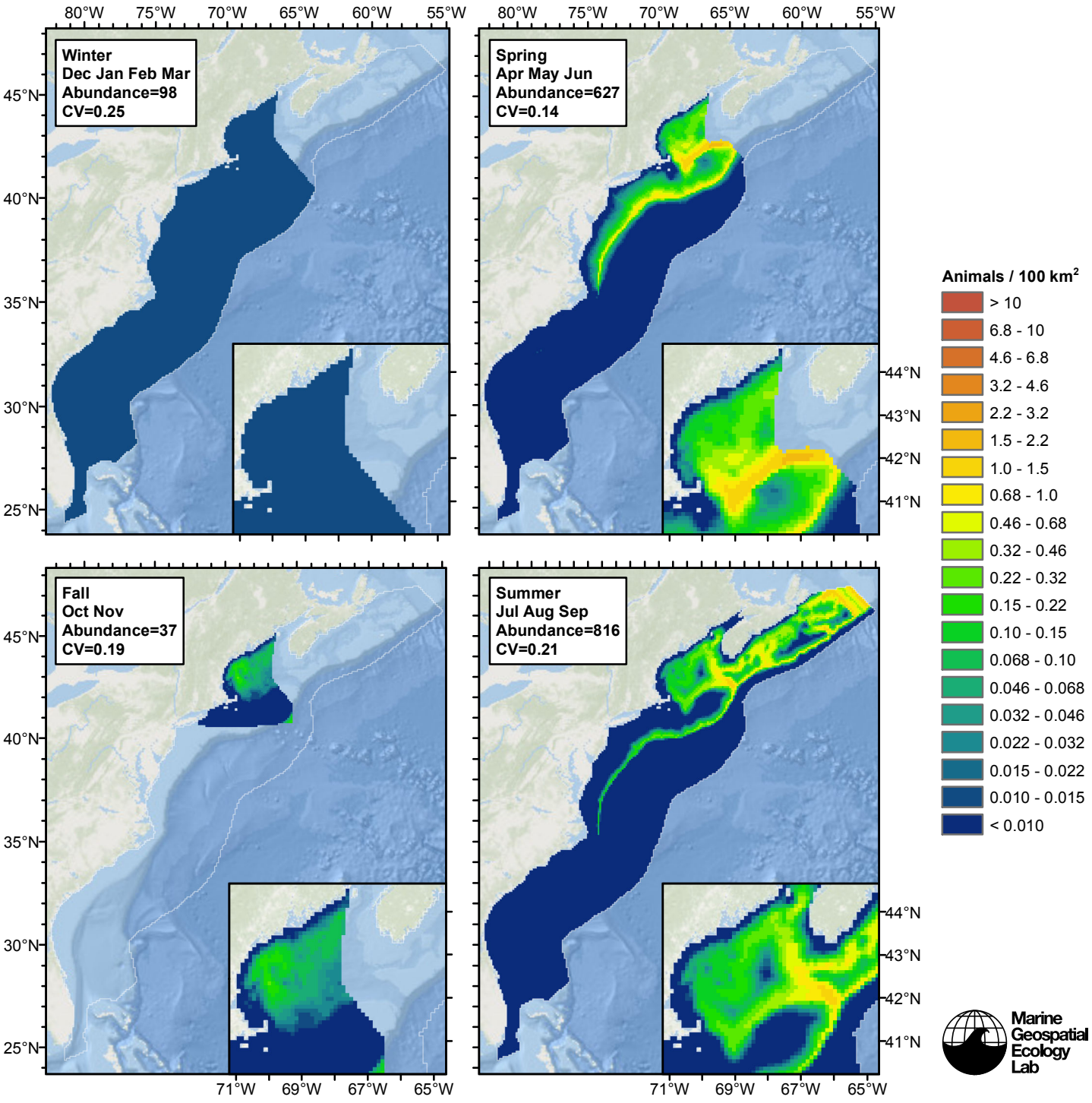

Figure 118: Sei whale density and abundance predicted by the contemporaneous model that explained the most deviance. Regions inside the study area (white line) where the background map is visible are areas we did not model (see text).

Climatological Same Segments Model

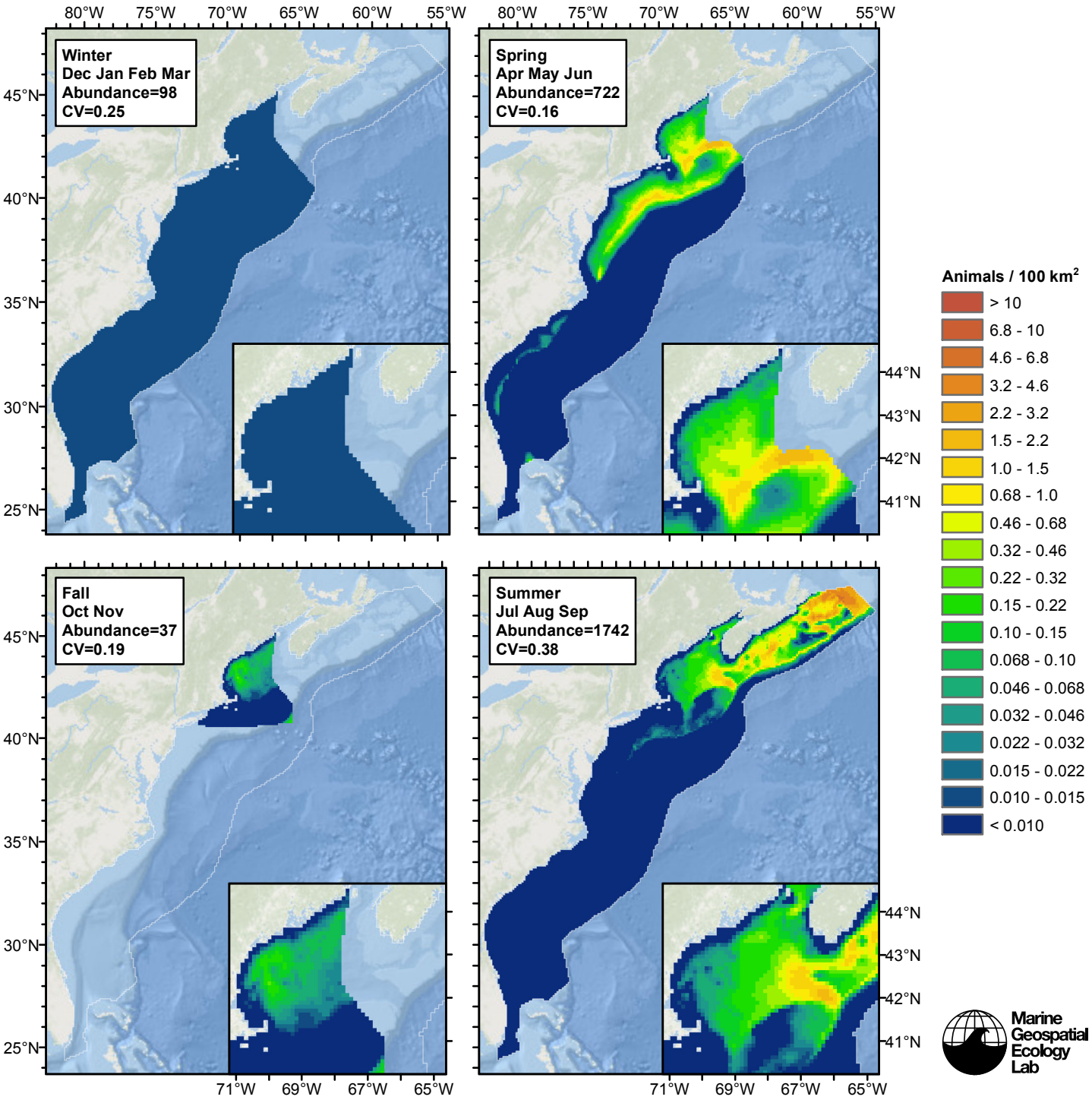

Figure 119: Sei whale density and abundance predicted by the climatological same segments model that explained the most deviance. Regions inside the study area (white line) where the background map is visible are areas we did not model (see text).

Temporal Variability

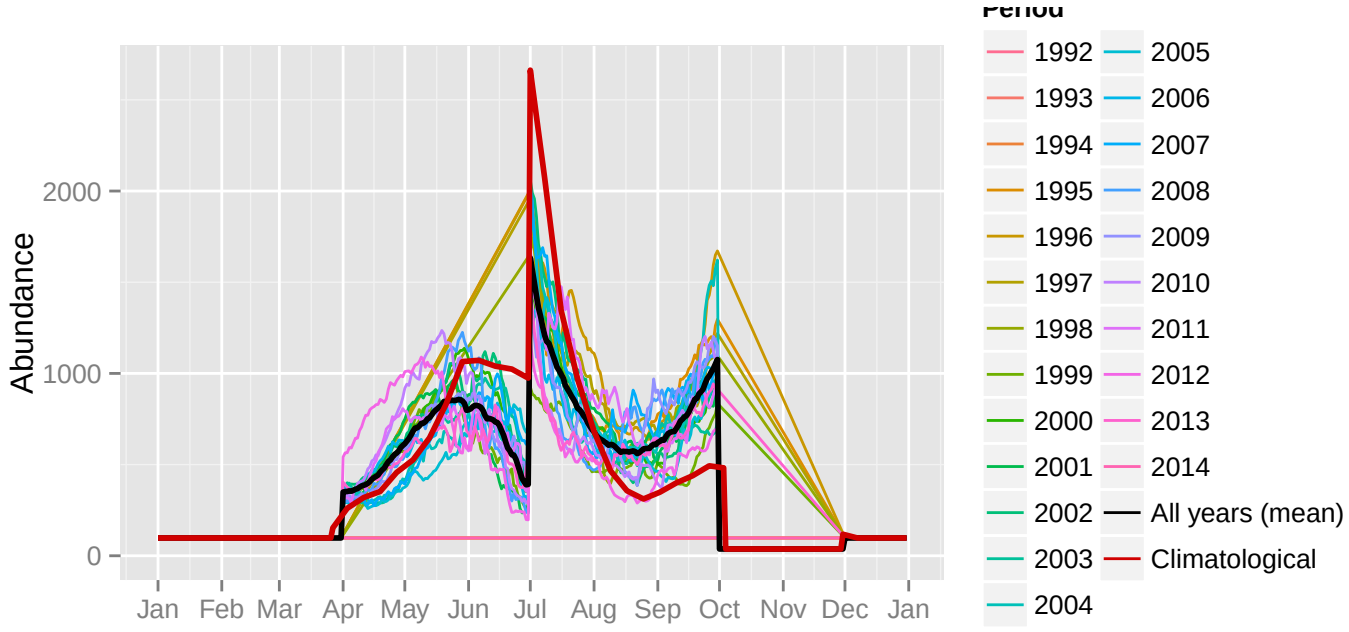

Figure 120: Comparison of Sei whale abundance predicted at a daily time step for different time periods. Individual years were predicted using contemporaneous models. "All years (mean)" averages the individual years, giving the mean annual abundance of the contemporaneous model. "Climatological" was predicted using the climatological model. The results for the climatological same segments model are not shown.

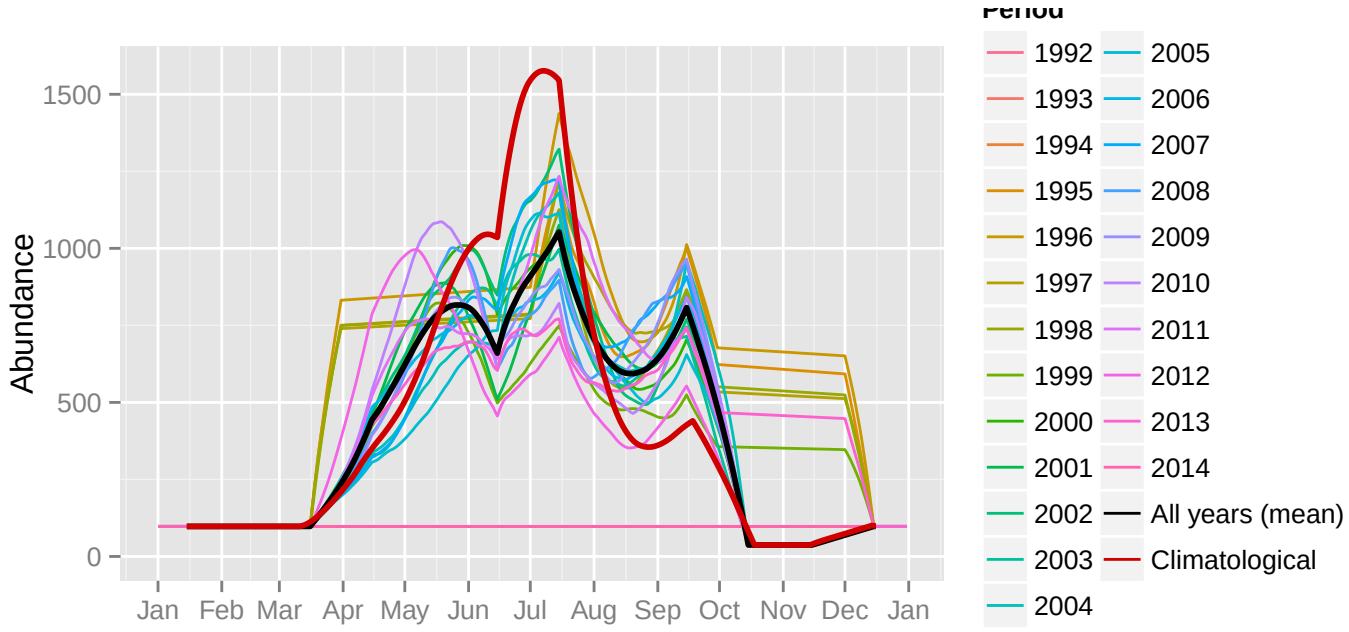

Figure 121: The same data as the preceding figure, but with a 30-day moving average applied.

Climatological Model

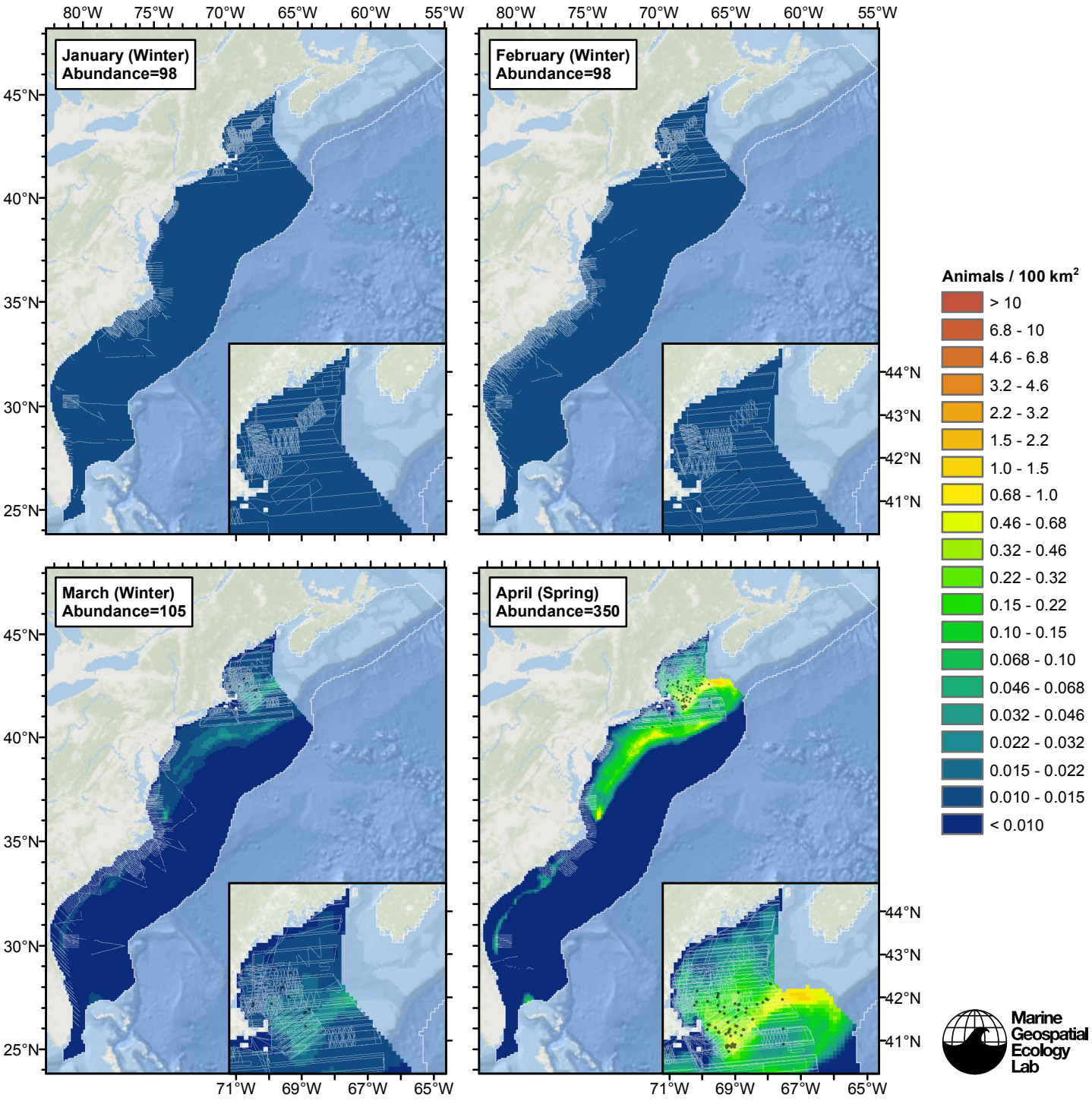

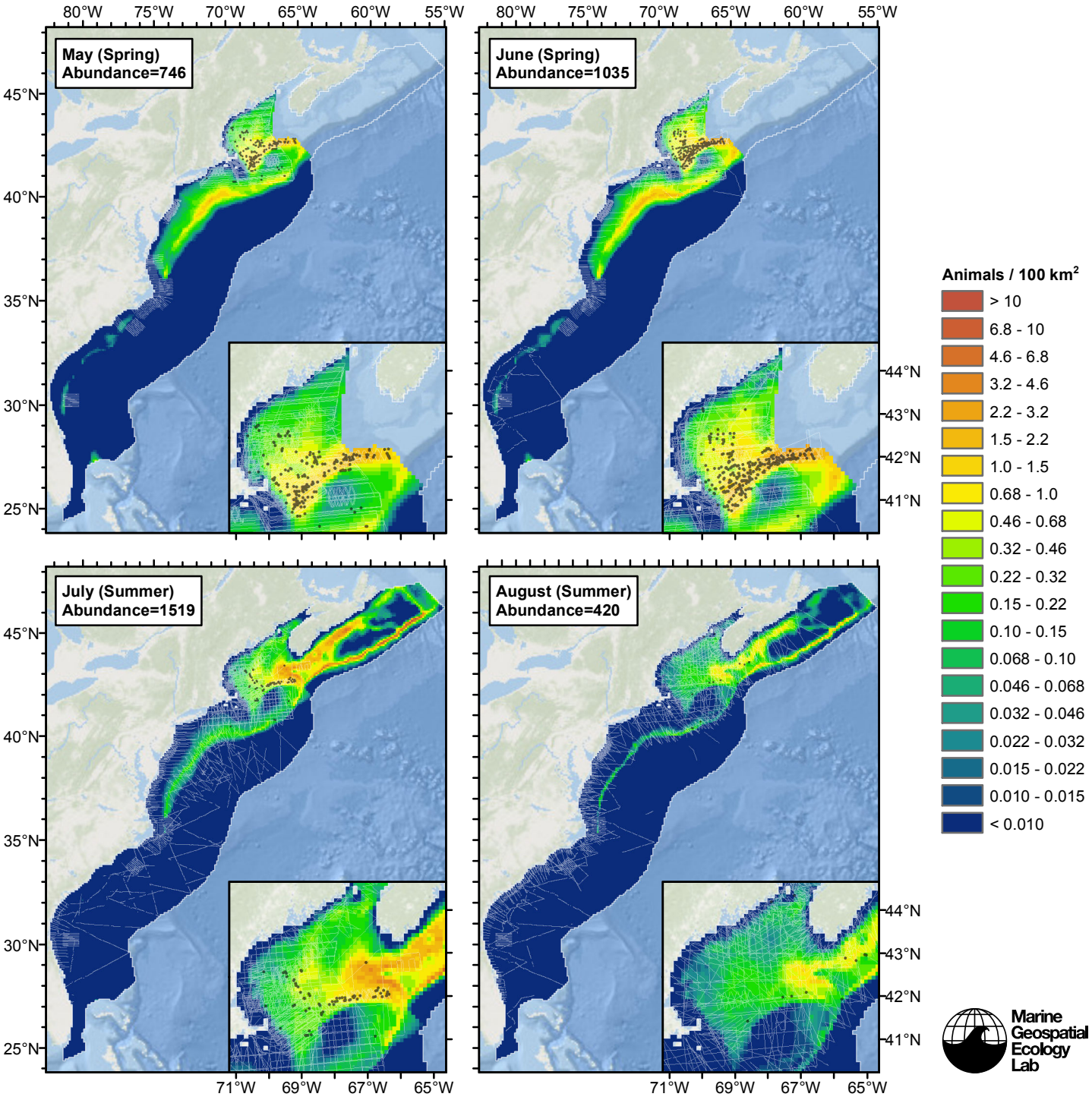
May (Spring)
Abundance=746
June (Spring)
Abundance=1035
July (Summer)
Abundance=1519
August (Summer)
Abundance=420
80°W
75°W
70°W
65°W
60°W
55°W
45°N
40°N
35°N
30°N
25°N
44°N
43°N
42°N
41°N
71°W
69°W
67°W
65°W
Animals / 100 km²
> 10
6.8 - 10
4.6 - 6.8
3.2 - 4.6
2.2 - 3.2
1.5 - 2.2
1.0 - 1.5
0.68 - 1.0
0.46 - 0.68
0.32 - 0.46
0.22 - 0.32
0.15 - 0.22
0.10 - 0.15
0.068 - 0.10
0.046 - 0.068
0.032 - 0.046
0.022 - 0.032
0.015 - 0.022
0.010 - 0.015
< 0.010
Marine
Geospatial
Ecology
Lab

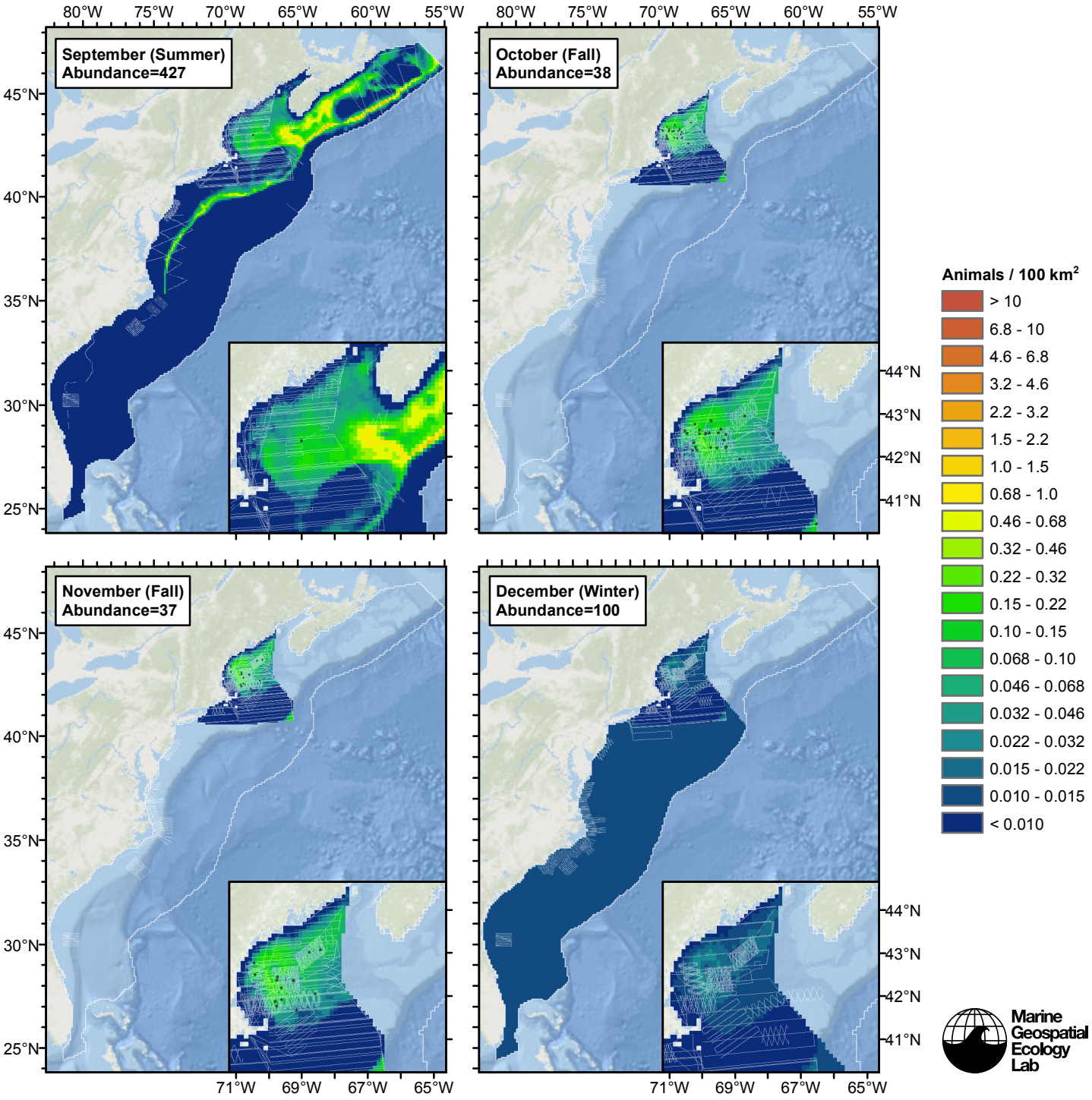
September (Summer)
Abundance=427
October (Fall)
Abundance=38
November (Fall)
Abundance=37
December (Winter)
Abundance=100
80°W
75°W
70°W
65°W
60°W
55°W
45°N
40°N
35°N
30°N
25°N
44°N
43°N
42°N
41°N
71°W
69°W
67°W
65°W
Animals / 100 km²
> 10
6.8 - 10
4.6 - 6.8
3.2 - 4.6
2.2 - 3.2
1.5 - 2.2
1.0 - 1.5
0.68 - 1.0
0.46 - 0.68
0.32 - 0.46
0.22 - 0.32
0.15 - 0.22
0.10 - 0.15
0.068 - 0.10
0.046 - 0.068
0.032 - 0.046
0.022 - 0.032
0.015 - 0.022
0.010 - 0.015
< 0.010
Marine
Geospatial
Ecology
Lab

Contemporaneous Model

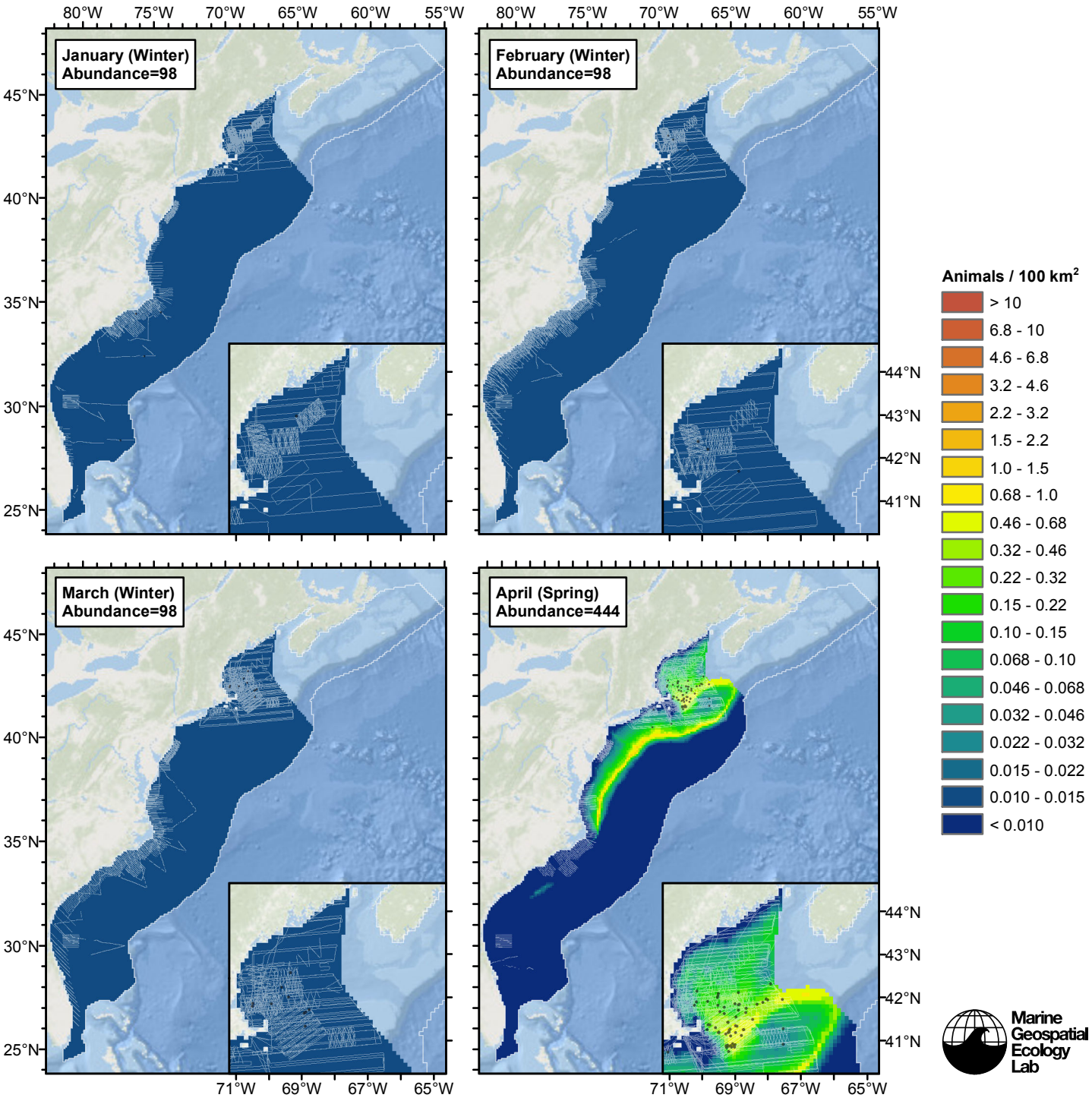

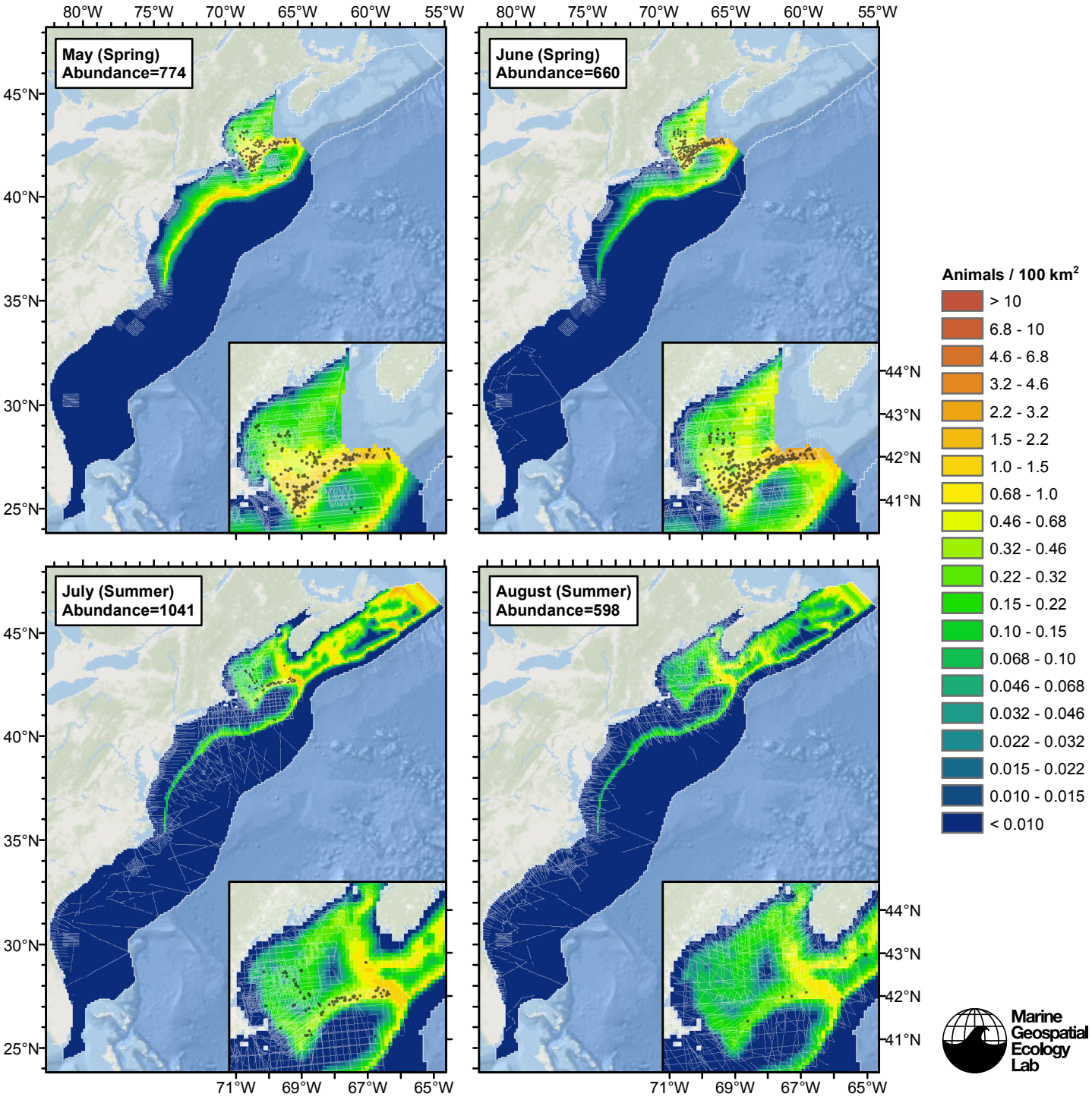
May (Spring)
Abundance=774
June (Spring)
Abundance=660
July (Summer)
Abundance=1041
August (Summer)
Abundance=598
80°W
75°W
70°W
65°W
60°W
55°W
45°N
40°N
35°N
30°N
25°N
44°N
43°N
42°N
41°N
71°W
69°W
67°W
65°W
Animals / 100 km²
> 10
6.8 - 10
4.6 - 6.8
3.2 - 4.6
2.2 - 3.2
1.5 - 2.2
1.0 - 1.5
0.68 - 1.0
0.46 - 0.68
0.32 - 0.46
0.22 - 0.32
0.15 - 0.22
0.10 - 0.15
0.068 - 0.10
0.046 - 0.068
0.032 - 0.046
0.022 - 0.032
0.015 - 0.022
0.010 - 0.015
< 0.010
Marine
Geospatial
Ecology
Lab

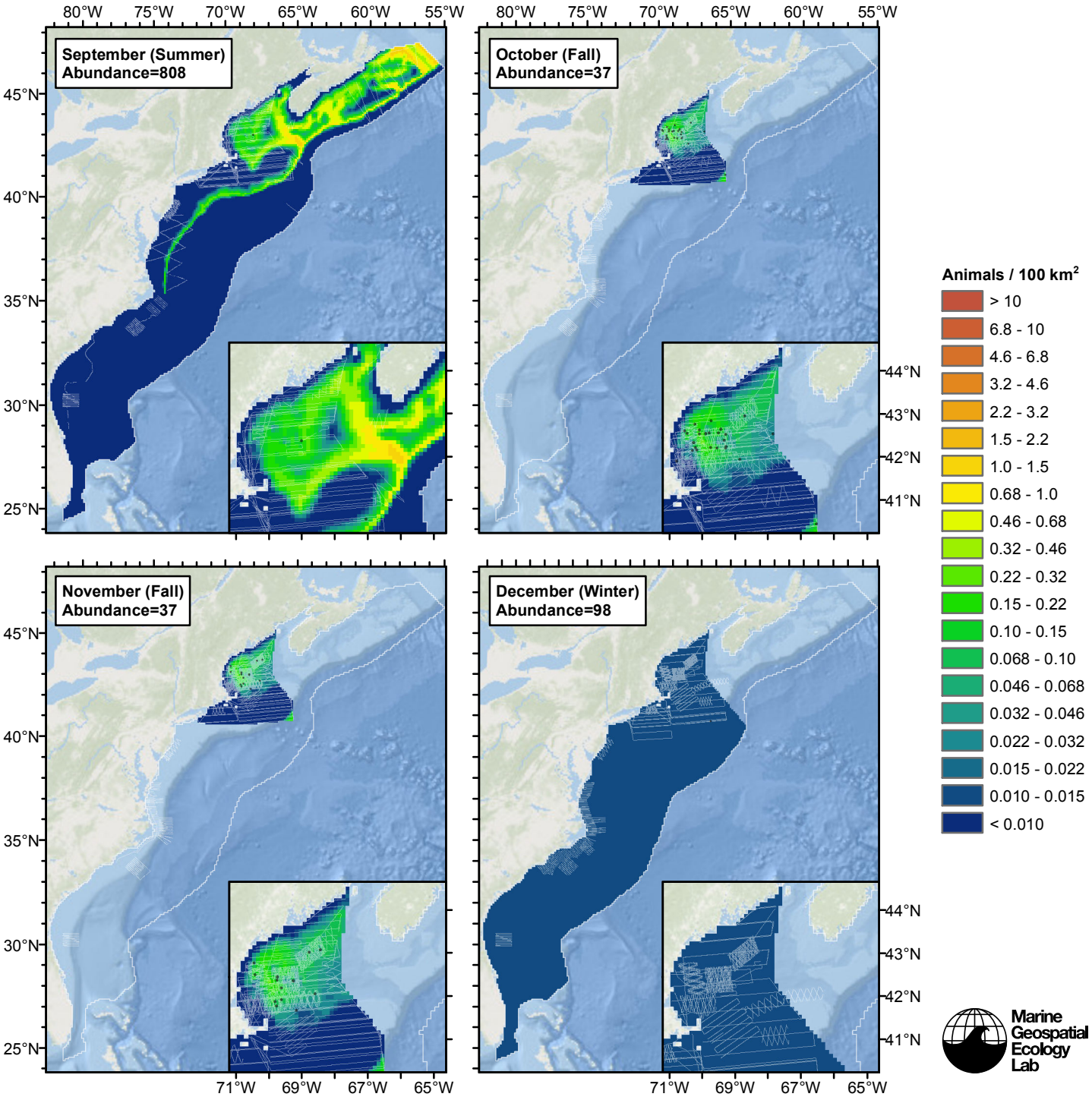
September (Summer)
Abundance=808
October (Fall)
Abundance=37
November (Fall)
Abundance=37
December (Winter)
Abundance=98
80°W
75°W
70°W
65°W
60°W
55°W
45°N
40°N
35°N
30°N
25°N
44°N
43°N
42°N
41°N
71°W
69°W
67°W
65°W
Animals / 100 km²
> 10
6.8 - 10
4.6 - 6.8
3.2 - 4.6
2.2 - 3.2
1.5 - 2.2
1.0 - 1.5
0.68 - 1.0
0.46 - 0.68
0.32 - 0.46
0.22 - 0.32
0.15 - 0.22
0.10 - 0.15
0.068 - 0.10
0.046 - 0.068
0.032 - 0.046
0.022 - 0.032
0.015 - 0.022
0.010 - 0.015
< 0.010
Marine
Geospatial
Ecology
Lab

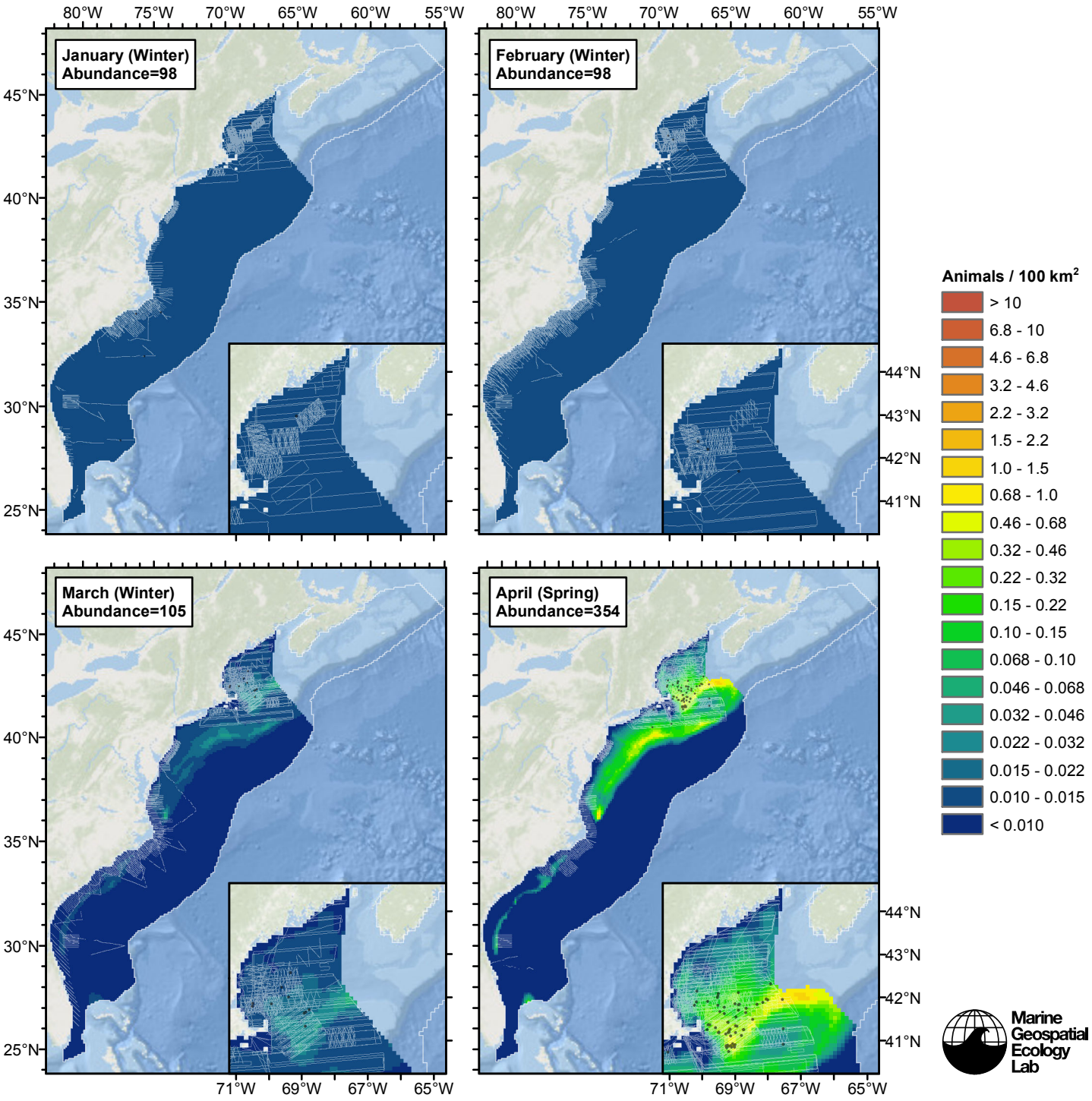
January (Winter)
Abundance=98
February (Winter)
Abundance=98
March (Winter)
Abundance=105
April (Spring)
Abundance=354
80°W
75°W
70°W
65°W
60°W
55°W
45°N
40°N
35°N
30°N
25°N
44°N
43°N
42°N
41°N
71°W
69°W
67°W
65°W
Animals / 100 km²
> 10
6.8 - 10
4.6 - 6.8
3.2 - 4.6
2.2 - 3.2
1.5 - 2.2
1.0 - 1.5
0.68 - 1.0
0.46 - 0.68
0.32 - 0.46
0.22 - 0.32
0.15 - 0.22
0.10 - 0.15
0.068 - 0.10
0.046 - 0.068
0.032 - 0.046
0.022 - 0.032
0.015 - 0.022
0.010 - 0.015
< 0.010
Marine
Geospatial
Ecology
Lab

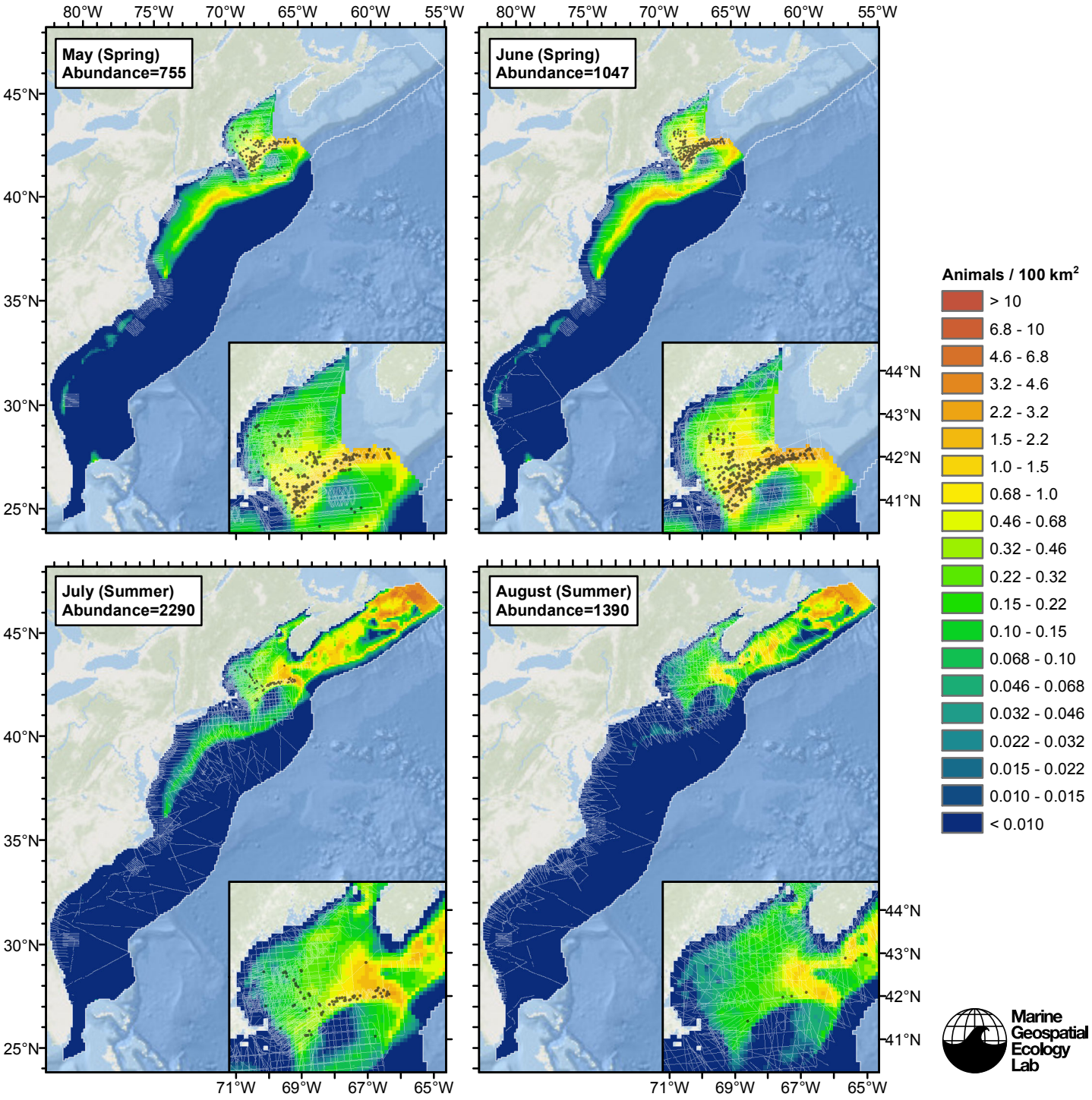
May (Spring)
Abundance=755
June (Spring)
Abundance=1047
July (Summer)
Abundance=2290
August (Summer)
Abundance=1390
80°W
75°W
70°W
65°W
60°W
55°W
45°N
40°N
35°N
30°N
25°N
44°N
43°N
42°N
41°N
71°W
69°W
67°W
65°W
Animals / 100 km²
> 10
6.8 - 10
4.6 - 6.8
3.2 - 4.6
2.2 - 3.2
1.5 - 2.2
1.0 - 1.5
0.68 - 1.0
0.46 - 0.68
0.32 - 0.46
0.22 - 0.32
0.15 - 0.22
0.10 - 0.15
0.068 - 0.10
0.046 - 0.068
0.032 - 0.046
0.022 - 0.032
0.015 - 0.022
0.010 - 0.015
< 0.010
Marine
Geospatial
Ecology
Lab

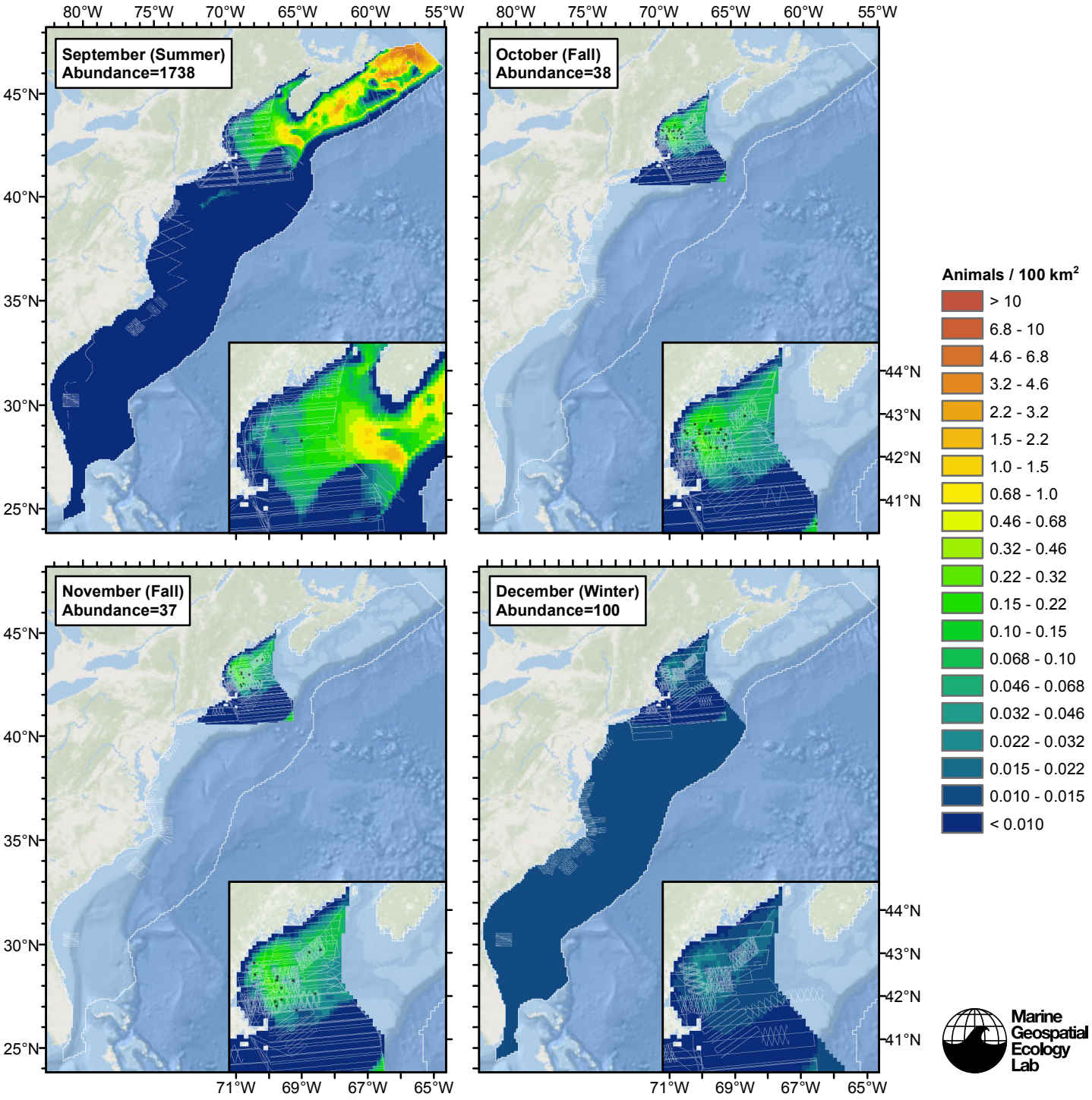

Discussion

Winter

In this season, we lacked sufficient sightings to model density from environmental predictors. Our stratified model estimated that mean density of sei whales was very low. Our model would benefit from additional surveying in this season, but given the apparent rarity of the species, substantial effort might be required to obtain enough sightings to attempt a model based on environmental predictors.

Spring

In this season, the model that used contemporaneous predictor variables explained slightly more deviance than the models that used climatological predictors; we selected the contemporaneous model as our best estimate of sei whale distribution and abundance in this season.

The model predicted high sei whale density in the Great South Channel and waters to the north, and along the northern edge of Georges Bank. No surveying was performed in Canada during these months except along the northern edge of Georges Bank. Lacking additional data in Canada, we were uncomfortable extrapolating our model further north. We recommend additional surveying be performed in Canada during these months to help elucidate the extent of sei whale distribution during this season.

The model also predicted high density along the continental shelf break around Georges Bank and south to Cape Hatteras. We urge caution with this prediction, as survey effort was very sparse across this area, but note that other studies offer some support to this prediction. The CETAP (1982) surveys, conducted over the period 1978-1982, not used in our models, reported numerous sei whales along the southeast edge of Georges Bank. Five acoustic monitors placed along the eastern and southern edge of Georges Bank in spring of 2012 and 2013 reported acoustic detections of sei whales at rates similar to those reported by recorders placed in the Great South Channel and the northern edge of Georges Bank (D. Cholewiak, pers. comm.). Finally, surveys conducted in the summer season that were incorporated into our analysis (see next section), and some that were not yet available to be incorporated (the NOAA AMAPPS surveys), reported sightings along the southern edge of Georges Bank (in summer). Under Mitchell's (1975) hypothesis, in which whales are believed depart the Gulf of Maine and vicinity and migrate up the Scotian Shelf in summer, it stands to reason that if some were still present along southern Georges Bank in summer, there were probably more there in the preceding months.

Our model predicted a mean springtime abundance of 627. At the time of this writing, NOAA had not produce an abundance estimate for this season. As we noted, our estimate does not extend north of Georges Bank, and our model predicted high density up to the northern edge of our modeled area along Georges Bank. This suggests our abundance estimate would be higher if additional (but currently unsurveyed) Canadian waters were included in the prediction.

Summer

In this season, the model that used climatological predictor variables and fitted to all segments explained markedly more deviance than the model that used contemporaneous predictors or the model that used climatological predictors and was restricted to the contemporaneous model's segments. We selected the climatological model that was applied to all segments as our best estimate of sei whale distribution and abundance in this season.

The model predicted a northward shift in abundance from spring, moving from the U.S. shelf break, Georges Bank, and the central Gulf of Maine to the Northeast Channel, Browns Bank and further up the Scotian Shelf, both along the shelf break and at moderate depths close to shore. Abundance was predicted to be highest in July, then fall in August. This overall pattern is roughly compatible with Mitchell's (1975) hypothesis, but we caution that survey effort was sparse on the Scotian Shelf and occurred mainly in August. The Canadian TNASS program surveyed the Scotian Shelf by aircraft from 21 July to 23 August, 2007 and sighted two sei whales (Lawson and Gosselin, 2009). We made several attempts to contact J. Lawson regarding this survey, in the hope of incorporating it into our models, but received no response. We remain hopeful that a collaboration can be established in the future, and the Canadian TNASS data may be incorporated into a new version of our models.

Our model predicted a mean abundance of 717 over the three month season, with a peak of 1519 in July and low of 420 in August. NOAA estimated 357 for the period June-August 2011 (Waring et al. 2014). The two results cannot be directly compared due to mismatching spatiotemporal extents. First, our estimate covers the entire EC study area while NOAA's covers a smaller area, from Central Virginia to Browns Bank. Second, NOAA's estimate is split between two strata: the shelf break, surveyed by ship 4-21 June 2011, and the Gulf of Maine / Bay of Fundy (GOM/BOF), surveyed by aircraft 8-26 August 2011. Our study predicted a dramatic difference in abundance between June and August; if this difference was real, it complicates the comparison to NOAA's estimate further, due to NOAA's shipboard shipboard transects occurring during a high abundance period and their aerial transects occurring during a low abundance period.

Similar spatiotemporal matchup problems also occur when comparing our model's predictions to NOAA's earlier surveys. NOAA's highest estimate came in 2004, when on-shelf aerial surveying of the Gulf of Maine occurred in late June and early July, rather than in August, as with their other surveys. In sum, NOAA's estimates and ours agree that sei whale abundance is higher in June and July and lower in August. In July, our models predict much higher abundance in Canadian waters than U.S. waters, particularly on the Scotian Shelf; this seems plausible based on historical records but it is an extrapolation that cannot be easily compared with NOAA's estimates because NOAA did not survey this area until August.

Fall

All three models we attempted for this season produced the same result: they discarded all dynamic predictors and retained only two static predictors. Therefore it did not matter which model we selected as best; the results were identical.

Predicted abundance was very low in this season. But, consistent with Mitchell's (1975) hypothesis that sei whales return to the Gulf of Maine in September and October, our model (spanning October and November) predicted higher abundance in the western Gulf of Maine than our summer model. As with winter and spring, NOAA had not produce an abundance estimate for fall months at the time of this writing.

Summing up all of our seasonal results at the broad scale, our models displayed plausible temporal dynamics for what has been reported in the literature for sei whales, with low abundance in winter months, an increase and peak in spring and early summer, a northward shift and decrease in late summer, and some suggestion of a return to the Gulf of Maine in fall. While our models would benefit from the introduction of additional survey data in non-summer months, and in Canada at all times of year, the temporal dynamics of our models resemble what is described in the literature well enough for us to recommend that our monthly predictions be used for federal regulatory purposes and marine spatial planning applications.

References

Byrd BL, Harms CA, Hohn AA, McLellan WA, Lovewell GN, et al. (2014) Strandings as indicators of marine mammal biodiversity and human interactions off the coast of North Carolina. Fishery Bulletin 112: 1-23.

CETAP (1982) A characterization of marine mammals and turtles in the mid-and north Atlantic areas of the US outer continental shelf. Final Report. Bureau of Land Management, Washington, DC. Ref. AA551-CT8-48.

Chelton DB, Schlax MG, Samelson RM (2011) Global observations of nonlinear mesoscale eddies. Prog. Oceanogr. 91: 167-216.

Debich AJ, Baumann-Pickering A, Sirovic A, Buccowich JS, Gentes ZE, et al. (2014) Passive Acoustic Monitoring for Marine Mammals in the Cherry Point OPAREA 2011-2012. MPL Technical Memorandum #545. Marine Physical Laboratory, Scripps Institution of Oceanography, University of California San Diego, La Jolla, California. 83 p. Available online: http://www.navymarinespeciesmonitoring.us/index.php/download_file/view/660/

Debich AJ, Baumann-Pickering A, Sirovic A, Kerosky SA, Roche LK, et al. (2013) Passive Acoustic Monitoring for Marine Mammals in the Jacksonville Range Complex 2010-2011. MPL Technical Memorandum #541. Marine Physical Laboratory, Scripps Institution of Oceanography, University of California San Diego, La Jolla, California. 57 p. Available online: http://www.navymarinespeciesmonitoring.us/index.php/download_file/view/465/

Hiby L (1999) The objective identification of duplicate sightings in aerial survey for porpoise. In: Marine Mammal Survey and Assessment Methods (Garner GW, Amstrup SC, Laake JL, Manly BFJ, McDonald LL, Robertson DG, eds.). Balkema, Rotterdam, pp. 179-189.

Hodge L, Reed A (2014) Passive Acoustic Monitoring for Marine Mammals in Onslow Bay (multiple documents). Reports by the Duke University Marine Laboratory, Beaufort, North Carolina. Available online: http://www.navymarinespeciesmonitoring.us/reading-room/atlantic/ under Technical Reports.

Jefferson TA, Webber MA, Pitman RL (2008) Marine Mammals of the World: A Comprehensive Guide to Their Identification. Academic Press/Elsevier, 573 pp.

Mitchell E (1975) Preliminary report on Nova Scotia fishery for sei whales (Balaenoptera borealis). Rep. Int. Whal. Comm. 25: 218-225.

Norris TF, Oswald JO, Yack TM, Ferguson EL (2014) An Analysis of Marine Acoustic Recording Unit (MARU) Data Collected off Jacksonville, Florida in Fall 2009 and Winter 2009-2010. Final Report. Submitted to Naval Facilities Engineering Command (NAVFAC) Atlantic, Norfolk, Virginia, under Contract No. N62470-10-D-3011, Task Order 021, issued to HDR Inc., Norfolk, Virginia. Prepared by Bio-Waves Inc., Encinitas, CA. 21 November 2012. Revised January 2014.

Palka DL (2005b) Shipboard surveys in the northwest Atlantic: estimation of g(0). In: Proceedings of a Workshop on Estimation of g(0) in Line-Transect Surveys of Cetaceans (Thomsen F, Ugarte F, Evans PGH, eds.). European Cetacean Society's 18th Annual Conference; Kolmarden, Sweden; Mar. 28, 2004. pp. 32-37.

Palka DL (2006) Summer Abundance Estimates of Cetaceans in US North Atlantic Navy Operating Areas. US Dept Commer, Northeast Fish Sci Cent Ref Doc. 06-03: 41 p.

Prieto R, Janiger D, Silva MA, Waring GT, Goncalves JM (2012) The forgotten whale: a bibliometric analysis and literature review of the North Atlantic sei whale Balaenoptera borealis. Mammal Review 42:235-272.

Rosel PE, Wilcox LA (2014) Genetic evidence reveals a unique lineage of Bryde's whales in the northern Gulf of Mexico. Endangered Species Research 25: 19-34.

Waring GT, Josephson E, Fairfield-Walsh CP, Maze-Foley K, eds. (2007) U.S. Atlantic and Gulf of Mexico Marine Mammal Stock Assessments – 2007. NOAA Tech Memo NMFS NE 205; 415 p.

Waring GT, Josephson E, Maze-Foley K, Rosel PE, eds. (2014) U.S. Atlantic and Gulf of Mexico Marine Mammal Stock Assessments – 2013. NOAA Tech Memo NMFS NE 228; 464 p.